LINCOLN LABORATORY

Vol. 120 Nos. 1-6

May-June 1958

PROCEEDINGS OF THE ACADEMY OF SCIENCES

OF THE USSR

(DOKLADY AKADEMII NAUK SSSR)

Physical Chemistry Section

A publication of the Academy of Sciences of the USSR

IN ENGLISH TRANSLATION

Year and issue of first translation:
vol. 112, nos. 1-6 Jan.-Feb. 1957

Annual subscription	*$160.00*
Single issue	*35.00*

Copyright 1959

CONSULTANTS BUREAU INC.
227 W. 17th ST., NEW YORK 11, N. Y.

NOTE: The sale of photostatic copies of any portion of this copyright translation is expressly prohibited by the copyright owners. A complete copy of any paper in this issue may be purchased from the publisher for $5.00.

Printed in the United States

PROCEEDINGS OF THE ACADEMY OF SCIENCES OF THE USSR

Physical Chemistry Section

Volume 120, Number 1-6 May-June 1958

CONTENTS

	PAGE	RUSS. ISSUE	RUSS. PAGE
The Surface Conductivity of Quartz in the Presence of Adsorbed Film. I. F. Abdrakhmanova and B. V. Deriagin	263	1	94
A Study of the Oxidation-Reduction Potentials of Plutonium in Nitric Acid. P. I. Artiukhin, A. D. Gel'man and V. I. Medvedovskii	269	1	98
The Problem of the Mechanism of Electrolytic Polishing and the Structure of the Electropolished Surface. G. S. Vozdvizhenskii, G. A. Gorbachuk and G. P. Dezider'ev	273	1	101
Reversible Isotherms for the Adsorption of Water on Quartz. S. P. Zhdanov	277	1	103
The Role of the Nonstationary Process in the Stimulation of Degenerative Branching Chain Reactions in the Liquid Phase. D. G. Knorre, V. L. Pikaeva and N. M. Emanuel'	283	1	107
The Thermodynamics of CsCl-RbCl Solid Solutions at 25°. L. L. Makarov and Iu. G. Vlasov	287	1	111
The Measurement of the Differential Capacity of the Electrical Double Layer on the Dropping Mercury Electrode in Solutions of KF, LiCl, NaCl and KCl in Methyl Alcohol. S. Mints and Ia. Iastshembskaia	291	1	114
The Mechanism of the Vertical Distribution of H_2O_2 Above a Solution. I. L. Roikh and I. P. Bolotich	293	1	116
The Kinetics of the Oxidation of Ferrocene by Iodine. A. V. Savitskii, and Ia. K. Syrkin	297	1	119
The Equilibrium Potentials of Zirconium in Chloride Melts. M. V. Smirnov and V. A. Chemezov	301	1	122
The Mechanism of the Emulsifying Action of Solid Emulsifiers. A. B. Taubman and A. F. Koretskii	305	1	126
The Dependence of the Lower Limit of the Structural Stability and the Critical Velocity Gradient on the Concentration of Oleogels of Aluminum Naphthenate. V. A. Fedotova and A. A. Trapeznikov	309	1	130
Electrocapillary Movement in Molten Slags. V. V. Khlynov and O. A. Esin	313	1	134
The Determination of Polarographic Diffusion Coefficients by the Use of the Rotating Disk Electrode. V. D. Iukhtanova	317	1	137
The Adsorptive Properties of Aluminosilicate Catalysts and Their Dependence on Composition. M. M. Egorov, Iu. A. Zarif'iants, V. F. Kiselev and K. G. Krasil'nikov	321	2	326

CONTENTS (continued)

	PAGE	RUSS. ISSUE	RUSS. PAGE
The Luminescence Spectra of the Coordination Compounds of Uranyl Nitrate. G. I. Kobyshev and D. N. Suglobov	325	2	330
The Catalytic Properties of Calcium Oxide. O. V. Krylov and E. A. Fokina	329	2	333
The Reactions of Free Radicals in Solution. The Interaction of Free Radicals with Internal and External Double Bonds. E. B. Milovskaia, B. L. Erusalimskii and B. A. Dolgoplosk	333	2	336
The Mechanics of Polymer Molecules. G. A. Patrikeev	337	2	339
The Nature of the Bonds and the Gas Permeability of Space Structured Polybutadiene. S. A. Reitlinger, A. S. Kuz'minskii and L. A. Fel'dshtein	341	2	343
The Formation of Free Radicals and Atoms by the Radiolysis of Hydrocarbons at a Temperature of 77° K. N. Ia. Cherniak, N. N. Bubnov, V. V. Voevodskii, L. S. Polak and Iu. D. Tsvetkov	345	2	346
The Influence of the Salts of a Series of Lower Fatty Acids on Emulsion Polymerization. A. I. Iurzhenko and S. S. Ivanchov	349	2	349
The Phenomenon of the Formation of Electrode Zones During the Electrocrystallization of Metals. V. V. Bondar' and Iu. M. Polukarov	353	3	552
The Theory of the Faraday Rectification. Iu. A. Vdovin	357	3	554
The Mechanism of the Anodic Dissolution of Magnesium. B. N. Kabanov and D. V. Kokoulina	363	3	558
The Mechanics of Extended Polymer Systems. G. A. Patrikeev	367	3	562
The Isotope Effect in the Critical Temperature. I. B. Rabinovich and V. A. Gorbushenkov	371	3	566
The Determination of the Specific Surface and the Pore Volume of Solid Polymeric Sorbents. A. A. Tager, M. V. Tsilipotkina and A. I. Suvorova	377	3	570
A Contribution to the Theory of the Surface Tensions of Solutions of Strong Electrolytes. V. E. Bravina	381	4	815
The Energy of Activation for Diffusional Creep in Metallic Disordered Solid Substitution Solutions. Ia. E. Geguzin	387	4	819
An Investigation of the Films on a Mercury Electrode. A. Ia. Gokhshtein and Ia. P. Gokhshtein	391	4	823
The Effect of Polarization on the Mechanical Properties of Steel. G. V. Karpenko and R. I. Kripiakevich	395	4	827
The Chemical Adsorption and Catalytic Oxidation of CO on ZnO, and on Various Solid Solutions of the Latter which Differ in Conductivity. N. P. Keier and G. I. Chizhikova	399	4	830
The Energy of Coulombic Interaction between Silica Gel Hydroxyl Groups and Benzene Molecules. A. V. Kiselev and D. P. Poshkus	403	4	834
The Chemical Reactions of Atoms with Energies Comparable to the Energy of Activation. B. N. Provotorov	407	4	838

CONTENTS (continued)

	PAGE	RUSS. ISSUE	RUSS. PAGE
The Effect of Concentration on the Critical Deformation and the Associated Structural Strength of Aluminum Naphthenate Oleogels. V. A. Fedotova and A. A. Trapeznikov	411	4	841
Effect of Nickel on the Electrochemical and Corrosion Behavior of Steel. G. M. Florianovich, Ia. M. Kolotyrkin and N. K. Smirnova	415	4	845
Effect of High Pressures on Self-Adhesion (Autohesion) of High-Polymers. L. A. Igonin, Iu. V. Ovchinnikov and S. A. Arzhakov	419	5	1062
Mechanism of the Protective Action of Colored Lacquer Coatings. V. A. Kargin, M. I. Kariakina and Z. Ia. Berestneva	423	5	1065
The Quasi-Stationary Thermal Regime in Explosion Reactions. A. G. Merzhanov and F. I. Dubovitskii	427	5	1068
Study of the Adsorption of Cations on Platinized Platinum by the Method of Measuring the Adsorption Potentials. A. D. Obrucheva	431	5	1072
X-Ray Diffraction from Regions Composed of Long Molecules. D. Ia. Tsvankin	435	5	1076
The Edge Problem in the Theory of Heat Explosion. V. V. Barzykin and A. G. Merzhanov	441	6	1271
The Thermodynamics of Formation of the Higher Antimonide of Iron. V. A. Geiderikh, Ia. I. Gerasimov and A. A. Vecher	445	6	1274
The Properties of Guttapercha in the Amorphous State. V. A. Kargin, T. I. Sogolova and B. I. Aikhodzhaev	449	6	1277
Relaxation Reaction of Impact Waves with a Zone of Combustion. S. M. Kogarko and V. I. Skobelkin	453	6	1280
Vapor Pressure of Saturated Selenium Vapors Below the Melting Point. A. A. Kuliev and M. G. Shakhtakhtinskii	457	6	1284
A Contribution to the Theory of Thermal Chain Flame Propagation. L. A. Lovachev	461	6	1287
A Study of the Dissociation of Oxygen Behind a Powerful Shock Wave. S. A. Losev	467	6	1291
Irreversible Catalytic Hydrogen Waves in Polarography. S. G. Mairanovskii	471	6	1294
The Electrical Conductivity of n-Semiconductors with Chemisorbed Atoms and Radicals. I. A. Miasnikov	475	6	1298
Application of the Irreversibility of Adsorption of Optical Sensitizers. Z. L. Petrushkina	479	6	1302
The "Deviations" from Raoult's Law Caused by Chemical Interaction Between the Components. M. Usanovich	481	6	1304

THE SURFACE CONDUCTIVITY OF QUARTZ IN THE PRESENCE OF ADSORBED FILMS

I. F. Abdrakhmanova and B. V. Deriagin, Corresponding Member, Academy of Sciences, USSR

INTRODUCTION

The donor properties of the surface atoms of a glass are affected by the double layers which are formed on contacting the glass with polymer coatings, these latter being, as a rule, negatively charged. At the same time, the charge of such double layer determines the strength of the resulting adhesional bonds. One of the methods for studying these bonds involves the study of those changes which occur in the surface conductivity on covering the surface with films of foreign molecules, beginning with mono-, and ending with polymolecular layers. An increase of the surface conductivity can, for example, serve as indication of a transfer of electrons into new energy levels, this being a factor plays a role in the formation of the double layer. (There are, of course, other mechanisms leading to an increase in the electrical conductivity).

Study has been made of the surface conductivity of quartz and of various glasses in the presence of water vapors, but there is no data on the effect of the adsorption of organic compounds. Tsekhnovitser [1], studied the surface conductivity of rock salt crystals in 1929 and found that the conductivity in the presence of benzene vapors rose to $10^{-12}\ \Omega^{-1}$, whereas in vacuum at room temperature it amounted to $10^{-15}\ \Omega^{-1}$.

The investigations of N. Chirkov [2] have shown that, as compared with its value in vacuum, the conductivity of sheet mica which had been treated with HCl was increased by the presence of ethyl alcohol vapors. These data indirectly indicate that the adsorption of vapors of organic compounds should also have an affect on the surface conductivity of quartz.

Technique. In this work the surface conductivity of quartz in vapors of water, benzene, CCl_4 and alcohols has been studied.

The apparatus for this study of the surface conductivity (Fig. 1) was prepared from quartz glass. Into the tube 1 there was poured the material whose vapor adsorption was to be investigated. The specimen 2 in the form of a bar with platinum leads was affixed in the middle portion of the apparatus; 4 is a guard ring and 3, a mercury seal. A potential was applied to one of the leads of the apparatus and the other lead was connected to the grid of the electrometer tube of an amplifier. This amplifier was in a bridge circuit [3] with the electrometer tube and with it the measurement of currents as small as 10^{-13} amp was possible.

Specimens in the form of bars of 1-3 mm diameter were drawn out in the blast lamp flame from cylinders of optical quartz. After these specimens had been repeatedly boiled in fresh portions of distilled water, electrodes were deposited on them by extrusion from a silver paste. This method of electrode deposition was applied earlier by G. I. Skanavi [4] and M. S. Aslanova [5], whose experiments have shown that silver electrodes thus obtained are assured of a firm contact and give most stable results.

Prior to measurements, the apparatus was pumped out by a two-stage fractionating pump working on "Octoil 5." The pressure was measured with a MacLeod gauge. In order to avoid contamination by the oil, a trap situated directly ahead of the apparatus was immersed in a Dewar flask with liquid nitrogen and the liquid in the tube 1 was frozen out. The apparatus was sealed off from the vacuum line after the pressure in it had fallen to 10^{-5} mm of Hg.

The pressure of the vapors was specified by fixing the temperature difference between the specimen 2, which was thermostated at constant temperature T_c, and the liquid in the tube 1. In the tube containing the liquid, the pressure of the vapors was varied by altering the tube temperature T, the pressure of the saturated vapors near the surface of the specimen remaining constant.

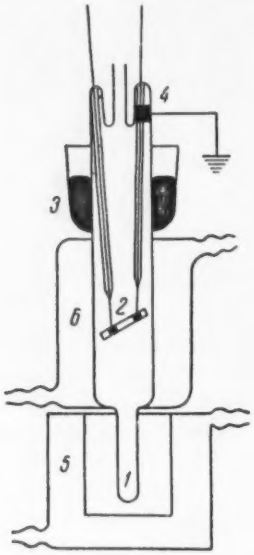

Fig. 1. Apparatus for the study of the surface conductivity in vacuum.

Thus it was possible to obtain any desired value of the relative pressure p/p_s, p and p_s (the pressures of saturated vapor at the temperatures T and T_c, respectively) being calculated from tabular data by the use of the customary interpolation equation, $\log p = A + B/T$, in which A and B are constants.

The specimen 2 was thermostated by passing water from a thermostat at temperature T_c through the jacket b. The tube containing the liquid which was under study was inserted in a second thermostat 5 whose temperature T was varied.

The temperatures T and T_c were measured with a Beckmann thermometer with 0.01° scale divisions. In order to determine to what extent a temperature difference as read from this Beckmann thermometer would correspond to the actual temperature difference between the specimen and the liquid in the apparatus, check was made with a differential thermocouple, one junction of which was inserted at the position of the specimen and the other in the tube. The accuracy of measurement of the temperature difference was 0.01°. The temperature differences, as determined from the thermometer and as measured by the thermocouple, did not differ by more than 0.01°.

Prior to an experiment, the quartz apparatus for the measurement of the surface conductivity was washed out with chromic acid solution and was then treated with steam for 5-6 hours. The quartz specimen was heated to incandesence. For comparison, several specimens were cleansed by treatment in a glow discharge, using a method which has been developed by V. V. Karasev [8] in the Laboratory for Surface Phenomena of the Institute of Physical Chemistry of the Academy of Sciences of the USSR.

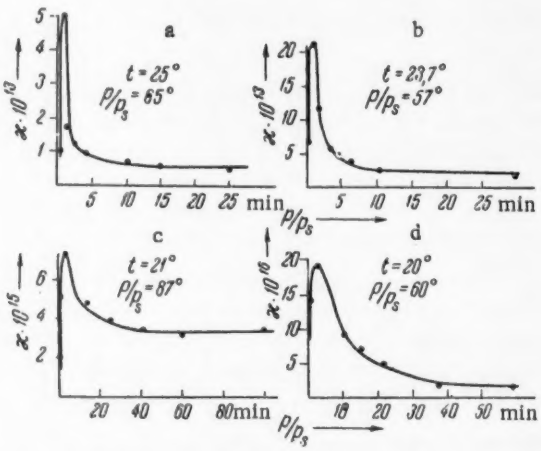

Fig. 2. The kinetics of the surface conductivity of quartz under adsorption of: a) water; b) ethyl alcohol; c) butyl alcohol; d) hexyl alcohol.

Experimental results. In vacuum, both the specimens which had been treated in the glow discharge and those which had been cleansed by heating showed a surface conductivity below the sensitivity of the technique, i.e., less than $10^{-17}\Omega^{-1}$.

At the beginning of each experiment, the surface conductivity of the specimen was measured at the temperature T_C and with the working material frozen out, i.e., with $p/p_s = 0$. In the case of the specimens of optical quartz, the surface conductivity was always less than $10^{-17}\Omega^{-1}$. The working material was then melted and tube 1 immersed in the thermostat 5. With a constant pressure ratio p/p_s, the surface conductivity at first rapidly increased, reaching a maximum, and then gradually fell, assuming in the course of 10-20 minutes an invariant value corresponding to the given p/p_s. Kinetic curves of this type were obtained for all of the substances studied with the exception of benzene and carbon tetrachloride; even at saturation, the vapors of these materials did not alter the surface conductivity of the quartz (to within an accuracy of $10^{-17}\Omega^{-1}$).

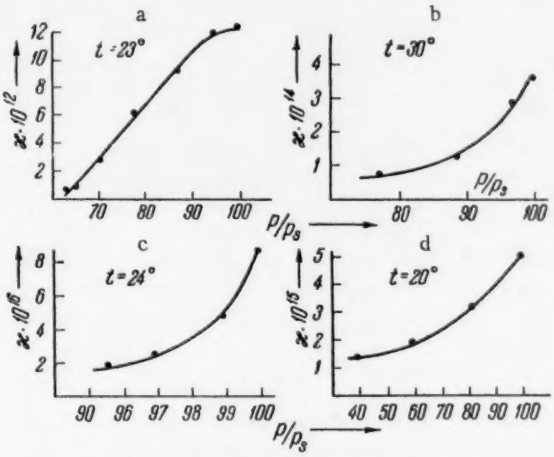

Fig. 3. Isotherms of the surface conductivity of quartz under adsorption of: a) water; b) butyl alcohol; c) hexyl alcohol; d) octyl alcohol.

Similar kinetics for the conduction of adsorbed water films has been observed in [9]. These papers explained the maxima as resulting from a transition of the original amorphous layers of adsorbed water into the crystalline state.

Kinetic curves for water, and for ethyl, butyl and hexyl alcohols are shown in Fig. 2. The maxima which are observed here are obtained only if the first point of the surface conductivity isotherm in a given experiment is plotted, i.e., only when there are no adsorbed molecules in the working material on the quartz surface.

In Fig. 3 there are shown isotherms for the surface conductivity of water, and of butyl, hexyl and octyl alcohols.

The water which was employed for these measurements had been twice distilled in quartz. The remaining materials were from the firm of Khalbaum and were dehydrated prior to experiment by being boiled under vacuum in the surface conductivity apparatus with chips of metallic calcium. In Table 1 there are presented values of the surface conductivity of quartz free of adsorption and of quartz saturated with the vapors of various substances.

DISCUSSION OF RESULTS

The surface conductivity of optical quartz has been measured in the vapors of water, benzene, carbon tetrachloride, and ethyl, butyl, hexyl, heptyl and octyl alcohols. The resulting isotherms for the alcohols indicate that the surface conductivity alters by 2-3 fold over an interval of relative pressures of 0.8–1; only in the case of ethyl alcohol is a considerably greater increase noted, the isotherm being very similar to that for the surface conductivity of water. With benzene and carbon tetrachloride, the surface conductivity lies, even

at saturation and supersaturation, outside the sensitivity limits of the method ($10^{-17}\,\Omega^{-1}$), although the work of B. V. Deriagin and Z. M. Zorin [6, 7] has shown that near saturation the depths of adsorbed films of these substances are even greater than is the case with the polar materials which we have studied.

A comparison of the rise in the surface conductivity of the investigated materials with increasing depth of adsorbed film, discloses a quantitative incompatibility: over a given interval of relative pressures, the film depth increases more rapidly than does the conductivity.

TABLE 1

Material adsorbed on the quartz	$\kappa_p \mid p_s = 0, \Omega^{-1}$	$\kappa_p \mid p_s = 1, \Omega^{-1}$
Water	$< 1 \cdot 10^{-17}$	$\sim 1 \cdot 10^{-11}$
Ethyl alcohol	$< 1 \cdot 10^{-17}$	$\sim 5 \cdot 10^{-12}$
Butyl alcohol	$< 1 \cdot 10^{-17}$	$\sim 5 \cdot 10^{-14}$
Hexyl alcohol	$< 1 \cdot 10^{-17}$	$\sim 1 \cdot 10^{-15}$
Heptyl alcohol	$< 1 \cdot 10^{-17}$	$\sim 5 \cdot 10^{-15}$
Octyl alcohol	$< 1 \cdot 10^{-17}$	$\sim 5 \cdot 10^{-15}$
Carbon tetrachloride	$< 1 \cdot 10^{-17}$	$< 1 \cdot 10^{-17}$
Benzene	$< 1 \cdot 10^{-17}$	$< 1 \cdot 10^{-17}$

A second result of this work is the development of the kinetics of that surface conductivity of the investigated materials which results from adsorption on a clean surface of optical quartz. It is clear that a nonequilibrated adsorption layer is initially formed on the quartz surface, the molecules of this layer, possessing nonequilibrium orientations, in the first place, and occupying, in the second place, positions which are inconsistent with maximum adsorption energy (due to the nonuniformity of the surface), to which there corresponds an increased surface conductivity. Subsequently, there begins an orientation of the adsorbed molecules and their transition to positions with higher adsorption energy.

The orientation process progresses from the lower layers to the upper, with the result that there is formed an adsorption layer of firmly adsorbed molecules which possesses an ordered structure, with a constant, considerably reduced, conductivity corresponding to the given relative pressure. On obtaining the following points on the isotherm of surface conductivity, the newly entering molecules either adsorb on the vacant positions, from which they cannot transfer to others with low energy levels since these latter are already occupied, or they are oriented by the already existing ordered layer and the surface conductivity reaches a value corresponding to the new relative pressure more rapidly and does not disclose the sharply elevated values of the initial stage.

The results which have been obtained still do not make it possible to say with certainty what mechanism of surface conduction is brought into play by the adsorbed layer of molecules or whether this mechanism be electronic or ionic.

LITERATURE CITED

[1] E. V. Tsekhnovitser, J. Russ. Phys. Chem. Soc. phys. sec. 61, No. 5, 487 (1929).

[2] N. M. Chirkov, J. Phys. Chem. 21, vol. 11, 1303 (1947).

[3] G. I. Berleev, Success Phys. Sci. 49, vol. 1, 93 (1953).

[4] G. I. Skanavi, Dielectric Polarization and Losses in Glasses and Ceramic Materials with High Dielectric Permeability (in Russian), 1952.

[5] M. S. Aslanova, Doc. Diss., Moscow (in Russian), 1954.

[6] B. V. Deriagin and Z. M. Zorin, Proc. Acad. Sci. USSR 98, 93 (1954).

[7] B. V. Deriagin and Z. M. Zorin, J. Phys. Chem. 29, vol. 6, (1955); 29, vol. 10, (1955).

[8] V. V. Karasev and G. I. Izmailova, J. Tech. Phys. 24, 871 (1954).

[9] Sh. Kyrosaki, Sh. Saito and G. Sato, J. Chem. Phys. 23, No. 10 (1955).

The Laboratory for Surface Phenomena of the
Institute of Physical Chemistry of the
Academy of Sciences of the USSR

Received January 1, 1958

A STUDY OF THE OXIDATION-REDUCTION POTENTIALS OF PLUTONIUM IN NITRIC ACID

P. I. Artiukhin, A. D. Gel'man and V. I. Medvedovskii

(Presented by Academician I. I. Chernaev, December 24, 1957)

Data on the formal potentials of various plutonium pairs in solutions of hydrochloric and perchloric acids is to be found in the literature [1-6]. On the other hand, the data on these formal potentials in nitric acid solutions are quite limited and very untrustworthy [2, 7-9].

There has, as well, been no investigation of the auto-oxidation and autoreduction of plutonium in nitric acid solutions.

Working in nitric acid solutions of various concentrations, we have studied the disproportionation of Pu (IV) and have determined the formal oxidation-reduction potentials of various plutonium pairs.

Measurement of the potentials of the Pu (IV) – Pu (III) pair was carried out in an apparatus similar to that described earlier [10], working at 25° in an atmosphere of nitrogen which had been carefully freed of oxygen. The Pu (III) was obtained by reduction of Pu (IV) on a platinized platinum cathode. The concentrations of Pu (IV) and Pu (III) were determined spectrophotometrically.

TABLE 1

The Formal Potentials of the Pu (IV) – Pu (III) Pair in Nitric Acid Solutions

Concentration of HNO_3, N	Potential, mv
0.20	942
0.40	930
1.00	914

Measurement of the oxidation-reduction potentials was carried out over the entire range of relative concentrations of Pu (IV) and Pu (III). From the resulting data there were graphically determined those values of the formal potentials which are presented in Table 1.

An attempted direct determination of the potentials of the Pu (VI) – Pu (IV) pair was unsuccessful. The experimental values fell in the interval 1010–1040 mv, and depended only weakly on the relative concentrations of the Pu (VI) and Pu (IV). For the determination of the formal potentials of the Pu (VI) – Pu (IV) pair use was made of the disproportionation of Pu (IV) at low concentrations of the nitric acid: 0.40; 0.30; 0.20; and 0.10 N.

The disproportionation of Pu (IV) was carried out at 25°, the concentrations of Pu (IV), Pu (III) and Pu (VI) being determined spectrophotometrically, just as in the first case. Measurement of the oxidation-reduction potentials was carried out after equilibrium had been attained.

From the equilibrium concentrations and the measured values of the oxidation-reduction potentials at equilibrium, formal potentials were calculated for the pairs: Pu (IV) – Pu (III), Pu (VI) – Pu (IV) and Pu (VI) – Pu (III), the resulting values being those presented in Table 2.

It is to be seen from Table 2 that the values of the formal potentials of the pairs Pu (VI) – Pu (IV) and Pu (VI) – Pu (III) increase markedly with a rise in the hydrogen ion concentration. Calculation shows that the potentials of these pairs depend on the fourth power of the H^+ concentration. Thus, the following reactions proceed at the electrode

$$PuO_2^{2+} + 4H^+ + 2e \rightarrow Pu^{4+} + 2H_2O, \quad (1)$$

$$PuO_2^{2+} + 4H^+ + 3e \rightarrow Pu^{3+} + 2H_2O. \quad (2)$$

Making use of these equations, the formal potentials of the pairs Pu (VI) – Pu (IV) and Pu (VI) – Pu (III) in 1 N HNO_3 were calculated, account being taken of complex formation [14, 15]; the resulting values proved to be 1054 and 1006 mv respectively.

TABLE 2

Formal Potentials of Plutonium in Nitric Acid Solutions

Concentration of HNO_3, N	Potentials in mv		
	Pu(IV) – Pu(III)	Pu(VI) – Pu(IV)	Pu(VI) – Pu(III)
0.40	927	993	972
0.30	935	973	961
0.20	939	949	946
0.10	952	925	934

In our opinion, the value which was earlier reported by Hindman for the formal potential of the Pu(VI) – Pu(IV) pair in 1 N HNO_3 (1110 mv) is too large, since it does not agree with the data on perchloric acid (1043 mv) and on hydrochloric acid (1053 mv) [4], or even with the data on complex formation in Pu (IV) in nitric acid.

The value which we obtained for the formal potential of the Pu (IV) – Pu (III) pair in 1 N HNO_3 (914 mv) is in good agreement with that of Hindman (916 mv).

In the disproportioning of Pu (IV) in 0.10 N HNO_3, it was observed that, at equilibrium, the sum of the concentrations of Pu (IV), Pu (III) and Pu (VI) was less than the original concentration of Pu (IV). The difference between the starting concentration of the plutonium and the sum of the concentrations of Pu (IV), Pu (III) and Pu (VI) was considered as representing the concentration of pentavalent Pu and a formal potential was calculated for the Pu (VI) – Pu (V) pair in 0.10 N HNO_3 The resulting 917 mv is in agreement with a value of 920 mv which we obtained later through direct measurement. There is no other data in the literature on the direct measurement of the potential of the Pu (VI) – Pu (V) pair in nitric acid. This agreement of the potential values supports our supposition as to the presence of pentavalent plutonium in solution.

Starting from the above, it is possible to propose the following scheme for the formal potentials of plutonium in nitric acid solutions:

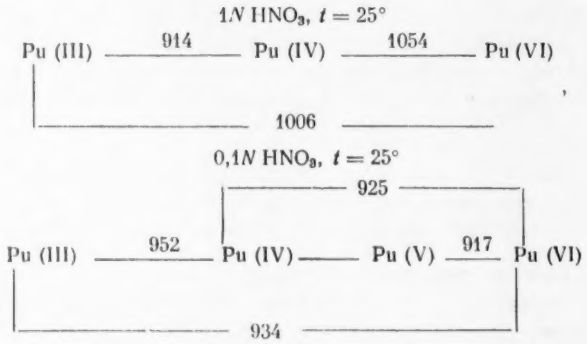

As has been said earlier, the disproportionation of Pu (IV) in nitric acid was also studied for the determination of the potentials. The alternation with time of the concentration of Pu (III), Pu (IV) and Pu (VI) in a 0.40 N HNO_3 solution is shown in Fig. 1.

These data confirm the fact that the disproportionation of Pu (IV) proceeded according to the following over-all equation which has been proposed by Kasha and Sheline [12, 13] for hydrochloric and perchloric acids

$$3\text{Pu (IV)} \rightleftarrows 2\text{Pu (III)} + \text{Pu (VI)}, \qquad (3)$$

and which can be written in the ionic form as:

$$3Pu^{4+} + 2H_2O \rightleftarrows 2Pu^{3+} + PuO_2^{2+} + 4H^+. \qquad (4)$$

It should be noted, however, that the equilibrium constant for Reaction (3) in nitric acid is inversely proportional to the 5.3 power of the hydrogen ion concentration, whereas the anticipated relation would be $K \sim (H^+)^{-4}$. It can be easily shown that this deviation is entirely accounted for by the formation of nitrate complexes of Pu (IV).

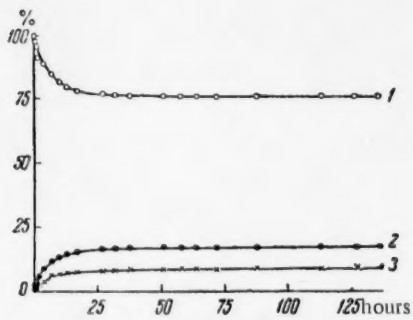

Fig. 1. The disproportionation of Pu (IV) in 0.40 N HNO_3. Total concentration of plutonium, $7.7 \cdot 10^{-3}$ M: 1) Pu (IV); 2) Pu (III); 3) Pu (VI).

In papers which have been published earlier [12, 13], it has been shown that the disproportionation of Pu (IV) in hydrochloric and in perchloric acids proceeds in two steps, following the equations:

$$\text{Pu (IV)} + \text{Pu (IV)} \underset{k_2}{\overset{k_1}{\rightleftarrows}} \text{Pu (V)} + \text{Pu (III)} \qquad (5)$$

$$\text{Pu (V)} + \text{Pu (IV)} \rightleftarrows \text{Pu (III)} + \text{Pu (VI)} \qquad (6)$$

The problem of the mechanism of the disproportionation of Pu (IV) in nitric acid has not been dealt with in the literature. We have carried out calculations for the velocity constant of the direct disproportionation reaction, by making use of the equation

$$-\frac{d\,[\text{Pu (IV)}]}{dt} = k_1\,[\text{Pu (VI)}]^2 - \frac{k_1}{K}\,\frac{[\text{Pu (III)}]^2\,[\text{Pu (VI)}]}{[\text{Pu (IV)}]}, \qquad (7)$$

This latter was derived from the Equations (5) and (6) by supposing that Reaction (6), which involves a single electron transfer, rapidly attains equilibrium and that reaction (5) is limiting. The calculated velocity constants for this reaction prove to be identical for the various stages of the process, and it is thus possible to affirm that the disproportionation of Pu (IV) proceeds in nitric acid according to Equations (5) and (6).

TABLE 3

Equilibrium Constants for the Disproportionation of Pu (IV) in Nitric Acid Solutions

Concentration of HNO_3, N	Total plutonium concentration, $M \cdot 10^3$	Equilibrium constant, K
0.40	7.7	$5.66 \cdot 10^{-3}$
0.30	7.6	$5.01 \cdot 10^{-2}$
0.20	3.04	$4.55 \cdot 10^{-1}$
0.10	2.25	7.91

Despite complex formation in the Pu (IV), however, the values which we have obtained for the velocity constant of its disproportionation are the same in nitric as in perchloric acid. This permits the supposition that not only the Pu^{4+} ions but also the complex ions of Pu (IV) participate in the reaction, the latter ions possessing the higher reactivity.

LITERATURE CITED

[1] B. G. Garvei, G. G. Gill, A. G. Meddok and E. L. Pauli, Sympos. The Chemistry of Isotopes (in Russian), 2, 9 (1948).

[2] J. J. Howland, J. C. Hindman and K. A. Kraus, The Transuranium Elements, 1949, p. 133.

[3] R. E. Connick and W. H. McVey, J. Am. Chem. Soc. 73, 1798 (1951).

[4] R. E. Connick and W. H. McVey, J. Am. Chem. Soc. 75, 474 (1953).

[5] K. A. Kraus and G. E. Moore, The Transuranium Elements, 1949, p. 550.

[6] S. W. Rabideau, J. Am. Chem. Soc. 78, 2705 (1956).

[7] K. A. Kraus, The Transuranium Elements, 1949, p. 241.

[8] E. F. Orleman and B. B. Brody, The Transuranium Elements, 1949, p. 118.

[9] G. T. Seaborg and J. Katz, The Actinides (in Russian) 1956, p. 231.*

[10] Papers on Radiation Chemistry (in Russian) 1955, p. 71.

[11] G. T. Seaborg and J. Katz, The Actinides (in Russian) 1956, p. 198.*

[12] M. Kasha, The Transuranium Elements, 1949, p. 295.

[13] M. Kasha and G. E. Sheline, The Transuranium Elements, 1949, p. 180.

[14] J. C. Hindman, The Transuranium Elements, 1949, p. 388.

[15] S. W. Rabideau, J. Am. Chem. Soc. 73, 2895 (1951).

The Institute of Physical Chemistry of the
Academy of Sciences of the USSR

Received December 24, 1957

*Russian translation.

THE PROBLEM OF THE MECHANISM OF ELECTROLYTIC POLISHING AND THE STRUCTURE OF THE ELECTROPOLISHED SURFACE

G. S. Vozdvizhenskii, G. A. Gorbachuk and G. P. Dezider'ev

(Presented by Academician A. N. Frumkin, January 2, 1958)

In recent years there has been persistantly advanced a hypothesis to the effect that the electrolytic polishing of metals proceeds in two steps of different mechanisms [1]. At relatively low polarization in a first, preliminary stage, there occurs a structural attack of the specimen surface and a preferential dissolving of its more elevated portions with the formation of clearly expressed etch figures. At high polarization in a second, decisive stage there begins a supression of the structural attack and the gradual production of a smooth surface which is free of any trace of structure.

In elucidating the mechanism of the first stage, it has been presumed that the crystallographic orientation of the metallic grains is a vital factor in fixing the dissolution process; whereas various other factors, having, naturally, no connection with the crystallographic orientation, are advanced for explaining the second stage mechanism. It is considered that the theory just outlined finds its direct experimental confirmation in the study of the structure and properties of the electropolished surface.

Thus, the question of the mechanism of electropolishing is directly related to the problem of structure in the electropolished surface. The presence of a structure must point to one mechanism and its absence to another.

Our electronmicroscopic studies of the electropolished surface [2] have shown that a theory presuming electropolishing to be accomplished in two different stages of different mechanisms is far from being unobjectionable, this being particularly true of the presumption of the suppression of the structural attack in the second stage.

Some of the results of these investigations are published in the present communication.

EXPERIMENTAL

Electropolished specimens of a polycrystalline copper (M-1) were studied. Electropolishing was carried out in a 5 M phosphoric acid solution with a potential of 1.2 v on the terminals, a current density of 12.5 amp/dm^2 and a bath temperature of 20°.

Collodion replicas were taken from specimens which were subjected to polishing over various periods of time (10, 25 and 180 sec) and these, after shading with chromium, were studied in the electron microscope at a magnification of 11500×. The photographs which are presented below were made in combination with optical magnification (up to 2300 ×).

The microphotographs of Figs. 1 and 2 show that during the primary stage of electropolishing (10 sec) there occurs an active structural attack whose magnitude depends on the degree of electrochemical inhomogeneity in the surface. Over some regions (Fig. 1), this structural attack appears in the form of coarse, deep, etch figures such as are associated with a relatively pronounced electrochemical nonuniformity. On other sections (Fig. 2), these figures are considerably finer and more shallow because of a less pronounced electrochemical nonuniformity. On both microphotographs, it is clearly to be seen that additional, much finer etch figures cover the surfaces of the coarser figures. These are obviously related to the presence of dislocation and deformations in the crystal bodies.

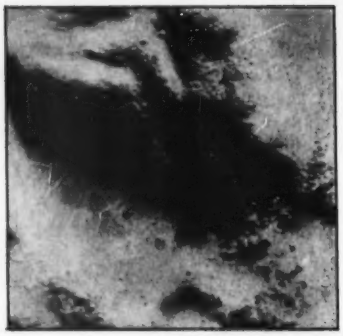

Fig. 1.

Fig. 2

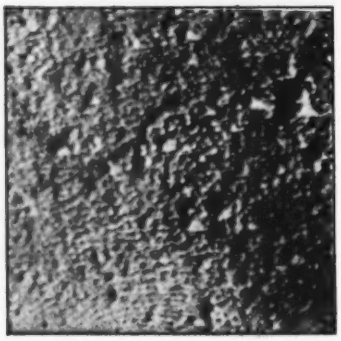

Fig. 3

Fig. 4

Thus, even in the initial stages of electropolishing, there is shown a pronounced variation in the degree of attack, this being related to the variability of the electrochemical nonuniformity in the initial surface.

Increasing the duration of electropolishing to 25 seconds (Fig. 3) leads to a further change in the degree of structural attack. Of the coarse etch figures there already remain only traces in the form of relatively dark patches, whereas the fine etch figures have experienced a certain development.

A further extension of the duration of the electropolishing to 180 seconds, i.e., passage into what is customarily considered to be the decisive stage of the process, leads to no essential qualitative change in the picture of the structural attack. The very finest of the etch figures, which arose even in the first stage, now undergo further development and give a clear cut structure to the electropolished surface (Fig. 4).

Over the entire course of the electropolishing, the microphotographs which have been presented fail to show any suppression of structural attack. There occurs only a regular alteration in the degree of attack such as results from changes in the degree of electrochemical nonuniformity of the surface. Actually, if suppression of the structural attack should occur it would so act as to eliminate first of all the finest of the etch figures, these being the ones most easily removed. The microphotographs, on the other hand, indicate a gradual development of these fine figures.

The results which have been presented give one more clear cut illustration of the theories of the structure of the electropolished surface which we have developed [3] and agree in their content with the data of other investigators [4].

LITERATURE CITED

[1] T. P. Hoar, and I. A. S. Mowat, Nature, 165, 64 (1950); K. Huber, Zs. Elektrochem. 55, 165 (1951); A. Politicki and H. Fischer, Zs. Elektrochem. 56, 326 (1952); S. I. Krichmar and V. P. Golushko, J. Phys. Chem; 30, 577 (1956); S. I. Krichmar, Outlines of the Reports at a Conference on the Mechanism of the Electrolytic Polishing of Metals (in Russian) Kazan, 1957, p. 8.

[2] S. I. Berezina, G. A. Gorbachuk and G. P. Dezider'ev, Proc. Conference on the Mechanism of the Electrolytic Polishing of Metals (in Russian) Kazan, 1957.

[3] G. S. Vozdvizhenskii, G. P. Desider'ev and V. A. Dmitriev, Proc. Acad. Sci. USSR 65, 697 (1949); J. Phys. Chem. 25, 547 (1951); G. S. Vozdvizhenskii, Outlines of the Reports at a Conference on the Mechanism of the Electrolytic Polishing of Metals (in Russian) Kazan, 1957, p. 4; G. S. Vozdvizhenskii, N. I. Berezina, G. A. Ivanova and R. N. Khavizov, ditto, p. 30.

[4] K. Huber, Helv. chim. Acta, 26, 1037 (1946); H. Reather, Optik, 1, 69 (1946); Quoted from Sympos. on Catalysis, The Investigation of Heterogeneous Processes (in Russian) Foreign Lit. Press, 1956, pp. 82-83;* H. Fischer and L. Koch, Metall. 17/18, 481 (1952); P. Bussy and G. Chaudron, Compt. rend. 236, 2323 (1953); P. Bussy, Compt. rend, 238, 247 (1954); P. Jacquet, Compt. rend. 242, 1990 (1956).

The Chemical Institute of the Kazan Affiliate
of the Academy of Sciences of the USSR

Received November 18, 1957

*Russian translation.

REVERSIBLE ISOTHERMS FOR THE ADSORPTION OF WATER ON QUARTZ

S. P. Zhdanov

(Presented by Academician M. M. Dubinin, December 30, 1957)

The adsorption of water vapors on quartz has been investigated in [1-3]. The adsorption isotherms for water which were obtained in these studies are represented in Fig. 1. Despite the fact that the adsorption was referred in every case to unit surface of quartz, the isotherms of Fig. 1 do not concide, but deviate markedly from one another even at the very lowest values of p/p_s. The results of these investigations have not been compared nor have they been subjected to discussion, but the observed incompatibility of the "absolute" adsorption isotherms for water on quartz is of fundamental interest, especially since it has been shown for various silica gels [4] that such adsorption isotherms coincide at low relative pressures when the adsorption is referred to unit surface. The present paper contains the results of an investigation of water vapor adsorption on four specimens of powdered quartz which differed in their origin and in their specific surface areas. Three of these specimens were prepared by grinding rock salt crystals from various localities, the powders being subsequently treated with HCl and a carefully freed of traces of Cl^- by washing with water. A fourth, more finely dispersed, powder was prepared in a similar fashion from crystals of milky quartz, but was elutriated with water for long time with a view to separating out the finest fraction.

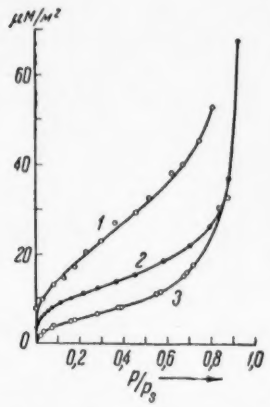

Fig. 1. A comparison of the adsorption isotherms of water on quartz, as described in the literature. 1) Livingston [1], 2) Sarakhov [2], 3) Stober, desorption [3].

Following the BET method, the specific surfaces were evaluated from the adsorption isotherms of nitrogen, argon and methyl alcohol. The following values were accepted for the areas (ω) occupied by the adsorbed molecules in the monolayer: $\omega_{N_2} = 16.2\,A^2$, $\omega_{Ar} = 15.4\,A^2$ and $\omega_{CH_3OH} = 25\,A^2$.

The calculated values of the specific areas of the investigated quartz powders are presented in Table 1.

Water vapor adsorption isotherms obtained from studying these quartz specimens by the volumetric method are shown in Fig. 2A. With the exception of 5, all of these isotherms are reversible. This is directly obvious for two of them and the reversibility of the remaining two follows from a comparison of the isotherm obtained after heating the specimen to 200° with a second isotherm obtained without prior heating. These facts indicate that neither heating nor a preliminary adsorption lead to a change in the properties of the surface or its total area. On heating the powders of milky quartz to 200° in vacuum there resulted a sharp increase in the adsorption and the isotherm became irreversible (Curve 5). The isotherms which are presented in Fig. 2A, just as those of Fig. 1, have the form of a series of curves branching out from the origin of coordinates, even though the adsorption was here referred to unit surface area of the quartz. It would, at first sight, seem possible to interpret these results as indicating a variation in the unit surface properties of the various quartz specimens. The isotherms of Figs. 1 and 2A give a straight lines in the coordinates $\frac{p/p_s}{\alpha\,(1 - p/p_s)}$, p/p_s and from them there can be calculated the area occupied by the water molecule in the adsorbed monolayer (ω_{H_2O}). The values of this quantity vary between 10.6 and 30 A^2. From this it follows that the various specimens of quartz differ in regard to the packing density of the water

molecules in that first adsorption layer which is directly bound to the surface. There are certain papers [5-9] in which values of ω_{H_2O} ranging from 10.8 to 55 A^2 have been obtained from adsorption isotherms of water on silica gels, aluminosilicates and porous glasses, acceptance of these values making it possible to bring the surface areas calculated from water and from nitrogen into concordance.

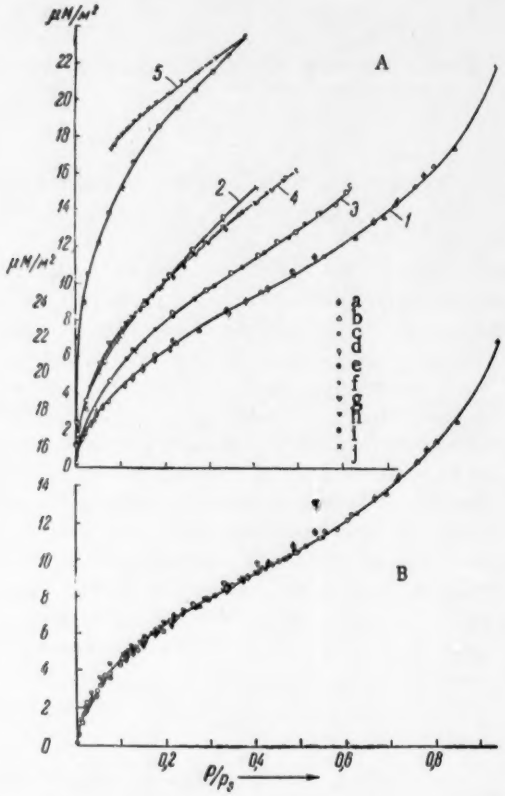

Fig. 2. A) Adsorption isotherms for water on various specimens of quartz, referred to unit surface; B) absolute isotherm for the adsorption of water on quartz. 1) Rock salt I: a) primary adsorption on a specimen which had been heated to 200° in vacuum; b) repetition of adsorption, without heating. 2) Rock salt II: c) primary adsorption on a specimen which had been heated to 200° in vacuum; d) repetition of adsorption, without heating. 3) Rock crystal III, degassed without heating: e) adsorption; f) desorption. 4) Milky quartz, degassed without heating: g) adsorption; h) desorption. 5) The same specimen but degassed at 200°: i) adsorption; j) desorption.

Because of the clearly expressed sensitivity of the adsorption of water to the surface state of siliceous adsorbents [10-15, 4], the above noted lack of agreement among the calculated values of might be related to differences in the nature of the investigated adsorbents and to the variation in their surface states. The isotherms 1, 2, 3, 4, and 5 of Fig. 2A were, however, obtained with a single crystalline substance, namely, low temperature quartz, and under uniform and comparable conditions of degassing. The reversibility of the first four of these isotherms indicates that in each case the adsorption of water proceeded on a SiO_2 surface which was in a state of maximal hydration. At low values of the ratio p/p_s, the adsorption of water on a siliceous surface has been shown [10-15] to proceed, in the first instance, on the surface hydroxyls and the magnitude of this adsorption is related to the degree of surface hydration. At maximum hydration, the number of hydroxyls on the surface must be the same for all specimens, since it is determined by the crystallographic structure of the quartz [11]. Thus, it is quite unlikely that the divergence of the isotherms of Fig. 2A could be due to

a lack of uniformity in the properties of the unit surfaces of the various quartz specimens or to differing densities of packing of the water molecules in the first adsorbed layer. A more probable cause for this divergence is the fact that a portion of that surface which is available to the small water molecules is unavailable for the larger nitrogens. Such an effect is well known from the case of the ultraporous crystalline aluminosilicates or zeolites [16]. In the instance of quartz, this effect could result from the presence of submicroscopic fissures in the crystals. It is clear that such fissures are present in all of the specimens of quartz which were investigated in the present work with the exception of rock salt I. They must have been particularly numerous in the crystals of the milky quartz. Confirmation of this fact is found in the evolution of large amounts of water when powders of this quartz were heated in vacuum over the temperature interval 100-200° and also by the anomalously large amount of structural water which was evolved from unit surface of the quartz on calcining it in the interval 200-1000° (about 25μ M/m^2), the surface being determined from nitrogen. This last effect has also been observed by Stober [3] in certain quartz specimens which he investigated, although he did not relate it to the presence of fissures in the crystal but rather ascribed it to the influence of siliceous contaminants. It is well known that the lack of transparency which is observed in certain specimens of quartz is considered by the mineralogists to result from strongly developed fissuring [17].

In determining the absolute adsorption isotherms of water, it is clear that an evaluation of the surface with nitrogen, or with other substances whose molecules are larger than those of water, will be acceptable only if the surface is in equal degree available for the water and for those molecules which are used for the surface determination. From the position of isotherm 1 in Fig. 2A, it can be concluded that rock salt I fulfills this condition better than any other of the investigated specimens.

The value of ω_{H_2O} which was calculated from isotherm 1 of Fig. 2A proves to be equal to 26 A^2. This is very close to the value of 25 A^2 which was found in [4] silica gels. It agrees with a value of 13.4 A^2 which was reported in [11] for the individual hydroxyl on a hydrated surface of low temperature α-quartz, if the assumption is made that it is the hydroxyl pair, rather than the individual hydroxyl, which is the initial adsorption center for the water molecules. This mechanism for the water adsorption follows from the observed concordance between the decrease in the number of hydroxyl pairs resulting from dehydration of a porous glass surface and the decreased adsorption of water in the region of build-up of the monolayer [13, 14]. The authors of [4] were led to a similar mechanism for the adsorption of water molecules on hydrated silica gel surfaces.

To within the limits of experimental error, all of the reversible isotherms of Fig. 2A lie on a common curve (Fig. 2B) when the specific surfaces of the investigated quartz specimens are determined from the adsorption isotherms of water and the value ω_{H_2O} = 26 A^2, and the absolute isotherms developed from the resulting figures.

A comparison of the isotherms of Fig. 2B with the absolute isotherms for the adsorption of water on silica gels [4] and on porous glasses [14] shows that in all cases where the adsorption occurs on a maximally hydrated surface, the absolute isotherms can be represented by a single curve in the region $\theta \leq 1$. The reversibility of the isotherms in the monomolecular region is one indication of this condition.

The incompatibility which has been observed by other authors in the absolute adsorption isotherms of water on quartz [1-3], silica gels [5, 9] and porous glasses [18] in the region of low p/p_s values, and the associated variation in the values obtained for ω_{H_2O}, are related to two factors which were not taken into account in earlier work: 1) the possibility of ultraporosity in the investigated materials which, in certain cases, appears even in the nitrogen adsorption; and 2) the clearly expressed sensitivity of the water adsorption to the condition of the siliceous adsorbent surface and the degree of its hydration.

In the case of a pronounced ultraporosity, evaluation of the surface area from the nitrogen adsorption isotherms leads to values which are too low. This can be the cause of the excessively high values which have been obtained for the adsorption of water per unit surface and for the correspondingly low values of ω_{H_2O} [1, 2, 5-8, 18]. One indication of the existence of such ultraporosity is the evolution during heating to 200° of a considerable quantity of water which is adsorbed in the finer pores and fissures; this leads to a marked irreversibility in the adsorption isotherms (Isotherm 5, Fig. 2A). Water can, however, be adsorbed completely reversibly on a part of the pores of a surface which shows ultraporosity with respect to nitrogen (Isotherms 3 and 4, Fig. 2A).

TABLE 1

Specimen and conditions of degassing	S, m^2/g			Accepted value
	N_2	Ar	CH_3OH	
Rock crystal I, 200°	–	0.195	0.195	0.195
Rock crystal II, 200°	–	0.290	–	0.290
Rock crystal III, 20°	0.57	–	–	0.57
200°	0.56	–	–	
Milky quartz 20°	5.15	–	4.85	5.15
200°	5.4	–	–	5.4

The excessively high values of ω_{H_2O} which were obtained in [5-9] result from the fact that in these works the adsorption of water was studied on silica gels which had been dehydrated to a considerable degree. In view of the above noted details of the mechanism of the water adsorption, the formation of a densely adsorbed monomolecular layer cannot occur on a dehydrated SiO_2 surface in the region of moderate values of p/p_s and the evaluation of ω_{H_2O} is therefore without real significance in such cases.

Thus, the properties of unit surfaces of various specimens of quartz and, to a certain degree, of other siliceous adsorbents as well, can be identical with respect to the adsorption of water only if adsorption occurs at maximum hydration. When irreversible adsorption occurs, the properties of the unit surfaces are not identical. Consistency in the conditions of heating prior to an adsorption experiment does not adequately guarantee the production of SiO_2 surfaces with uniform adsorptional properties in regard to water.

With a nonporous material such as quartz is considered to be, the existence of those extremely fine fissures which reveal themselves in the water adsorption despite their impenetrability for nitrogen requires that a certain caution be exercised regarding values of surface areas which have been measured in other cases by the use of nitrogen, especially when the data obtained from water and from nitrogen is employed for the calculation of the area occupied by the water molecule in an adsorbed monomolecular film [1, 19].

The author expresses his thanks to M. M. Dubinin and to A. V. Kiselev for their interest in this work and to E. B. Koromal'd for participating in the measurements.

LITERATURE CITED

[1] H. K. Livingston, J. Am. Chem. Soc. 66, 569 (1944).

[2] A. N. Sarakhov, Bull. Acad. Sci. USSR, Div. Chem. Sci. 1956, 150.*

[3] W. Stöber, Koll. Zs. 145, 1, 17 (1956).

[4] L. D. Beliakova, O. M. Dzhigit and A. V. Kiseleva, J. Phys. Chem. 37, 1577 (1957).

[5] K. S. W. Sing and J. D. Madeley, J. Appl. Chem. 4, 365 (1954).

[6] J. P. Quirk, Soil Sci. 80, 423 (1955).

[7] P. H. Emmett and M. Cines, J. Phys. Coll. Chem. 51, 1248 (1947).

[8] B. L. Harris and P. H. Emmett, J. Phys. Coll. Chem. 53, 811 (1949).

[9] M. M. Egorov, T. S. Egorova, V. F. Kiselev and K. G. Krasil'nikov, Proc. Acad. Sci. USSR 114, 579 (1957).*

[10] S. P. Zhdanov, Proc. Acad. Sci. USSR 68, 99 (1949).

[11] S. P. Zhdanov and A. V. Kiselev, J. Phys. Chem. 31, 2213 (1957).

[12] S. P. Zhdanov, Proc. Acad. Sci. USSR 100, 1115 (1955).

[13] S. P. Zhdanov, Sympos., The Surface Chemical Compounds and Their Role in Adsorption Phenomena (in Russian) Moscow, 1957, p. 129.

*Original Russian pagination. See C. B. Translation.

[14] S. P. Zhdanov, J. Phys. Chem. 32, vol. 3 (1958).

[15] A. V. Kiselev, Sympos., The Surface Chemical Compounds and Their Role in Adsorption Phenomena (in Russian) Moscow, 1957, p . 90, 199.

[16] S. Brunaeur, The Adsorption of Gases and Vapors (in Russian) 1948.*

[17] A. G. Betekhin, Minerology (in Russian) 1950.

[18] D. P. Dobychin, Sympos., The Surface Chemical Compounds and Their Role in Adsorption Phenomena (in Russian) Moscow, 1957, p. 166.

[19] W. Harkins and G. Jura, J. Am. Chem. Soc. 66, 1362 (1944).

The Institute of Silicate Chemistry of the Academy of Sciences of the USSR

Received December 30, 1957

*Russian translation.

THE ROLE OF THE NONSTATIONARY PROCESS IN THE STIMULATION OF DEGENERATIVE BRANCHING CHAIN REACTIONS IN THE LIQUID PHASE

D. G. Knorre, V. L. Pikaeva and N. M. Emanuel'

(Presented by Academician V. N. Kondrat'ev, December 25, 1957)

In a series of papers, it has recently been shown by one of us that the oxidation of liquid hydrocarbons [1-5] and combustible gaseous hydrocarbons [6] can be considerably accelerated if some initiator of oxidation (the gaseous catalysts HBr [1] NO_2 [2, 3]; incident radiation; inert radioactive gases [5]) acts, even briefly, on the process while the reaction is still in the induction period. Further action of the initiator proves to be unnecessary, or even detrimental, to the development of the process because of the undesirable secondary reactions which arise. In these same papers the observed phenomena were interpreted from the point of view of the theory of degenerative branching chain reactions which has been advanced by N. N. Semenov [7].

In a hydrocarbon oxidation which proceeds according to a degenerative chain branching mechanism, the formation of active centers takes place along two paths:

1) from the original materials, the hydrocarbon RH and oxygen O_2, by the reaction

$$RH + O_2 \rightarrow R^{\cdot} + HO_2^{\cdot} \qquad (1)$$

which proceeds at a low, constant, velocity, w_0 (chain iniation);

2) as the result of decomposition, or of some other transformation, in an intermediate product P (in the instance of liquid phase oxidation, this is usually by breakdown of the peroxide ROOH), the reaction proceeding with a velocity $k_p[P]$, (degenerative branching).

When $w_0 + k_p[P]$ is small, the rate of oxidation is low, and the reaction is in its induction period. The reaction is accelerated and its time of induction is diminished if application is made of some initiator which will give a higher initiation rate, w_i. The initiator will accelerate the reaction only if $w_i > w_0 + k_p[P]$. When the concentration of the hydroperoxide reaches such a value that $k_p[P] \gg w_i$, the initiator ceases to influence the rate of oxidation, i.e., it ceases to have a positive effect on the system.

In the case of a linear chain rupture, a mathematical consideration of the kinetics of degenerative branching chain reactions and their dependence on the intensity and the duration of initiation shows that an increase in w_0 definitely shortens the induction period [3, 4, 6]. In liquid phase oxidation, however, a second power process of chain rupture predominates. A corresponding kinetic analysis has been carried out in the work of E. T. Denisov and one of the present authors [8]. In the calculations of this latter paper, the concentration of the active centers was assumed to be quasi-stationary. Such an approximation is only valid, however, when the rate of initiation is sufficiently high. In actuality, in the case of a second power breakdown, the equation for the build-up of the active centers has the form $dn/dt = w_i - k_g n^2$, and, for fixed w_i, this leads to the relation $n = \sqrt{w_i/k_g}\,\mathrm{th}\,\sqrt{k_g w_i}\,t$. The time required for the establishment of a stationary concentration is thus of the order of $1/\sqrt{k_g w_i}$. For small values of w_i, this time can prove to be long. In particular, the supposition of a stationary condition leads to the conclusion that the reaction proceeds without an appreciable induction period this is in many instances in contradiction with the experimental data.

In the present work calculations have been carried out on the kinetics of chain reactions with degenerative branching and second power rupture, account being taken of the fact that the process is not stationary in the initial period of the reaction. Here the fundamental question is that of the influence of the rate and duration of initiation on the initial stage of the reaction and, in particular, on the magnitude of the induction period. For this reason, the calculations were carried out without taking the consumption of the intermediate product into account, this being a factor which begins to influence appreciably the reaction kinetics only in the more advanced phases of the transformation. It is further assumed that rupture occurs through recombination of the RO_2 radicals, which is, as a rule, true at oxygen pressures close to one atmosphere. With such suppositions, the system of equations describing the kinetics of build-up of the intermediate product takes the form

$$\frac{d[RO_2]}{dt} = w_0 + k_P[ROOH] - k_g[RO'_2]^2,$$
$$\frac{d[P]}{dt} = k[RO_2][RH]. \qquad (2)$$

Here, k_g and k are, respectively, the rate constants for the recombination of the RO'_2 radicals and for the chain propagation

$$RO'_2 + RH \rightarrow ROOH + R'.$$

We will now introduce the dimensionless variables ξ, η and τ, and the dimensionless parameter ω_0

$$[RO_2] = \frac{\sqrt{kk_P[RH]}}{k_g}\xi;\ [ROOH] = \frac{k[RH]}{k_g}\eta;$$
$$t = \frac{\tau}{\sqrt{kk_P[RH]}};\quad \omega_0 = \frac{k_g w_0}{kk_P[RH]}.$$

Written in these dimensionless variables, the differential Equations (2) take the form

$$\frac{d\xi}{d\tau} = \omega_0 + \eta - \xi^2,\ \frac{d\eta}{d\tau} = \xi. \qquad (3)$$

Under the initial conditions $\eta = 0$, $\xi = 0$ and at $\tau = 0$, integration of the System (3) leads to

$$\tau = \int_0^{\eta} \frac{dx}{\sqrt{x - \left(\frac{1}{2} - \omega_0\right)(1 - e^{-2x})}}.$$

Since we have neglected the consumption of the hydroperoxide, this relationship can be considered as acceptable only for small degrees of transformation of the order of 1%.

Designating the percentage transformation by p, we obtain for η

$$\eta = \frac{p}{100} \cdot \frac{k_g}{k}.$$

In view of the fact that all of the experiments on initiation in the initial stage of reaction have been carried out with paraffin hydrocarbons, the present calculations were set up for the case of the typical branched paraffin isodecane. In the absence of quantitative data on the energy of the tertiary C–H bond in isodecane and the rate of decomposition of isodecyl hydroperoxide, use is made of the corresponding data on isobutane and tertiary butyl hydroperoxide [9]:

$$k_P = 10^{15} e^{-39000/RT}.$$

The heat change accompanying Reaction (1) is equal to − 42 kcal (taking the energy of rupture of the C–H bond to be 89 kcal [10] and the energy of the H–O_2 bond to be 47 kcal [11]) and, since such process can scarcely have a pronounced activation barrier (a strongly endothermic process with a linear activated complex), it follows that

$$w_0 = f \cdot 10^{-10} e^{-42000/RT}[RH][O_2].$$

With [RH] = 10^{21} and [O_2] = 10^{18}, this gives at 127°C, i.e., at 400°K,

$$\omega_0 \approx \frac{k_g}{k} f \cdot 10^{-9}.$$

The full curves of Fig. 1 show the kinetics of the build-up of the hydroperoxide as calculated for the cases $k_g/k = 10^3$ (a) and 10^5 (b). In this same figure there are shown dotted curves which have been developed by assuming a quasi-stationary condition. It is clear that this leads in both cases to a sharp increase in the value of η, the induction period disappearing.

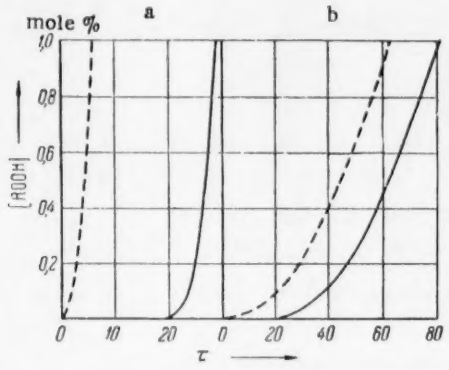

Fig. 1. Calculated kinetic curves for the build-up of hydroperoxide as obtained by an exact solution of the System (3) (full curves) and by assuming a quasi-stationary condition (dotted curves), etc.. a) $k_g/k = 10^3$, $\omega_0 = 10^{-10}$; b) $k_g/k = 10^5$, $\omega_0 = 10^{-8}$.

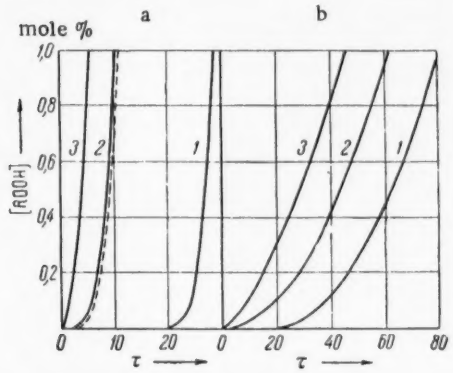

Fig. 2. Calculated kinetic curves for the build-up of hydroperoxide. a) $k_g/k = 10^3$, $\omega_0 = 10^{-10}$ (1) (uninitiated oxidation), $\omega_i = 10^{-2}$ (2) and $\omega_i = 1$ (3); b) $k_g/k = 10^5$, $\omega_0 = 10^{-8}$ (1), $\omega_i = 1$ (2) and $\omega_i = 100$ (3). In dotted form there is shown the curve for initiation with $\tau = 1.2$. The time of breaking off initiation is indicated with an arrow.

In Fig. 2 there are given kinetic curves for the build-up of the hydroperoxide under these same values of the parameter k_g/k and for various values of w_0. In determining w_0 for the uninitiated reaction, it was assumed that $f = 10^{-4}$, since it is known that the stearic factor in liquid phase hydrocarbon reactions is much less than unity. For the initiated process, the values of w_0 were taken as 10^{10} and 10^{12} moles/cm^3·sec, this corresponding approximately to the experimental conditions for the paraffin oxidation initiated by the γ-radiation from a cobalt source [4], and the isodecane oxidation [5] initiated by radon. It is clear that increasing w_0 (ω_0) leads to a shortening of the induction period or to its complete disappearance at a sufficiently high value of ω_0.

From Fig. 3 it is to be seen that those calculations which presume a quasi-stationary process give a completely false idea as to the influence of the initiator on the kinetics of oxidation.

The curves for the initiated oxidation which are presented in Fig. 2 have been developed by supposing direct initiation over the entire course of the process. Calculations have also been carried out for the case of initiation over the period $\tau = 1.2$, use being made of the parameter values $k_g/k = 10^3$ and $\omega_0 = 10^{-2}$. The resulting kinetic curves are practically identical with the curve obtained for continuous initiation at the same intensity. The kinetic curves which have been obtained by calculation are of the same type as those which have been developed experimentally. Thus the curves of Fig. 2A are similar to the kinetic curves obtained by initiating the oxidation of paraffin in its initial period with nitric oxide or the γ-radiation of Co^{60} [4]. The curves of Fig. 2B are of approximately the same type as the kinetic curves for the radon initiated oxidation of isodecane [5]. It is of essential significance that these curves were obtained with different values of the parameters ω_0 and ω_i.

The absence of information concerning the initiating action of NO_2 does not permit the evaluation of ω_0 in this case, and for gaseous initiation it is possible to speak only of a qualitative agreement between the calculated and the experimental curves.

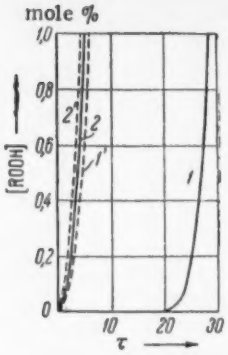

Fig. 3. Calculated kinetic curves for the build-up of the hydroperoxide in the case that $k_g/k = 10^3$, without initiation (Curves 1, 1') and with initiation at $\omega_i = 1$ (Curves 2, 2') as obtained by exact solution of the System 3 (full curves) and by the application of a quasi-stationary condition (dotted curves).

Thus an exact solution of the system of differential equations describing the kinetics of the build-up of the intermediate product in an oxidation reaction with second power chain rupture permits an elucidation of the experimentally observed induction period and an understanding of the effect of the initial stimulation of these processes.

LITERATURE CITED

[1] N. M. Emanuel', Proc. Acad. Sci. USSR, 102, No. 3, 559 (1955).

[2] E. A. Blumberg and N. M. Emanuel', Bull. Acad. Sci. USSR, Div. Chem. Sci. 1957, 274.*

[3] N. M. Emanuel', J. Phys. Chem. 30, vol. 4, 847 (1956).

[4] N. M. Emanuel', Proc. Acad. Sci. USSR 11, No. 6, 1286 (1956).*

[5] N. M. Emanuel', E. A. Blumberg, D. M. Ziv and V. L. Pikaeva, Proc. Acad. Sci. USSR 119, No. 6 (1958).

[6] N. M. Emanuel', Proc. Acad. Sci. USSR 110, No. 2, 245 (1956).*

[7] N. N. Semenov, Chain Reactions (in Russian) 1934.

[8] E. T. Denisov and N. M. Emanuel', J. Phys. Chem. 31. vol. 6, 1266 (1957).

[9] E. R. Bell and H. Raley, et al., Disc. Farad. Soc. No. 10, 242 (1951).

[10] T. Cottrell, The Strength of Chemical Bonds (in Russian), Foreign Lit. Press, 1956, p. 254.**

[11] S. N. Foner and R. L. Hudson, J. Chem. Phys. 23, 1364 (1955).

Received December 22, 1957

*Original Russian pagination. See C. B. Translation.

**Russian translation.

THE THERMODYNAMICS OF CsCl-RbCl SOLID SOLUTIONS AT 25°

L. L. Makarov and Iu. G. Vlasov

(Presented by Academician A. N. Terenin, December 27, 1957)

X-ray investigations [1] and crystallographic characteristics (lattice types, ionic dimensions) permit one to anticipate that the miscibility of CsCl and RbCl would be limited at low temperatures. To study the thermodynamic properties of CsCl-RbCl solid solutions and fix the limits of their existence, the system CsCl-RbCl-H_2O was investigated at 25°. The experimental data and the results of thermodynamic calculations carried out in conformity with the relations of A. V. Storonkin and M. M. Shul'ts [2] are presented in Table 1, $\underline{m}$ representing the concentration in moles per 100 g of water; $\underline{x}$, the mole fraction; P_{H_2O}, the pressure of water vapor above the solution, in mm of Hg; $\underline{f}$, the rational activity coefficient in the solid phase, $\lim_{x \to 1} f \to 1$; $\gamma_{\pm}$, the mean ionic activity coefficient in an aqueous solution at the indicated concentrations m_{CsCl} and m_{RbCl}; and $D_{2,1}$, the crystallization coefficient as determined from the relation $D_{2,1} = \frac{x_2}{1 - x_2} \cdot \frac{m_1}{m_2}$ where the indices 1 and 2 refer, respectively, to the solvent and solute substances in the solid phase (in the solid phase, that substance which is present in the larger amount will be designated as the solvent).

In order to attain a state of equilibrium between the liquid and solid phases, use was made of the technique developed by V. G. Khlopin [3] this involving the isothermal establishment of supersaturation, followed by extended agitation (10 hours). The solid phase was analyzed according to the Schreinmaker method. Use was made of the radioisotopes Rb^{86} and Cs^{134} for the purpose of analysis. The vapor pressure of the water above the solutions was determined by the isopiestic method. The experimental results show (Table 1) that CsCl and RbCl form solid solutions with a miscibility range running from 10.7 to 93.3 mole % CsCl (these limits for the existence of the CsCl-RbCl solid solutions were calculated from the value of $D_{2,1}$ and the composition of the liquid phase at the triple point).

TABLE 1

Composition of liquid phase		Composition of solid phase	$D_{2,1}$	P_{H_2O}	f_{CsCl}	$\gamma_{\pm CsCl}$	f_{RbCl}	$\gamma_{\pm RbCl}$
m_{RbCl}	m_{CsCl}	x_{RbCl}						
7,78	10^{-3}	1,000	0,05	17,82	8,6	0,496	1,00	0,573
7,46	0,66	0,996	0,05	17,60	7,3	0,41	0,99	0,571
7,06	1,60	0,985	0,06	17,27	6,7	0,505	1,00	0,566
6,76	2,26	0,982	0,05	17,04	8,9	0,516	0,99	0,566
6,45	2,87	0,977	0,05	16,83	8,6	0,512	1,00	0,568
6,17	3,49	0,970	0,05	16,61	8,9	0,519	0,99	0,570
5,91	4,04	0,966	0,05	16,41	9,1	0,518	0,99	0,571
5,54	5,01	0,956	0,05	16,07	9,2	0,517	0,99	0,570
5,02	6,16	0,944	0,05	15,66	9,5	0,516	0,99	0,576
4,56	7,79	0,914	0,05	15,08	8,6	0,516	1,00	0,570
4,35	8,36	0,891	0,06	14,88	7,4	0,512	1,01	0,571
4,14	9,10	0,789	0,12	14,62	8,6	0,514	0,99	0,573
4,09	9,02	0,094	0,22	14,65	0,98	0,514	13,3	0,574
3,23	9,55	0,037	0,12	14,65	0,98	0,517	21,3	0,615
2,65	9,86	0,042	0,16	14,81	0,99	0,517	14,8	0,615
1,28	10,76	0,012	0,10	15,28	0,98	0,512	15,7	0,490
10^{-3}	11,41	0,000	0,16	15,61	1,00	0,516	13,3	0,573

From Table 1, it is to be seen that the activity coefficients remain constant, to within the limits of the experimental error, over the entire range of the solubility isotherms. The following relations are valid in the case of extreme dilution of one of the components:

$$\gamma_{\pm CsCl(RbCl\ m=7,78)} = \gamma_{\pm CsCl\ m=7,78},$$

$$\gamma_{\pm RbCl(CsCl\ m=11,4)} = \gamma_{\pm RbCl\ m=7,78}.$$

In the solid phase, the activity coefficient of the solvent component which fixes the crystal structure of the solid solution is, to a high degree of accuracy, equal to unity. The activity coefficient of the solute maintains a constant value which is different from unity and shows larger deviations from the mean, this last being one of the peculiarities of the method which was employed for the calculations.

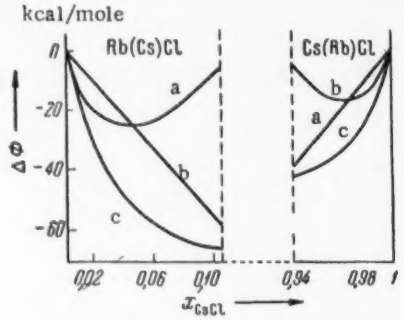

Fig. 1. The free energy of formation of CsCl-RbCl solid solutions at 25°: a) $x\Delta\mu_{CsCl}$, b) $(1-x)\Delta\mu_{RbCl}$, c) $\Delta\Phi$.

TABLE 2

x_{CsCl}	$-\Delta\mu_{CsCl}$	$-\Delta\mu_{RbCl}$	$-\Delta\Phi$
	kcal per 1 mole of ionic pairs		
0,000	∞	0,0	0,0
0,020	1037	12,0	32,5
0,040	626	24,2	48,2
0,060	383	36,7	57,5
0,080	215	49,4	62,6
0,090	145	56,0	64,0
0,095	113	59,2	64,3
0,100	82,6	62,5	64,5
0,107	41,1	67,0	64,2
	Miscibility limits		
0,933	41,1	67,0	42,8
0,935	39,9	87,4	43,0
0,940	36,7	134	42,5
0,960	24,2	374	38,2
0,980	12,0	783	27,5
1,000	0,0	∞	0,0

In Table 2,* and Fig. 1, there are presented the results of the final calculations for the change in the chemical potentials and the alteration in the free energy accompanying the formation of CsCl-RbCl solid solutions.

From the form of the resulting curve showing the dependence of $\Delta\Phi$ on composition (Fig. 1), it follows that formation of a solid solution occurs when the condition

$$\frac{\partial\Delta\Phi}{\partial x_2} < 0,$$

is fulfilled, x_2 being the mole fraction of the solute substances.

The following relation is valid near the limits of stability of the solid solutions:

$$\left(\frac{\partial\Delta\Phi}{\partial x}\right)_{\cong x^{sat}} = 0,$$

or

$$\Delta\mu_1 \cong \Delta\mu_2,$$

from which it follows that

$$x_1^{sat} = \frac{f_2}{f_1+f_2}$$

$$x_2^{sat} = \frac{f_1}{f_1+f_2}$$

Thus the composition of the saturated solution, x^{sat}, is fixed by the activity coefficients of the two components.

LITERATURE CITED

[1] R. J. Havighurst, E. Mach, Jr., and F. C. Blacke, J. Am. Chem. Soc. 47, 1 (1925).

*In the calculations for $\Delta\Phi$, use was made of the values of the activity coefficients of the dissolved substances at the triple point: $f_{CsCl} = 8.6$ and $f_{RbCl} = 13.3$.

[2] A. V. Storonkin and M. M. Shul'ts, Bull. Leningrad State Univ. No. 11 (1954).

[3] V. G. Khlopin, Proc. State Radiation Inst. 4 (1938).

The A. A. Zhdanov State University,
Leningrad

Received December 24, 1957

THE MEASUREMENT OF THE DIFFERENTIAL CAPACITY OF THE ELECTRICAL DOUBLE LAYER ON THE DROPPING MERCURY ELECTRODE IN SOLUTIONS OF KF, LiCl, NaCl AND KCl IN METHYL ALCOHOL

Stefan Mints and Iadviga Iastshembskaia

(Presented by Academician A. N. Frumkin, January 2, 1958)

The question as to whether an alteration in the ionic polarizability* would affect the structure and the capacity of an electric double layer is one that has been considered as very important in our studies.

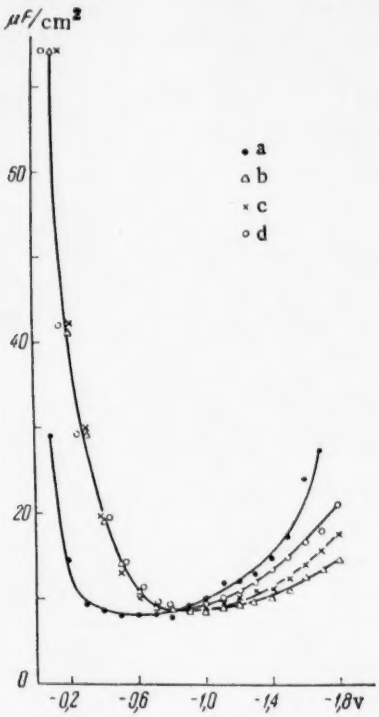

Fig. 1. The relation between the potential and the differential capacities of solutions of KF (a), LiCl (b), NaCl (c) and KCl (d) in methanol.

By measurements carried out on aqueous solutions of salts of the alkali metals, it has been shown that there is a wide variation in the differential capacities of the double layers on a dropping mercury electrode in solutions containing Li^+, Na^+ and K^+ ions, these capacities being equal to from 15.5 to 16.5 $\mu F/cm^2$ at a potential of about -1.1 v. These values change only slightly on increasing the applied potential [1, 2].

Supposing the methyl alcohol molecules in the dense portion of the electric double layer to show a compressibility approximately twice as large as that of the water molecules, we have postulated that the interaction between ions and electrode would be stronger in alcohol than in water, and that it would be, accordingly, easier to detect the effect of the varying ionic polarizability [3].

On the basis of measurements which we have carried out (the technique of these measurements has been described earlier [4]) on 0.1 N solutions of LiCl, NaCl and KF, and on a saturated solution of KCl (approximately 0.05 N), in methyl alcohol, it can be said that capacity differences are met at potentials sufficiently in excess of -1.2 v (Fig. 1).

The appended diagram of the capacity vs potential relation shows that, at a given potential, the capacity is the greater, the smaller the cation polarizability.

*In agreement with Born and Heisenberg, we use the term ionic polarizability to designate the ratio of the ion charge to the ion radius. Its value is: 1.7 for Li^+, 1.0 for Na^+ and 0.6 for K^+.

From these rough measurements it follows that cations possessing the same polarizability should form double layers of the same capacity under identical applied potentials.

The fact that the negative branch of the KCl curve falls beneath the corresponding branch of the KF curve, is related to the differences in the concentrations of the solutions which were employed. As our measurements have shown, the negative branch of the curve of the differential capacity of the saturated, i.e., approximately 0.05 N, solution practically coincides with the negative branch for 0.05 N KF.

LITERATURE CITED

[1] D. C. Grahame, J. Electrochem. 98, 343 (1951).

[2] A. N. Frumkin, B. B. Damaskin and N. V. Nikolaeva Fedorovich, Proc. Acad. Sci. USSR 115, No. 4, 751 (1956).*

[3] J. R. MacDonald, J. Chem. Phys. 25, 364 (1956).

[4] S. Minc and J. Jastrzebska, Rocz. Chem. 31, 735 (1957).

The Electrochemical Laboratory of the
University of Warsaw
The Electrochemical Laboratory of the
Institute of Physical Chemistry of the
Polish Academy of Sciences

Received December 15, 1957

*Original Russian pagination. See C. B. Translation.

THE MECHANISM OF THE VERTICAL DISTRIBUTION OF H_2O_2 ABOVE A SOLUTION

I. L. Roikh and I. P. Bolotich

(Presented by Academician A. N. Frumkin, January 2, 1958)

It has been established in [1] that the number of photographically active particles evolved from a metallic surface which is undergoing atmospheric corrosion falls off with distance according to an exponential law. In view of the fact that these particles are molecules of H_2O_2, it is to be expected that there would also be a vertical distribution in the hydrogen peroxide vapors which are liberated from solution. To test this point the following experiments were set up.

Into a cell there was poured an aqueous solution of hydrogen peroxide of known concentration and a photographic plate was so placed as to be inclined at a slight angle to the solution surface. The experimental conditions were as follow. The photoplate was an emulsion No. 747 of 5 minute exposure time, which, after exposure, was heated for 10 minutes [5] in a thermostat at 100°; the development was for 3 minutes at 20°, the relative humidity in the laboratory building was 62% and the room temperature, 20°.

From the experimental results there was established a linear relation between the degree of blackening, D, and the height, h, of the plate above the surface of the peroxide solution,

$$D = -bh + A, \tag{1}$$

here, b and A are constants.

The curves of Fig. 1 were obtained by averaging the data of 10 experiments at fixed exposure time.

Further study was aimed at elucidating the mechanism of the vertical distribution of the material vaporizing from a H_2O_2 solution. If it is supposed that the H_2O_2 molecules decompose on dust motes in the air, it must then follow that in volume dv the diminution in the number of hydrogen peroxide molecules will be proportional to the number of molecules originally present in this volume, n, and to the number, N, of dust particles responsible for their breakdown:

$$-dn = knN_p.$$

Since

$$N_p = n_p\,dv = n_p\,s\,dh,$$

(n_p is here the number of those dust particles per unit volume which are responsible for the decomposition), then

$$-dn = kn\,n_p\,s\,dh.$$

From this it follows that

$$-\ln n = kn_p sh + C$$

when h = 0, n = n_0 and C = $-\ln n_0$.
Then

$$n = n_0 e^{-kn_p sh}. \qquad (2)$$

Equation (2) shows that the number of hydrogen peroxide molecules falls off exponentially with the height above the solution. Assuming the law of interchangeability to be valid, as would be justified in the present case, the equation of the linear portion of the characteristic curve of the photoplate takes on the form

$$D = \gamma(\ln Et - \ln E_i t_i). \qquad (3)$$

The existence of a direct proportionality between the number of particles of H_2O_2 evolved from the solution and the number impinging on the photoplate has been demonstrated in [7]. On this basis, it can be considered that E = k'n. Then

$$D = \gamma(\ln k' n_0 e^{-kn_p sh} t - \ln k' n_i t_i),$$
$$D = \gamma(\ln k' n_0 t - \ln k' n_i t_i - kn_p sh).$$

We will set

$$A = \gamma \ln \frac{n_0 t}{n_i t_i}; \quad b' = \gamma ks.$$

We then obtain

$$D = -b' n_p h + A, \qquad (4)$$

i.e., a relation analogous to the experimentally developed Equation (1). It follows from Equation (4) that the slope of this straight line depends on the number of dust particles (n_p). With a decrease in the number of those dust particles which are responsible for the decomposition, there is an increase in the angle of inclination of the straight line to the axis of abscissas.

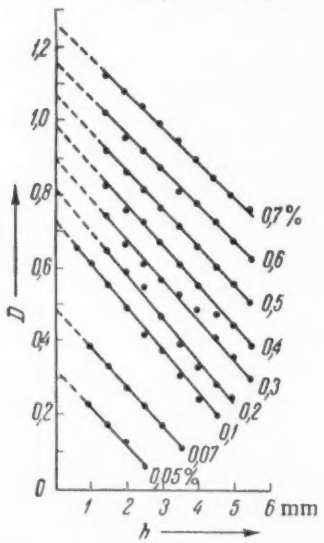

Fig. 1. The relation between the degree of photoplate blackening and the height above the surface of H_2O_2 solutions of various concentrations.

In order to experimentally test Equation (4), we have established the dependence of D on h with dusty air, and with air which was partially dust free, above the surface of the H_2O_2 solution. An isoorthochromatic plate, emulsion No. 3, with a light sensitivity of 32 according to GOST and an exposure time of 4 minutes was employed. Air which had been sucked up by a pump was rendered partially free of dust by electrofiltration and was then passed into a vessel containing the photoplate and the solution of hydrogen peroxide. Exposure was carried out after purification of the air in the vessel. The electrofilter was in the form of a metallic cylinder along whose axis there was stretched a wire which was connected to the negative pole of an induction coil, the cylinder itself being grounded. This filter functioned in the region of the corona discharge. In order to avoid blackening of the plate under the action of the ozone which was formed in the discharge, the purified air, prior to the admission into the vessel, was passed through a heater in which the ozone was made to undergo dissociation. The results shown in Fig. 2 respresent the mean of 5 experiments. Values of the optical densities of the straight lines I and II were found to lie in the region of the photometric interval which was established by plotting the characteristic curve. In conformity with Equation (4), the straight

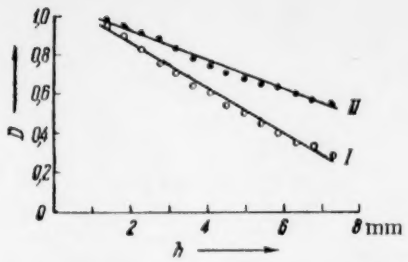

Fig. 2. The relation between the degree of blackening of a photoplate and its height above the surface of a H_2O_2 solution. I) in dusty air, II) in air partially freed of dust.

line II which was obtained in partially purified air had a more gradual course than I which was obtained with dusty air above the H_2O_2 solution.

The experimental data indicate that the fall-off with height of the molecules evaporating from a solution of hydrogen peroxide is connected with the existence of dust particles in the air.

We count it our pleasant duty to express our thanks to Academician A. N. Frumkin who pointed out to us the possibility of explaining the vertical distribution of the H_2O_2 in terms of the breakdown of the peroxide on dust particles.

LITERATURE CITED

[1] I. L. Roikh, Proc. Acad. Sci. USSR 70, No. 2, 253 (1950).

[2] I. L. Roikh and D. M. Rafalovich, Proc. Acad. Sci. USSR 60, No. 4, 603 (1953).

[3] I. L. Roikh, Proc. Acad. Sci. USSR 64, No. 6, 1117 (1954).

[4] I. L. Roikh, Proc. Acad. Sci. USSR 108, No. 6, 1102 (1956).

[5] I. L. Roikh, J. Phys. Chem. 30, vol. 4, 954 (1956).

[6] I. L. Roikh and D. M. Rafalovich, Ukr. Chem. J. 24, No. 2, 198 (1958).

[7] I. L. Roikh, J. Phys. Chem. 31, No. 9, 1959 (1957).

The I. V. Stalin Technological Institute,
Odessa

Received November 21, 1957

THE KINETICS OF THE OXIDATION OF FERROCENE BY IODINE

A. V. Savitskii and Ia. K. Syrkin, Corresponding Member,
Academy of Sciences, USSR

The transformation of ferrocene into ferricinium ion is of interest as a process of electron transfer in the dissolved state. The mechanism of reactions of this kind has been repeatedly studied, especially in the case of ions of like charge. For example, it is possible that water molecules are involved in the isotopic reaction between Fe^{2+} and Fe^{3+}, these molecules serving as a chain for the transfer of electrons [1-3]. Because of the great electrostatic repulsion between similarly charged ions, such reactions must take place over a sufficiently large distance. These reactions can be characterized by low transmission coefficients.

In the case of the electrically neutral molecules of ferrocene, $Fe(C_5H_5)_2$, (abbreviated in what follows, as Fn), and iodine, the electron transfer can take place over small distances.

It is natural to propose two possible schemes for the course of this reaction

$$\left.\begin{aligned} Fn + I_2 &\underset{k_2}{\overset{k_1}{\rightleftarrows}} Fn^+ + I_2^- \\ Fn + I_2^- &\xrightarrow{k_3} Fn^+ + 2I^- \end{aligned}\right\} \quad \text{Scheme 1}$$

or

$$\left.\begin{aligned} Fn + I_2 &\rightleftarrows Fn^+ + I + I^- \\ Fn + I &\rightarrow Fn^+ + I^- \end{aligned}\right\} \quad \text{Scheme 2}$$

In a number of reactions, it has been shown [4-6] that the breakdown of I_2^- into I^- and I does not take place in solution. In this light, Scheme 1 is the more probable of the two. It can be supposed that k_2 and k_3 are of the same order of magnitude. This would result from the instability of the ion radical I_2^- which rapidly reacts either with the molecule of ferrocene or with the ferricinium ions. For example, the reaction

$$2Fe^{3+} + 2I^- = 2Fe^{2+} + I_2$$

proceeds through the stages

$$Fe^{3+} + 2I^- \underset{k_a}{\overset{}{\rightleftarrows}} Fe^{2+} + I_2^-$$

and

$$Fe^{3+} + I_2^- \xrightarrow{k_b} Fe^{2+} + I_2,$$

with $k_a \approx 0.2\, k_b$ [5]. The reaction of $Fe(CN)_6^{3-}$ with iodine follows a similar mechanism; in this case $k_a = 4.3\, k_b$ [6]. By assuming that I_2^{-1} does not build up in the course of the reaction, the following expression can be obtained for the rate of oxidation of the ferrocene:

$$\frac{d[Fn^+]}{dt} = \frac{2k_1k_3[Fn]^2[I_2]}{k_2[Fn^+] + k_3[Fn]}, \quad (1)$$

when $k_2 \approx k_3$ this takes the form:

$$\frac{d[Fn^+]}{dt} = \frac{2k_1 [Fn]^2 [I_2]}{[Fn]_0}, \quad (2)$$

$[Fn]_0$ being the initial concentration of the ferrocene.

It is possible that the reaction proceeds through a preliminary formation of the molecular compound FnI_2, the ferrocene being the electron donor. There are data pointing to the formation of ferrocene complexes with halide derivatives of the hydrocarbons [7], even though it is a fact that the ability of the latter to form molecular compounds by electron transfer is much less than that of iodine. The formation of FnI_2 could be reflected in the form of the kinetic curves at high iodine and ferrocene concentrations when the equilibrium

$$Fn + I_2 \rightleftarrows FnI_2$$

is markedly displaced to the right. If the reaction does proceed through the formation of FnI_2, it is marked by: 1) zero activation energy for the formation of FnI_2, 2) molecular polarization in forming the molecular compound, 3) the transfer of an electron from ferrocene to iodine which proceeds in all likelihood more readily in the molecular compound than in a bimolecular reaction.

TABLE 1

The Reaction of Ferrocene with Iodine in 96.5% Alcohol at 25°

No. experiment	$[Fn]_0$, 10^{-4} moles·l^{-1}	$[I_2]_0$, 10^{-4} moles·l^{-1}	k, $l \cdot moles^{-1} \cdot sec^{-1}$	$k' = k[Fn]_0[I_2]_0$ $l \cdot moles^{-1} \cdot sec^{-1}$
1	0,463	7,75	256	15,3
2	0,463	15,5	669	20,0
3	0,463	27,1	1100	18,8
4	0,925	15,5	335	20,0
5	0,925	31,0	558	16,7
6	0,925	31,0	707	21,1
7	1,85	7,75	58*	13,9
8	1,85	15,5	178*	21,2
9	1,85	31,0	299	17,8
10	1,85	31,0	300	17,9

* Determined from the initial reaction rate.

With initial ferrocene concentrations not exceeding 10^{-4} mole·l^{-1} and with a 10-50-fold iodine excess, the ferrocene oxidation was studied in 93 and 96% alcohol solutions over a 5-40° temperature interval. The concentration of the ferricinium ions was determined spectrophotometrically from the adsorption maximum at 619 mμ as observed at constant temperature on the SF2M instrument. With an excess of iodine, the resulting data showed the equilibrium to be displaced in the direction of the formation of the ions. With a 25-fold excess of iodine and at 25°, the equilibrium concentration of the ferricinium ions proved to be approximately 98% of the initial ferrocene concentration. Thus, under the experimental conditions, the rate of the reverse reaction is not large and this process can be left out of account in studying the kinetics of the ferrocene oxidation. The side reaction between the iodine and the solvent [8] is without essential influence on the main process since the latter proceeds considerably more rapidly. Under the experimental conditions, the larger part of the ferrocene is oxidized by the iodine in the course of several minutes.

$$Fn + {}^3/_2 I_2 \rightleftarrows Fn^+ + I_3^-$$

In each experiment, the change in the ferricinium ion concentration was described by the equation

$$\frac{d[Fn^+]}{dt} = k([Fn]_0 - [Fn^+])^2, \quad (3)$$

k being a constant. A change in the initial concentrations of the ferrocene and of the iodine leaves the character of the kinetic curves unaltered, although the quantity k varies in proportion to $[I_2]_0/[Fn]_0$, $[I_2]_0$ being the initial iodine concentration (see Table 1).

The experimental equation (4) for the rate of oxidation of ferrocene agrees with Equation (2) which was derived for the first reaction scheme:

$$\frac{d[Fn^+]}{dt} = \frac{k'([Fn]_0 - [Fn^+])^2 [I_2]_0}{[Fn]_0}. \quad (4)$$

The kinetic data are, therefore, not in contradiction with the assumption of the formation of an intermediate, unstable, ion-radical I_2^-.

TABLE 2

Values of the Rate Constant for the Reaction $Fn + I_2 = Fn^+ + I_2^-$

Temperature, °C	Concentration of solvent alcohol, %	$k_1 = {}^1/_2 k'$, $l \cdot moles^{-1} \cdot sec^{-1}$
5.4	93	3.0 ± 0.3
20.0	93	10.6 ± 1.2
21.0	93	11.1
30.0	93	27.3 ± 1.8
40.0	93	52.6
25.0	96.5	9.1 ± 1.0

The energy of activation and the exponential multiplier for the electron transfer from ferrocene to iodine were determined graphically from the temperature dependence of the reaction rate. Values of k_1 at various temperatures shown in Table 2.

Experiment gives for the energy of activation, 14.6 kcal · mole^{-1} and for the multiple of the exponent, $9 \cdot 10^{11}$ l · moles^{-1} sec^{-1} ($\Delta S = -5.85$ cal · mole^{-1} · deg^{-1}). From the associated cyclic process, the energy of solvation of the ferricinium ion can be evaluated. This value must be in excess of 50 kcal · mole^{-1}. The comparatively high value of this energy of solvation permits the supposition that the positive charge of the ion resides, to a considerable degree, on the iron atom.

The exponential multiplier differs but little from the usual value. It must be kept in view that if the reaction proceeds through the molecular compound FnI_2, the observed activation energy will be equal to the true value diminished by the heat effect accompanying compound formation. In this case, the observed entropy of activation would equal the sum of the entropy of formation of the molecular compound and the entropy of activation of the reaction whose velocity was measured. It should be pointed out that the entropy of activation can take on high negative values [9] in reactions involving electron transfer between ions of like charge. In our case the conditions of electron transfer are clearly quite different, and there is no reason to expect a low value for the exponential multiplier.

LITERATURE CITED

[1] J. Hudis and A. C. Wahl, J. Am. Chem. Soc. 75, 4153 (1953).

[2] J. Hudis and R. W. Dodson, J. Am. Chem. Soc. 78, 911 (1956).

[3] F. S. Dainton, G. S. Laurence, W. Schneider, D. R. Stranks and M. S. Vaidya, Internat. Confer. of Radioisotopes in Scientific Research, Paris, 1957.

[4] J. C. Roy, W. H. Hamill and R. R. Williams, J. Am. Chem. Soc. 77, 2953 (1955).

[5] A. J. Fudge and R. W. Sykes, J. Chem. Soc. 1952, 119.

[6] C. Wagner, Zs. phys. Chem. 113, 261 (1924).

[7] J. C. D. Brand and W. Snedden, Trans. Farad. Soc. 53, 894 (1957).

[8] A. Batley, Trans. Farad. Soc. 24, 438 (1928).

[9] B. J. Zwolinski, R. Marcus and H. Eyring, Chem. Rev. 55, 157 (1955).

The M. V. Lomonosov Institute of Exact Chemical Technology

Received January 14, 1957

THE EQUILIBRIUM POTENTIALS OF ZIRCONIUM IN CHLORIDE MELTS

M. V. Smirnov and V. A. Chemezov

(Presented by Academician A. N. Frumkin, January 2, 1958)

The literature shows an absence of work dealing with the equilibrium potentials of metallic zirconium in molten chlorides. The dependence of the equilibrium potential of thorium on the temperature and the concentration of thorium ions in chloride melts has been established in one of the papers from our laboratory [1]. It was shown that metallic thorium reduces the Th^{4+} ion to Th^{2+} in such melts. A similar reduction could be expected to occur in the other tetravalent cations of the Ti subgroup. To investigate this point, we have carried out special experiments.

Into a molybdenum crucible there was loaded a molten eutectic mixture of lithium and potassium chlorides, which had been previously treated with dry hydrogen chloride, and to this there then was added a definite amount of zirconium tetrachloride (zirconium tetrachloride was prepared by chlorination of a dense mixture of zirconium dioxide and carbon in a current of chlorine. The reaction product was subjected to triple sublimation for the removal of traces of carbon dioxide). This crucible was affixed to a molybdenum rod and inserted into a quartz tube filled with argon. Special attention was given to the removal of moisture, nitrogen and oxygen from the argon. The tube was placed in a massive metallic block which served as a thermostat. This latter was heated in an electrical resistance furnace with an automatic control which allowed the temperature to be held constant to within ± 1°. Into the salt melt there was immersed a zirconium electrode which had been prepared by the iodine method. This metal was weighed prior to experiment. In the melt, the course of the ionic reduction was followed by measuring the potentials of the zirconium and molybdenum electrodes (the crucible serving as the latter electrode). These potentials were measured against a chlorine electrode which was contained in a quartz tube filled with a salt melt of the same composition. This tube was raised above the level of the electrolyte in order to avoid interaction between the quartz and the low valence zirconium ions. Contact with it was made by means of a wick-like asbestos diaphram which tightly covered an opening in the bottom of the tube containing the chloride electrode. The end of this asbestos wick was immersed into the melt.

In Fig. 1 there are shown graphs of the results of two experiments which were carried out at 560 and 585°C. In both cases the melt contained 2.27% Zr by weight. It is to be seen that the inert molybdenum electrode was at first more negative than the zirconium. As reduction proceeded, the potentials of the two chlorides approached one another, finally becoming equal and constant. This gives evidence of the attainment of equilibrium in the reduction reaction:

$$Zr_s + Zr^{4+}_{melt} \rightleftarrows 2Zr^{2+}_{melt}.$$

In actuality, at equilibrium, the potential of the zirconium electrode relative to the ions of higher and lower valences

$$E_{Zr} = E^0_{Zr|Zr^{2+}} + \frac{RT}{2F} \ln a_{Zr^{2+}} = E^0_{Zr|Zr^{4+}} + \frac{RT}{4F} \ln a_{Zr^{4+}},$$

must be equal to the oxidation-reduction potential of the system represented by the inert molybdenum electrode:

$$E_{Mo} = E_{Zr^{4+}|Zr^{4+}} + \frac{RT}{2F} \ln \frac{a_{Zr^{4+}}}{a_{Zr^{2+}}}.$$

From the loss in weight of the zirconium electrode and the increase in the concentration of zirconium in the melt, it follows that it is predominately divalent zirconium which is formed in the reduction. Within the limits of experimental error (several mg), the amount of zirconium in the melt increased to twice its initial value in the course of the equalization of the potentials of the molybdenum and the zirconium electrodes. A dichloride of zirconium has not as yet been described in the literature. Only in one recent paper has the formation of zirconium trichloride been reported [2]. Melts of zirconium dichloride possess strong reducing properties. They interact with glass and with porcelain. On contact with the air, a fine suspension of ZrO_2 rapidly forms in them. Congealed salt mixtures containing $ZrCl_2$ decompose water, with the evolution of hydrogen.

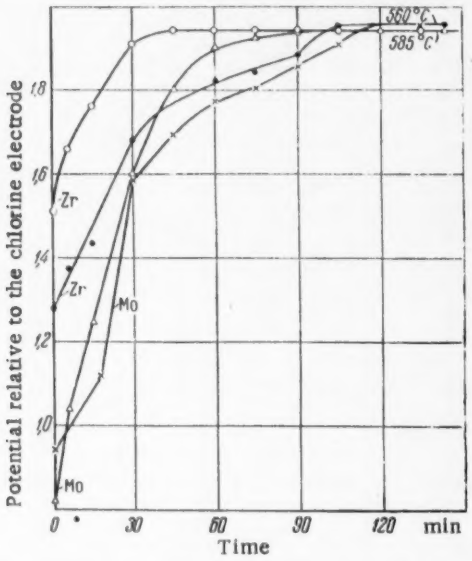

Fig. 1. The variation of the potentials of the zirconium and molybdenum electrodes in the course of the reduction of Zr^{4+} ions to Zr^{2+} in the melt.

After having cleared up the nature of the zirconium ions which are present in chloride melts that have come into equilibrium with metallic zirconium, the equilibrium potentials of the metal were then measured over wide intervals of temperatures (400-820°C) and of concentrations (0.0 to 24.9 weight % $ZrCl_2$).

These measurements were carried out in the cell which is schematically represented in Fig. 2. The initial electrolyte was a eutectic mixture of the chlorides of lithium and potassium, to which there was added a certain amount of zirconium tetrachloride. Into the molybdenum crucible there was placed the salt mixture and some powdered metallic zirconium, the latter in an amount several times in excess of that required for the reduction of the Zr^{4+} to Zr^{2+}. A separate zirconium electrode was not introduced into the melt since the potentials of the molybdenum and the zirconium electrodes are equal at equilibrium. The cell's second electrode was a chloride electrode such as was described above. The cell EMF was measured with a high resistance potentiometer of the PPTV-1 type. Values obtained under the given conditions were considered to be trustworthy if they remained constant to within 1 mv over an extended period of time (not less than 1 hour). Over the investigated intervals of temperature and concentration, there was no detectable sublimation of zirconium chloride out of the electrolyte. At higher temperatures and concentrations, the loss of zirconium from the melt began to make itself felt.

The results of the EMF measurements at the various temperatures are shown graphically in Fig. 3. At each of the investigated concentrations, the experimental points fell on straight lines which could be represented by the following empirical equations.*

In Fig. 4 there are presented EMF isotherms at 700, 800, 900, 1000 and 1100°K, these being constructed on the basis of the experimentally observed temperature dependence of the EMF for the investigated electrolyte concentrations of zirconium (mole fractions of Zr^{2+}: $8.33 \cdot 10^{-5}$, $7.73 \cdot 10^{-4}$; $4.21 \cdot 10^{-3}$; $1.38 \cdot 10^{-2}$ and $4.74 \cdot 10^{-2}$). At mole fractions of zirconium in excess of 10^{-3}, and especially at high temperatures (above 1000°K), the EMF isotherms have the form of straight lines whose slopes closely approximate RT/2F. This once more confirms the fact that when a melt is in equilibrium with metallic zirconium, the major portion of the zirconium which it contains is in the form of divalent ions. We have measured the EMF of the cell when filled with a molten eutectic mixture of the chlorides of lithium and potassium which contained no added zirconium trichloride. The resulting potentials were the same as in the case of melts containing 0.05 weight % $ZrCl_2$.

*Equations omitted in original text – Publisher's note.

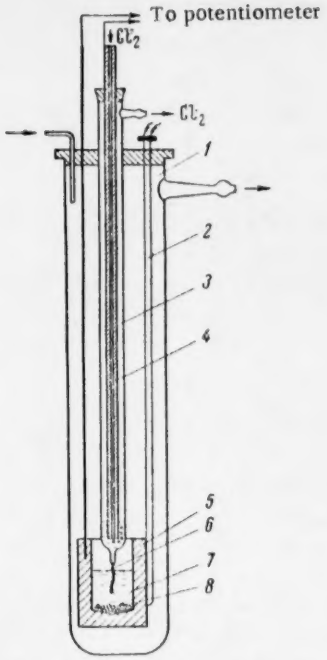

Fig. 2. Measuring cell: 1) tube of quartz glass; 2) thermocouple; 3) tube of quartz glass; 4) chlorine electrode; 5) molybdenum electrode; 6) asbestos wick; 7) salt melt; 8) zirconium powder.

Thus in the melt layer which is formed in contact with the metal as the result of the latter's autodissolution, the concentration of zirconium exceeds 0.05 weight % $ZrCl_2$. It is exactly through this fact that there is to be explained the apparent falling of the points on the EMF isotherms which were developed for melts with low concentrations of zirconium. From the experimental data it is clear that the equilibrium mole fraction of Zr^{2+} in the pre-electrolyte layer resulting from the dissolution of the metal is approximately $3 \cdot 10^{-4}$.

The smallest spread of points was obtained in the experiments with a melt containing 24.9 weight % $ZrCl_2$, this clearly being the result of the more exact determination of the concentration and the smaller relative variation of this concentration in the course of the measurements. Filled with this electrolyte, the EMF of the cell varied with temperature according to the empirical equation:

$$\varepsilon_{mes} = (2{,}442 - 6{,}28 \cdot 10^{-4} T) \pm 0{,}004 \text{ v}.$$

Into the measured value of the EMF there enters not only the difference of the electrochemical potentials but also the thermoelectric force between the molybdenum and the carbon (chlorine electrode), these quantities being of opposite sign.

As experiments carried out in our laboratory have shown, the latter value varies with temperature according to the equation: $\epsilon_T = (0.008 + 0.17 \cdot 10^{-4} T) \pm 0.001$. Thus the desired EMF value is

$$\varepsilon = (2{,}434 - 6{,}11 \cdot 10^{-4} T) \pm 0{,}005 \text{ v}.$$

From this it is possible to evaluate the quantity $E^0_{Zr/Zr^{2+}}$ which enters into the equation for the equilibrium potential of zirconium in molten chlorides: $E = E^0_{Zr/Zr^{2+}} + \frac{RT}{2F} \ln a_{Zr^{2+}}$. Supposing the melt containing 24.9 weight % $ZrCl_2$ to behave as an ideal solution, we obtain

$$E^0_{Zr|Zr^{2+}} = (-2{,}434 + 7{,}42 \cdot 10^{-4} T) \pm 0{,}005 \text{ v}$$

relative to the chlorine electrode.

Con. $ZrCl_2$, wt. %	$\epsilon_1 \cdot 10^4$, v
24.90	2.442 − 6.28
7.90	2.456 − 5.94
2.65	2.474 − 5.54
0.45	2.512 − 5.12
0.05	2.519 − 4.78

From the earlier determined value of $E_{Th/Th^{2+}}$ [1], it is possible to find the difference between the potentials required for the separation of thorium and zirconium out of chloride melts of the same concentrations: $E_{Th} - E_{Zr} = (-0.80 + 3.55 \cdot 10^{-4} T)$ v. As is to be seen, thorium is more electronegative than zirconium. Thus, at a temperature of 1000°K, it should precipitate out at a potential approximately 0.44 v more negative than zirconium, provided, of course, that the electrolysis is not complicated by the formation of alloys on the cathode. From the temperature dependence of the EMF of the cell: Zr | 24.9 weight % $ZrCl_2$, KCl, $LiCl_{melt}$ | Cl_2, C, it is possible to calculate the change in the free energy which accompanies the formation of the molten dichloride from its elements: $Zr_s + Cl_{2g} = ZrCl_{2_l}$, it being assumed that solutions of $ZrCl_2$ in the molten eutectic mixture of lithium and potassium chlorides behave ideally right up to the pure molten salt:

$$\Delta Z = (-112\,300 + 31{,}82\,T) \pm 230 \text{ cal/mole}$$

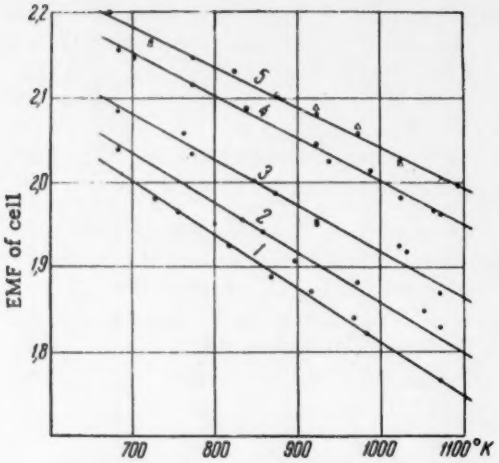

Fig. 3. The temperature dependence of the EMF of a cell containing a melt with 13.95 weight % Zr^{2+} (1), 4.44 weight % Zr^{2+} (2), 1.41 weight % Zr^{2+} (3), 0.26 weight % Zr^{2+} (4), 0.03 weight % Zr^{2+} (5), points designated by triangles represent values obtained without the addition of $ZrCl_4$.

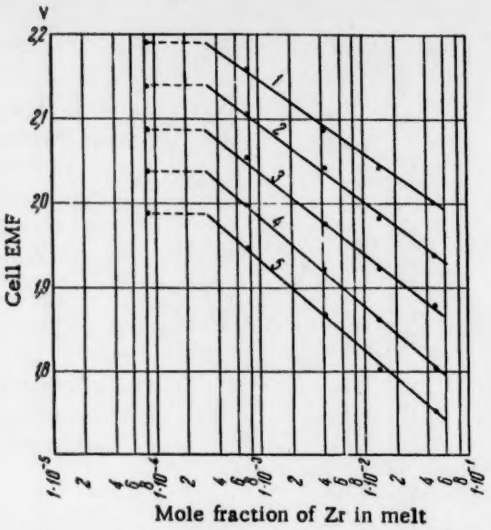

Fig. 4. Cell EMF isotherms. 1) 700°; 2) 800°; 3) 900°; 4) 1000°; 5) 1100°K.

From this there follows the heat of formation of liquid zirconium dichloride, $\Delta H = -112.3$ kcal/mole and the entropy change for the reaction, $\Delta S = -31.82$ kcal/deg·mole. On the basis of the literature values [3] for the standard entropies of chlorine and zirconium, it is possible to calculate the standard entropy for liquid zirconium dichloride $S^0_{ZnCl_2} = \Delta S + S^0_{Zr_s} + S^0_{Cl_{2g}}$ by using the value found for ΔS. This proves to be equal to 30.67 cal/deg·mole.

LITERATURE CITED

[1] M. V. Smirnov and L. E. Ivanovskii, J. Phys. Chem. 31, 802 (1957).

[2] E. M. Larsen and J. J. Leddy, J. Am. Chem. Soc. 78, 5983 (1956).

[3] W. Latimer, The Oxidation States of the Elements and their Potentials in Aqueous Solutions (in Russian), Foreign Lit. Press, 1954.*

The Electrochemical Laboratory of the
Ural Affiliate of the Academy of Sciences
of the USSR

Received December 10, 1957

*Russian translation.

THE MECHANISM OF THE EMULSIFYING ACTION OF SOLID EMULSIFIERS

A. B. Taubman and A. F. Koretskii

(Presented by Academician P. A. Rebinder, December 30, 1957)

According to the modern conceptions of the mechanism of the emulsification of liquids by solid emulsifiers [1], the type of the emulsion (O/W or W/O), and its stability, are determined by the selective wetting of the highly dispersed solid particles by the liquid phases forming the emulsion.

The nonuniformity in the separate portions of the solid surfaces (mosaic structure) results in their being wetted to various degrees and, at the same time, makes possible the adhesion of these particles to the drop surfaces. This presupposes that stability in an emulsion can be achieved by the formation of external monomolecular layers which jacket the drops, and that the physicochemical nonuniformity in the particle surfaces is sufficiently marked so as to assure their simultaneous partial wetting by both phases.

The results which are presented below on the emulsification of a hydrocarbon oil in aqueous suspensions of bentonite clay (the most widely employed of the solid emulsifiers) have shown that these conceptions are inadequate for interpreting the mechanism of those phenomena which lie at the basis of the formation of high-stability emulsions of the O/W type through the action of highly dispersed powders.

Bentonite clay which had been activated by the addition of electrolytes ($FeCl_3$, $Al_2(SO_4)_3$, etc.) was earlier employed by us [2] as a cheap and effective emulsifier for the removal of viscous petroleum products from oil tankers by the conversion of these substances into low viscosity fluid emulsions. The experiments which are described in the present work permit the elucidation of the essential features of the activation of bentonite by electrolytes and allow the establishment of a physicochemical method for emulsifying petroleum products by solid emulsifiers.

In emulsions formed by energetic mechanical agitation, we have determined the stability, and the structural-mechanical properties of the interphase layers, and the dependence of these factors on the concentration of the solid emulsifier, as observed at a constant ratio between the volumes of the liquid phases (water: oil = 1 : 1) and in the presence of organic additives (oleic acid, in the oil phase) and electrolytes ($AlCl_3$, in the aqueous phase).

As experimental materials there were chosen vaseline oil (medicinal), carbon tetrachloride which had been carefully freed from traces of polar contaminants by the use of silica gel, and a bentonite clay from the Oglanlinskii region (Turkmen SSR) [3] in the form of suspensions of various concentrations (up to 6%) which had been prepared by maintaining the clay in water for an extended period of time to complete peptization. Since the pH of these suspensions fell in the region 7.5-9.5, it followed that the oleic acid neutralized in forming the emulsion passed as sodium oleate from the oil into the water phase. The stability of these emulsions was evaluated in terms of the time (τ) which elapsed between their formation and their partial breakdown with the separation of 50% of the oil in the free state. Since, however, there were not only emulsions which disintegrated relatively rapidly (τ not exceeding several hours) but others which possessed practically unlimited stability ($\tau \gg$ 2–3 days), the term stable will be used in what follows to designate emulsions showing absolutely no separation of free oil in the course of 48 hours (in Figs. 1, 2, such emulsions are indicated by the sign ∞). Using a simple torsion apparatus, the structural-mechanical properties of the surface layers were measured at the CCl_4–water interface in the presence of the solid phase which settled out from the upper aqueous medium in a quantity which corresponded, for practical purposes, to the depth of the bentonite layers on the emulsion droplets.

The measurements show, in the first instance, that with pure vaseline, stable emulsions can be obtained with such comparatively high concentrations (4%) of bentonite in the aqueous medium (Fig. 1, Curve 1) as correspond to the formation of a coagulation structure throughout the entire volume [4]. On lowering the concentration of the emulsifier, the stability of the emulsion falls precipitously and it is clear that neither the monomolecular layers which are directly bound to the droplet surfaces by the forces of wetting, nor even considerably thicker layers, are in a condition to form any sort of stable emulsion because of the insufficient strength of the spatial structure in the bulk of the aqueous medium.

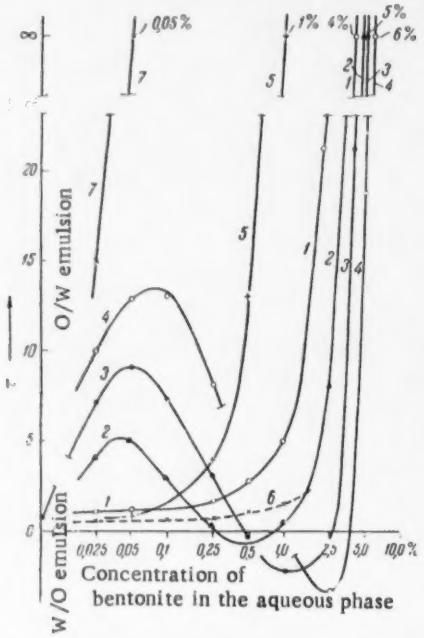

Fig. 1. The emulsion stability (τ, min.), concentration relation in the system bentonite, oleic acid and $AlCl_3$. 1) An emulsion of pure oil; 2-5) oil emulsions containing, respectively, 0.001; 0.01; 0.1 and 1% oleic acid; 6) an emulsion of pure oil in a 0.01 N aqueous solution of $AlCl_3$; 7) an emulsion of an oil containing 0.1% oleic acid, in 0.01 N aqueous solution of CCl_4.

The introduction of oleic acid into the oil sharply changes the condition for emulsification since the sodium oleate which is formed on the droplet surfaces hydrophobizes the particles by chemadsorption (on the calcium containing portions of the surface, for instance)• when it passes into the aqueous medium.

The effect of such an alteration in the properties of the solid surface varies, depending on the concentration of the bentonite. With the appearance in the aqueous phase of emulsions with a coagulation structure of bentonite and at a concentration of the latter > 4%, hydrophobization decreases the strength of the emulsion [5], this effect being the greater, the higher the oleic acid concentration (Curves 2-4). As a result, the emulsion stability falls so markedly that the emulsion either does not form at all or unstable emulsions of the reverse type (W/O) appear because of the stabilization of the water droplets by the oleofaction of the particles of the bentonite which have passed into the oil phase.

Further increase of the acid concentration to 1% leads to still another result: the stability of the emulsion sharply increases (Curve 5) as a result of the stabilizing action of sodium oleate which is not found in the chemadsorbed layers on the solid surface, but is formed in excess in the aqueous phase and assures the stability of the emulsion regardless of the presence of the dispersed solid phase. This gives a ready explanation of the fact that many authors [6] have been able to obtain stable emulsions of technical oils by using 1% suspensions of bentonite clay; from what has been said above, this could not have been done with pure oils or with oils which were only lightly contaminated.

Surface modification by the adsorbed layers makes its influence felt in a different manner in the region of bentonite suspensions of low concentrations (below 1%) in which there is practically no structuralization in the aqueous phase, since under these conditions a second stabilizing factor, the force of weting (adhesion) between the first monomolecular layer of the emulsifier and the surface of separation, comes into play. This is obvious from the course of the Curves 1-4 in the left portion of Fig. 1. A comparison of Curve 1 and Curves 2-4, which show clearly marked maxima, indicates that the emulsion stability rises as hydrophobization proceeds and the strength of the adhesion of the particle increases, the optimum emulsification corresponding to complete coverage of the droplet surface with a monomolecular layer. Up to the maxima (at bentonite concentrations less than 0.05-0.1%) the solid phase is insufficient for this, whereas above the maxima there comes into play the "oiling" of the particle surfaces, resulting from that increase in the sodium oleate concentration of the aqueous phase which accompanies a rise in pH.

• Hydrophobization of surface can occur also as the result of its direct adsorptional interaction with the oleic acid during contact between the particles and the drop surface.

At the same time, the magnitude of the maxima indicate that it is not possible to obtain stable emulsions by increasing the mosaic nature of the particle surfaces through partial hydrophobization and by the adhesion of the monomolecular layer to the drops of oil.

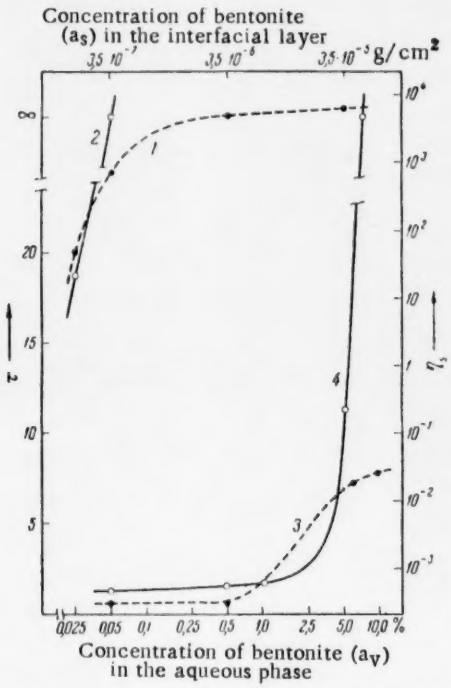

Fig. 2. The surface viscosity of the interfacial layers (η_S, surface poises), and the stability (τ, min), of emulsions. 1) η_S at the CCl_4 + 0.1% oleic acid – 0.01 N aqueous solution of $AlCl_3$ interface, in the presence of bentonite; 2) τ for emulsions of CCl_4 containing 0.01% of oleic acid, in 0.01 N aqueous $AlCl_3$ solution; 3) η_S at the CCl_4 – water interface, in the presence of bentonite; 4) τ for CCl_4 emulsions in water.

The effect of the addition of electrolytes on the emulsion stability varies markedly, depending on the existence of a fatty acid in the oil. Despite the strong coagulation of the bentonite particles resulting from adsorption of the potential-determining Al^{3+} ions and the increased mosaic nature of the particle surface to which this gives rise, the introduction of $AlCl_3$ into a pure oil emulsion not only fails to give the anticipated increase in the emulsion stability but actually diminishes it strongly (Curve 6). In the emulsification of an oil containing 0.1% of oleic acid, this same addition of electrolyte brings about that exceptionally sharp increase in stability which is characteristic of Curve 7. Similar results are given by the ions of Fe, Cu, Co, Zn, Th, etc.

It is clear that under these conditions, a stable emulsion will form at bentonite concentrations which are two orders less than is required in the absence of the electrolyte and the fatty acid. This quantity of emulsifier corresponds to the coverage of the emulsion droplet with a layer approximately one particle in depth.

In this case the structural-mechanical barrier, or structure formation in the adsorbed layers of the soaps of polyvalent metals, is the stabilizing factor.

It should be noted that pronounced stabilization of emulsions is met only over a strictly defined region of of pH values in the aqueous phase, this region being one in which it is possible to form partially replaceable basic metal soaps [7] whose adsorbed monomolecular layers possess enhanced stability.

The extent to which the mechanical properties of these layers make themselves felt can be seen from Fig. 2 in which there are presented: Curve 1 – the viscosity of adsorbed layers of aluminum oleate which were formed at the interface between CCl_4 + 0.1% oleic acid and water + 0.01 N $AlCl_3$ in the presence of a bentonite layer, and the corresponding Curve 2 – the stability in water of CCl_4 emulsions which have been obtained at the same concentrations of the indicated components. For comparison, similar data characterizing the behavior of these same systems in the absence of oleic acid and $AlCl_3$ are also presented (Curves 3 and 4).

It follows from what has been said that stable emulsions (O/W) of pure oils can be obtained only if a bulk coagulation structure is formed in the aqueous phase by the bentonite and that a monomolecular layer of the solid emulsifier can stabilize the emulsion only in conjunction with the formation of structured metallic soaps of basic character in the surface layer. It is important to note here that although the "hydrophobic" (oleophilic) emulsifiers (metallic soaps) usually stabilize only emulsions of the reverse type, they can also strengthen emulsions of the direct type when a monomolecular layer of solid phase of hydrophilic character is present. This indicates that the influence of the mechanical properties of the emulsifiers predominate over the effect of the second stabilizing factor, the wetting, which thus obviously plays a secondary role and cannot by itself assure the formation of high-stability emulsions.

We wish to express our deep thanks to Academician P. A. Rebinder for the interest which he has shown in this work and for his valuable advice.

LITERATURE CITED

[1] P. A. Rebinder, Colloid J. 8, 157 (1946); V. Clayton, Emulsions, Their Theory and Technical Applications (in Russian), Foreign Lit. Press, 1950, pages 26, 256, 357;* J. H. Schulman and J. Leja, Trans. Farad. Soc. 5, 598 (1954).

[2] A. B. Taubman and A. F. Koretskii, Bull. Acad. Sci. USSR, 9, 62 (1954); A. F. Koretskii and M. L. Rabei, New Methods of Mechanizing the Cleaning of Oil Barges (in Russian) 1955.

[3] A. V. Danov, Bull. Turkmen Affiliate, Acad. Sci. USSR 5 (1943).

[4] L. A. Abduragimova, P. A. Rebinder and N. N. Serb-Serbina, Colloid J. 17, 184 (1955);** P. A. Rebinder, Sympos., The Viscosity of Liquids and Colloidal Solutions (Reports of Conference) (in Russian) 1, 361 (1941).

[5] N. N. Serb-Serbina and S. A. Nikitina, Colloid J. 8, 63 (1946).

[6] R. M. Woodman and E. M. Taylor, J. Phys. Chem. 34, 229 (1930); L. N. Mukerjee and S. N. Srivastava, Koll. Zs. 150, 144 (1957).

[7] J. A. Spink and J. V. Sanders, Trans. Farad. Soc. 51, 1154 (1955); H. Kimizuka, Bull. Chem. Soc. Japan, 29, 123 (1956).

The Institute of Physical Chemistry of the Academy of Sciences of the USSR

Received December 26, 1957

*Russian translation.

**Original Russian pagination. See C. B. Translation.

THE DEPENDENCE OF THE LOWER LIMIT OF THE STRUCTURAL STABILITY AND THE CRITICAL VELOCITY GRADIENT ON THE CONCENTRATION OF OLEOGELS OF ALUMINUM NAPHTHENATE

V. A. Fedotova and A. A. Trapeznikov

(Presented by Academician M. M. Dubinin, December 28, 1957)

It has been shown in [1, 2] that many intermediate (in the rheological sense) systems, such as the oleogels of the aluminum soaps of napthenic acid in decalin which we have studied, have the particularly interesting property of simultaneously possessing all of the characteristics of both the completely fluid (liquid-like, non-Newtonian)systems and the practically nonfluid (plasto-solid and elasto-friable) systems. It has been explained [2] that it is necessary to consider the presence of a structural lattice even in those liquid-like systems which show flow under arbitrarily low shear stresses. Although such lattices show extremely slow relaxation in those systems which behave as if they were solid, they are mobile in liquid systems and are characterized by small relaxation times.

It has been further established [2] that among the great number of physicomechanical parameters which are required for the complete characterization of the behavior of structured systems over wide intervals of velocity gradients, $\dot{\epsilon}$, and shear strengths, P, the most important rheological constants are the lower limit of structural stability, P_k and the critical value $\dot{\epsilon}_k$ corresponding to it. These constants P_k and $\dot{\epsilon}_k$ are tied up with the transition out of the region of constant relaxational viscosity, η_1 = const., i.e., out of the region of a statistically indestructible structure which is fully re-established in the deformation process, into the field of diminishing viscosity $\eta_2(P)$ which is associated with the breakdown of those structural bonds which fail to relax and re-establish in deformation.

An investigation of the dependence of these constants on the concentration of aluminum naphthenate oleogels has lead to the discovery interesting relationships.

A series of kinetic curves for the development of deformation under constant shear stress $\epsilon(\tau)_P$ (P = const. method) and for the development of shear stress under constant rotational velocities of the inner cylinder $P(\tau)_\Omega$ (Ω = const. method) was obtained with the complex elastoviscosimeter [2] and led to the establishment of a relation between the viscosity of the system, the applied shear stress and the velocity gradient; this, in turn, made possible the evaluation of P_k and $\dot{\epsilon}_k$ for each gel concentration.

In Figs. 1 and 2 there are shown the η (P) and η ($\dot{\epsilon}$) relations for gels of aluminum naphthenate in decalin over the interval of concentrations, C, from 6 to 20%.* Although the systems with C < 6% possessed elasticity, they proved to be quite fluid and resembled liquids, whereas systems in which C = 8-20% behaved as true high-elastic gels with high shear moduli. At the same time, a slow, but completely measurable, flow was to be observed in these gels even under the very lowest P values, and corresponding relatively high viscosities of the order of 10^5-10^6 poise. In this respect the high-concentration aluminum naphthenate oleogels approach those systems which are classed as plastico-solid bodies, an example of which would be the hydrodispersions of bentonite clays in which maximum constant viscosities of almost the same order as those indicated above have recently been measured.

* The study of these oleogels was carried out 20 days after their preparation. The data at C < 6% have been published earlier [2]. In the present work there was employed an aluminum naphthenate which had been prepared by G. V. Belugina, following a procedure calling for 36% free NaOH and pH = 5 [3]. In [2] this specimen of soap was designated as type V.

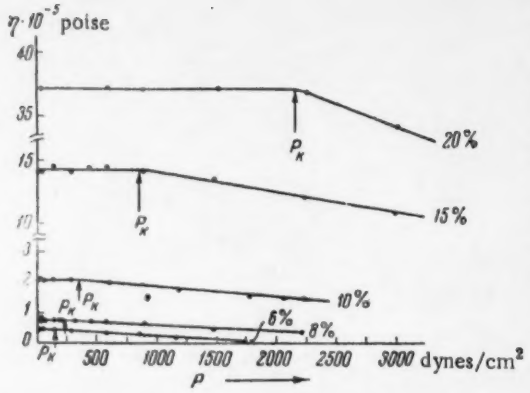

Fig. 1. The η (P) relation for 6-20% oleogels of aluminum naphthenate in decalin. The arrows indicate the values of the lower limit of structural stability, P_k.

From Figs. 1 and 2 it is completely clear that under all of the investigated oleogel concentrations, the viscosity diminishes at higher P and $\dot{\epsilon}$ values after having been constant over the low range of P and $\dot{\epsilon}$. It also follows from Fig. 1, that, with increasing gel concentration, there is a pronounced rise in the value of the maximal constant viscosity η_1 = const, and the lower stability limit P_k. Because of their inherently low relaxation rates, Y_{rel} [5], not all of the structural elements succeed in relaxing at a given value of $\dot{\epsilon}$ when $P > P_k$, but break down as the development of deformation moves along the P (τ) curve up to the point where $P = P_s$ [2]. This, together with the orientation of the particles in the flow, leads to a diminution of the viscosity in the region $P > P_k$.

The increase in the lower limit of structural stability, P_k, with increasing C can be explained by the rise in the number of local (cross) linkages in the structural lattice of the gel, increase in concentration resulting in a pronounced rise in the number of these interlocks per unit volume of the system and in the degree of interaction between the thread-like high polymer particles of the aluminum naphthenate. It is natural that an increase in the number and strength of the bonds existing between the structural elements of the gel lattice should lead to an increase in the shear strength necessary for initiating the breakdown of the system's structural bonds.

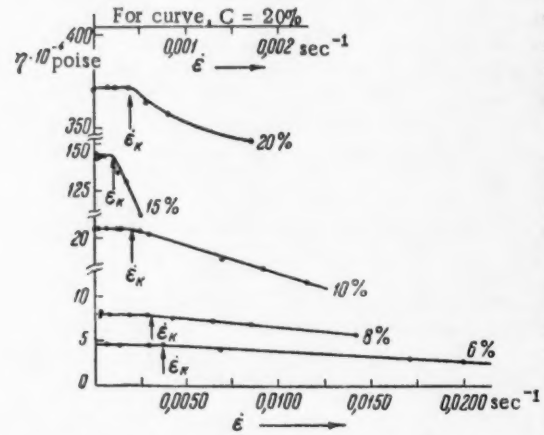

Fig. 2. The η ($\dot{\epsilon}$) relation for 6-20% oleogels of aluminum naphthenate in decalin. The arrows indicate values of $\dot{\epsilon}_k$ corresponding to P_k.

An increase in P_k with rising C, analogous to that which we have reported in [2] and similar to that described above, has also been found in hydrosuspensions of bentonite clays [4]. This once again underscores the earlier proposal [1, 2] for describing liquid-like and solid-like systems in terms of general parameters.

It is to be seen from the curves of Fig. 2 that the η (P) and the η ($\dot{\epsilon}$) relations are formally similar, even though they are fundamentally different. With increasing C, the value of $\dot{\epsilon}_k$ does not increase, but diminishes. The diminution of $\dot{\epsilon}_k$ with increasing C obviously results from the fact that the rate of true relaxation of elastic loading of the system diminishes, on the whole, with an increase in the concentration of the oleocolloid. The lower the value of the system's relaxation rate, the less is the likelihood that the system can succeed in relaxing all of its strained bonds at fixed deformation rate and the lower the value of $\dot{\epsilon}$ which it can sustain without structural breakdown.

Especial interest attaches to the regularities existing between our measured values of P_k, $\dot{\epsilon}_k$ and C. The corresponding curves are shown in Fig. 3. In Fig. 4 the same relations are plotted in semilogarithmic coordinates.

It is to be seen from Fig. 4 that both relationships (log P_k vs C, and log $\dot{\epsilon}_k$ vs C) are well described by straight lines of almost identical slopes. This indicates that the powers of the exponents are here practically identical, differing only in regard to sign:

$$P_к = P_{к_1} e^{\alpha(C-C_1)} \text{ and } \dot{\varepsilon}_к = \dot{\varepsilon}_{к_1} e^{-\alpha_1(C-C_1)},$$

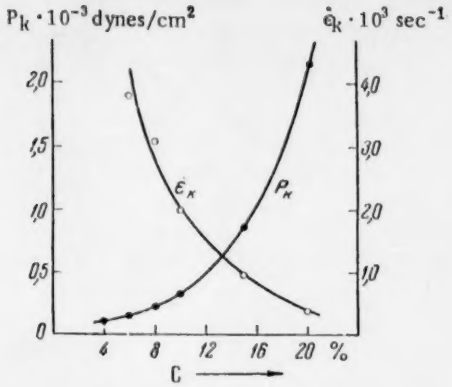

Fig. 3. The variation of the lower limit of the structural stability, P_k, and of the corresponding critical velocity gradient, $\dot{\epsilon}_k$, with the concentration of the oleogel.

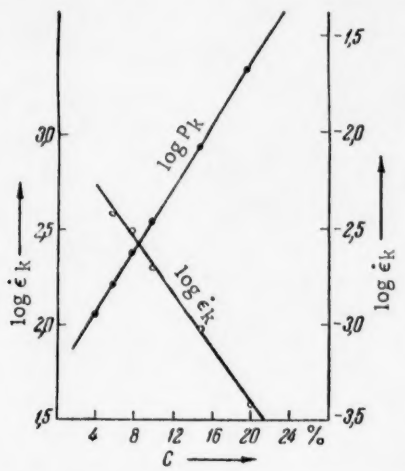

Fig. 4. The dependence of log P_k on C, and of log $\dot{\epsilon}_k$ on C, for oleogels of aluminum naphthenate in decalin.

C_1 is a certain arbitrary concentration and $\alpha \approx \alpha_1$. It follows that there is an internal relation between P_k and $\dot{\epsilon}$. In actuality, the equations presented above show that the product of the corresponding quantities have a fixed value which is independent of C:

$$P_к \dot{\varepsilon}_к = P_{к_1} \cdot \dot{\varepsilon}_{к_1} = W_к = \text{const.}$$

The product of the value of P required for maintaining stationary flow and the corresponding value of $\dot{\epsilon}$ represents the current strength per unit volume of the body, or the energy dissipation. Thus over the concentration interval from 6 to 20%, the critical energy dissipation is independent of the C value of the gel (for a given aluminum naphthenate). As is to be seen from the data of Table 1, the value of W_k actually increases somewhat with increasing C, a fact which is related to the small difference between α and α_1, but for changes of P_k and amounting to 10-13 fold, the alteration in W_k is very minute.

It might be supposed that the independence of W_k and C is a reflection of the fact that on increasing W_k identical bonds in the gel begin to break down at various values of C. In other words, that the increase in the total number of bonds per unit volume of system which accompanies a rise in concentration must be compensated for by a corresponding diminution in $\dot{\epsilon}$ so that during the deformation of the system in stationary flow it is possible to completely reestablish a definite number of bonds in unit time. Thus, the value of W_k might be used for interpreting the minimum rate of bond re-establishment. Earlier, there was developed [5] the concept of sets of aluminum naphthenate gels bonds possessing various values of $\dot{\epsilon}_{ki}$ and ϑ_i and various rates of regeneration. It can be supposed that the constancy of W_k is determined by the shortest elements of structure, these showing the smallest values of $\dot{\epsilon}_{ki}$ and being most slowly regenerated. The weak increase of W_k with C which is actually observed can probably be related to a certain intensification of the interaction of the closely neighboring aluminum naphthenate chains.

The concept of a critical strength has also been used by Ramaiia in the treatment of his data on the viscosimetry of oils [6]. The constancy of $P_k \cdot \dot{\epsilon}_k$ under varying oil temperature was noted by him. Although our experimental materials and methods of investigation have been quite different from those employed by Ramaiia, the close concordance of the independently obtained results deserves attention and confirms the importance of the idea of a critical strength.

TABLE 1

C, %	P_k dynes · cm^{-2}	$\dot{\epsilon}_k$ 10^3 sec^{-1}	$W_k = P_k \cdot \dot{\epsilon}_k \cdot 10^3$ erg · cm^{-3} · · sec^{-1}
6	160	3.8	607
8	240	3.1	744
10	350	2.0	700
15	860	0.98	844
20	2160	0.40	864

LITERATURE CITED

[1] A. A. Trapeznikov, Colloid J. 12, 67 (1950); Sympos., New Methods of Phys.-Chem. Investigation of Surface Phenomena 1, 20, 1950; Reports of the Second All-Union Conference on Colloidal Chemistry, Kiev 1952.

[2] A. A. Trapeznikov and V. A. Fedotova, Proc. Acad. Sci. USSR 81, 1101 (1951); 82, 97 (1952); Reports of the Third-All-Union Conference on Colloidal Chemistry, Acad. Sci. USSR Press, 1956.

[3] A. A. Trapeznikov and G. V. Belugina, Proc. Acad. Sci. USSR 87, 635, 825 (1952); 94, 97 (1954).

[4] L. A. Abduragimova, P. A. Rebinder and N. N. Serb-Serbina, Colloid J. 17, 184 (1955).

[5] A. A. Trapeznikov , Proc. Acad. Sci. USSR 102, 1177 (1955); Colloid J. No. 3 (1958).

[6] K. S. Ramaiia, The Anomaly in the Viscosities of Oils and its Influence on the Friction in Machines (in Russian) 1949.

Received December 26, 1957

ELECTROCAPILLARY MOVEMENT IN MOLTEN SLAGS

V. V. Khlynov and O. A. Esin

(Presented by Academician A. N. Frumkin, January 2, 1958)

Metal is lost in the slags from the metallurgy of the light metals, not only by solution, but also, and principally, by the formation of suspensions of both fine and coarse droplets [1]. The dissolved metal can be extracted by electrolysis [2], but in view of the high concentration and mobility of the slag ions [3], it is very unlikely that there is any possibility of the removal of these droplets by electrophoresis.

In aqueous solutions, however, a number of investigators have observed [4-7] the so-called electrocapillary motion, i.e., the displacement of mercury droplets in electrolytes under the action of an electric field. A quantitative theory of these phenomena has been given by Frumkin and Levich [8-10]. From this theory it follows that there is a good possibility of the electrocapillary movement in slags since the liquid metals and sulfides with which they are loaded are electrically charged [11, 12].

In conformity with these ideas, we have observed at temperatures of 1370-1500°C the movement of droplets of Cu, Ni, Mn, Ag, and Ni_3S_2 along the surface of a slag containing 52% CaO, 41% Al_2O_3, and 7% SiO_2 toward a definite electrode.

A π-shaped tube of fused magnesia was completely filled with molten slag so that the depth of the latter in the horizontal canal amounted to 3 mm. Graphite leads were introduced into the lower part of the vertical canals through special inclined housings. A droplet whose diameter of 0.5-3 mm had been previously determined, was carefully deposited on the slag surface. This droplet did not run off (FeS was an exception), nor did it sink into the surface. Subsequently, the dimensions of the droplet were checked in the tube with the aid of a telescope fitted with an measuring eyepiece. On passage of a direct current (0.5-5 amp) the droplet was displaced along the horizontal canal and the time of its movement was determined with a stop watch. By changing the direction of the current, it was possible to make the droplet move in the one direction or the other an indefinite number of times. In a series of experiments employing liquid Ni_2S_3 electrodes with graphite leads, it was possible to observe the simultaneous movement of a large number (20-30) of droplets of various dimensions (from 0.5 to 3 mm).

In agreement with the theory, such movement was not observed with solidified metallic droplets or with pieces of solid magnesium oxide. This detail, together with the rate of movement of the liquid droplets, indicated the displacement to be electrocapillary, rather than electrokinetic, in nature. The rate of displacement (U) was directly proportional to the potential gradient (E) and depended on the composition and the dimensions (r) of the droplet, as well as on the nature of the atmosphere.

The results of experiments carried out in an oxidizing atmosphere are shown in Table 1. Values are also given for the specific mobility (v), i.e., the rate of displacement referred to unit potential gradient and to unit radius.

In view of the fact that metallic nickel and nickel sulfide moved in opposite directions, it was of interest to determine the sulfur concentration corresponding to zero displacement rate. Experiments which were carried out at gradients E = 5-6 v/cm showed that decreasing the S content of Ni–S melts from 26% (Ni_2S_3) to 0.4% was practically without influence on the mobility. In all likelihood, this comes about from the high capillary activity of sulfur which results in the composition of the surface layer of the droplet remaining constant despite a marked alteration in its bulk composition. This type of behavior is in agreement with the fact

that the surface tension of nickel (σ_{Ni} = 1756 ergs/cm² [13]) is strongly depressed by the addition of sulfur ($\sigma_{Ni_2S_3}$ = 452 ergs/cm² [14]). A further decrease in the sulfur concentration caused a diminution of the mobility, which at 0.15% S reached zero value and then changed sign, i.e., the droplet was displaced toward the cathode, as were metals.

Thus, at low sulfur concentrations, the surfaces of Ni–S alloys are positively charged, whereas at high and medium concentrations their charge is negative. This last agrees with earlier obtained electrocapillary curves [12] and indicates the double layer to be formed here as the result of the transfer of cations from the metal into the slag:

$$Me \rightarrow Me^{2+} + 2e. \qquad (1)$$

In reducing atmosphere, or more exactly, on blowing a mixture of nitrogen and hydrogen (72% N_2 and 28% H_2, traces of O_2 not being excluded) through the cell, the Ni_2S_3 was displaced toward the anode, as before, and with the same velocity. With nickel, on the other hand, the mobility of the metallic droplets diminished to zero, and with copper and silver the mobility changed sign, becoming equal to 0.8 and to 20 cm/sec · v, respectively. This clearly resulted from the following causes.

TABLE 1

Metal	E (v/cm)	r (cm)	U (cm/sec)	v (cm/sec · v)	Direction of movement
Cu	2,3	0,07	5,8	36	To cathode
Ni	2,0	0,05	2,8	28	" "
Mn	2,8	0,075	6,3	30	" "
Ni_3S_2	2,3	0,05	4,8	42	To anode
Ni_3S_2	6,6	0,025	7,5	46	" "
Ni_3S_2	6,6	0,05	15	46	" "
Ni_3S_2	6,6	0,075	15	30	" "
Ni_3S_2	6,6	0,16	6	5,7	" "

Whereas the composition of the sulfides remains practically unaltered, the metallic droplets can undergo partial oxidation or reduction, depending on the composition of the atmosphere. In the presence of O_2, the slag layer in the neighborhood of the droplet is enriched with MeO* and the formation of the double layer can proceed by a transfer of the Me^{2+} cations from the slag into the metal.

$$Me^{2+}_{(slag)} + 2e \rightarrow Me. \qquad (2)$$

There is not to be excluded the possibility that the reverse movement occurs in the oxygen which is dissolved in the drop:

$$O_{(met)} + 2e \rightarrow O^{2-}_{(slag)} \qquad (3)$$

Both of these processes lead to the appearance of a positive charge on the droplet surface. In an atmosphere containing hydrogen, the latter partially reduces the oxide MeO, this reduction being the more nearly complete the more noble the metal. For this reason, with copper and silver the concentration of the oxides in the nearest neighboring slag layers becomes so low that the transfer of the cations from the metal into the slag, (1), begins to predominate over the reverse process (2), and in the less noble metal, nickel, the rates of these two reactions become equal.

For a quantitative comparison of the theory of electrocapillary movement with the results of our measurements, the specific mobilities of the Ni_3S_2 droplets (v = U/Er) were calculated from the equation of Frumkin and Levich [9].

* The moving droplet leaves behind a dark track which gives evidence of the appearance of MeO in the slag.

$$U = \frac{\varepsilon E r}{2\eta + 3\eta' + \frac{\varepsilon^2}{\varkappa}}, \tag{4}$$

which is valid when

$$Er \ll \varepsilon / C. \tag{5}$$

Here η and η' are the viscosities of the metal and of the slag, κ is the electrical conductivity of the latter and ϵ and C are the specific charge and the capacity of the double layer.

In the case which is under consideration, $\epsilon = 15 \cdot 10^{-6}$ coul/cm^2 [12], C = 15 μ f/cm^2 [15], $\eta \cong 15$ poise [16], and $\kappa \cong 0.5$ ohm^{-1} cm^{-1}, according to our rough measurements. Since for us $\epsilon^2/\kappa \ll 2\eta$ and $\eta' \ll \eta$, Equation (4) gives

$$v = \frac{\epsilon}{2\eta} \tag{6}$$

The inequality (5) is valid for Ni_2S_3 droplets with $\underline{r} < 0.15$ cm when E = 6.6 v/cm. As is to be seen from Table 1, however, deviations begin for Ni_2S_3 droplets of somewhat smaller radii.* At $\underline{r} \cong 0.075$ cm, the rate of displacement U ceases to increase with increasing $\underline{r}$, and sharply diminishes at $\underline{r} = 0.16$, facts which are in contradiction to Equation (4). In this connection, for comparison with the theory, there were taken the mobilities v_{exp} = 42-46 cm/sec · v, the calculations according to Equation (6) giving v_{theo} = 50 cm/sec · v.

The concordance between the order of magnitude of v_{exp} and v_{theo} once more confirms that the observed displacements represent an electrocapillary movement of the droplet over the surface of the slag. Concerning the quantitative difference between these two terms, it can be said that it arises, principally, from the simplifying assumptions which were introduced in the derivation of Equation (4). In particular, the rate of movement would be lowered, as Frumkin and Levich have shown [9], by taking the incomplete polarizability into account, i.e., in our case, v_{theo} would approach v_{exp}. It should also be considered that Equation (4), and the quantities η and κ which enter into it, refer to droplets moving within a liquid rather than on its surface.

LITERATURE CITED

[1] V. I. Smirnov, The Metallurgy of Copper and Nickel (in Russian) Sverdlovsk-Moscow, 1950, pp. 67, 523.

[2] O. A. Esin, N. P. Diev, L. L. Chermak and S. E. Liumkis, Patent No. 107869, 15 VII, 1957.

[3] O. A. Esin, J. Phys. Chem. 30, 3 (1956).

[4] C. Christiansen, Ann. Phys. (4) 12, 1072 (1903).

[5] A. N. Frumkin, J. Russ. Phys.-Chem. Soc. 49, 207 (1917).

[6] S. R. Craxford, Phyl. Mag. 16, 268 (1933).

[7] I. A. Barotskaia, J. Phys. Chem. 23, 1231 (1949).

[8] A. N. Frumkin, Bull. Acad. Sci. USSR, Div. Chem. Sci. 1945, 223.

[9] A. N. Frumkin and V. G. Levich, J. Phys. Chem. 19, 573 (1945).

[10] V. G. Levich, J. Phys. Chem. 21, 689 (1947).

[11] O. A. Esin, Iu. P. Nikitin and S. I. Popel', Proc. Acad. Sci. USSR 83, 431 (1952).

[12] Iu. P. Nikitin and O. A. Esin, Proc. Acad. Sci. USSR 107, 847 (1956).

[13] V. I. Smirnova and B. F. Ormont, Proc. Acad. Sci. USSR 82, 751 (1952).

* It is possible that this results from the second requirement of the theory, which is that $R_e = Ur/\nu$ should be less than unity. Here $\nu = \eta/\rho$, and ρ is the density of the slag, which is approximately equal to 3 g/cm^3 [17].

[14] I. T. Sryvalin, O. A. Esin and Iu. P. Nikitin, Bull. S. M. Kirov Ural Polytech. Inst. Coll. 49, 95 (1956).

[15] Iu. P. Nikitin and O. A. Esin, Proc. Acad. Sci. USSR 111, 133 (1956).

[16] V. V. Mikhailov and S. G. Bratchikov, Bull. S. M. Kirov Ural Polytech. Inst. Coll. 67, 70 (1957).

[17] S. I. Popel', N. N. Krasovskii, O. A. Esin and Iu. P. Nikitin, ditto, 49, 77 (1954).

The S. M. Kirov Ural Polytechnic Institute

Received October 15, 1957

THE DETERMINATION OF POLAROGRAPHIC DIFFUSION COEFFICIENTS BY THE USE OF THE ROTATING DISK ELECTRODE

V. D. Iukhtanova

(Presented by Academician A. N. Frumkin, August 28, 1957)

In view of the fact that there is at the present time a lack of trustworthy data on the so-called polarographic diffusion coefficients, i.e., on diffusion coefficients measured in the presence of an excess of a foreign electrolyte, it has been the aim of the present work to determine these coefficients by the accurate and comparatively simple method of the rotating electrode.

The following expression for the diffusion coefficient results from the theory of convectional diffusion at the rotating disk electrode, as developed by V. G. Levich [1]:

$$D^{2/3} = \frac{1{,}62\, i \nu^{1/6}}{FnC\sqrt{\omega}}, \qquad (1)$$

i being the current density; ω, the angular velocity; c, the concentration in the body of the solution of the ion which is undergoing reduction; ν, the kinematic viscosity and n, the number of electrons participating in the reaction.

Making use of the Levich equation, we have calculated the diffusion coefficients of the ions: Cd^{2+}, Tl^{+}, Pb^{2+} and Zn^{2+}. This work was carried out with the aid of an amalgamated copper electrode which had the form of a disk (diameter, 4.997 ± 0.002 mm). Prior to experiment, this electrode was amalgamated for twenty-four hours; it was then polished, washed in double-distilled water and immersed in mercury for 2 hours. The electrode potential was measured against a normal calomel electrode, using a standard potentiometer circuit. The experiments were carried out in a hermetically sealed cell, in an atmosphere of hydrogen. The capacity of the cathode compartment of the cell was equal to 80 ml; into a side-arm there was inserted the platinum anode which was separated from the cathode space by a stop-cock. The determinations were carried out at t = 25 ± 0.1°. The rate of rotation of the electrode was usually 600-1000 rotations/min., but a lower rate was employed in one series of experiments. All solutions were prepared, either from salts which had been twice recrystallized, or by dissolving the pure metals. The salt for the background underwent an additional purification for 4-5 hours on platinum gauge in an atmosphere of hydrogen. The concentrations of the solutions which were employed were, as a rule, 10^{-3}–10^{-4} moles/l in the reducible ion.

The polarization curves which were constructed from the experimental data on the ions Cd^{2+}, Tl^{+}, Pb^{2+} and Zn^{2+} have well defined regions of limiting current and from these the limiting diffusion currents were calculated. By way of an example, the polarization curve of Pb^{2+} is given in Fig. 1. Over the entire range of the measurements, a proportionality is observed between the limiting current and the concentration of the ions which are undergoing reduction, the data showing good reproducibility. Into the results there was introduced a correction for the background current, this being less than 1% of the total current.

In Table 1, data are presented on the diffusion coefficients of Cd^{2+}, Tl^{+}, Pb^{2+} and Zn^{2+} against a background of KCl, comparison being made with the data of other authors. These coefficients are expressed in $cm^2/sec \cdot 10^{-6}$.

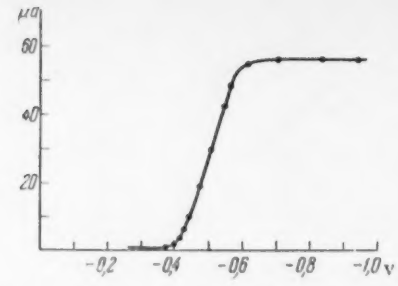

Fig. 1. Polarization curve for the reduction of lead ion against a 1 N KCl background, c = $3.27 \cdot 10^{-4}$ mole/l.

It is clear from Table 1 that the values of the diffusion coefficients which were determined with the rotating disk electrode are in good agreement with those obtained by Stackelberg by the Cottrel method, or with those calculated from the Il'kovich equation through the introduction of the corresponding semiempirical corrections (data designated by stars); the divergence does not exceed 2%. The divergences are somewhat greater in the case of the diffraction micromethod.

In the case of the ions of Zn^{2+} and Tl^{+}, the diffusion coefficients were also measured over a wide range of background concentrations. In order to have a more detailed comparison with the data which have been obtained by Mitska with the dropping electrode [5], the diffusion coefficients of the zinc ion were determined against a $KClO_3$ background ranging over the interval of concentrations from 0.6 to 0.01 N.

In Fig. 2 there is shown the dependence of the diffusion coefficient of Zn^{2+} on the square root of the background concentration ($KClO_3$). It is to be seen from this figure that at the higher $KClO_3$ concentrations, the diffusion coefficient increases with a rise in the background concentration. Exactly this same dependence of the diffusion coefficient on the concentration of the background has been observed by Stackelberg who explained the increase in terms of complex formation.

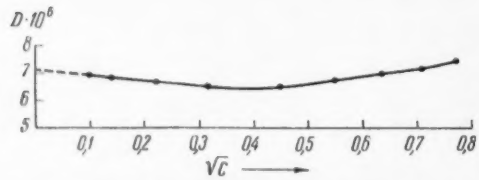

Fig. 2. The dependence of the diffusion coefficient of Zn^{2+} on the square root of the background ($KClO_3$) concentration. c is expressed in moles/l.

At the lower $KClO_3$ concentrations, the value of the diffusion coefficient diminishes with an increase in the background concentration, a fact which is obviously related to the action of the interionic forces. Points lying in the region of low background concentrations (beginning with 0.1 N $KClO_3$, and below) fall on a straight line which, on extrapolation to infinite dilution, gives the value Dex = $7.10 \cdot 10^{-6}$ cm^2/sec for the diffusion coefficient, a result which is in good agreement with that calculated from the Nernst Equation for infinite dilution, using the mobility λ 52.8; namely D = $7.04 \cdot 10^{-6}$ cm^2/sec. Comparing the data on the diffusion coefficients of zinc as determined on the rotating electrode, with the polarographic coefficients of diffusion obtained by Mitska, we see that there is a fundamental difference both in the values of the coefficients (his lying above those obtained by us) and in the dependence of these values on the background concentration. According to the figures of Mitska, the diffusion coefficient increases with the background concentration over the entire concentration range. As he has carried it out, extrapolation to infinite dilution somewhat corrects for experimental errors, but leads, none the less, to the value D = $7.6 \cdot 10^{-6}$ cm^2/sec, which is clearly too high.

TABLE 1

Ion	Normality of KCl background	Rotating electrode method	Nonstationary diffusion in a capillary [2]	Diffraction micromethod [3, 4]
Cd^{2+}	1	7,72	7,89	7,16
	0,1	7,07	7,16	6,58
Tl^{+}	1	15,28	15,67*	
	0,1	17,52	17,44*	
Pb^{2+}	1	8,95	9,17	8,06
	0,1	8,60	8,69	8,12
Zn^{2+}	1	7,30	7,23*	7,54
	0,1	6,62	6,73*	6,41

In order to be convinced of the validity of the theory of the influence of complex formation on the value of the diffusion coefficient, these experiments were repeated with the Tl^{+} ion, which shows less inclination to complex formation than does Zn^{2+}. The diffusion coefficients were measured against a background of sodium perchlorate. These measurements were extended into the region of high background dilution, going down to c = $2 \cdot 10^{-4}$ N with a Tl concentration of 10^{-4} N. The determinations were carried out at low rates of rotation of the electrode (130-150 rot/min) in order to avoid the ohmic potential drop which distorts the form of the polarization curve. Into the calculations there was introduced a correction for migration, the diffusion current, i_d, being determined from the observed current, i, by the equation *

* This equation is obtained from formulas which are derived in [7], expansion being carried out in powers of c_0/c and the first three members retained.

$$i = i_d\left[1 + \frac{1}{4}\frac{c_0}{c} - \frac{1}{8}\left(\frac{c_0}{c}\right)^2\right],$$

c_0 being the concentration of the discharging cation and $\underline{c}$, the concentration of the background. In addition a correction was introduced for the concentration change which accompanied the process; this did not exceed 1%.

In Fig. 3 there is shown the dependence of the diffusion coefficient of thallium on the square root of the background concentration. It is to be seen that, in this case, the diffusion coefficient continuously falls as the background concentration increases. The first score of points lie nicely on a straight line which, when extrapolated to infinite dilution, gives $D = 19.90 \cdot 10^{-6}$ cm^2/sec. The diffusion coefficient for the Tl^+ ion as calculated from the Nernst Equation for infinitely dilute solutions with the mobility $\lambda = 74.7$ [6] at 25°, is equal to 19.94, 10^{-6} cm^2/sec.

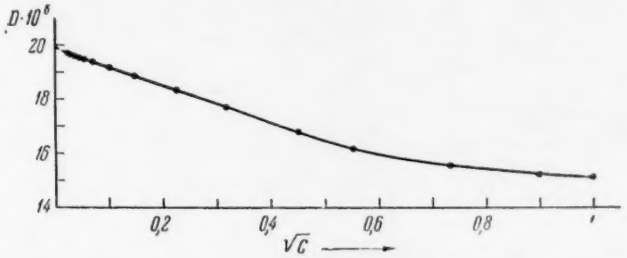

Fig. 3. The dependence of the diffusion coefficient of Tl^+ on the square root of the background ($NaClO_4$) concentration. $\underline{c}$ is expressed in moles/l.

The good agreement between the extrapolated values of the diffusion coefficients and the values calculated from the Nernst Equation speaks for the suitability of the rotating electrode method for the exact determination of the polarographic diffusion coefficients.

I express my deep thanks to Academician A. N. Frumkin for his continued interest in this work and for valuable remarks during the discussion of the results, and I also thank A. I. Fedorova for aid in carrying out the operations.

LITERATURE CITED

[1] V. G. Levich, Physicochemical Hydrodynamics (in Russian), 1952; A. I. Fedorova. Report at the Fourth Conference on Electrochemistry, Moscow, 1956.

[2] H. Stackelberg, H. Pilgram and V. Toome, Zs. Elektrochem. 57, 342 (1953).

[3] Ia. P. Gokhshtein, J. Phys. Chem. 31, 404 (1957).

[4] Ia. P. Gokhshtein, J. Phys. Chem. 30, 1584 (1956).

[5] K. Micka, Chem. Listy 50, 203 (1956).

[6] B. Conway, Electrochemical Data, 1952, p. 145; E. Potter, Electrochemistry, 1956, p. 125.

[7] A. Eucken, Zs. phys. Chem. 59, 72 (1907).

Received September 27, 1957

THE ADSORPTIVE PROPERTIES OF ALUMINOSILICATE CATALYSTS AND THEIR DEPENDENCE ON COMPOSITION

M. M. Egorov, Iu. A. Zarif'iants, V. F. Kiselev and K. G. Krasil'nikov

(Presented by Academician M. M. Dubinin, January 15, 1958)

The marked influence of the degree of surface hydration on the adsorptive properties of unit silica surface in regard to the molecules of water and methyl alcohol has been pointed out earlier [1-4]. This dependence is not a single valued function of the temperature of treatment of the specimen but depends on a number of factors including the crystal-chemical details of the specimen's structure and the magnitude of its specific surface. It has proven to be of interest to extend these investigations to a series of aluminosilicates which differ in composition but which have surfaces containing hydroxyl groups just as does silica [5], i.e., to study the extent to which the replacement of silicon atoms by aluminums in the aluminosilicate structures [6] would be reflected in the degree of the surface hydration and in the adsorptive properties of the surface.

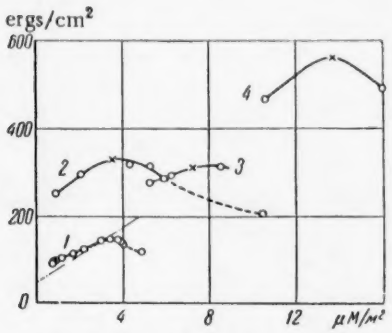

Fig. 1. The heat of wetting with water and its dependence on the amount of structural water in silica gel K-2 (1), and in aluminosilicates containing 15% (2), 30% (3) and 50% (4) Al_2O_3. Data for specimens which had been treated at 300° are designated by crosses.

As the first step in these investigations, we have studied the adsorption of water vapor and methyl alcohol, and the heat of wetting by water, of synthetic aluminosilicate catalysts containing 15% (Houdry catalyst), 30%, and 50% Al_2O_3. Prior to the experiments, these specimens were washed with redistilled water and then treated in air for 24 hours at each of the indicated temperatures. The specific surface of each specimen was evaluated from the nitrogen adsorption isotherm by the BET method. The technique of preparing the specimens for the determination of the heats of wetting, and that of the measurements of the adsorption and the specific surface, were the same as in [1-4, 7]. The adsorption measurements were carried out in an adsorption apparatus with quartz spiral balances; the determinations of the heats of wetting, in a calorimeter with constant heat interchange and a temperature sensitivity of $5 \cdot 10^{-5}$ °C. Structural water was estimated from the loss on calcination [1] (Table 1).

For each of the investigated aluminosilicates, the heat of wetting by water and its dependence on the amount of structural water are shown in Fig. 1. Just as in the case of the silica gel (Curve 1), these curves have maxima which correspond to a preliminary thermal treatment at 200-300°. The heats of wetting of unit surfaces of the aluminosilicates by water prove, however, to be higher than that of the silica gel [1]. The considerable quantity of structural water, especially in the specimens having a high Al_2O_3 content, is noteworthy. In this case, it is possible that a part of this water enters not only into the surface hydrate, but into the bulk compound, as well. By comparing points which were obtained for specimens treated under similar conditions, at 300°C, for example, it can be seen that there is an approximate two-fold difference between the heats of wetting of silicagels and aluminosilicates with low Al_2O_3 contents (15%) even at approximately identical surface hydrations.

Isotherms for the adsorption of water vapor and methyl alcohol were studied on these same specimens. The initial sections of the resulting isotherms are shown in Figs. 2 and 3. In conformity with the data on the heats of wetting, the isotherms for the initial adsorption and desorption* of water vapors indicate that the higher adsorptions are given by the aluminosilicates with the higher Al_2O_3 contents. In distinction to silica gel [3], a comparison of the isotherms which are presented in Fig. 2 shows that for each specimen the curve for desorption lies considerably below that for adsorption. This is clearly related to the fact that the irreversible adsorption of water is extensive in the case of the aluminosilicates (Table 1), desorption proceeding from a surface whose energy is less than that of the original surface, as is to be seen from Fig. 1. A similar phenomenon is not observed with silica gel, the irreversible adsorption of water on specimens which have been treated at 300° being very small [3]. The adsorption isotherms for methanol vapors were obtained on specimens which had been hydrated at $p/p_s = 1$ and then degassed at 250°. The data presented in Fig. 3 show adsorption differences which are less than in the case of water vapor, although the sequence of the isotherms is maintained. In each instance, the adsorption isotherm for methanol vapor differs from that obtained on silica gel, this being true even for specimens with low Al_2O_3 contents (15%).

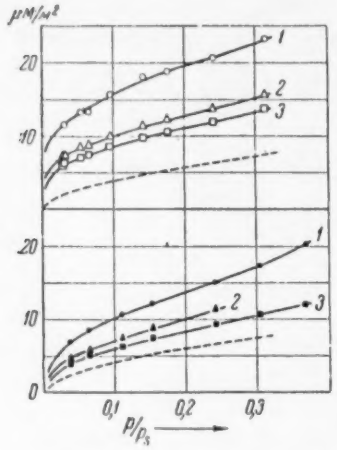

Fig. 2. Isotherms for the adsorption (open points) and the desorption (full points) of water vapor on aluminosilicates containing 50% (1), 30% (2) and 15% (3) Al_2O_3. The dotted curves show the corresponding isotherms for silica gel [3].

In their structure, the aluminosilicates are closely related to silica, the SiO_4 tetrahedral in the lattices of these compounds being capable of isomorphic replacement by AlO_4 [6] to form other structures which are either disordered or, in the case of many natural aluminosilicates, layered. On the surface, the hydroxyl groups are bound to the Si atoms as well as to the Al atoms [8, 9]. The chemical properties of these groups are different from those of the similar groups of silica. The water which is contained in the aluminosilicates may be more "acidic" in its properties than the original oxides, SiO_2 and Al_2O_3 [6], a fact which is supported by work on the ion exchange properties of these substances. There are also indications that into the structure of the aluminosilicate surfaces there may enter OH groups whose chemical function is of more "basic" type [10]. Thus, aluminosilicate surfaces are more heterogeneous than a silica surface. The composition of aluminosilicate surfaces and, in particular, the degree of their hydration, depend on their previous history and type of treatment: in all likelihood it is through these facts that there is to be explained the difference in the hydration of our specimens as compared with those which were studied in [10]. As our data shows, there is a difference in the energetic and adsorptional properties of silica surfaces and of surfaces of aluminosilicates even when these have been prepared under completely similar conditions. Clearly, these differences relate to the hydrated, as well as the dehydrated, portions of the surfaces of these adsorbents.

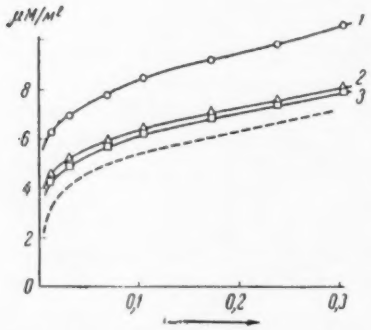

Fig. 3. Isotherms for the adsorption of methanol vapor on aluminosilicates containing 30% (1) and 15% (2) Al_2O_3. The dotted curve shows the isotherm for silica gel [3].

*For ease of comparison, the desorption isotherms have been carried to zero, i.e., the value of the irreversible water sorption has been subtracted from each ordinate.

On the basis of the correspondence between the "absolute" adsorption isotherms for methanol vapors on silica gel and on aluminosilicates containing 10-20% Al_2O_3 [11, 12] and the isotherms for the adsorption of benzene vapors on natural materials which are of similar composition [14], and the agreement among the values of the "absolute" heats of wetting of these adsorbents, the authors of [11, 13, 14] draw the conclusion that "the physical adsorption of methanol vapors is quite indifferent to the atoms which lie under the surface hydroxyl groups and oxygen atoms, whether these be atoms of aluminum or silicon" [11], this adsorption being determined by the interaction of the alcohol molecules with the OH groups or the oxygen atoms. From our point of view such conclusions are unjustified.* It is impossible to reduce the consideration of the mechanism of adsorption to the mere interaction of the adsorbed molecules with the active centers, no account being taken of the topography or the concentration of these centers on the surface or of the affect of the stochiometric composition and structure of the bulk phase on the energetic properties of the surface. In those cases where the interaction of the molecules with the adsorption centers is determined by the forces, not only of physical, but of chemical adsorption, including hydrogen bonding, as well, the adsorbent and the adsorbed molecules should be considered [16] as a single quantum mechanical system whose adsorptive properties are very sensitive to various defects in the adsorbent's structure, together with the variation in the concentration and the nature of the accidentally existing, or designedly introduced, additives. The chemosorbed molecules themselves should be numbered among the latter.

TABLE 1

Adsorptive Characteristics of Aluminosilicate Catalysts

Content of Al_2O_3	Temperature of calcination, °C	Specific surface, m^2/g	Heat of wetting, ergs/cm^2	Content of structural water, μ moles/m^2	Irreversible sorption of water after degassing, μ moles/m^2	
					at 20°	at 250°
15	300	257	330	3,62	7,92	0,61
30	300	496	310	7,3	8,31	0,56
50	300	357	518	12,6	14,5	1,34

The authors express their deep thanks to B. V. Il'in for his support of this work and to K. V. Topchieva for continued interest in the work and for having furnished the specimens.

LITERATURE CITED

[1] M. M. Egorov, K. G. Krasil'nikov and E. A. Sysoev, Proc. Acad. Sci. USSR 108, 103 (1956).**

[2] G. I. Aleksandrova and V. F. Kiselev, et al., Proc. Acad. Sci. USSR 108, 283 (1956).**

[3] M. M. Egorov, T. S. Egorova, V. F. Kiselev and K. G. Krasil'nikov, Proc. Acad. Sci. USSR 114, 579 (1957).*

[4] B. V. Il'in, V. F. Kiselev and K. G. Krasil'nikov, Bull. Mos. State Univ. No. 6 (1957).

*In determining the specific surfaces of their specimens from the experimental isotherms, the authors of [1] did not take into account the nature of the adsorbent surface and its effect on the adsorption and on the area occupied by the alcohol molecule [2, 4, 15]. a fact which would naturally be reflected in the resulting values of the specific surface. From a comparison of "absolute" isotherms determined in this way, it is impossible to draw conclusions concerning the uniform adsorptive properties of unit surfaces of these adsorbents. From this it also follows that the recommended procedure of determining the specific surfaces of silica gels and aluminosilicates from one point on the isotherm [11, 13] and from the "absolute" heats of wetting [12, 13] can lead to considerable error.

**Original Russian pagination. See C. B. Translation.

[5] A. N. Terenin, Sympos. The Surface Chemical Compounds and Their Role in Adsorption Phenomena (in Russian) (Moscow, 1957) p. 206.

[6] V. I. Vernadskii and S. M. Kurbatov, The Natural Silicates, Aluminosilicates and Their Analogy (in Russian) (1937).

[7] K. G. Krasil'nikov, V. F. Kiselev, N. V. Kapitonova and E. A. Sysoev, J. Phys. Chem. 31, 1448 (1957).

[8] R. K. Iller, The Colloid Chemistry of Silica and Silicates (N. Y., 1955).

[9] K. V. Topchieva, K. Yun-Pin and I. V. Smirnova, Sympos., The Surface Chemical Compounds and Their Role in Adsorption Phenomena (in Russian) (Moscow, 1957) p. 311.

[10] M. A. Kaliko, The Surface Chemical Compounds and Their Role in Adsorption Phenomena (in Russian) (Moscow, 1957) p. 155.

[11] A. V. Kiselev and N. M. Kamakin, Proc. Acad. Sci. USSR, 80, 393 (1951).

[12] N. M. Kamakin, A. V. Kiselev, Ia. V. Mirskii and I. I. Starostin, Petroleum Economy 9, 41 (1953).

[13] A. V. Kiselev, Methods for Investigating the Structures of Highly Dispersed and Porous Bodies (in Russian) (Acad. Sci. USSR, Press, 1953) p. 86.

[14] V. T. Bykov, Reports of the Scientific-Investigational Work of the Primorskii Section of the Mendeleev All-Union Chemical Society, Vol. 2, 61 (1953).

[15] V. A. Dzis'ko and V. N. Krasnopol'skaia, J. Phys. Chem. 26, 1841 (1952).

[16] F. F. Vol'kenshtein, Prog. Phys. Sci. 60, 249 (1956).

The Physics Faculty of the M. V. Lomonosov State University, Moscow

Received January 6, 1958

THE LUMINESCENCE SPECTRA OF THE COORDINATION COMPOUNDS OF URANYL NITRATE

G. I. Kobyshev and D. N. Suglobov

(Presented by Academician A. N. Terenin, March 18, 1958)

In the past, the photoluminesence of the uranyl salts has been very fully studied. In particular, the influence of the number of molecules of water of crystallization on the luminescence of uranyl nitrate has been treated in detail [1]. This spectrum has been ascribed to the electron transfer in the uranyl ion, onto which there is superposed the vibrations of the O – U – O group and the crystal lattice. It is clear, however, that the mere presence of the uranyl ion is an insufficient condition for the appearance of that structure in the luminescence spectrum which is characteristic of the uranyl salts. Thus, B. E. Gordon [2] pointed to the absence of luminescence in a uranyl nitrate which had been fully deprived of its water of crystallization. Katz and Gibson [3], having obtained especially pure specimens of anhydrous uranyl nitrate, noted the very weak luminescence of the powders of this salt as observed at 90°K, without, however, giving particular attention to it. In contradiction to these authors, A. N. Sevchenko, V. M. Vdovenko and T. V. Kovaleva [1], and later L. V. Volod'ko and A. N. Sevchenko [4], obtained discrete luminescence spectra of powders of anhydrous uranyl nitrate, in which there was observed that frequency interval between the separate lines which is characteristic of the uranyl salts. This result called forth objections, however, since the method of preparing anhydrous uranyl nitrate by the dehydration of the crystal hydrate in vacuum, which had been employed in these papers, is unsatisfactory. Salt specimens obtained in this manner are always heavily loaded with the products of partial decomposition, a fact which has been repeatedly pointed out earlier [2, 5]. Anhydrous uranyl sulfate [2, 6, 7] and the anhydrous chloride (according to our data) are similar to the anhydrous nitrate [2, 3] in that they do not show the discrete luminescence spectra which is characteristic of the uranyl salts.

According to M. Freymann and Chantrel [8], M. Freymann and R. Freymann [9] and Volod'ko and Sevchenko [4], on the other hand, the coordination compounds of uranyl nitrate with acetone, ethyl ether, dioxane, nitromethane and other molecules, clearly luminesce at the temperature of liquid air and have structured spectra, the exact structure of the bands which result from the crystal lattice vibrations having been studied in the last of these papers.

It can thus be presumed that the existence of a structured luminescence spectrum is not a specific property of the uranyl nitrate crystal hydrate, but arises from a more general effect, namely, the coordination of addenda molecules with the uranyl ion.

The luminescence spectra of anhydrous uranyl nitrate and its coordination compounds with various addenda have been studied in the present work, the aim being to elucidate the effect of coordination, and the influence of the properties of the addenda molecules. Luminescence spectra were obtained for microcrystalline powders of the following coordination compounds of uranyl nitrate: UN · $2H_2O$, UN · $3H_2O$, UN · $6H_2O$, UN · nHN_3, UN · · $2C_5H_5N$, UN · $2(C_2H_5)_2O$, UN · $2(C_4H_9)_2O$, UN · $2(C_2H_4Cl)_2O$, UN · $2O(CH_2)_4O$, UN · nC_2H_5OH, UN · $2CH_3CN$, UN · $2C_6H_5NO_2$, UN · $2CH_3NO$, UN · $2NO_2$, UN being used to designate $UO_2(NO_3)_2$. Mixed complexes of the compositions UN · $2H_2O$ · $2(C_2H_5)_2O$ and UN · $2H_2O$ · $2NO_2$ were also studied. Anhydrous uranyl nitrate was prepared by the method of Katz and Gibson [3], following the reaction $UO_3 + 3N_2O_4 \rightarrow UO_2(NO_3)_2 \cdot 2NO_2 + N_2O_3$. The resulting complex compound $UO_2(NO_3)_2 \cdot 2NO_3$ was then broken down in vacuum (10^{-5} mm of Hg) at 165°C with the formation of $UO_2(NO_3)_2$. The above enumerated complex compounds were obtained either by condensation of vapors of the addendum substance onto the anhydrous uranyl nitrate in vacuum or, when this was

possible, by saturation of the corresponding organic liquid with the anhydrous uranyl nitrate, followed by crystallization out of a supersaturated solution. The mixed complexes $UN \cdot 2H_2O \cdot 2NO_2$ and $UN \cdot 2H_2O \cdot 2(C_2H_5)_2O$ were prepared by the method described in [3, 10].

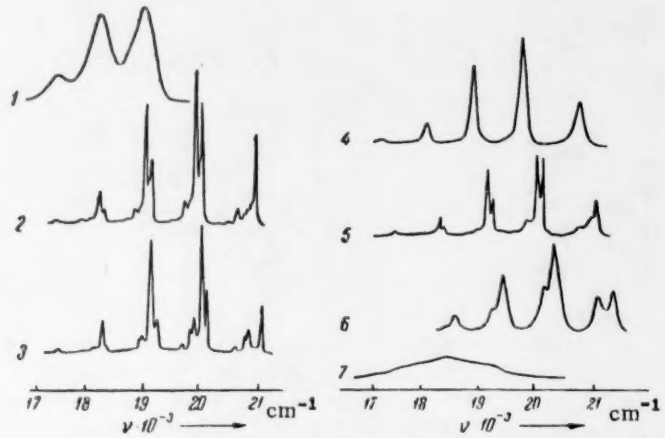

Fig. 1. The luminesence spectra of coordination compounds of uranyl nitrate. 1) $UN \cdot 2C_5H_5N$; 2) $UN \cdot 2(C_2H_5)_2O$; 3) $UN \cdot 2CH_3CN$; 4) $UN \cdot 2C_6H_5NO_2$; 5) $UN \cdot 2CH_3NO_2$; 6) $UN \cdot 2NO_2$; 7) Un.

The compositions of the resulting complex compounds were controlled by determining their content of uranium and water. Luminescence was excited by a PRK-4 mercury lamp using a UFS-4 filter. The spectra were recorded both photographically and photoelectrically on a ISP-51 spectrograph with a FEP-1 attachment. All of these luminescence spectra were obtained at a temperature of 77°K. The vibrational structures of the electron bands of the coordinated cations were investigated without resolving the finer structure resulting from the crystal lattice. The investigated specimen of uranyl nitrate did not show luminescence at room temperature and, in comparison with the crystal hydrate, luminesced very weakly at 90°K. As is to be seen from the spectrograms of Fig. 1, the luminescence spectrum of this anhydrous salt had the form of a wide band in the region from 4965 to 6100 A, with a maximum at 5455 A and a background in which other poorly expressed maxima can be noted. In distinction to the anhydrous uranyl nitrate, all of the above enumerated complex compounds in which the addenda were electron-donor molecules, luminesced clearly at 90°K (and certain of them, such as $UN \cdot 2NO_2$, $UN \cdot 2C_5H_5N$, $UN \cdot 2CH_3CN$, for example, even at room temperature) showed luminescence spectra with sharply defined vibrational structures such as are characteristic of the uranyl salts. Certain of these spectra are shown in Fig. 1. The vibrational frequency is determined in the basic uranyl ion and depends only slightly on the nature of the addendum. The uranyl nitrate amine which has a structureless luminescence spectrum, is an exception. On condensing NO, SO_2 or vaporous benzene or cyclohexane – substances which do not form vacuum-stable complex compounds with $UO_2(NO_3)_2$ on anhydrous uranyl nitrate, there was observed a regular diminution in the intensity of luminescence of the anhydrous compound at 90°K, and in some instances luminescence was almost completely lacking.

It follows from what has been said that the necessary condition for the existence of the structured luminescence spectrum which is characteristic of the uranyl compounds, is the coordination of the uranyl ion with electron-donor molecules so as to form a stable compound.

It should also be pointed out that with increasing donor properties of the addenda molecules, there was observed a regular displacement of the intensity maxima in the luminescence spectra of the investigated compounds (with the exception of $UN \cdot 2C_6H_5NO_2$), this displacement being in the direction of lower frequencies. The displacement of the short-wave band in the luminescence spectra proceeds in a similar fashion, the position of this band characterizing, in a certain way, the magnitude of the pure electron transfer. In Table 1 there are presented the intensity maxima in the structured luminescence spectra of the complexes. To

TABLE 1

A Comparison of the Intensity Maxima in the Spectra of the Coordination Compounds of Uranyl Nitrate with Quantities Characterizing the Electron-donor (Basic) Properties of the Addenda

Addendum	λ_{max}, cm^{-1}	Basicity constant [11]	Infrared absorption		Raman scattering
			$\frac{\Delta\nu}{\nu}$, % (13)	$\frac{\Delta 3\nu}{3\nu}$, % (13)	$\frac{\Delta\nu}{\nu}$, % (14)
NH_3	18850	10^{-5}	21,0		
C_6H_5N	18970	$8 \cdot 10^{-8}$	23,0		7,2
C_2H_5OH	19150	10^{-10}			
$(C_2H_5)_2O$	19850	10^{-16}	12,0	7,1	4,2
$O(CH_2)_4O$	19800	$2 \cdot 10^{-18}$			4,2
$(CH_3)_2CO$	19800	$2 \cdot 10^{-18}$	9,5	8,0	3,8
CH_3CN	18950				
$C_6H_5NO_2$	19800	$4 \cdot 10^{-25}$		3,1	
CH_3NO_2	20000			2,7	
NO_2	20270				
C_6H_6	—		2,9	2,5	1,7
C_6H_{12}	—				

characterize the donor properties of the addenda, reference is made to certain of their basicity constants [11]. In the last columns there are presented values of the relative decrease in the frequencies of the valence vibration and the second overtone of the OH group of the hydroxyl-containing molecules (phenol, methanol, surface OH), these being displaced as the result of interaction with the addenda which are under consideration [12-14]. This quantity also characterizes the donor properties of the addenda.

LITERATURE CITED

[1] A. N. Savchenko, V. M. Vdovenko and T. V. Kovaleva, J. Exp. Theoret. Phys. 21, 204 (1951).

[2] B. E. Gordon, Bull. Acad. Sci. USSR, phys. ser. 15, 624 (1951).

[3] J. J. Katz and G. Gibson, J. Am. Chem. Soc. 73, 5436 (1951).

[4] L. V. Volod'ko and A. N. Sevchenko, Optics and Spectroscopy 4, 40 (1958).

[5] M. de Forkrand, Compt. rend. 150, 1044 (1913); Ann. Chem. 9, 12 (1915).

[6] V. L. Levshin and G. D. Sheremet'ev, J. Exp. Theoret. Phys. 17, 204 (1947).

[7] D. D. Pant, J. Sci. Res. Benares Hinder Univ. 3, 19 (1952).

[8] M. Freymann and H. Chantrel, Compt. rend. 227, 1029 (1948).

[9] M. Freymann and R. Freymann, Compt. rend. 227, 1096 (1948).

[10] V. M. Vdovenko, M. P. Koval'skaia and T.V. Kovaleva, J. Inorg. Chem. 2, 1677 (1957).

[11] W. Gordy and S. C. Stanford, J. Chem. Phys. 9, 204 (1941); W. Gordy, J. Chem. Phys. 9, 215 (1941).

[12] A. N. Sidorov, J. Phys. Chem. 30, 995 (1956).

[13] R. Mecke, Discussions Faraday Soc. 9, 161 (1950).

The Physics Institute and the
Chemical Institute of the
A. A. Zhdanov State University,
Leningrad

Received March 4, 1958

THE CATALYTIC PROPERTIES OF CALCIUM OXIDE

O. V. Krylov and E. A. Fokina

(Presented by Academician S. I. Vol'fkovich, January 2, 1958)

Several years ago we observed the strong catalytic activity of the solid bases, the oxides and hydroxides of the metals of the second group; CaO, $Ca(OH)_2$, SrO and BaO, in the dehydrogenation of isopropyl alcohol [1, 2]. At that same time, attention was called to the small amount of study which had been given to heterogeneous alkaline catalysis. A number of investigators have recently observed catalytic activity in the solid bases; the oxides and hydroxides [3, 4], the hydrides [5], the amides [6-8], the alcoholates [9] and the alkaline metals.

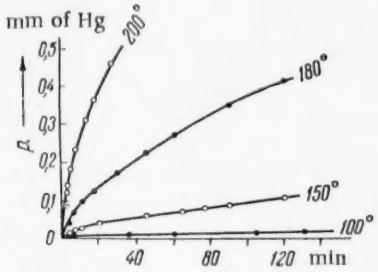

Fig. 1. Kinetic curves for the dehydrogenation of isopropyl alcohol in the adsorbed layer on CaO.

It is of interest to investigate the laws of alkaline catalysis, as distinct from acid, and from oxidation-reduction catalysis. The present work has involved the study of the dehydration of cyclohexane, and the breakdown of isopropyl alcohol and hydrazine, on calcium oxide.

Calcium oxide was prepared by the dehydrogenation of $Ca(OH)_2$ in vacuum at 600° in the same vessel in which the catalytic reactions were to be carried out. For the experiments on the breakdown of cyclohexane and hydrazine, 2 g of this oxide was taken; for the decomposition of the isopropyl alcohol, 1 g. The surface of the CaO was determined from the adsorption of n-heptane and amounted to 48.5 m^2/g. The breakdown of iso-C_3H_7OH and N_2H_4 was studied in the adsorption layer and the decomposition of C_6H_{12} under static conditions in vacuum. The reaction products were analyzed by freezing. In addition, a supplementary analysis for H_2 was carried out by passing the latter through a palladium capillary.

In Fig. 1 there are shown the kinetic curves for the dehydrogenation of isopropyl alcohol in the adsorption layer at 100-200°. The amount of hydrogen desorbed at 180-200° was equal to the amount of acetone. At lower temperatures the hydrogen was in excess of the acetone by 10-20%. This is explained by the strong adsorption of acetone on CaO. Study has shown that acetone adsorbed at 190° can be completely removed by degassing at this time temperature, whereas at 100°, only 4% of the acetone can be so removed. Under the experimental conditions, an adsorption of H_2 could not be detected (it corresponded to a coverage of less than 0.1%). The dehydrogenation products made up 10-20% of the total amount of the reaction products. Within any one series of experiments the reproducibility was satisfactory. "Activation" was observed, after some 20 experiments, the last at low temperature (75-100°), had been carried out under standard conditions, the rate of dehydrogenation increasing by 20-30%. The kinetic curves for the dehydrogenation of isopropyl alcohol were linear in the coordinates log p, log t. In view of the approximate constancy in the values of the initial coverage of the CaO (0.236 mmoles/g at 100°, 0.225, at 150° and 0.177 at 100°), the energy of activation, E, for dehydrogenation of the iso-C_3H_7OH could be determined by comparing the logarithms of the times required for attaining a certain degree of transformation, with 1/T. At low temperatures (100-150°) this led to E values of

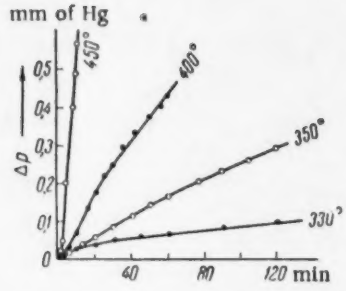

Fig. 2. Kinetic curves for the dehydrogenation of cyclohexane on CaO at 350-450°.

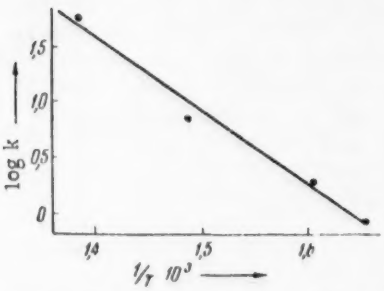

Fig. 3. The log k vs 1/T relation for the dehydrogenation of C_6H_{12} on CaO.

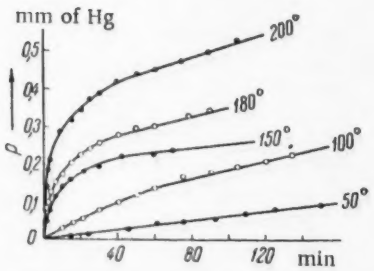

Fig. 4. Kinetic curves for the breakdown of hydrazine in the adsorption layer on CaO.

21-30 kcal/mole, depending on the degree of coverage, and at 180-200°, to 32-36 kcal/mole. It is possible that these differences in the energy of activation were related to the fact that the breakdown proceeded on the hydrated surface at the low temperatures and on the pure CaO at the high. The "activation" of the CaO at low temperatures speaks in favor of this.

For an initial C_6H_{12} pressure of 0.2 mm, the kinetic curves of Fig. 2 show the dehydrogenation of cyclohexane to proceed with satisfactory velocity at 300-450°. At this initial pressure, adsorption measurements carried out with the MacBain balance indicated that the cyclohexane adsorbed on the CaO to the extent of 0.044 mmoles/g at 300° and 0.030 mmoles/g at 350°, i.e., to each molecule of C_6H_{12} there corresponded 300-400 A^2 of surface. Benzene was adsorbed in smaller quantities under these same conditions. The adsorption was rapidly concluded and the adsorbed material could be removed by degassing. At these coverages, the reaction was not retarded by the adsorption of the components and in its kinetics, it followed a first order law. The dependence of the initial reaction rate on the cyclohexane pressure was also linear. The H_2 made up 52-59% of the reaction products in various experiments at 350-400° and 69-74%, at 450°. The reproducibility of the results was good. After a series of experiments (12 runs at 300-450° with P_{init} = 2 mm), the decrease in the rate amounted to only 5-8%.

In Fig. 3 the logarithm of the rate constant for the first order decomposition of cyclohexane on CaO has been plotted as a function of 1/T. As calculated from this straight line, the energy of activation for the dehydrogenation is equal to 30.5 kcal/mole. This is considerably higher than the energy of activation, E, for the dehydrogenation of C_6H_{12} on metals and is close to the value obtained by Baladin and Brusov [10] and by Kagan and Flid [11] for the dehydrogenation on Cr_2O_3. According to the data of these authors, the oxide catalysts are distinct from the metals, in that on them there is the possibility of the formation of cycloolefins and cracking products. Our data also indicate that the stoichiometric breakdown of C_6H_{12} into $C_6H_6 + 3H_2$ was not observed.

In Fig. 4 there are presented certain kinetic curves for the breakdown of hydrazine in the adsorbed layer on CaO at 50-200°. The activity of CaO in regard to the decomposition of hydrazine was not constant and its variation in certain repetitions of the experiments reached 20-25%. The products of decomposition were analyzed for: ammonia, (the volume of that gas which condensed in liquid nitrogen), the amount varying from 11.1% at 100° to 20.4% at 200°; hydrogen, (the noncondensable gas which passed through the Pd capillary), the amount being very slightly dependent on the temperature, varying within the range 46.8-55.7%, and nitrogen, (the residual, noncondensable gas) the amount varying from 31.1 to 35.5% at temperatures of 100-200°.

Thus, on CaO, the breakdown of hydrazine proceeded according to the same equation as in strong alkaline solutions [13]:

$$(3 + x)N_2H_4 \rightarrow 2NH_3 + (2 + x)N_2 + (3 + 2x)H_2$$

and differed from the decomposition on metals and on semiconductors, where special experiments showed the formation of only ammonia and nitrogen:

$$3N_2H_4 \rightarrow 4NH_3 + N_2.$$

At temperatures of 150-200°, the kinetic curves for the breakdown of hydrazine were linear in the coordinates p, log t and were nonlinear in these coordinates at 50-100°. Calculations for E at various degrees of coverage led to values varying from 6200 to 7400 cal/mole at 50-100°, and from 12000 to 28000 cal/mole at 100-200°. In view of the great variability in the activity of the CaO, it is necessary to underscore the coarsely approximate character of these values. It is possible that the variation in the energy of activation and the difference in the forms shown by the kinetic curves for the breakdown of N_2H_4 on CaO at high and low temperatures, were the result of the low temperature hydration of the CaO surface, the water involved serving as a contaminant for the entering hydrazine.

These experiments have pointed up the possibility that three reactions of hydrogen splitting which are usually considered as being of the oxidation-reduction or homolytic type might be carried out on CaO. Two of these reactions, the dehydrogenation of the alcohol and the cyclohexane, proceed in the same direction as on the electron semiconductors, and the third, the breakdown of hydrazine, in a direction opposite to that which is followed on metals and on semiconductors.

A comparison with zinc oxide, the neighboring oxide from the subordinate subgroup of Group 2 of the periodic table [13], (a typical electron semiconductor) shows approximately identical values for the energy of activation in the breakdown of isopropyl alcohol, under streaming conditions (12-16 kcal/mole on CaO, 12-13, on ZnO) and in the adsorption layer (21-36 and 25-46, respectively), while the fact that the reaction proceeds over the same temperature interval speaks for similar values of the multiplier, k_0, of the exponential term.

The authors express their thanks to S. Z. Roginskii, Corresponding Member of the Academy of Sciences of the USSR, for his advice and for many valuable discussions.

LITERATURE CITED

[1] O. V. Krylov, Sympos., Heterogeneous Catalysis in Chemical Industry (in Russian) (Moscow, 1955) p. 430.

[2] O. V. Krylov, S. Z. Roginskii and E. A. Fokina, Bull. Acad. Sci. USSR, Div. Chem. Sci. 1956, 668.*

[3] J. C. Ghosh, S. K. Bhattacharyya, S. N. Sen and D. K. P. Chaudhuri, Petroleum 19, No. 358 (1956).

[4] S. Malinowski and H. Jedrzejewska, et al., Roczniki Chem. 30, No. 4, 1129 (1956).

[5] L. Wright and S. Weller, J. Am. Chem. Soc. 76, 5302, 5305, 5948 (1954).

[6] I. V. Gostunskaia and B. A. Kazanskii, J. Gen. Chem. 26, 1992 (1955).*

[7] I. V. Gostunskaia, N. I. Tiun'kina and B. A. Kazanskii, Proc. Acad. Sci. USSR 108, 473 (1956).*

[8] B. A. Kazanskii, P. A. Liberman, M. Iu. Lukina and I. V. Gostunskaia, Chem. Sci. and Indus. 2, 172 (1957).

[9] H. Pines and L. Schaap, J. Am. Chem. Soc. 79, 2956 (1957).

[10] A. A. Balandin and A. A. Brusov, J. Gen. Chem. 7, 18 (1937).

[11] M. Ia. Kagan and R. M. Flid, J. Gen. Chem. 20, 503 (1946).

*Original Russian pagination. See C. B. Translation.

[12] L. Odrid and B. Ogg, The Chemistry of Hydrazine (in Russian) (Foreign Lit. Press, 1954).••

[13] O. V. Krylov, S. Z. Roginskii and E. A. Fokina, Bull. Acad. Sci. USSR, Div. Chem. Sci. 1957, 421.•

Received December 31, 1957

•Original Russian pagination. See C. B. Translation.
••Russian translation.

THE REACTIONS OF FREE RADICALS IN SOLUTION

THE INTERACTION OF FREE RADICALS WITH INTERNAL AND EXTERNAL DOUBLE BONDS

E. B. Milovskaia, B. L. Erusalimskii and B. A. Dolgoplosk

(Presented by Academician B. A. Kazanskii, December 24, 1957)

It has been shown that double bonds of the vinyl type are effective acceptors of free radicals [1]. In the present work data is presented to characterize the relative activities of internal and external double bonds in their interactions with free radicals.

The interaction of free methyl radicals with hydrocarbon polymers. Methylphenyltriazine was employed as a source of free methyl radicals, this substance decomposing on warming in solution, according to the equation:

$$CH_3N = N - NHC_6H_5 \rightarrow CH_3\cdot + N_2 + \cdot NHC_6H_5. \quad (1)$$

The degree of interaction of the free radicals with the double bonds was indirectly evaluated in terms of the decrease in the yield of methane from the reaction:

$$R\cdot + LH \rightarrow RH + L\cdot \quad (2)$$

(LH is the hydrocarbon molecule) relative to the observed yield of CH_4 when the reaction was carried out in a saturated hydrocarbon medium. The results showed that an internal double bond is much less capable of uniting with free radicals than is a double bond of the vinyl type. Data from the study of the interaction of free methyl radicals with polymers led to this same conclusion (see Table 1). In this last case, reaction was in concentrated isopropyl benzene solutions, polystyrene solutions of the same concentrations serving as standards The fact that the values for polystyrene were practically identical with those for natural rubber, permitted the supposition that the free radicals united with the double bonds of the latter substance in only an insignificant degree. On the other hand, a sharp decrease was noted in the yield of methane in the case of synthetic polyisoprene which had a high proportion of vinyl double bonds.

It was established that the yield of methane was only 9% of the theoretical in the case of a swollen polystyrene containing 10% isopropylbenzene, whereas it was 49% of the theoretical in pure isopropylbenzene The diminution in the yield of methane which accompanied the transition to a highly viscous medium was the result of the enhanced role of the recombination of the free radicals which were formed in Reaction (1). Confirmation of this was found in the fact that the yield of methylaniline (the product of initial recombination) was 16% in the pure solvent and 43% in the swollen polystyrene. This same fact explains the decreased yield of methane in the decomposition of triazine in saturated rubber solutions.

Thus, the transition into a highly viscous medium led to a decrease in the proportion of effective radical reactions.

The interaction of dimethylcyanomethyl free radicals with 2-butene. The dinitrile of nitroisobutyric acid was used for the generation of dimethylcyanomethyl free radicals. In Table 2 data are presented on the various compounds which were found in the products from the thermal decomposition of dinitrile of nitroisobutyric acid in 2-butene.

TABLE 1

The Yield of Methane in the Thermal Decomposition of Methylphenyltriazine in Various Hydrocarbons (Triazine Concentration, 3 Mole %) and in Polymers Containing 34% Isopropylbenzene (Triazine Concentration, 15 Wt. % with Respect to the Polymer). Temperature, 110°

Hydrocarbon	Yield of CH_4, % theoretical	Hydrocarbon	Yield of CH_4, % theoretical
n-Butane	54	Polystyrene	29
1-Heptene*	12	Natural rubber	27
Isobutylene	8	Polyisoprene containing up to 70% linkages 1,2, and 3, 4	14
α-Methylstyrene*	0		
2-Butene	30		

*Data obtained at other temperatures and concentrations and presented in an earlier communication [1].

TABLE 2

The Yield of Products from the Reaction of Dimethylcyanomethyl Free Radicals in a Butene Medium, in %, of Theoretical. Temperature, 80°. Concentration of the Azo-compound, 5 Mole %.

R–R	RH	RAR	$RA_{(+H)} + RA_{(-H)}$
79	3	3.5	2

(R is the radical and A, the molecule, of the hydrocarbon)

From these data it follows that the dimethylcyanomethyl free radicals combined to only a very insignificant extent with the internal double bonds. The recombination of these radicals predominated under the prevailing experimental conditions. Under similar conditions, the principal reaction which takes place with the hydrocarbons containing the vinyl group is, as we have shown earlier [1], that of uniting the free radicals with the double bond. The RA· free radicals which result from the interaction of the initial radicals R· with the 2-butene are characterized by a distinctively low reactivity. This results from the nature of the products of their further transformation, these arising from the reactions:

$$RA\cdot \xrightarrow{R\cdot} RAR \qquad (3)$$

$$RA\cdot \xrightarrow{RA\cdot} RA_{+H} + RA_{-H}\,. \qquad (4)$$

To the compound RAR there should be ascribed the structure of 2, 2', 3, 4, 5, 5'-hexamethyladipic acid. The product from the disproportionation of the RA· radicals (Reaction (4)) could not be separated into individual compounds, but was characterized as an equimolar mixture of saturated and unsaturated components. The formation of the nitrile of isobutyric acid (RH) at the same yield as when the reaction was carried out in other hydrocarbons [1], clearly arose from the disproportionation of the initial free radicals.

EXPERIMENTAL

The decomposition of methylphenyltriazine in various media. The experiments with low boiling hydrocarbons were carried out in a small autoclave with an average charge of 1 g of triazine (concentration, 3 mole %). The experiments with the polymers were performed in ampules, each of which was equipped with an inlet

tube and an outlet that connected with a gas burette. Upon completion of disintegration (8 hours at 110°), water was introduced through the inlet tube and the contents of the ampule were boiled until there was no longer any evolution of the gas which had been "entrapped" in the polymer. 2 g of the polymer was taken in the experiment; the relationships among the various components are shown in Table 1.

The determination of the yield of methylaniline from the breakdown of triazine in isopropylbenzene and in swollen polystyrene was by means of successive application of the bromide-bromate procedure and the rapid method of Shchetinina [2].

The products from the decomposition of the dinitrile of azoisobutyric acid in 2-butene. 20 g of the dinitrile was decomposed in an autoclave in 135 g of 2-butene at 80°. After distilling off the butene which had not entered into reaction, the following products were separated:

a) The dinitrile of tetramethylsuccinic acid, 13 g (yield, 79% of theoretical), m. p. 168-168.5°; accepted value, 169° [3]. Mixing test, 168.5°.

b) The nitrile of isobutyric acid, 0.64 g (yield, 3% of theoretical), determined by the saponification of the toluene fraction which was obtained by distilling off toluene which had been earlier introduced into the reaction mixture after freeing the latter of 2-butene and the basic mass of the dinitrile of tetramethylsuccinic acid; this latter compound did not saponify [4] under the conditions employed in this method.

c) A fraction with b. p. 25-26°/0.5 mm. Yield, 0.7 g (2% of theoretical), $d_4^{19.5}$ 0.8123; $n_D^{19.5}$ 1.4248.

Found %: N 11.19, 11.39; M 118.5. Iodine number 102. $C_8H_{15}N$(RAH). Calculated %: N 11.20; M 125. Iodine number 0. $C_8H_{13}N$(RA(−H)). Calculated %: N 11.38; M 123. Iodine number 206.

d) A fraction with b. p. 102-105°/0.5 mm, d_4^{20} 0.9250, n_D^{20} 1.4620. Yield, 0.85 g (3.5% of theoretical).

Found %: C 72.27, 73.35; H 10.27, 10.30; N 14.34, 14.45; M 187.5. MR 57.24. $C_{12}H_{20}N_2$ (RAR). Calculated %: C 75.00; H 10.41; N 14.58; M 192; MR 57.07.

e) A tarry, nonvolatile residue, 1.5 g.

The content of bound dimethylcyanomethyl radicals (according to % of nitrogen) was 6.5 % of the initial amount.

LITERATURE CITED

[1] E. B. Milovskaia, B. A. Dolgoplosk and B. L. Erusalimskii, Bull. Acad. Sci. USSR, Div. Chem. Sci. 1957, 494.*

[2] P. L. Lastovskii, Technical Analysis in the Production of Intermediate Products and Dye Stuffs (in Russian), 1949, pp. 166, 212.

[3] F. K. Beilstein, Handbuch der organischen Chemie, 2, S. 707.

[4] P. Bruin, A. F. Bickel and E. C. Kooyman, Rec. Trav. Chim. 71, 1115 (1952).

The Institute for High-Polymer Compounds of the Academy of Sciences of the USSR

Received June 20, 1957

THE MECHANICS OF POLYMER MOLECULES

G. A. Patrikeev

(Presented by Academician V. A. Kargin, January 2, 1958)

1. Many of the observations which have been made on the rolling, crushing, and physical deformation of polymeric substances have been theoretically interpreted as the result of rupture of the polymer molecules [1].

In recent years it has been shown that polymer free radicals (macroradicals) arise in the breakdown of polymer molecules and that these can serve as centers for radical polymerization [2, 3].

The new scientific disciplines of mechano-chemistry [3] and physicochemical mechanics [4] have been developed.

2. The concepts of intermolecular mechanical stresses [5] and of valence bonds resembling quasi-elastic bars [6] are old ones.

If it is supposed that mechanical rupture is preceded by an interval of elastic distension, it then becomes possible to apply the methods of mechanics to the study of the elementary acts of distortion and rupture in the polymer molecule. The initial step in the distension of a flexible polymer molecule is known to be the straightening of the latter under the action of external forces, this leading to an alteration in the molecular configuration and to a decrease in the system's entropy. The mean-statistical value of the modulus of elasticity, (a_s), for the "entropy-configurational" deformation of an idealized hydrocarbon polymer molecule must be considered to be of the order of $1 \cdot 10^{-8}$ dynes/bond [7, 8]. For a formal evaluation of the energy changes accompanying the mechanical deformation of the molecule, it is useful to introduce the concept of "specific energy density," (g_s), this quantity being defined as the quotient of the work of distension and the volume of the deformed portion of the molecule. In configurational deformation, the specific energy density is not large and has the expression $g_s \simeq 0.05\, V_s$ kcal/mole, where V_s is the work of distension in kcal/mole. With V_s values of the order of 200 kcal/mole, $g_s \simeq 10$ kcal/mole.

Only after the molecule has been fully straightened does there become possible that elastic distension of the polymer which has been postulated to arise from the deformation of the valence angles and bonds. Taking the length of the completely straightened molecule as unity, the modulus of elasticity, (a_c), for the initial step in the extension of the hydrocarbon polymer chain has been roughly evaluated as a quantity of the order of $2.5 \cdot 10^{-3}$ dynes/bond [9] or $5.6 \cdot 10^{-3}$ dynes/bond [7]. Approximating the stress (σ), distension (ϵ) relation through Hook's law, the strength of the C–C bond can be crudely fixed at $5.7 \cdot 10^{-4}$ dynes/bond [7]. In our opinion, these evaluations of the rigidity and strength of the polymer molecule are much too low, the latter especially so, since they take no account of the increase in the slope of the potential curve which accompanies an extension of the covalent bond or of the role of other factors. It can be supposed that the order of the modulus is $a_c \simeq 7 - 12 \cdot 10^{-3}$ dynes/bond; if the strength of the C–C bond is taken to be $0.2 \cdot 10^{-2}$ dynes/bond,* the relative extension at rupture (ϵ_z) then proves to be no less than 0.2–0.3. Regardless of the values

* Taking the mean effective cross section (s_0) of the polymer molecule to be equal to $25 \cdot 10^{-16}$ cm^2, we obtain the corresponding values of the modulus of elasticity, $E_c = \frac{a_c}{s_0} \simeq 3.5 \cdot 10^6$ kg/cm^2, and the strain at rupture $f_z = \frac{\sigma_z}{s_0} \simeq 0.8 \cdot 10^6$ kg/cm^2.

of the mechanical parameters, the potential energy stored up during elastic distension must be commensurable with the energy of dissociation (V_0), of the covalent C—C bond, since the deformation must assure the extension of all of the valence bonds and angles which enter into the molecular chain. In elastic distension, the specific energy density, (g_c) is quite large and is covered by the expression $g_c \simeq 54\, V_c$ cal/cm^3, V_c being the work of distension in kcal/mole; when V_c = 20 kcal/mole, g_c is about 10^3 cal/cm^3, i.e., as compared with the case of the entropy-configuration deformation, it is greater by two orders. Such are the conclusions which follow from the extension of the basic propositions of mechanics to the mechanical deformation of the polymer molecule.

Because of the potential energy which accumulates during deformation, the elastically distended polymer chain can be looked on as a quasi-elastic bar which spontaneously contracts on diminishing the external interaction, and thereby performs work against the external forces. This process proves to be reversible if there is no excitation (activation) of the valence bonds and no chemical reactions occur. Due to the very considerable increase in the internal energy which accompanies the elastic extension of the valence bonds, there is a high probability of excitation-activation; there can scarcely be any doubt of the statistical character of this effect. The degree of activation during the rupture of an elastically distended polymer molecule must be especially large. Attempts have been made to evaluate experimentally the energy of activation without theoretically considering the elementary acts of distension and rupture of the polymer molecule [10].

4. For the mechanics of polymer molecules, a consideration of the elementary act of rupture of the elastically strained molecule is of fundamental significance. The thermodynamic equilibrium of the elastically distended molecular chain is determined by the relationship of the elastically strained state of the molecule and the action of the external forces. In mechanical rupture of the chain, i.e., in the breakdown of even a single bond, the state of thermodynamic equilibrium is destroyed simultaneously with the breaking of the covalent bond, since the possibility of the action of the external forces on the molecule is then precluded.

For an evaluation of the relation of the work of the external forces in the elastic distension of the molecular chain and in the formation of macroradicals through mechanical rupture, it is sufficient to take account of the number of valence bonds (n) in the distended molecule. Supposing rupture to occur at one of these bonds, the relative contribution of the external forces to the formation of the two macromolecules proves to be quite insignificant, since it amounts to only 1/n-th part of the total work of distending the molecule of n links. This important detail must be considered, not only in a theoretical evaluation of the work of formation of macromolecules, but also in determining the magnitude of the surface energy in the production of an interface during the rupture of the polymer body [11].

The energy which accumulates during elastic distension of the molecular chain is very considerable and proves to be the larger, the closer the values of the work of distension of the individual valence bond and the dissociation energy of the C—C bond are to being equal. Due to the appearance of statistical variations in the energy of the valence bonds, the value of the energy of dissociation alone proves to be insufficient for an estimation of the energy density prior to molecular rupture. The strength of the elastically distended molecular chain must, therefore, vary with time. Thermodynamic equilibrium must be instantaneously broken down by the mechanical rupture of the elastically distorted molecular chain. Then, as a result of the impossibility of the performance of mechanical work, the process of activation of the valence bonds must be accompanied by a transformation and redistribution of energy. The establishment of the relative energy quantities involved in these processes is an important, but as yet unsolved, problem. When the rate of the spontaneous contraction is sufficiently high, the dissipative processes in the mechanical rupture of the elastically strained polymer molecule must be explosive.

There is reason to suppose that these dissipative processes are fundamental to the elastic rupture of the polymer molecule. In particular, it is natural to believe that the strong electrification and evolution of heat which are observed during the "cold" plasticization of polyisobutylene (15-20°C) by rolling result from the mechanical elastic rupture of the molecules. Dissipative effects are, naturally, not to be expected in the thermal dissociation of elastically unstrained polymer molecules. Attention should also be given to the fact that there is no ground for anticipating such dissipation of energy in the mechanical rupture of localized molecular van der Waals' bonds or hydrogen bonds, the considerably lower mechanical rigidity of these bonds and the resulting possibility of their sequential rupture assuring that there will be no elastic distension here.

For a consideration of this problem it is, however, impossible to limit oneself to the mechanics of the polymer molecule; it is necessary touch also on the question of the deformation of the polymer system. It should be specially noted that the ideas which are being developed are ones based on an affirmation of the astonishingly high rigidity and mechanical strength of the covalent chemical bonds (C–C, C–O, C–S). In the same way these concepts are based on an affirmation of the essential qualitative difference between the strong covalent chemical bonds and the considerably weaker physical bonds. It is exactly this detail of the structure of the polymer molecules which proves to be basic from the chemical, as well as from the mechanical, point of view. Unfortunately, this fact is not only not taken into account, but frequently is tacitly set in doubt, or even refuted.

5. At the present time there is no possibility of the direct experimental study of the elastic distension and rupture of the polymer molecule. There is even an absence of trustworthy basic data for a theoretical, qualitative evaluation of the mechanical and energetic parameters which have been considered in this work. These facts must not, however, stand in the way of a development of the mechanics of the polymer molecule.

The concept of the mechanical rupture of polymer molecules, with the formation of polymer radicals and activation of the valence bonds has served as the basis for the development of a program of work on the synthetic modification of polymers [2, 3], as well as for work in the field of certain technological problems and in the in the study of the details of the molecular mechanism of the deformation of polymer bodies [12].

The concept of the elastic distension of the polymer molecules is, however, not as yet, fully utilized and that of the dissipative processes which accompany the elastic rupture of the polymer molecules, has not been employed at all. Among other things, the recognition of the existence of an energy redistribution in the elastic rupture of the polymer molecule makes it possible to note new approaches to the solution of certin important problems in the polymer field.

The development of a program of work can be based on the general rule that a study of the mechanical deformation of polymer bodies should take account of the possibility of the appearance of elastic distension and mechanical rupture of the polymer molecules, this last being accompanied, not only by the formation of radicals and the activation of valence bonds, but by dissipative processes as well. The rule which has been just formulated can also be used to advantage in a solution of the problem of the strength of solid bodies; for this purpose it is recommended that a decision be reached as to whether the solid body in question contains polymer molecules which because of their high strength and rigidity could, in elastic distortion, exert a marked influence on the mechanical properties, even at very low polymer contents.

6. An important branch of the recommended program of work is the study of the mechanical distension of polymeric systems. We have already pointed to the possibility of developing a molecular theory based on an admission of the fundamental significance of the elastic distension of polymeric hydrocarbon molecules for the deformation of elastic bodies [13].

Acknowledging the importance of elastic rupture, it is possible to understand the nature of the triboelectricity which accompanies the mechanical breakdown of polymeric bodies, and to comprehend the cause of the electrification which arises during the rubbing of polymer bodies on solid objects. Finally, if it is supposed that an elastic rupture of polymer molecules occurs during the deformation of plant and animal fibers, it then becomes possible to formulate a theory interpreting the cause of the directed growth of these fibers. The ideas which have been developed can thus be used for the study of a rather wide circle of phenomena in the field of polymeric and solid bodies.

LITERATURE CITED

[1] H. Staudinger and W. Heuer, Ber. 67, 1159 (1934); N. V. Mikhailov and V. A. Kargin, Proc. Fourth Confer. on High-Molecular Compounds, Acad. Sci. USSR Press.* 1948, pp. 138-157; V. A. Kargin and G. L. Slonimskii, Proc. Acad. Sci. USSR 105, No. 4, 751 (1955); N. K. Baramboim, Proc. Acad. Sci. USSR 114, No. 3, 568 (1957).**

[2] D. J. Angier and W. F. Watson, Polym. Sci. 20, 235 (1956); V. A. Kargin and B. M. Kovarskaia, et al., Proc. Acad. Sci. USSR 112, No. 3, 485 (1957).*

*In Russian.

**Original Russian pagination. See C. B. Translation.

[3] A. A. Berlin, Proc. Acad. Sci. USSR 110, No. 3, 401 (1956); L. C. Bateman, Ind. and Eng. Chem. 49, No. 4, 704 (1957).

[4] P. A. Rebinder, Proc. Third All-Union Confer. on Colloidal Chem. Acad. Sci. USSR Press, 1956, pp. 7-18.*

[5] A. Bayer, Ber. 18, 2277 (1885).

[6] N. Bierrum, Verh. Deutsch. Phys. Ges. 16, 737 (1914).

[7] P. P. Kobekov, Amorphous Substances (in Russian), Acad. Sci. USSR Press, 1952.

[8] L. Treloar, The Physics of the Elasticity of Rubber (in Russian) Foreign Lit. Press, 1953.**

[9] W. Kuhn and H. Kuhn, Helv. Chim. Acta 29, 1095 (1946).

[10] A. S. Kuz'minskii, M. G. Maizel's and N. N. Lezhnev, Proc. Acad. Sci. USSR 71, No. 2, 319 (1950).

[11] G. A. Patrikeev, The Strength of the Bonds between the Elements of Multilayer Rubber Fabric Objects in Production and Use, Scientific-Tech. Conf. 22-24 December, 1954, Leningrad, 1956, pp. 78-86.

[12] V. A. Kargin, T. I. Sogolva, G. L. Slonimskii and E. V. Reztsova, J. Phys. Chem. 30, No. 8, 1903 (1956).

[13] G. A. Patrikeev, Reports of the Ninth Confer. on the General Problems of the Physics and Chemistry of High-Polymer Compounds (in Russian), Acad. Sci. USSR Press (1956), p. 145; Rubber and Latex No. 4, 37 (1957).

Received December 26, 1957

*In Russian.

**Russian translation.

THE NATURE OF THE BONDS AND THE GAS PERMEABILITY OF SPACE-STRUCTURED POLYBUTADIENE

S. A. Reitlinger, A. S. Kuz'minskii and L. A. Fel'dshtein

(Presented by Academician P. A. Rebinder, January 13, 1958)

The effect of the formation of a space structure on the gas permeability of a polymer has been studied by a number of investigators. One important practical instance of such structuralization is found in the formation of a space lattice during vulcanization of rubber as the result of combination with sulfur. Barrer and Skirrow [1] have shown that the gas permeability of a rubber decreases nonlinearly with an increase in the amount of sulfur which is bound to the rubber. At the same time, increasing the density of the space lattice leads to a diminution of the diffusion constant and the solubility of gas in the polymer, with the result that the permeability constant, or product of these two quantities, proves to be a very sensitive indicator in the study of structure formation in polymers. In addition to an overall decrease in the gas permeability, a rise in the density of the lattice of a polymer in the high-elastic condition is also accompanied by an increase in the constant D_0 and in the apparent energies of activation for penetration and diffusion, factors which characterize the temperature dependence of these latter processes [1].

A decrease in the penetrability and an increase in the activation energy for penetration are also observed in the oxidation of rubber [2], in the action of short-wave radiation on polyethylene [3] and in other cases of space structuralization in polymers. An increase in the number of junctions in the space lattice of a polymer is accompanied by a rise in the latter's vitrification temperature. Taking account of the fact that the temperature of vitrification and the gas permeability of a polymer both depend on the flexibility of the molecular chain, it follows that there must be a relation between the variations which occur in these quantities during structure formation in the polymer. This can be expressed in the form of a function relating the logarithm of the gas permeability at the temperature of vitrification, a relation which is linear in the case of sulfur vulcanizates of rubber [4].

The specific properties of space structured polymers are dependent on the density of the cross linkages, the regularity of their distribution and their chemical character [5]. A determination of the relation between the gas permeability and the amount of sulfur bound in a rubber does not make it possible to give a definitive answer to the question of the effect of the density of the cross linkages, since it is known that sulfur not only forms intermolecular bonds but can unite intramolecularly as well. Groups such as $-S-S-$, $H-S-$, etc., result from the combination of sulfur, and these possess a high polarity which aids in the development of the intermolecular forces and the diminution of the gas permeability. In actuality, diminished gas permeability characterizes linear polymers which contain considerable amounts of sulfur, either in the basic chain – the thiokols [6] – or in the form of additions of the basic chain [7]. A very low value of the gas permeability is also shown by ebonite [8], a space structured product from the combination of rubber and sulfur. Much interest attaches to the possibility of clearing up the distinct effects of the crossed linked covalent bonds and the intermolecular bonds on the gas permeability.

For the solution of this problem, we have investigated spatially structured polybutadienes which differed from one another in the chemical nature of their cross linkages, the density of these latter being characterized by the value of the equilibrium high-elastic modulus, as determined by the method of [9].

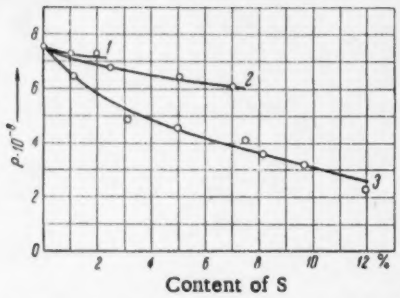

Fig. 1. The dependence of nitrogen permeability of polybutadiene at 20° on the sulfur content. 1) Dissolved sulfur, 2) intramolecularly bound sulfur, 3) vulcanized rubber with sulfur and diphenylguanidine.

The formation of a space lattice in polybutadine (SKB-40) was brought about by heating in a press at 220°, by the action of the radiation from Co^{60}, by heating with sulfur and diphenylguanidine, and by heating with sulfur and thiuram. The lattice density was varied, either by altering the time of heating or of irradiation, or by changing the amount of the vulcanizing agent. It was presumed that space structuralization proceeded at the high temperature (220°), principally by the breaking of double bonds; that the irradiation with Co^{60} gave rise to bonds of the C–C– type; and that vulcanization with thiuram produced monosulfide bonds, whereas with diphenylguanidine it was principally polysulfide bonds which were formed [10, 11]. Specimens, 80 mm in diameter and 0.5 mm in thickness, which had been prepared by hot pressing, served as test objects. The determination of the gas permeability was carried out in a thermostated Shuman apparatus [12]. Tank nitrogen (99.6% N_2) served as the test gas, this being subjected to a preliminary purification prior to introduction into the apparatus. The values of the gas permeability were expressed in cm^3 (STP)·sec^{-1}·cm^{-1}·at^{-1} and values of the equilibrium modulus, E_∞, in kg/cm^2.

In order to evaluate the effect on the gas permeability of those additional intermolecular forces which arise through the introduction of sulfur, a preliminary study of the permeability of a polybutadiene rubber containing dissolved, intramolecularly bound, and cross linked sulfur was carried out.

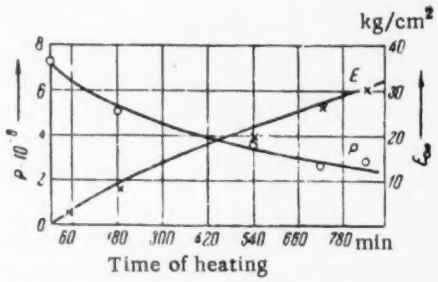

Fig. 2. The alteration of the equilibrium modulus and the nitrogen permeability of polybutadiene heated at 220°.

The results which were obtained are shown in Fig. 1. There was no appreciable influence on the nitrogen permeability of the rubber from dissolved sulfur whose supersaturated solutions in the polybutadiene did not exceed 2% concentration at 20°. The observed change in permeability was also small in the case of intramolecularly bound sulfur (Curve 2, for the product of the interaction of dienes with mercaptan). The largest effect in lowering the permeability of the polybutadiene was brought about by the sulfur which was capable of forming a space structure (Curve 3, for a sulfur vulcanizate of diphenylguanidine). Thus the cross linked sulfur bonds which arise between the molecular chains prove to have a stronger influence in decreasing the gas permeability than does a similar amount of sulfur in groups which are tied-up in the molecule.

The existence of a relationship between the gas permeability and the concentration of linkages in the space lattice makes it possible to establish a tie-up between the permeability and the equilibrium high-elastic modulus.

By way of an example, there is shown in Fig. 2 the characteristic relations which exist between the equilibrium modulus, the nitrogen permeability, and the time of heating of the polybutadiene at 220°. The diminution in the gas permeability which is observed in the process of space structuralization, is inversely proportional to the accompanying increase in the equilibrium modulus. The relationship between the gas permeability and the equilibrium modulus can be expressed in the form of a simple equation:

$$\log P = \log P_1 - kE_\infty,$$

P and P_1 being the gas permeability of the vulcanizate and the rubber, respectively, E_∞, the equilibrium high-elastic modulus and k, a coefficient of proportionality. For various temperatures, the log P, E relation is shown in Fig. 3. It follows from this experimental data that the chemical nature of the bonds is without essential influence on the alteration of the gas permeability resulting from spatial structuralization. At a fixed value of the high-elastic modulus, the value of log P is approximately the same for lattices of different chemical nature. This conclusion is valid, however, only in the case of lattices which are not too dense (up to E_∞ = 30-40 kg/cm^2) since at higher lattice densities, the specific influence of the bond nature begins to affect the gas permeability. In the case of the less dense lattices, the basic role in decreasing the flexibility of the molecular chain and diminishing the gas permeability belongs to the cross linkages, which, in comparison with the intermolecular forces whose magnitude is fixed by the nature of the bond, are, to a first approximation, without essential significance.

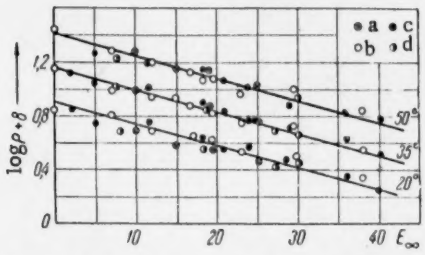

Fig. 3. The dependence of the logarithm of the nitrogen permeability on the equilibrium modulus. a) Irradiated by Co^{60}, b) heated with sulfur and diphenylguanidine, c) heated with sulfur and thiuram, d) heated at 220°.

LITERATURE CITED

[1] R. M. Barrer and G. Skirrow, J. Polymer Sci. 3, 549, 564 (1948).

[2] L. L. Shanin, Proc. Acad. Sci. USSR 99, 1053 (1954).

[3] J. Sobolev et al., J. Polymer Sci. 17, 417 (1955).

[4] G. M. Bartenev, S. A. Reitlinger and B. E. Rubinshtein, J. Phys. Chem. 30, 592 (1956).

[5] B. A. Dogadkin and M. M. Reznikovskii, Prog. Chem. 24, 801 (1955).

[6] T. R. Sager, J. Res. Nat. Bur. Stand. 19, 181 (1937).

[7] G. E. Meyer et al., Rubb. World 136, 532 (1957).

[8] R. M. Barrer, Trans. Farad. Soc. 36, 644 (1940).

[9] N. N. Lezhnev and Iu. S. Zuev, Proc. Scientific-Research Ins. Rubber Inds. 2, 35 (1955).

[10] B. A. Dogadkin and Z. N. Tarasova, Proc. Acad. Sci. USSR 85, No. 5, 1069 (1952).

[11] B. A. Dogadkin and Z. N. Tarasova, Colloid. J. 15, 347 (1953).*

[12] A. C. Shuman, Ind. and Eng. Chem. 16, 58 (1944).

The Scientific-Research Institute of the Rubber Industry

Received January 13, 1958

*Original Russian pagination. See C. B. Translation.

THE FORMATION OF FREE RADICALS AND ATOMS BY THE RADIOLYSIS OF HYDROCARBONS AT A TEMPERATURE OF 77°K

N. Ia. Cherniak, N. N. Bubnov, V. V. Voevodskii, L. S. Polak and Iu. D. Tsvetkov

(Presented by Academician N. N. Semenov, January 22, 1958)

There is indication in the literature that there is a formation of free radicals during the action of ionizing radiations (x-rays, γ-radiation, high speed electrons, etc.) on hydrocarbons and that this is the result of the rupture of C—C or C—H bonds [1]. In the radiolysis of the liquid hydrocarbons, the lifetime of these radicals is very short and their stationary concentrations quite low, so that radical formation can be only conjectured from the composition of the final product. Thus [2], in the irradiation of liquid heptane (Co^{60} source of the L. Ia. Karpov Physicochemical Institute), the degree of reaction increases linearly with a rise in the dosage, reaching $\approx 10\%$ with a dose of $3 \cdot 10^8$ r.

In addition to liquid substances containing one and two conjugated double bonds, H_2 and $C_{14}H_{30}$ appear as basic products of this radiolysis; the last of these can be considered as a dimer of the heptyl radical if it be supposed that the initial products from the heptane dissociation are atomic hydrogen and the C_7H_{15} radical. In order to directly confirm this supposition, there was carried out a low temperature irradiation of heptane in the frozen condition; because of the low mobilities of the radicals and atoms which are formed under the action of the γ-quanta, recombination would be retarded here and it could be expected that it would be possible to build up considerable concentrations of the thus frozen free radicals. The irradiation of frozen heptane, and of other hydrocarbons, was carried out in the above mentioned apparatus. The sample of hydrocarbon in a carefully evacuated and sealed quartz ampule (d = 2 — 4 mm) was placed on the bottom of a tall-form Dewar flask which was completely filled with liquid nitrogen. As evaporation proceeded, more liquid nitrogen was added to the flask so that the ampule continually remained beneath the nitrogen surface. As compared with the case of heptane irradiated in the liquid state, the resulting yield of tetradecane proved to be less by a factor of 2.

In order to detect the radicals, identify them, and determine their concentrations, the irradiated specimen was placed, without melting, into a special Dewar flask of phenoplast,* which was then inserted in the resonator of an electron paramagnetic resonance (EPR) spectrometer. Two EPR setups were employed. To establish the presence of the radicals and to determine the hyper-fine structure of the corresponding EPR spectra of the investigated substances there was employed an apparatus having a high frequency modulation of the magnetic field, this permitting the first derivative of the spectrum to be photographed on the screen of an electron oscillograph. When working at a wave length of ~ 3 cm, the sensitivity of this apparatus was approximately $4 \cdot 10^{-10}$ moles of diphenylpicrylhydrazyl. Themeasurement of the splitting of the hyper-fine structure of the spectra was carried out with a nuclear probe of the magnetic field. The evaluation of the concentration of free radicals in the test specimen was by means of a comparison of the integral intensity of the EPR signal on an ordinary visual spectrometer with the corresponding value for a fixed amount of the paramagnetic salt $CuSO_4 \cdot 5H_2O$.

The hydrocarbons; hexane, heptane, octane, dodecane, cetane, isooctane, cyclohexane, benzene and toluene, were studied. In every case, the observed EPR signals were intense and the g-factor was close to 2.0. With the paraffin hydrocarbons and cyclohexane, the observed hyper-fine splitting was quite clear cut, and, as a result, the total line width amounted to from 100 to 170 oersteds.

* "Penoplast" in original — Editor.

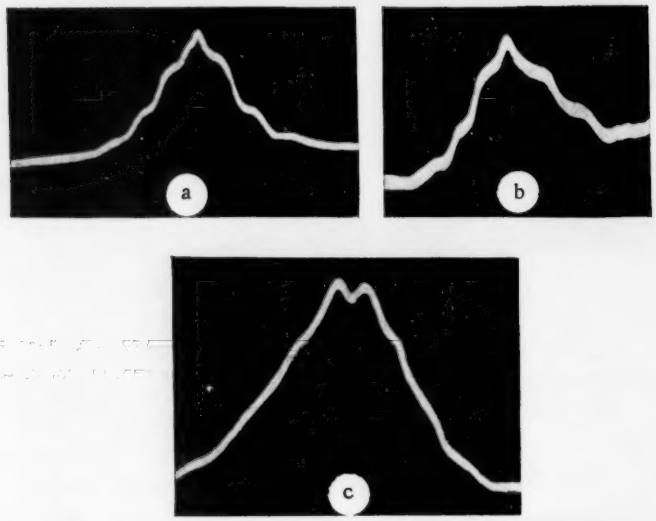

Fig. 1. The electron paramagnetic resonance spectra of the alkyl radicals resulting from the γ -irradiation of: hexane (a), heptane (b) and cetane (c).

From the accompanying photographs (Fig. 1), it is to be seen that the character of the hyper-fine structure was profoundly altered by a change in the structural characteristics of the initial molecules. Spectra of this same type have been observed by Gordy and McCormick [3] in the irradiation of dimethyl and diethyl mercury, diethyl zinc, etc., with x-rays and have been ascribed by these authors to the alkyl radicals. The production of spectra of this type by the irradiation of the hydrocarbons has not as yet been reported in the literature.

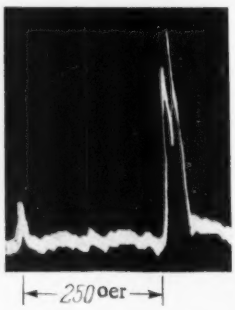

Fig. 2. The doublet components in the spectra of atomic hydrogen (1), and the alkyl radical (2).

Another peculiarity of the EPR spectra of the substances which we have irradiated in the frozen condition, is the presence of hydrogen atoms at considerable concentrations, this being indicated by two narrow signals symmetrically spaced on both sides of the alkyl radical signal at a distance of approximately 250 oersteds (see Fig. 2). Hydrogen atoms have been observed [4] in the γ -irradiation of solid acids (phosphoric, sulfuric, and hydrochloric) frozen at 77°, but it would have been difficult to have imagined that, under our conditions, their lifetimes would prove to be sufficient for the maintenance of measurable concentrations over any extended period. Subsequent measurements over two weeks showed that both the alkyl radicals and the hydrogen atoms are adequately stable at the temperature of liquid nitrogen. By direct experiment, it was also shown that the concentration of atomic hydrogen began to diminish only 10-12 seconds, and the concentration of the radicals, only 30-35 seconds, after removal of the liquid nitrogen. From this it followed that in introducing the ampule into the resonator, the transfer from one Dewar to the other could not have resulted in any appreciable alteration in the concentration of the active particles.

On this basis it could be supposed, on the other hand, that the hydrogen atoms were stabilized, not in the bulk of the frozen hydrocarbon, but on the inner surface of the quartz ampule. The possibility of this type of stabilization of atomic hydrogen during irradiation of ice has already been pointed out in [4].

A detailed analysis of the EPR spectra of the free radicals lies outside the scope of the present article. However, several qualitative remarks should be made. First of all, the very existence of a hyper-fine structure is noteworthy, as is the anomalously large value of the splitting (of the order of 25 oersteds). According to Gordy [3], this indicates: first, the possibility of some sort of displacement of the H atoms in the radical with respect to the inflexible carbon skeleton, these displacements assuring the appearance of the hyper-fine structure, and, second, the existence of a high density of unpaired electrons on the hydrogen atoms. The large number of components in the hyper-fine structure (see Fig. 1) clearly shows that in the splitting there participate not only the hydrogen atoms which are directly connected to the carbon carrying the free valence, but also, and at least, the hydrogen atoms which are located in the β-position. A comparison of the spectra of hexane, heptane and cetane, proves the hyper-fine structure to consist of an odd number of components in the first two cases and of an even number in the third. Since the relative probability of the rupture of the bonds in the CH_2 group is greater in cetane than it is in hexane, splitting on the nearest hydrogen atom must lead to the even case. The odd number of components in the case of n-hexane and n-heptane must be considered as an indication that in these compounds there is principally a rupture of the CH bonds in the CH_3 groups.

In Table 1 there have been compared the quantitative measurements which were carried out on the concentration of free radicals in heptane at a dosage of $\sim 10^7$ r and the chemical analyses of a sample which had been irradiated under exactly similar conditions.

Quantity of Radicals	
According to the data of paramagnetic resonance, per 1 g	According to calculations based on the amount of the resulting products of radiolysis, per 1 g
$(4.9 \pm 1) \cdot 10^{18}$ $(7.1 \pm 1) \cdot 10^{18}$	$6.1 \cdot 10^{18} \pm 10\%$

In view of the possibility of a large error in the dosage (10-15%), the agreement between the results of these two measurements is completely satisfactory. The close agreement with the analytic data confirms, on the one hand, the correctness of the method of evaluating the concentrations, and indicates, on the other hand, that the radicals resulting from the dissociation of about 0.1% of the molecules at the temperature of liquid nitrogen do not participate in any sort of side reaction.

LITERATURE CITED

[1] Sympos., Radiation Chemistry, Foreign Lit. Press, 1953; Sympos., Work on Radiation Chemistry, Acad. Sci. USSR Press, 1955; Disc. Farad. Soc. 12 (1952).

[2] L. S. Polak, A. V. Topchieva and N. Ia. Cherniak, Proc. Acad. Sci. USSR 119, No. 2 (1958).*

[3] W. Gordy and C. G. McCormick, J. Am. Chem. Soc. 78, 3243 (1956).

[4] R. Livingston, H. Zeldes and E. H. Taylor, Disc. Farad. Soc. 19, 166 (1955).

The Petroleum Institute of the
Academy of Sciences of the USSR
The Institute of Chemical Physics of the
Academy of Sciences of the USSR

Received January 11, 1958

*Original Russian pagination. See C. B. Translation.

THE INFLUENCE OF THE SALTS OF A SERIES OF LOWER FATTY ACIDS ON EMULSION POLYMERIZATION

A. I. Iurzhenko and S. S. Ivanchov

(Presented by Academician P. A. Rebinder, January 13, 1958)

The influence of inorganic electrolytes on the polymerization of styrene in emulsion has been studied in the papers of a number of investigators. Thus, Fryling and John [1] have pointed to the accelerating action of these salts on polymerization in emulsion. The influence of certain anions and cations on emulsion polymerization has been treated in the paper of Apukhtina and Liagalova [2]. In studying the effect of certain inorganic salts on the kinetics of emulsion polymerization, Tsvetkov and Iurzhenko [3] reduced this effect to the alteration of the colloidal properties of the emulsifier under the action of the electrolytes. John and his collaborators [4] have shown that electrolytes affect the mechanical properties of the resulting polymer by hindering the formation of cross linkages (chain binding). In each of these investigations, it was only the chlorides and the sulfates of the alkali metals which were subjected to study. The present work is devoted to an investigation of the effect of the sodium salts of a series of the lower fatty acids, from acetic to lauric, on the polymerization of styrene in emulsion. This choice was dictated by the fact that these salts have surface active cations, so that they can affect the micell formation of the emulsifier, and its dissolving action, and can thus specifically influence the polymerization of styrene in emulsion. On the other hand, technical emulsifiers of the type of the salts of the fatty acids, always contain mixtures of salts of various chain lengths, and an elucidation of the role of the various components is therefore important for the selection of emulsifying systems having more desirable properties. In the literature, there is a complete absence of data on the influence of such salts on polymerization in emulsion.

The test styrene (containing 99.8% of the monomer) was treated with a 20% NaOH solution, held over metallic sodium, and then distilled in vacuum. The emulsifier was a Nekal (a sodium salt of dibutylnaphthalenesulfonic - acid) which had been carefully freed of electrolytes. The salts were obtained by the neutralization of the corresponding fatty acids (chemically pure) with sodium alcoholate, following the method of Harkins [5]. $K_2S_2O_8$ (chemically pure) was employed as the initiator. Polymerization was carried out in a special dilatometer which was equipped with a magnetic stirrer and an outlet for any gases that might be formed in the breakdown of the initiator. The composition of the polymerization system (in moles per liter) was: emulsifier, 0.029; initiator, 0.029; salts, from 0 to 0.3 (all in the aqueous phase). The ratio between the volumes of the aqueous and the hydrocarbon phases was 1 : 9 and the temperature of polymerization, 50 ± 0.1°.

Data on the effect of the investigated salts on the rate of polymerization, V, is presented in Fig. 1. The value of V was obtained by graphing the linear relation between the degree of polymerization, S, and the time, t, using the equation:

$$V = 0{,}01 \frac{\Delta S}{\Delta t} \mu \frac{1000 d_m}{M_0 \gamma},$$

in which μ is the relative proportion of the monomer; γ, the relative proportion of the aqueous phase in the polymerization system; d_m, the specific gravity of the monomer and M_0, the molecular weight of the latter.

Up to 0.02 M, the introduction of small amounts of the salts led to an increase in the rate of polymerization; at concentrations in excess of 0.02 M, these electrolytes acted differently, the action depending on the nature of the anion. In the mechanism of their action on the polymerization process, the salts of the lower homologs from the acetate to the caproate, inclusive, differed from sodium caprylate and the higher members.

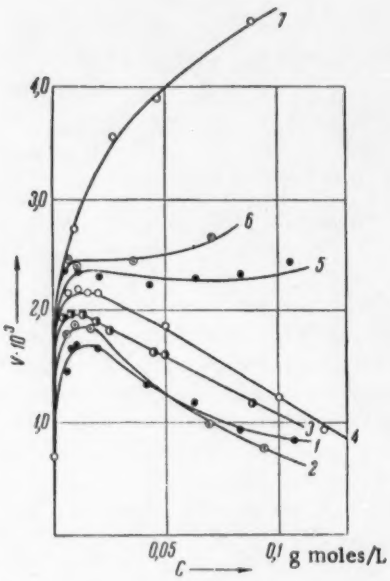

Fig. 1. The relation between the rate of polymerization of styrene and the nature and the concentration of the added salt; 1) Na acetate; 2) Na proprionate; 3) Na butyrate; 4) Na caproate; 5) Na caprylate; 6) the Na salts of the C_7–C_9 fraction; 8) Na laurate.

For the lower homologs up to and including sodium caproate, it was characteristic that the increase in the polymerization rate which resulted from the addition of salts to the polymerizing system in concentrations up to 0.02 M was replaced at higher concentrations by a retardation of polymerization. In passing from sodium acetate to sodium caproate there was an increase in the rate of polymerization, although the nature of the effect of the salt on the process and the position of the maximum rate remained the same in all cases.

An increase in the rate of polymerization was observed on introducing sodium caprylate at concentrations up to 0.02 M; beyond this point, the rate remained practically constant and that decrease in rate which is characteristic of the salts of the lower series was not observed. In the case of the higher members of the series, the rate of polymerization rose in parallel with the concentration of the added material and the more sharply the longer the anion chain in the salt.

Depending on their effect on the polymerization process, it was thus possible to divide the salts of the fatty acids into two groups: 1) the salts of the lower fatty acids (from acetic to caproic), these showing maximum rates of polymerization which depended on the concentration, and 2) the salts of the higher acids (above caproic) which gave a continual increase in the polymerization rate with rising salt concentration in the reaction mixture (and in greater measure, the longer the hydrocarbon chain of the anion). These salts affected the molecular weights of the resulting polymers in exactly the same way (see Fig. 2). On adding the salts of the fatty acids in the series from the acetic to caproic , the characteristic polymer viscosity at first rose sharply (similarly to the polymerization rate), then passed through a maximum at concentrations of the order of 0.04 M, and finally diminished. In this series, the nature of the added salt was practically without influence on the characteristic polymer viscosity, the respective curves for sodium butyrate, caproate and propionate coinciding. With respect to the maximum in the polymerization rate, the maximum in the characteristic viscosity was displaced in the direction of higher concentrations (from 0.02 to 0.04 M).

With sodium caprylate and the higher members of the series, increasing the salt concentration did not lead to a maximum in the characteristic viscosity and this quantity steadily increased with increasing salt content, the rise being the more pronounced the longer the hydrocarbon chain in the anion radical.

From the resulting data on the rates of polymerization and the characteristic polymer viscosities, rates of initiation of polymerization were calculated for various salt additions. It is to be seen from Fig. 3 that the addition of the sodium salts of the lower fatty acids from acetic to caproic inclusive, resulted in a diminution in the rate of initiation, this being the more sharply expressed, the shorter the chain of the salt's anion.

With increasing concentration of the added salt, a decrease was observed in the rate of initiation although there was a certain maximum in V_{in} at a concentration of 0.02 M.

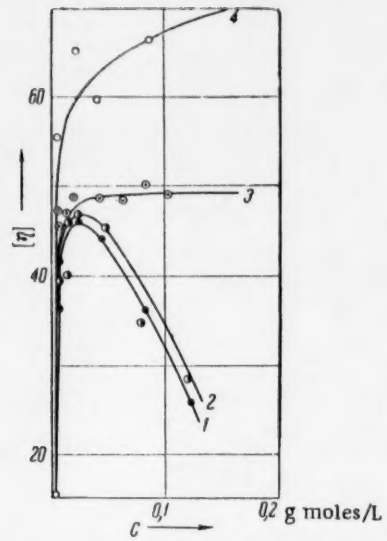

Fig. 2. The relation between [η] for the prepared polymers and the nature and the concentration of the added salt: 1) Na propionate; 2) Na caproate;, 3) Na caprylate; 4) Na laurate.

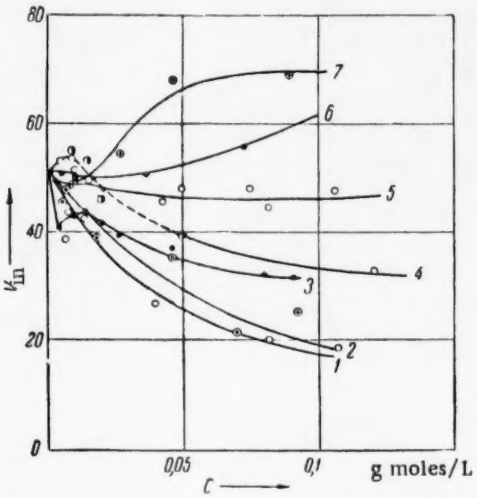

Fig. 3. The dependence of the values of V_{in} for polymerization on the nature and the concentration of the added salt: 1) Na acetate; 2) Na propionate; 3) Na butyrate; 4) Na caproate; 5) Na caprylate; 6) Na salts of C_7–C_9; 7) Na laurate.

With sodium caprylate, the initation rate remained practically constant, whereas with the salts of the higher acids, (lauric, and beyond) after a slight decrease (0.02 M), the rate increased both with increasing concentration and with increasing length of the hydrocarbon chain in the salt anion.

The following principal factors must be taken into account in considering the effect of the investigated salts on the process of emulsion polymerization:

a) Because of salt hydrolysis, the introduction of the sodium salts of the fatty acids into a polymerization system increases the pH of the aqueous phase from 6.8 to 9.3-9.5.

Such a jump in the pH must lead to an increase in the rate of emulsion polymerization [6]. We, too, have observed this effect on adding the first portions of one of the investigated salts. This effect was practically absent when the polymerization was carried out in a buffered system.

b) The investigated organic salts exert a salting-out effect, just as do inorganic salts. But with an increase in the length of the hydrocarbon radical there is a rise in the surface activity and in the stabilizing action of the anion. Thanks to this, stabilization is imposed on the salting-out effect, the latter factor predominating at a certain length of the hydrocarbon chain.

For the homologous series of salts, up to and including the caproate , the results which have been outlined above indicate a predomination in the salting-out effect on the emulsifier (Nekal, in this case), this leading to a gradual diminution in both the rate of polymerization and in V_{in}, i.e., these salts behave similarly to inorganic salts [3].

With the salts of caproic acid, and beyond, the stabilizing effect becomes predominant, so that with increasing concentration of salt in the system an increase in the polymerization rate is observed.

Such an evaluation of the influence of the investigated salts is in agreement with data on the scattering of light by aqueous solutions of Nekal containing these salts.

c) The investigated salts affect the rate of decomposition of the initiator $K_2S_2O_8$, the results of our experiments showing (Fig. 4) that the effect here is, to a considerable degree, analogous to that exerted by these salts in the process of polymerization in emulsion.

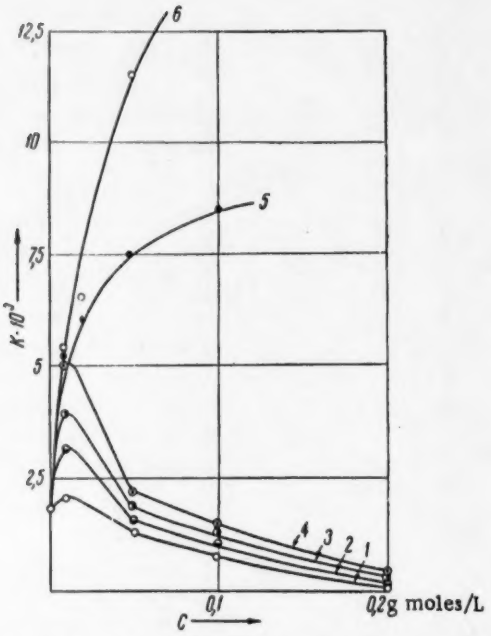

Fig. 4. The relation between the rate constant, K, for the decomposition of potassium persulfate and the nature and the concentration of the added salt; 1) Na acetate; 2) Na propionate; 3) Na butyrate; 4) Na caproate; 5) Na caprylate; 6) Na laurate.

LITERATURE CITED

[1] C. F. Fryling and W. M. John, Ind. and Eng. Chem. 42, 2164 (1950).

[2] N. P. Apukhtina and A. M. Liagalova, Colloid. J. 17, 415 (1956); 18, 340 (1956).

[3] N. S. Tsvetkov and A. I. Iurzhenko, Colloid. J. 18, 362 (1956).

[4] W. M. John, C. A. Uraneck and C. F. Fryling, Polym. Sci. 7, 159 (1951).

[5] W. Harkins, J. Am. Chem. Soc. 51, 1675 (1929).

[6] A. I. Iurzhenko, O. N. Brazhnikova and N. M. Likholet, Ukrainian Chem. J. 21, 586 (1956).

The Ivan Franko State University,
Lvov

Received January 13, 1958

THE PHENOMENON OF THE FORMATION OF ELECTRODE ZONES DURING THE ELECTROCRYSTALLIZATION OF METALS

V. V. Bondar' and Iu. M. Polukarov

(Presented by Academician A. N. Frumkin, October 4, 1957)

Nobili discovered the formation of colored rings of lead peroxide on an iron anode during the electrolysis of solutions of lead salts containing a pointed cathode placed near the anode [1]. For this case, the distribution of the current on the electrode has been considered by Riemann [2] and by Weber [3] and it has been shown that the current density gradually falls on moving away from the center, with the result that there must be a decrease in the depth of the precipitate in going from the center toward the edge of the electrode. For thin films, such a distribution of the precipitate leads to the appearance of Newton's interference rings.

Arndt [4] attempted to investigate the dispersion of the electrolyte during the electrodeposition of copper, using a cell closely resembling that which had been employed by Nobili. Here, the role of the pointed electrode was filled by an opening in a partition separating the cathode and anode spaces. A plane cathode was set opposite the opening in the partition at a distance of approximately 2 mm. Arndt found the copper deposit to show a series of concentrically spaced zones which differed in the character of the light which was reflected from them and in the dimensions of the crystals. He explained the formation of such zones by starting from the idea of preferential crystal growth in the direction of the lines of force, these lines being variously inclined to the cathode under the experimental conditions.

Shemiakin and Mikhalev [5] attempted to interpret these, and a number of other periodic phenomena, in terms of the de Broglie Equation, considering the ring formation to result from ion diffraction.

We have carried out investigation of the electrodeposition of alloys (Cu – Pb, Cu – Zn, Cu – Bi, Cd – Bi, Cu – Sn) and pure metals (Cu, Ni, Co, Zn, Bi, etc.) and the anodic dissolution of copper, under conditions analogous to those of the Arndt experiments.* In each case, there was observed the formation of clearly delineated, concentrically arranged zones** (see Fig. 1). X-ray studies have shown that the alloy deposits in the various zones were different in regard to phase composition.

The nonuniformity in the current distribution on the cathode which was noted by Reimann must lead to different values for the potential at the center and on the periphery of the cathode. We have carried out potential measurements over the various regions of the cathode. In Fig. 2, there are presented curves characterizing the change which occurs in the potential as one moves away from the cathode center.

Resting on data concerning the interval of potentials within which some particular phase will form, it is possible in the usual electrolysis to obtain this phase by observing the corresponding electrochemical regime.

---

* The phenomenon of zone formation was observed in every case in which the area of one of the electrodes was considerably less than that of the other. The zone form was fixed by the shape of the small electrode. For example, the zones had the form of rings in the case of circular electrode (opening), but they were ovals in the case of a slit. The cell which was used in our experiments had a 2.5 mm partition opening and the cathode was situated at a distance of 3-10 mm from it.

** The maximum number of rings was observed when the saturation current for the more electronegative metal was established in the central zone.

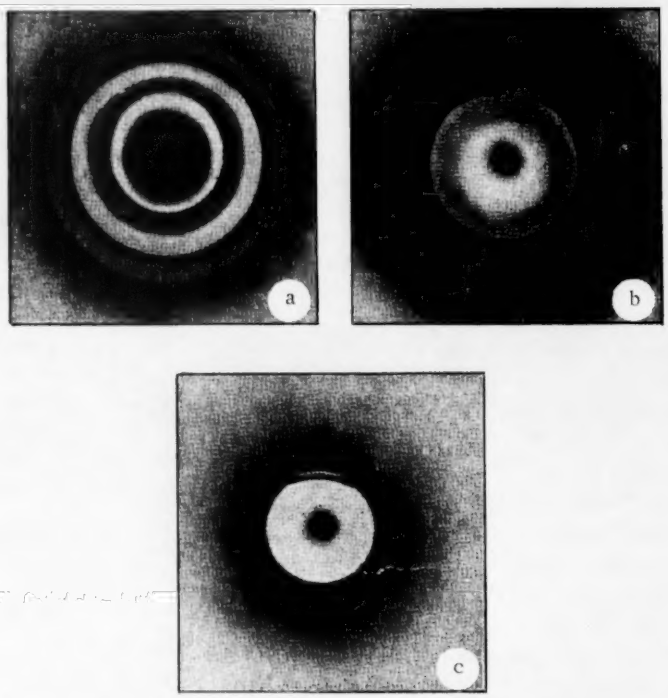

Fig. 1. The relation between the various zones on the electrode and the conditions under which they were formed. A) 0.5 N $Cu(ClO_4)_2$, 0.5 N $Bi(ClO_4)_3$, 2N $HClO_4$; I = 300 ma; distance from opening, 4 mm, B) 0.05 N $Cu(ClO_4)_2$, 0.5 N $Bi(ClO_4)_3$, 2 N $HClO_4$; I = 300 ma; distance from opening, 7 mm. C) 0.6 $Cu(ClO_4)_2$, 0.4 N $Cu(ClO_4)_3$, 2 N $HClO_4$; I = 300 ma; distance from opening, 4 mm.*

Thus, the appearance of zones during the co-deposition of two metals is the result of a variation in the current density, and the potential, in the direction from the center to the periphery of the cathode, this variation being accompanied by an alteration in the composition of the deposit, which ranges from the pure, more noble metal up to an alloy containing the maximum amount of the electronegative component which it is possible to obtain in the given electrolyte.

On the basis of the material which has been obtained, it is possible to formulate the conclusion that transition from one zone to another occurs at sharply defined potentials.

As Fig. 1 shows, the character of the zone distribution depends on both the electrolyte composition and the current distribution on the electrode surface. With the aid of the given cell, it was possible to control the electrolyte composition and thus obtain the optimal conditions for the electrodeposition of metals and alloys.

Zone formation was also observed in the electrodeposition of pure metals. In this case, x-ray (Table 1), optical and electron microscopic studies made it possible to establish the fact that the zones differed from one another in regard to the size of the crystals, their orientation, and the nature of the grain boundaries.

*The figure has been reproduced from a color photograph therefore some detail has been lost. – Publisher.

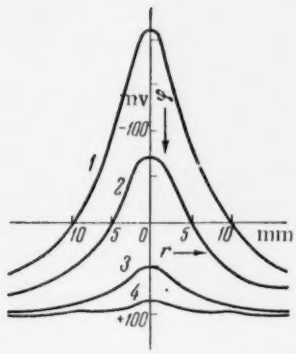

Fig. 2. Curves showing the potential distribution on the cathode. Electrolyte composition, $CuSO_4 \cdot 5H_2O$, 200 g/l; H_2SO_4, 50 g/l. 1) 10 ma, 2) 40 ma, 3) 100 ma, 4) 200 ma.

TABLE 1

Zone	Cu	Ni	Co	Zn
	Crystal orientation			
Center	None	[001]	Weak [111]	None
I	None	[001],[011]	Strong [111]	[112]
II	[111]	None	Medium [111]	None
III	[001],[112]	None	None	—

From data obtained in this way, and from the results of earlier investigations (under ordinary conditions) on the orientation of the crystals in copper and nickel deposits [6], and the nature of the boundaries of copper crystals [7] and their dependence on the experimental conditions, it was possible to conclude that zone formation in the deposition of pure metals does not arise from variations in the inclinations of the lines of force, as Arndt has supposed, but from differences in the electrochemical conditions of deposition (current density, overvoltage). The existence of characteristic angles under which maximum intensity of reflected light is observed results from the fact that the crystals in each zone are limited by quite definite grain boundaries.

It is interesting to note the establishment of a region of potentials within which pitting takes place during the deposition of nickel. It is clear that bubbles of hydrogen adhere most firmly to the cathode surface over this potential interval [8]. With the aid of the given cell, it was thus possible to determine rapidly the interval of potentials in which pitting was to be observed.

LITERATURE CITED

[1] L. Nobili, Bibliotheque universelle, Geneve, 1826.

[2] B. Riemann, Mathematische Werke und wissenschaftlicher Nachlass, Leipzig, 1892, S. 55.

[3] H. Weber, J. reine u. angew. Math. 75, 92 (1873).

[4] J. Arndt, Technische Elektrochemie, 1929, S. 368.

[5] F. M. Shemiakin and P. F. Mikhalev, Physicochemical Periodic Processes (in Russian), 1938, p. 37.

[6] S. M. Kochergin, Proc. Kazan Chem.-Tech. Ins., vol. 18, p. 48 (1953); F. Denis and H. Leidheiser, J. Elektrochem. Soc. 100, 490 (1953); B. C. Banerjee and A. Goswami, J. Sci. and Ind. Res. (B) 14, N 7, 322 (1955); A. Goswami, J. Sci. and Ind. Res. (B), 15, N 6, 322 (1956).

[7] S. Okada and S. Magari, J. Elektrochem. Soc. 102, 580 (1955); S. Okada, S. Magari and K. Katsui, J. Elektrochem. Soc. 103, 557 (1956).

[8] A. Gorodetskaia and B. N. Kabanov, J. Phys. Chem. 4, 529 (1933); B. N. Kabanov and A. N. Frumkin, J. Phys. Chem. 4, 534 (1933); N. N. Kabanov, J. Phys. Chem. 4, 549 (1933).

Received October 4, 1957

THE THEORY OF THE FARADAY RECTIFICATION

Iu. A. Vdovin

(Presented by Academician A. N. Frumkin, January 15, 1958)

In addition to an alternating potential, the passage of an alternating current through an electrolyte also gives rise to a certain constant potential drop at the electrode [1-3]. For the case of low currents, attempts at a theoretical explanation of this phenomenon have been made in [4-6]. In the work of Doss and Agarwal [4, 5] it was supposed, however, that the oxidizing agent and the reducing agent had the same volume concentrations and equal diffusion coefficients. But as will be shown below, even small differences in the diffusion coefficients can be of vital significance. The general case was considered in a paper of Oldham [6], in which there was proposed the name of Faraday rectification which has been adopted here. In that work essential terms were neglected, however, and the results obtained are fundamentally different from our own.

The present work is a theoretical investigation of this effect. There are two possible paths for the passage of an alternating current across the electrode surface. One of these involves the charging and discharging of the double layer at the electrode surface. Here the phenomena are similar to those in the passage of an alternating current through a condenser. The second path is exactly that which gives rise to the Faraday component of the alternating current and it is directly connected with the oxidation-reduction reactions on the electrode surface. At frequencies which are not too high and concentrations of reactive particles which are not too low, the phenomena in the double layer can be neglected and attention concentrated on the Faraday component of the alternating current. The relation between the Faraday component of the current and the alternating potential on the electrode has been studied in a number of papers [2, 7-10].

Let an alternating current $\underline{i}$ pass through an electrode of area A cm^2:

$$i = I \cos \omega t. \tag{1}$$

The passage of the current will be accompanied by an oxidation-reduction reaction on the electrode

$$\mathrm{Ox} + ne \rightleftarrows \mathrm{Rd}. \tag{2}$$

I. We will suppose that the solution contains ions of both the oxidizing agent, at a volume concentration $\bar{c}$, and the reducing agent, at a volume concentration $\bar{c}'$. The Fe^{3+}, Fe^{2+}/Pt electrode system, which has been studied in [4, 5], could serve as an example.

With U representing the electrode potential measured against a reference electrode at i = 0, the equilibrium condition for the system can be written as:

$$i = \overleftarrow{i} - \overrightarrow{i} = nAFk_2 \bar{c}' e^{\frac{n(1-\alpha)FU}{RT}} - nAFk_1 \bar{c} e^{-\frac{n\alpha FU}{RT}} = 0. \tag{3}$$

Here $\overleftarrow{i}$ and $\overrightarrow{i}$ are the exchange currents. At equilibrium, these are equal to one another. k_1 and k_2 (cm/sec) characterize the reaction rate and α is a coefficient whose value lies between zero and unity.

The electrode potential is altered by the passage of the alternating current. We will designate this alteration by φ. The current being a periodic function of time, it is clear that the electrode potential will vary with the same period. In this case:

$$i = I\cos\omega t = \overleftarrow{i} - \overrightarrow{i}, \tag{4}$$

$$\overleftarrow{i} = nAFk_2 c_0' \exp\left\{\frac{n(1-\alpha)}{RT} F(U+\varphi)\right\},$$

$$\overrightarrow{i} = nAF\, k_1 c_0 \exp\left\{-\frac{n\alpha}{RT} F(U+\varphi)\right\}. \tag{5}$$

We will suppose a condenser to be connected in series with the electrode so that a direct component of the current cannot appear.

Let c_0 and c_0' be the ion concentrations at the electrode surface. These quantities can be evaluated by solving the diffusion equation $\frac{\partial c}{\partial t} = D\frac{\partial^2 c}{\partial x^2}$ under the boundary conditions $c = \bar{c}$, when $x \longrightarrow \infty$ and $\underline{t}$ is arbitrary, and $\underline{t}$ and $(c)_t = (c)_{t+\frac{2\pi}{\omega}m}$ when $\underline{m}$ is an integer and $\underline{x}$ is arbitrary. (Similarly for c'). In addition, we must relate the current to the concentration gradient on the electrode surface:

$$i = -\left[e_1 D\left(\frac{\partial c}{\partial x}\right)_0 + e_2 D'\left(\frac{\partial c'}{\partial x}\right)_0\right] FA. \tag{6}$$

Here e_1 and e_2 are the ion charges of Ox and Rd, and D and D' are their diffusion coefficients. The Ox and Rd ion currents are readily related to one another. Since there is one Ox ion for each Rd ion, and since these ion currents are oppositely directed, it follows that $D\left(\frac{\partial c}{\partial x}\right)_0 = -D'\left(\frac{\partial c'}{\partial x}\right)_0$. Ion migration will not be taken into account, it being supposed that the solution contains an excess of a foreign electrolyte.

Under these conditions we have:

$$c_0 = \bar{c}\left[1 + q\sin\left(\frac{\pi}{4} + \omega t\right)\right] \tag{7}$$

with a similar expression for c':

$$q = \frac{I}{nAF\bar{c}\sqrt{D\omega}}; \quad q' = -\frac{I}{nAF\bar{c}'\sqrt{D'\omega}}. \tag{8}$$

The resulting expressions for the concentration we will set into (5). Equation (4) gives the relation between the current and the potential φ. From this relation, we will eliminate the equilibrium potential $U\left(e^{\frac{nF}{RT}U} = \frac{k_1}{k_2}\frac{\bar{c}}{\bar{c}'}$, from (3)$\right)$. Considering the current, and the potential drop corresponding to it, to be small, and expanding the exponential into a series which is exact to within infinitesimals of the second order, we obtain:

$$\frac{I\cos\omega t}{nAFk\bar{c}}\left(\frac{\bar{c}}{\bar{c}'}\right)^{\alpha} = \frac{nF}{RT}\varphi + \frac{1-2\alpha}{2}\left(\frac{nF}{RT}\varphi\right)^2 + (q-q')\sin\left(\frac{\pi}{4}+\omega t\right) + \tag{9}$$

$$+ [q'(1-\alpha)\varphi + q\alpha\varphi]\frac{nF}{RT}\sin\left(\frac{\pi}{4}+\omega t\right),$$

where $k = k_1^{1-\alpha}k_2^{\alpha}$.

The periodic function φ we will expand in a Fourier series. Here it will be enough to limit ourselves to the first harmonic, since the remaining terms give only very small corrections.

$$\varphi = \psi + V_1 \cos \omega t + \tilde{V}_1 \sin \omega t = \psi + V \cos (\omega t + \vartheta). \tag{10}$$

By comparing the coefficients for the various harmonics, we find from Equation (9) the relation between the amplitude of the alternating potential, V, and the current, I, the phase angle ϑ of the alternating potential, and the dependence of the direct component of the potential drop, ψ, on the alternating potential. The last of these relations is the most interesting:

$$\psi = \left(\alpha - \frac{1}{2}\right)\frac{nF}{2RT}V^2 - \frac{nF}{2RT}\frac{V^2}{G}\left(\alpha - \frac{\tau\sqrt{\frac{D}{D'}}}{1+\tau\sqrt{\frac{D}{D'}}}\right)\left(1 + \frac{\sqrt{D\omega}\tau^{\alpha}}{\sqrt{2}\,k\left(1+\tau\sqrt{\frac{D}{D'}}\right)}\right), \tag{11}$$

where

$$\tau = \frac{\tilde{c}}{\tilde{c}'}; \quad G = \left[1 + \frac{\tau^{\alpha}\sqrt{2D\omega}}{k\left(1+\tau\sqrt{\frac{D}{D'}}\right)} + \frac{\tau^{2\alpha}D\omega}{k^2\left(1+\tau\sqrt{\frac{D}{D'}}\right)^2}\right]. \tag{12}$$

The existence of a direct potential drop at the electrode during the passage of an electrical current through the latter is easily explained by taking account of the fact that Relation (5) is antisymmetric with respect to the sign of φ. The value of ψ compensates, in a certain fashion, the rates of the direct and the reverse reactions. From these considerations, it is clear that ψ must reduce to zero when Equation (5) is symmetric, and that this will be the case when c = c', D = D' and $\alpha = 1/2$.

Actually, under these conditions, $\psi = 0$, as can be seen from (11). The corresponding equations of [6] show ψ reducing to zero at c = c', D = D', for any α. The error here is found in the fact that with the method of calculation which was adopted in [6], it is necessary to retain in the exponential, not only terms coming from the first harmonic, but those from the second harmonic of the development of φ. Equation (11) is somewhat simplified when the volume concentrations of the reacting ions are equal to one another, i.e., when $\tau = 1$. In this case:

$$\psi = \left(\alpha - \frac{1}{2}\right)\frac{nF}{2RT}V^2 - \frac{nF}{2RT}\frac{V^2}{G'}\left(\alpha - \frac{1}{1+\sqrt{\frac{D'}{D}}}\right)\left(1 + \frac{\sqrt{D\omega}}{\sqrt{2}k\left(1+\sqrt{\frac{D}{D'}}\right)}\right), \tag{13}$$

where G' = G when $\tau = 1$.

In the limiting case, $k \gg \sqrt{D\omega}$

$$\psi = \frac{nF}{2RT}V^2\left(\frac{1}{1+\sqrt{\frac{D'}{D}}} - \frac{1}{2}\right) + \frac{nF}{2RT}V^2\left(\alpha - \frac{1}{1+\sqrt{\frac{D'}{D}}}\right)\frac{\sqrt{D\omega}}{\sqrt{2}\,k\left(1+\sqrt{\frac{D}{D'}}\right)}. \tag{14}$$

When $k \ll \sqrt{D\omega}$

$$\psi = \left(\alpha - \frac{1}{2}\right)\frac{nF}{2RT}V^2 - \frac{nF}{2RT}V^2\left(\alpha - \frac{1}{\sqrt{\frac{D}{D'}}+1}\right)\frac{k\left(1+\sqrt{\frac{D}{D'}}\right)}{\sqrt{2D\omega}}. \tag{15}$$

From the resulting expressions, it is clear that the value of ψ depends on α. Having experimentally measured V and ψ, α can be found from these equations. Doss and Agarwal [4, 5] were the first to call attention to this fact. The equationderived by them corresponds to (13) when D = D'. If α is close to one half, however, even a small difference in the diffusion coefficients can prove to be significant, and so for the determination of this quantity it is necessary to use Equation (11) or (13).

II. A potential drop ψ is also met in the case where the solution contains only ions of the oxidizing agent. A metallic electrode immersed in a solution of its own ions, could serve as an example.

In this case, the surface layer contains an excess of the reducing agent, and the rate of oxidation is independent of the latter's concentration. Here we must set q' = 0 in Equations (5) and (9). The calculations are carried out in the same manner as before. The final result is:

$$\psi = \left(\alpha - \frac{1}{2}\right)\frac{nF}{2RT}V^2 - \frac{\alpha}{2}\frac{nF}{RT}V^2\,\frac{1+\dfrac{\tau^{\alpha}\sqrt{D\omega}}{\sqrt{2}k}}{1+\dfrac{\sqrt{2D\omega}\,\tau^{\alpha}}{k}+\dfrac{D\omega}{k^2}\tau^{2\alpha}}. \qquad (16)$$

With $k \gg \tau^{\alpha}\sqrt{D\omega}$

$$\psi = -\frac{1}{4}\frac{nF}{RT}V^2. \qquad (17)$$

In the diametrically opposite limiting case, $k \ll \tau^{\alpha}\sqrt{D\omega}$,

$$\psi = \left(\alpha - \frac{1}{2}\right)\frac{nF}{2RT}V^2 - \frac{\alpha}{2}\frac{nF}{RT}V^2\,\frac{k}{\tau^{\alpha}\sqrt{2D\omega}}. \qquad (18)$$

The $Hg_2^{2+} + 2e \rightleftharpoons 2Hg$ system has been studied in [6]. For reasons which have already been pointed out, the general equation given there for ψ is incorrect, but in the limiting case of $k \gg \tau^{\alpha}\sqrt{D\omega}$, there is agreement with (17). The experimental test as carried out in [6] refers, in actuality, to this limiting case, although the frequency ω varied from 20 to 5000 vib/sec (at high frequencies it is necessary to take account of the current which is involved in charging the double layer). It proved to be so (through the measurements of V and ψ) that the value of $\frac{2RT\psi}{FV^2}$ varied from -1.26 to -0.84, i.e., Equation (17) was well confirmed (n = 2).

However, in order to confirm the general equation (and to determine α), it is necessary to experimentally investigate the situation when $k \leq \tau^{\alpha}\sqrt{D\omega}$.

In these calculations we have not taken account of the effect of the double layer, particularly with respect to the value of the surface concentration.

In conclusion, I would like to take this opportunity to express my thanks to Academician A. N. Frumkin for having directed my attention to this problem, and to Professor V. G. Levich for valuable discussion.

Note added in correcting the proofs: The letter [11] containing an equation for the potential drop which is obviously similar to ours, appeared when the present work was already in press.

LITERATURE CITED

[1] K. S. G. Doss and H. P. Agarwal, Proc. Ind. Acad. Sci. 34, sec. A, 229 (1951).

[2] R. Hillson, Trans. Farad. Soc. 50, 385 (1954).

[3] M. Le Blanc and K. Schick, Zs. Phys. Chem. 46, 213 (1903).

[4] K. S. G. Doss and H. P. Agarwal, Proc. Ind. Acad. Sci. 34, sec. A, 263 (1951).

[5] K. S. G. Doss,and H. P. Agarwal, Proc. Ind. Acad. Sci. 35, sec. A, 45 (1952).

[6] K. B. Oldham, Trans. Farad. Soc. 53, 80 (1957).

[7] P. Dolin and B. Ershler, J. Phys. Chem. 14, 886 (1940); P. Dolin, B. Ershler and A. Frumkin, J. Phys. Chem. 14, 907, 917 (1940).

[8] D. C. Grahame, J. Electrochem. Soc. 99, 370C (1952).

[9] J. E. B. Randles, Disc. Farad. Soc. 1, 11 (1947).

[10] H. Gerisher, Zs. Phys. Chem. 198, 286 (1951); G. C. Barker, R. L. Faircloth and A. W. Gardner, Nature 181, 247 (1958).

Received January 10, 1958

THE MECHANISM OF THE ANODIC DISSOLUTION OF MAGNESIUM

B. N. Kabanov and D. V. Kokoulina

(Presented by Academician A. N. Frumkin, January 15, 1958)

Because of experimental and theoretical difficulties, it has not been possible up to the present to develop the mechanism for a rapid step in the anodic oxidation of metals when it is accompanied by a slower one. This can now be done in the case of metals showing a "negative difference effect," i.e., in the case of metals whose anodic dissolution leads to a transition state of a univalent ion, unstable in solution [1, 2].

The process of dissolution of magnesium in acid solutions can proceed according to the following scheme:

$$1.\quad Mg \longrightarrow Mg^{+}_{ads} + \theta;$$

$$2.\quad Mg^{+}_{ads} \longrightarrow Mg^{++} + \theta;$$

$$3.\quad Mg^{+}_{ads} \longrightarrow Mg^{+}_{sol}$$

and then

$$4.\quad Mg^{+}_{sol} + H^{+} \longrightarrow Mg^{++} + \frac{1}{2} H_2$$

or in neutral and weakly alkaline solutions:

$$4'.\quad Mg^{+}_{sol} + H_2O + OH \longrightarrow Mg(OH_2) + \frac{1}{2} H_2.$$

The slowest of the electrochemical steps of this process is the oxidation of metallic magnesium to the univalent ion, since after this there follow two parallel steps, one of which, the diffusion in solution, is almost always rapid because of the instability of the univalent ions. The electrochemical oxidation of magnesium is very markedly retarded by the adsorption of oxygen, i.e., by passivation [3]. It could be expected that the electrochemical oxidation of the intermediate substance, the univalent magnesium ion, to the divalent state (at a constant surface concentration of the univalent magnesium) would not be retarded by passivation of the metal, just as the oxidation of divalent to trivalent iron can proceed with considerable velocity on a passive iron on which the oxidation of the metal has practically ceased [4]. By that adsorption of oxygen which results in passivation it is possible to alter the structure of the metallic surface and of that part of the electric double layer which attaches to the surface and this process is then significant, primarily, for the transition of the metal into the hydrated ionic form. Further oxidation of the hydrated cation proceeds without the transfer of ions across the metal – solution interface, and is therefore not affected by an alteration in the work of liberation of the electron if there is no variation in the ψ_1-potential (in the case of the evolution of hydrogen, A. N. Frumkin pointed to an absence of an effect from the work of liberation as early as 1931 [5]). The explanation for this last is found in the fact that an alteration in the work of electron liberation in vacuum, or in the contact potential, at fixed total electrode potential is compensated by an equivalent alteration in the potential drop in the ionic electric double layer.

Let us consider the situation for the oxidation of univalent magnesium. Supposing the rate, i_2, of the anodic process $Mg^+ \rightarrow Mg^{++}$ to be determined by the retardation of the electron transfer (which is accompanied by increased hydration), it is possible to write the following expression:

$$i_2 = k_2 [Mg^+]_s \exp \frac{\beta F \varphi}{RT}. \quad (1)$$

We will consider the constant β to have the same value as in the oxidation of magnesium into the univalent form i.e., $\beta = 0.23$ (according to our data). For the parallel process of the diffusional transfer of Mg^+ from the electrode surface into solution, we have:

$$i_3 = FD \frac{dc}{dx} = FD \frac{[Mg^+]_{x=0}}{\delta} = k_3 [Mg^+]_s, \quad (2)$$

where k_3 depends on the rate of agitation, if the oxidation of the Mg^+ by the water is not completed in that portion of the diffusion layer which directly adjoins the electrode. Since it is comparatively low, it has been supposed that the concentration of magnesium ions in solution near the surface, $[Mg^+]_{x=0}$, is proportional to the surface concentration, $[Mg^+]_s$.

From a comparison of Equations (1) and (2), it is to be seen that the distribution of magnesium between the two parallel processes, i.e., the ratio i_2/i_3, is independent of the surface concentration of the univalent magnesium, $[Mg^+]_s$, and is fixed for the potential alone.

$$\frac{i_2}{i_3} = \frac{k_2}{k_3} \exp \frac{\beta F \varphi}{RT} = k \exp \frac{\beta F \varphi}{RT}. \quad (3)$$

In order to have a comparison of this theoretical result with the experimental data, it is necessary to find a relation between the effective valence, n_i, of the dissolving magnesium [1] and the electrode potential, φ. It is easily shown that the effective valence of the magnesium is:

$$n_i = \frac{1 + 2i_2/i_3}{1 + i_2/i_3}. \quad (4)$$

Combining Equations (3) and (4), we obtain the desired result:

$$n_i = \frac{1 + 2k \exp \frac{\beta F \varphi}{RT}}{1 + k \exp \frac{\beta F \varphi}{RT}}. \quad (5)$$

On the other hand, our experiments have shown the potential of anodic dissolution of magnesium to be almost independent of the current density in activationg solutions ($MgCl_2$, $MgBr_2$, $MgSO_4$); with decreasing anodic current density, there is a rise in the passivity of the magnesium.* At fixed potential, the effective valence, n_i, and the ratio i_2/i_3 (Equation (4)) remain constant under varying current density, i.e., according to Equation (3), the constant k is independent of the passivity of the metal, although there is a hundred fold

*This follows from the inverse diminution of the capacity of the double layer and from the course of the logarithmic curves of the alteration of the electrode potential after a sharp decrease in the current density, it being clear that the potential gradually returns to its original value.

variation in i_2 and i_3. In other words, with passivation of the magnesium, the rate of anodic oxidation of the Mg^+ ions at constant φ is altered only by changes in $[Mg^+]_s$ and in the diffusion of these ions from the electrode (it can be supposed that the apparent current density and the true density, the latter determined by considering the change in the total actual surface and the possibility of the mechanical coverage of a part of this surface with an oxide film, will alter in different degrees, but this fact is without influence on our conclusions).

When graphed, the theoretical n_i, φ relation of Equation (5) gives an S-shaped curve which is in general similar to that obtained experimentally. Additional evidence of this similarity is furnished by the slopes of these curves at $n_i = 1.5$, i.e., at the inflexion point. Let us differentiate (5) with respect to φ:

$$\frac{dn_i}{d\varphi} = \frac{k\beta F}{RT} \exp\left(\frac{\beta F\varphi}{RT}\right)\left[1 + k\exp\left(\frac{\beta F\varphi}{RT}\right)\right]^{-2},$$

we then have for the inflexion point:

$$\left(\frac{dn_i}{d\varphi}\right)_{n_i = 1.5} = \frac{\beta F}{4RT} = 2{,}3\text{v}^{-1}.$$

Within the limits of the experimental error, the slopes of the theoretical and experimental curves are the same at the inflexion point. In general, the similarity of the experimental and the theoretical curves supports the assumption that the process branches into diffusion and delayed discharge. It canthus be supposed that the velocity of electron transfer determines the rate of the second stage of the anodic oxidation of magnesium. Naturally, this velocity does not noticeably depend on the passivity of the electrode. At the extremities, however, the experimental curve departs from the theoretical. In distinction to the experimental curve, the theoretical curve tends toward the limit $n_i \cong 1.3$, instead of $n = 1$, at large negative values of φ.* Within the given interval of negative potential values, it can thus be supposed that either the rate of oxidation of Mg^+ is independent of φ or the passage of every two Mg^+ ions into solution is accompanied by the formation of one Mg^{++}. With this latter a assumption, the mechanism of activation and the existence of stationary anode potential in "activating" solutions could be explained. It can be assumed that the state of the magnesium in the passive adsorption layer is similar to that of the divalent ion in the bulk oxide. If the passage of two univalent Mg^+ ions and one structurally bound passivating MgO group into solution were the elementary act of anodic dissolution of magnesium, then this latter group, when in solution, would be attracted by the univalent ions and an activation proportional to the anode current would result.

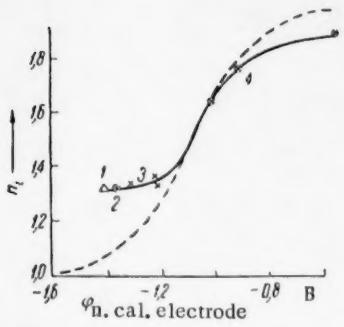

Fig. 1. The dependence of the effective initial magnesium valence on the potential of the magnesium anode. The dotted curve is the theoretical, the full one, the experimental. Solutions: 1) $MgCl_2$ (1 N); 2) $MgBr_2$ (1 N); 3) $MgSO_4$ (0.01 N and 1 N); 4) $KClO_3$ (0.5 N).

After increasing the current density, activation will continue as long as the effective surface does not increase to the point where the true current density falls to its initial value; this will automatically restore the initial potential under which there is a fixed number of passivating groups per unit effective surface.

* The potential φ is here read off from the inflexion point, i.e., it is assumed that $k = 1$.

Equation (5) makes it possible to obtain a general relation connecting the rate of hydrogen evolution (in amps/cm^2) and the potential [2]:

$$V = V_1 + V_2 = \frac{k' \exp\left(\frac{\beta' F\varphi}{RT}\right)}{1 + k \exp\frac{\beta F\varphi}{RT}} + k'' \exp\left(-\frac{\alpha F\varphi}{RT}\right),$$

here k' and β' are the coefficients for the Mg → Mg^+ reaction (we suppose β' = β) and k'' is the rate of the autodissolution of magnesium when $\varphi = 0$.

Considering the instability of the Mg^+ ion and the assumptions which we have made concerning the sequence of anodic processes in the formation of Mg^+ and Mg^{++}, it can be concluded that the potential of the Mg^+/Mg^{++} system is considerably more negative than the most negative potential under which the formation of Mg^+ can still proceed on the anode, i.e., −1.4 volts against the normal calomel electrode; its value can be approximated as −1.7 volts. According to Liuter's rule, the normal electrode potential of the Mg/Mg^+ system should be approximately −3 volts in this case, a value which would correspond to the normal potential for an alkali metal.

By using other suitable acceptors for the univalent ions in the place of water, it is hoped that it will be possible to obtain similar n_i (φ) curves for other more noble metals having 2 as the lower valence state of the ion and thereby deduce the slow step in these processes.

LITERATURE CITED

[1] R. L. Petty, A. W. Davidson and J. Kleinberg, J. Am. Chem. Soc. 76, 363 (1954); M. D. Rausch, W. E. McEwen and J. Kleinberg, Chem. Rev. 57, 417 (1957); J. H. Greenblatt, J. Electrochem. Soc. 103, 539 (1956).

[2] D. V. Kokoulina and B. N. Kabanov, Proc. Acad. Sci. USSR 112, 692 (1957).*

[3] E. V. Barelko and B. N. Kabanov, Proc. Acad. Sci. USSR 90, 1059 (1953).

[4] B. N. Kabanov and D. I. Leikis, J. Phys. Chem. 20, 1001 (1946).

[5] M. I. Temkin and A. N. Frumkin, J. Phys. Chem. 30, 1162 (1956).

The Institute of Physical Chemistry of the Academy of Sciences of the USSR

Received January 13, 1958

*Original Russian pagination. See C. B. Translation.

THE MECHANICS OF EXTENDED POLYMER SYSTEMS

G. A. Patrikeev

(Presented by Academician V. A. Kargin, January 2, 1958)

1. The basic problem of the molecular theory is that of establishing relations between the mechanical properties of polymer molecules and the mechanical characteristics of a body considered as an aggregate of these molecules. According to tradition, this is a problem which is to be solved by the methods of statistical thermodynamics [1]. The results which are available have been obtained from a study of the nonequilibrium deformation of polymers [2]. Up to the present time, however, there has been no systematic application of the methods of mechanics to the treatment of this problem.

2. In developing the mechanics of polymer molecules, it is assumed that the act of mechanical rupture follows after a stage of elastic extension of the polymer molecule [3]. Using rubber as an example, this paper will consider the fundamental problems of the "mechanical" theory of the extension of polymer systems, this theory being based on the assumption that such elastic extensions of polymer molecules are of fundamental significance for the extension of an idealized rubber [4]. The basic theorem of mechanics is that which postulates a balance of forces among the stressed structural elements of a deformed body, and thus the principal task in the development of the theory is the study of the conditions required for an "internally compensated" equilibrium.

3. The molecular structure of the idealized rubber is generally described in terms of "molecular" segments of fixed length, (α), which are united at "junctions" (C–C, C–S, etc.) by strong covalent chemical bonds. These molecular "segments" are looked on as unit structural parameters [5]. It is now proposed to introduce a second structural parameter, the length (μ) of that closed cyclic polymeric network, or polymer cycle, which is formed by the system of molecular segments united at the junctions; obviously, the length of the shortest of these "polycycles" is many times greater than that of a segment [6]. The extended idealized rubber is then a system of configurationally and elastically distended segments which are not only mutually joined by bonds, but are also directly united by the "molecular meshes." Under the conditions which are being considered, namely equilibrium between the elastically extended segments, it is not necessary to take direct account of the weak, localized intermolecular bonds, although their indirect influence is great, as is that of the stearic hinderances.

4. In the case of sufficiently slow extension, a mutual contraction along the chain must be postulated as the principal means for bringing the elastically stressed segments into equilibrium. In Fig. 1 there is a sketch of a stressed structnral element (SSE) which has the form of an elastically strained segment, No. 1, and a number of other similar segments which have brought the stress in this first segment into equilibrium by contraction along the chain. With increased branching, the degree of stress in the segments must diminish and, in the first approximation, diminish in direct proportion to the number of segments, so that constant total stress is maintained in every section of the SSE:

$$\sigma_c = A^{k_1}\sigma_2 = A^{k_2}\sigma_3 = \ldots = A^{k}\sigma_s \text{ dynes} \qquad (1)$$

A is here the mean number of branches in the segment ($2 < A \leq 4$); $\underline{k}$ is the order number of the segment or junction, counted from junction No. 1 to which segment No. 1 is united; σ_c is the stress in the maximally

elastically extended segment No. 1, $\sigma_c = a_c \epsilon_c \approx 7.5 \cdot 10^{-3} \epsilon_c$ dynes per molecule; σ_2 and σ_3 are the stresses in the equilibrating segments Nos. 2 and 3, etc.; σ_s is the statistical mean stress in the configurationally extended segments, $\sigma_s = a_s \epsilon_s \approx 1 \cdot 10^{-8} \epsilon_s$ dynes per molecule, and a_c, a_s and ϵ_c, ϵ_s are respectively, the moduli of elasticity and the relative extensions for the elastic, and the configurational, extensions of the segments [3].

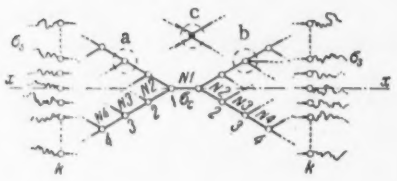

Fig. 1. Scheme of a SSE. a) Junction A-3, b) junction A-4, c) molecular mesh.

Mention should be made of the possibility of applying the mathematical apparatus of the theory of chain reactions to these calculations. The number of the configurationally extended segments which finally bring the elastic stress of the one elastically extended segment, No. 1, into equilibrium, can be considered as being of the order $10^4 - 10^5$. Such are the conclusions which follow from applying the methods of the mechanics of equilibrium to the direct interaction of the elastically extended polymer molecules.

5. Quantitative relations can be introduced if the "skeleton" hypothesis is accepted [4]. According to this hypothesis, on extending a rubber specimen, there arises a continuous, equilibrated system of elastically extended segments which is designated as the skeleton ("elastic lattice"), this system expanding as the extension proceeds so as to take up the better share of the external load and that part of the stress of the internal force field ("elastic lattice") which can not be brought into equilibrium by the action of the external forces. It is thus considered that the stress in the extended specimen is fixed by the potential energy of the elastically extended polymer molecules. The ideas which have been developed here can be brought into conformity with the concept of "forced elasticity" [7], but, contrary to general belief [1, 3, 5, 8] it is not possible to establish a direct relationship between the mechanical and the thermodynamical parameters, even though correlations can be expected in certain instances. It should be noted that the skeleton hypothesis considers an entropy deformation of the segments to be, for the most part, compensated within the specimen and to be without influence on the external stress. The thermodynamic theories of the thermal effects remain valid, although corrections are required in order that the role of the elastic extension of the segments be taken into account. Sections of the skeleton must penetrate the elastic medium; thus, the deformation mechanism of the specimen may be a microvolume mechanism rather than a molecular one. These concepts are in agreement with the idea of the existence of a special "chemical flow" which accompanies the mechanical deformation of polymers [9]. If the number of continuous longitudinal "sections" of the skeleton is presumed to correspond to the mean number of SSE units in the specimen cross section, a relation can then be established between the stress, (f), in the specimen, or the stress in the maximally distended segment No. 1, and the number of such segments (n), in the section. According to [1] this supposition is fully justified, the strain in any SSE section remaining constant and equal to σ_c. The condition of logitudinal equilibrium will then be described by the equation:

$$f = 10^{-6} \sigma_c \sum_1^x (n_1 + n_2 + n_3 + \ldots + n_x)$$

or

$$f = 10^{-6} \sigma_c n \text{ kg/cm}^2, \qquad (2)$$

where $\sigma_c = a_c \epsilon_c$; $n_1, n_2, n_3 \ldots n_x$ are the numbers of the sections formed in the respective elongations of the specimen and $\underline{n}$ is the mean over-all number of sections in the cross section of the distended specimen.

The maximum number, n', of independent, noninteracting SSE's in the cross section of the extended specimen, can be determined if a value is given for σ_c. With $\sigma_c = 1 \cdot 10^{-4} - 1 \cdot 10^{-3}$ dynes per molecule and $f = 1$ kg/cm^2, $n' = 1 \cdot 10^{10} - 1 \cdot 10^9$ cm^{-2} per 1 kg of stress in the distended specimen, the total area of the maximally stressed segments in the extended specimen makes up only $1 \cdot 10^{-5} - 1 \cdot 10^{-6}$-th part of the total cross section. According to the ideas which have just been developed, the experimentally determined "stress-strain" curve must reflect the probability of an increase in the number, (n), of sections of the skeleton during distension of the specimen; to this there is to be attributed the great significance of experiments on the extension of polymeric substances, a method of study which is widely applied in practice.

6. In studying the conditions which prevail during the formation of the skeleton, it is useful to consider three stages. The first stage is the formation of the individual SSE's; the second is the interaction of these SSE's and the establishment of internal force fields which are brought into equilibrium by the various segments of the skeleton; and the third is the formation of the continuous "longitudinal" (x) and "transverse" (y, z) sections of the skeleton. With increasing concentration, the SSE's must interact and unite with one another. Rigid, difficultly distendable sections of the skeleton must arise from subsequent longitudinal interaction; the relative extension of these sections must be the same as that of the specimen, if the initial length is taken to be that extension under which the given section was formed. If the SSE's interact, first in parallel and then in series, elastically stressed networks will then result from the secondary interaction of the elastically extended, transverse and longitudinally equilibrated structures, and subsequent interactions of these networks must led to the formation of three-dimensional equilibrated branched sections of the skeleton.

There are at least three facts which are responsible for the existence of different extensions, in the sections of the distended skeleton and in the specimen; the difference in the initial absolute lengths of the specimen and the section, the fact that the network is a three-dimensional structure and that the section is warped, and the discrepancy between micro- and macroextensions, this last being especially marked for rubbers which are loaded with fillers [10]. A scale factor (λ) takes account of the ratio between the relative length of the emerging section (x_n) and the relative length of the specimen (x) at which this section is formed, $\lambda = \frac{x_n}{x}$, when $x_n < x$. Another scale factor π takes account of the details of the skeleton structure; of the fact that this structure is three-dimensional (x, y, z), of the longitudinal distance (e) between the SSE's in the section, of the transverse distance between sections of one and the same network (i_y, i_z), and of the twist of the longitudinally (j_x) and transversally (j_y, j_z) network-bound sections: $\pi = j_x + 2\frac{i}{e} j_y$. Since $j_x > 1$, j_y, $j_z < 1$ and $i > e$, π must also be greater than 1. A third scale factor φ takes care of the increased extension of those microvolumes of vulcanizate which are situated between the particles of the filler: $\varphi = \frac{x'}{x}$, x' being the mean relative length of the microvolume at a relative specimen length x. As a result of the diminution in the transverse section during extension of the specimen, the longitudinal sections must be extended at the expense of the transverse, so as to maintain constancy of stress in the network and in the sections of the skeleton. Thanks to the internal shifting of the "elastic medium," the sectional stress will diminish; this explains certain relaxational processes and the increase in the residual extensions. For bringing the transverse sections of the skeleton into equilibrium, the degree of extension of the surface layers must be considerably greater than that of the underlying layers; this is not true of the internal interfaces, but even here, the stresses must be considerable.

7. Without additional suppositions, it is possible to establish relations between the parameters characterizing the elastic extension of polymer molecules and the parameters of the mechanical properties of a slowly distended rubber. If the total length of the sections is evaluated, the work of the elastic extension of the segments calculated, and account taken of the scale factors, it is then possible to derive the following equation:

$$\beta_1 = \pi\varphi\varepsilon_c = \frac{2(A_p - a)}{fx}, \qquad (3)$$

In which A_p is the work of distension in kg·cm/cm^3 as determined by graphical integration of the experimental load-extension curve, and a is a correction for the work directly expended on the entropy deformation of the polymer molecules. Because of an additional transmission through the skeleton, it is impossible to determine the work expended in the entropy deformation of the basic part of the molecule from extension experiments; such is one prediction from the mechanical theory. It is possible to evaluate the degree of fall off of the stress at the beginning of the contraction of a strongly extended specimen by calculating the number of sections from Equation (2) and introducing the scale factor

$$\beta_2 = \pi \cdot \varphi \cdot \bar{\varepsilon}_c = -\frac{f}{xE_\beta}, \qquad (4)$$

in which E_β is the nonequilibrium modulus of elasticity in kg/cm^2, as determined from the slope of the contraction curve, the value of this quantity being numerically equal to the fall in the strain when the specimen contracts by 100%. Despite the crude approximations which were made in the derivation of Equations (2), (3) and (4), the experimental results which have been obtained on a wide selection of rubbers of various types, including the filled, are in rather good agreement with the predictions of the mechanical theory of the extension of polymeric systems.

8. The fraction (η) of the segments which are elastically distended can be evaluated through the equation: $\eta \approx \frac{Fs_0}{10^{-6}\sigma_c}$, where F = fx and s_0 is the effective cross section of the molecule of natural rubber: $s_0 = 25 \cdot 10^{-16}$ cm^2; when F = $1 \cdot 10^3$ kg/cm^2 and $\sigma_c = 0.25 \cdot 10^{-3}$ dynes, and the "coefficient of nonuniformity," $\eta \approx 1\%$.

It is essential to note that the skeleton hypothesis is based on the assumption that the strength of the polymer molecule is very high [3]. The ideas which have been developed here can be applied to the development of a program of work in the field of polymeric and colloidal bodies.

LITERATURE CITED

[1] P. P. Kobekov, Amorphous Substances (in Russian), Acad. Sci. USSR Press, 1952; L. Treloar, The Physics of the Elasticity of Rubber (in Russian) Foreign Lit. Press, 1953.*

[2] P. P. Kobekov, E. V. Kuvshinskii and G. I. Gurevich, Bull. Acad. Sci. USSR, phys. ser. No. 6, 329 (1937); A. P. Aleksandrov and Iu. S. Lazurkin, J. Tech. Phys. 9, 1249 (1939).

[3] G. A. Patrikeev, Proc. Acad. Sci. USSR 120, No. 2 (1958).**

[4] G. A. Patrikeev, Reports of the Ninth Confer. on General Problems in the Chemistry and Physics of High-Polymer Compounds, Acad. Sci. USSR Press 1956, p. 145; Rubber and Latex No. 4, 37 (1957).

[5] B. A. Dogadkin and M. N. Reznikovskii, Prog. Chem. 24, 801 (1955).

[6] G. A. Patrikeev, cited in V. A. Kropachev, Colloid. J. 18, No. 4, 509 (1956).**

[7] A. P. Aleksandrov, Proc. First and Second Confer. on High-Molecular Compounds, Acad. Sci. USSR Press, 1945, pp. 49-59.***

[8] E. Guth, G. James and G. Mark, The Chemistry of Large Molecules, Sympos. 1 (in Russian) Foreign Lit. Press, 1948, p. 72; G. M. Bartenev, Colloid J. 13, No. 4, 233 (1951).

[9] V. A. Kargin, T. I. Sogolova, G. L. Slonimskii and E. V. Reztsova, J. Phys. Chem. 30, No. 8, 1903 (1956).

[10] G. A. Patrikeev, Sympos., The Strength of the Bonds between the Elements of Multilayer Rubber Fabric Objects, Leningrad, 1956, pp. 78-86.***

Received December 26, 1957

*Russian translation.

**Original Russian pagination. See C. B. Translation.

***In Russian.

THE ISOTOPE EFFECT IN THE CRITICAL TEMPERATURE

I. B. Rabinovich and V. A. Gorbushenkov

(Presented by Academician A. N. Frumkin, February 19, 1958)

The literature contains only a limited amount of data on the effect of isotopic substitution on the critical constants (Table 1), and the rules governing this effect are still not clear. In the series $H_2 - HD - D_2$, it has been shown [9] that the critical temperature (T_c) increases with increasing molecular weight (M) and that it varies almost linearly with $1/\sqrt{M}$. The opposite effect of diminishing T_c results, however, from the isotopic replacement by deuterium of the hydrogen in H_2O [7], PH_3, and HBr [8].

TABLE 1

The Critical Constants of Isotopic Compounds

Substance	T_c, °K	P_c, atm	V_c, cm³/mole	Substance	T_c, °K	Substance	T_c, °K	P_c, atm [7]	V_c, cm³/mole [7]	Substance	T_c, °K [8]
He^3	3,34 [1]	1,15 [1]	73,0 [24]	HCl	324,2	H_2S	373,3			H_3P	325,1
He^4	5,26 [3]	2,26 [3]	57,8 [10]	DCl	323,5	D_2S	372,2 [8]			D_3P	323,6
H_2	33,24 [11]	12,80 [11]	66,9 [12]	HBr	363,1	H_2Se	414,4			H_3As	373,1
HD	35,91 [4]	14,64 [4]	62,8 [4]	DBr	362,0	D_2Se	412,4 [8]			D_3As	372,1
D_2	38,35 [5]	16,43 [5]	60,3 [4] *	HI	423,9	H_2O	647,4	218,5	55,6	H_3N	405,7
				DI	421,8	D_2O	644,7 [7]	218,6	55,2	D_3N	405,5

* This value refers to a deuterium containing 0.022 p-D_2 and 0.978 o-D_2.

In the present work, the T_c values of eleven deuterium compounds (Table 2) and their hydrogen analogs have been compared. The synthesis of deuterochloroform has been described in [14] and that of the deuteroalcohols in [16]. In order to obtain deuteronitromethane, ordinary nitromethane was repeatedly exchanged with a 0.02 M solution of NaOD in D_2O in sealed ampules at 110°C. Deuterobenzene, C_6D_6, and methyldeutrobenzene, $C_6D_5CH_3$, were prepared by long and repeated exchange with a 52 mole % solution of D_2SO_4 in D_2O. These substances were carefully purified and dehydrated. The densities (ρ_4^{20}), refractive indices (n_D^{20}), and boiling temperatures of the hydrogen compounds agreed with the data of the literature [17] to within $1 \cdot 10^{-4}$ g/cm³, $1 \cdot 10^{-4}$ and 0.1-0.2°, respectively.

T_c was determined from the appearance and disappearance of a meniscus. The apparatus and the experimental technique were those which have been described in [7]. Each substance was used to fill three capillary tubes. Capillaries with the isotopic analogs were placed in the thermostat under the same conditions. On each pair of these capillaries, 20 measurements were carried out. In addition to measurements of the difference $\Delta T_c = T_{c,H} - T_{c,D}$, absolute values of T_c were determined in those cases where this quantity did not exceed 300°C. The results for the hydrogen compounds (Table 2) agreed to within 0.1-0.2° with the T_c values given

TABLE 2

The Isotopic Effect in the Critical Temperature

Substance	D **, %	ΔT_c, deg	T_c, °K	V, cm³/mole, at 293°K	Substance	D **, %	ΔT_c, deg	T_c, °K	V, cm³/mole, at 293°K
C_6H_6	0		562,1	88,87	C_2H_5OH	0		515,8	58,36
C_6D_6*	91	1,4 ***	560,7	88,69			0,9		
					C_2H_5OD	98		514,9	58,45
$C_6H_5CH_3$	0		594,0	106,29	$CH_3(CH_2)_2OH$	0		537,1	74,79
		1,0 ****					1,0		
$C_6D_5CH_3$*	65		593,0	106,20	$CH_3(CH_2)_2OD$	99		536,1	74,89
CH_3NO_2	0		588,0	53,65	$(CH_3)_2CHOH$	0		508,7	76,55
		1,0					0,3		
CD_3NO_2*	96		587,0	53,66	$(CH_3)_2CHOD$	99		508,4	76,67
$CHCl_3$	0		536,8	80,17	$CH_3(CH_2)_3OH$	0		560,9	91,56
		0,9					0,5		
$CDCl_3$	98		535,9	80,19	$CH_3(CH_2)_3OD$	98		560,4	91,73
CH_3COOH	0		594,8	57,24	$(CH_3)_2CHCH_2OH$	0		549,7	92,41
		0,7					0,3		
CH_3COOD	99		594,1	57,27	$(CH_3)_2CHCH_2OD$	97		549,4	92,67
					$CH_3CH_2CHOHCH_3$	0		538,1	91,90
							0,4		
					$CH_3CH_2CHODCH_3$	96		537,7	92,13

* The investigated substances did not exactly correspond to this formula, containing, as it did, isotopic analogs with a smaller number of deuterium atoms.

** In the group or ring where it was substituted.

*** By linear extrapolation to 100% D, $\Delta T_c = 1.6°$.

**** With 100% D, $\Delta T_c = 1.5°$.

in the review [15] as the most trustworthy from among the data of a number of authors. Above 300°C, it was only ΔT_c which was measured, the T_c values being taken from [15]. For each substance, the squared error of the ΔT_c determinations amounted to about 0.1°, this representing 20-30% of the ΔT_c values of the butanols and isopropanols, and about 10% of the ΔT_c values for the other substances.

It was found that the substitution of the light isotope by the heavy led, in every case, to a decrease in T_c. It is to be seen from Table 1 that this isotopic effect carries the same sign as that which has been observed in earlier investigated substances (hydrogen and helium are exceptions). It is thus clear that in the region of moderate temperatures, the relation

$$T_{c,D} < T_{c,H}, \tag{1}$$

is generally valid for substances taken from various classes of organic and inorganic compounds. Introducing the well known equations $a = 27R^2T_c^2/64P_c$ and $a = 9RT_cV_c/8$, (a is the van der Waals' constant), we have

$$\frac{a_D}{a_H} = \frac{T_{c,D}^2 P_{c,H}}{T_{cH}^2 P_{c,D}}, \tag{2}$$

$$\frac{a_D}{a_H} = \frac{(T_cV_c)_D}{(T_cV_c)_H}. \tag{3}$$

According to (3), $a_D/a_H = 0.989$ for the isotopic analogs of water. V_c and P_c have not been studied for the deutero compunds which are represented in Table 2. A rough idea as to the difference between V_D

and V_H in the neighborhood of T_c can be obtained from a knowledge of the volumes and mean coefficients of thermal expansion, $\bar{\alpha}_D$ and $\bar{\alpha}_H$, at lower temperatures. We have measured the densities of these substances at 5° intervals over the range from 293-343°K and have calculated values for V and $\bar{\alpha}$.

For chloroform, nitromethane and acetic acid, Table 2 shows that at 293° and to within the limits of the experimental error (0.05%), $V_D = V_H$. With C_6D_6 and $C_6D_5CH_3$, V_D is less than V_H by 0.1-0.2%. This is to be explained by the fact that the molar volumes of these compounds are markedly affected, even at room temperature, by the decrease in the amplitude of the null point molecular vibrations which results from the substitution of H by D [21]. With the alcohols, on the other hand, V_D exceeds V_H by 0.1-0.2%, this being possibly due to increased association from hydrogen bonding as the result of the substitution of the hydrogen of the hydroxyl by deuterium [13]. The effect of these two factors must be insignificant, however, when the temperature is close to T_c, since $h\nu$* is then small in comparison with kT and there is almost no association. In the region of study (293-343°), $\bar{\alpha}_D > \bar{\alpha}_H$ in every case, but these quantities differ by so little that the difference between the isothermal values of V_D and V_P is of the order of $1 \cdot 10^{-4}$ per degree. In addition, the values of $\bar{\alpha}_D$ and $\bar{\alpha}_H$ sharply diminish as T rises toward T_c, this being due to the weakening of the intermolecular interaction. With substances which are liquid at moderate temperatures there is thus reason to suppose that

$$V_D = V_H. \tag{4}$$

in the neighborhood of T_c and to within an accuracy of 0.1%. The condition $T_{c,D} < T_{c,H}$ can only lead to a diminution of V_{cD} relative to V_{cH} and not to the opposite effect. Thus, in view of (4), it is likely that

$$V_{c,D} \leqslant V_{c,H}. \tag{4'}$$

For compounds in which ΔT_c amounts to about 1°, we then find from (1), (3) and (4) that

$$a_D < a_H, \tag{5}$$

from which, in view of (4), it follows that

$$\pi_D < \pi_H, \tag{6}$$

where $\pi = a/V^2$ is the internal pressure. At moderate values of T, the substitution of hydrogen by deuterium thus clearly leads to a decrease in the van der Waals' interaction.

From the point of view of the dispersive forces, this result follows from the equation of Slater and Kirkwood [18]. Applying this equation to the isotopic analogs and replacing $(r_D/r_H)^3$ (r is the distance between the molecules) in a first approximation by V_D/V_H, we obtain

$$\frac{\varepsilon_D}{\varepsilon_H} = \left(\frac{V_H}{V_D}\right)^2 \left(\frac{\alpha_{0,D}}{\alpha_{0,H}}\right)^{2/3}, \tag{7}$$

ϵ being the molecular dispersive energy and α_0 the static polarizability. A diminution of the null point energy of the respective atomic bonds results from the substitution of hydrogen by deuterium and this leads to an increase in the frequency of electron transfer. It follows from the dispersion equation [19] that this will bring about a decrease in the polarizability, the identity of the electron clouds resulting in a probability for electron transfer which will differ only insignificantly in the isotopic analogs. A decrease in the polarizability on substituting hydrogen by deuterium has been experimentally confirmed in water [13, 20], hydrogen peroxide [20], benzene and cyclohexane [21], and the deuteroethanes [22]. At the same time, $V_D \geqslant V_H$ at moderate temperatures for all of the investigated substances with the exception of C_6D_{12}, C_6D_6 and $C_6D_5CH_3$. For these last, V_H exceeds V_D at room temperatures by 0.1-0.2% but this percentage-wise difference is several times less than the isotopic effect in α_0 [21]. In view of (7), it follows from this that

$$|\epsilon_D| < |\epsilon_H| \tag{8}$$

*ν is the frequency of the intermolecular vibrations (several cm^{-1}).

A diminution of the van der Waals interaction on substituting hydrogen with deuterium is also indicated by the existence of an accompaning increase in compressibility [16]. The diminished strength of the van der Waals' forces in the deuterocompounds, as compared with their hydrogen analogs, can also explain the higher $\bar{\alpha}$ values shown by the former.

The described isotopic effects in a, π and ϵ, and the deduction of decreased van der Waals interaction resulting from the substitution of the light isotope by the heavy, cannot, however, be extended to the region of low temperatures. Since molar volumes at low temperatures are strongly affected by the amplitude of the null-point molecular vibrations, the molar volumes of liquid tritium, deuterium and He^4 are considerably less than those of the light analogs at the same temperature. For D_2 and H_2 at 19.5°K this difference amounts to 17% [23]. In such cases, the difference in the molar volumes predominates over the decrease in the polarizability, and it then follows from (7) that the dispersive interaction is stronger in liquid D_2 and in He^4 than it is in H_2 and in He^3, respectively. The isotopic effect in the critical constants shows this be the actual case. Setting the values of P_c and T_c into (2), we obtain $a_D/a_H = 1.037$ for D_2 and H_2 and $a_4/a_3 = 1.26$ for He^4 and He^3 for although the percentage difference in the molecular weights of the hydrogen isotopes is three times that of the helium isotopes, the percentage differences in T_c, P_c and a on the other hand, are 3-7 times larger in the case of helium. This is due to the especially low T_c value of the latter. Since, at low temperatures, the heavy isotope has a smaller molar volume than its light analog, it follows from the relation $\pi_D / \pi_H = (a_D / a_H)(V_H / V_D)^2$ that we would have for hydrogen and helium: $\pi_D > \pi_H$ and $\pi_4 > \pi_3$.

Thus at temperatures in the field of existence of liquid hydrogen and helium, replacement of the light isotope by the heavy leads to an intensification of the van der Waals' interaction, i.e., to an effect which is the opposite to that met at moderate temperatures.

We wish to express our thanks to A. I. Brodskii, Corresponding Member, Academy of Sciences of the USSR, for a discussion of these results, and to S. D. Ravikovich for advice in the measurements.

LITERATURE CITED

[1] S. G. Sydoriak, E. R. Grilley and E. F. Hummel, Phys. Rev. 75, 303 (1949).

[2] B. M. Abraham, D. W. Osborne and B. Weinstock, Phys. Rev. 80, 366 (1950).

[3] H. K. Onnes and S. Weber, Proc. Acad. Sci. Amsterdam 18, 493 (1916).

[4] J. Hoge and J. W. Lassiter, J. Res. Nat. Bur. Stand. 47, 75 (1951).

[5] A. S. Friedman, D. White and H. L. Johnston, J. Am. Chem. Soc. 73, 1310 (1951).

[6] R. D. Arnold and H. J. Hoge, J. Chem. Phys. 18, 1295 (1950).

[7] E. H. Riesenfeld and T. L. Chang, Zs. Phys. Chem. B, 28, 408 (1935); B, 30, 61 (1930).

[8] H. Kopper, Zs. Phys. Chem. A, 175, 469 (1936).

[9] A. S. Friedman, D. White and H. L. Johnston, J. Chem. Phys. 19, 126 (1951).

[10] E. Mathias, C. A. Crommelin, H. K. Onnes and J. C. Swallow, Proc. Acad. Sci. Amsterdam 28, 526 (1925).

[11] D. White, A. S. Friedman and H. L. Johnston, J. Am. Chem. Soc. 72, 3565 (1950).

[12] H. W. Woolley, R. B. Scott and F. G. Brickwedde, J. Res. Nat. Bur. Stand. 41, 379 (1948).

[13] A. I. Brodskii, The Chemistry of Isotopes (in Russian) Moscow, 1957.

[14] I. B. Rabinovich, P. N. Nikolaev, Z. E. Gochaliev and N. N. Tret'iakova, Proc. Acad. Sci. USSR 110, 241 (1956).

[15] K. A. Kobe and R. E. Lynn, Jr., Chem. Rev. 52, 117 (1953).

[16] I. B. Rabinovich, V. G. Golov, N. A. Efimova and S. M. Rustamov, Proc. Acad. Sci. USSR 114, 590 (1957).*

*Original Russian pagination. See C. B. Translation.

[17] J. Timmermans, Physicochemical Constants of Pure Organic Compounds, 1950; Technical Encyclophedia, Handbook of Phys. Chem. Tech. Constants, 1931-1933.

[18] J. C. Slater and J. G. Kirkwood, Phys. Rev. 37, 682 (1931).

[19] M. V. Vol'kenshtein, The Structure and Physical Properties of Molecules (in Russian) Moscow, 1955.

[20] M. K. Phibbs and P. A. Giguere, Canad. J. Chem. 29, 173 (1951).

[21] J. A. Dixon and R. W. Schiessler, J. Am. Chem. Soc. 76, 2197 (1954).

[22] J. Verhulst and J. C. Jungers, Bull. Soc. Chim. Belges 58, 73 (1949).

[23] E. R. Grilly, J. Am. Chem. Soc. 73, 5307 (1951).

[24] V. P. Peshkov, J. Exp. Theo. Phys. 33, 833 (1957); E. C. Kerr, Phys. Rev. 96, 551 (1954).

The Scientific-Research Institute of Chemistry
of the N. I. Lobachevskii State University
Gorki

Received December 28, 1957

THE DETERMINATION OF THE SPECIFIC SURFACE AND THE PORE VOLUME OF SOLID POLYMERIC SORBENTS

A. A. Tager, M. V. Tsilipotkina and A. I. Suvorova

(Presented by Academician V. A. Kargin, December 26, 1957)

The work of recent years has established the existence of a definite relationship between the physical condition of a polymer and the thermodynamics of its dissolution. Thus an evolution of heat and a sharp decrease in the entropy of the sorbing liquid accompany the interaction of a number of glassy polymers with low molecular liquids (polystyrene [1], polymethylmethacrylate [2], cellulose [3] etc.). Such changes are characteristic of the adsorption of vapors by porous solid sorbents [3] and from this the conclusion has been drawn that these polymers behave in the glassy state as microporous sorbents. The microporosity of such polymers arises from the loose packing of the micromolecules. At the same time, it was shown that an adsorption of heat and a small increase in the entropy of the sorbing liquid were to be observed in the sorption of vapors by polyvinyl alcohol, and that these facts are related to the dense packing of the macromolecules of this polymer [1]. All of this work has permitted a new formulation of the problem of the intermediate position which the high-molecular compounds occupy between the low-molecular liquids, on the one hand, and the colloidal sorbents, on the other [1]. Directly after the low-molecular liquids, there are placed the high-elastic polymers with flexible chains, and then follow the dense packed high-molecular glasses, the polymeric, loosely packed glasses and the solid porous sorbents, such as activated charcoal and silica gel.

By taking account of the great similarity between low-molecular liquids and solutions of elastic polymers, it has proved possible in the last 20 years to apply successfully to these solutions the thermodynamic principles which had been developed for true solutions of low-molecular compounds [4]. These principles have proven to be completely inadequate, however, for a consideration of the dissolving and swelling of glassy polymers [1]. In particular, it is impossible to consider as generally valid the rule which postulates a sharp increase in entropy, exceeding by many fold the ideal value, to be characteristic of solutions in which the molecules of one component are of large dimensions [5].

All of this points to the necessity for the development of a new approach to the interaction of the high-polymer glasses with solvents. Such a new approach could be that of considering glassy polymers as being similar to solid sorbents, and applying to them those methods which permit a quantitative evaluation of the porosity.

One such method which has been widely applied is that of sorption. The sorption isotherms which have been obtained up to the present time cannot, however, give definite information about polymer porosities. There are two reasons for this ambiguity; 1) all of the experiments have involved vapors of liquids which cause polymer swelling, that is to say, the sorption processes have been accompanied by a structural change in the sorbent; and, 2) in the event of swelling, the sorbability of a polymer depends, not only on the degree of packing of the macromolecules, but on the flexibility of the molecular chains as well.

These difficulties can be avoided by the use of vapors of liquids which are inert to the given glassy polymer. In such case, the polymer structure is not altered by the sorption process and the chain flexibility does not come into play.

We have investigated the sorption of vapors of inert liquids by polystyrene, polyvinyl alcohol, cellulose and triacetylcellulose. As sorbents there were employed two fractions of polystyrene of molecular weights

456000 and 133000, powdered triacetylcellulose of molecular weight 140000, polyvinyl alcohol of molecular weight 17000 and an industrial linter. Methyl alcohol was chosen as a liquid inert to polystyrene, and n-hexane, was used with the other polymers. The sorption of these liquids on activated charcoals and silica gels has been well studied [6, 7]. The apparatus described earlier in [1] was used for the measurements. At 25°, equilibrium was established in the course of 3-5 hours. The results of the measurements are shown in Figs. 1 and 2, from which it is clear that the isotherms differed from one another.

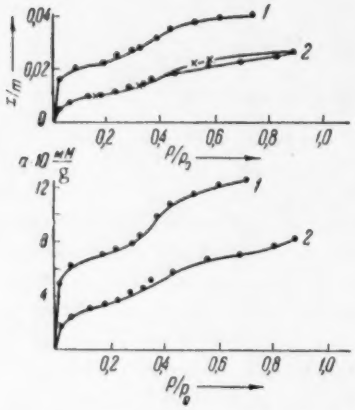

Fig. 1. Sorption isotherms for methyl alcohol on polystyrene. 1) Molecular weight 456000, 2) molecular weight 133000.

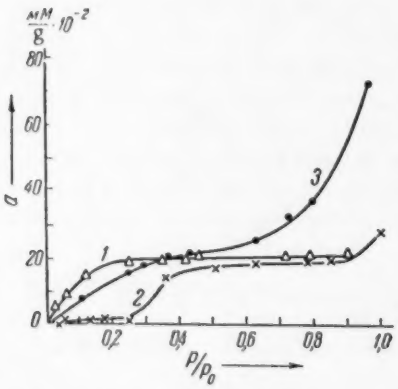

Fig. 2. Sorption isotherms for n-hexane. 1) Cellulose, 2) polyvinyl alcohol, 3) triacetylcellulose.

The isotherms for the sorption of methyl alcohol on polystyrene and n-hexane on cellulose are identical with isotherms for the sorption of the vapors of these same liquids on silica gel [3]. According to the classification of A. V. Kiselev [9], this type of sorption isotherm is characteristic of the homogeneous, finely porous sorbents. In this case a slight adsorption hysteresis was observed with the small molecules of methyl alcohol. The sorption isotherm for n-hexane on polyvinyl alcohol recalls the isotherms which have been obtained with nonporous sorbents [3]. Finally, with triacetylcellulose there was obtained a typically S-shaped isotherm, convex toward the axis of ordinates at low relative pressures of vapor and concave toward this axis at high relative pressures. Such isotherms are characteristic of the more coarsely porous sorbents. Thus, from a consideration of the external forms of these isotherms, it follows that polystyrene and cellulose are finely porous sorbents, that triacetylcellulose is more coarsely porous and that polyvinyl alcohol is a nonporous sorbent. These data are in complete agreement with the work of previous investigators, in which it has been shown that the molecular packing is open in polystyrene [1, 10], triacetylcellulose [1] and cellulose [2], whereas in polyvinyl alcohol, the packing is dense [1, 11]. From Fig. 1 it is seen that the sorption isotherm for the specimen with molecular weight 133000 fell below that of the specimen with molecular weight 456000. This points to an increase in the openness of the packing with increasing molecular weight of the polystyrene, a fact which has been noted earlier [12].

Following the BET method and the method of M. M. Dubinin and L. V. Radushkevich, an attempt was made to quantitatively evaluate the porosity of these polymers.

As is known, the basic equation of Brunauer, Emmett and Teller (BET) was derived for the S-shaped isotherm [13]. In a number of works, however, this method has been formally applied for calculating the specific areas and pore volumes of sorbents of various degrees of porosity, even including such nonporous sorbents as $BaSO_4$ and $PbSO_4$ [8]. The method of M. M. Dubinin and L. V. Radushkevich is applicable to finely porous sorbents.

In our cases, the BET equation was used over the region of relative pressures ranging from 0.03 to 0.05, that is, over that range in which it is generally valid. The equation of M. M. Dubinin and D. V. Radushkevich is applicable at low relative vapor pressures.

TABLE 1

Specific Surfaces and Pore Volumes

Sorbent	S, M^2/g	W_0, cm^3
Polystyrene, mol. wt. 456000	61.09	0.0315
Polystyrene, mol. wt. 133000	30.52	0.0154
Cellulose	42.64	0.0323
Triacetylcellulose	50.69	0.0838
Polyvinyl alcohol	3.59	–

In Table 1 there are shown the calculated values of the specific surfaces and the pore volumes of the investigated polymers. From this table it follows that high-molecular polystyrene, cellulose, and triacetyl cellulose can be classified as finely porous sorbents with poorly developed specific surfaces. With decreasing molecular weight of the polystyrene there is a decrease in the specific surface and the pore volume. The pore volume amounts to 1.5% of the total volume in high-molecular polystyrene, to 3% in cellulose and to 8% in triacetylcellulose. The specific surface of the polyvinyl alcohol is very small, its value corresponding to that of the nonporous sorbents [8].

The results which have been obtained indicate the possibility of quantitatively estimating the porosity of polymers by studying the sorption of inert liquids on them.

LITERATURE CITED

[1] A. A. Tager, Dissertation, L. Ia. Karpov Physicochemical Ins. Moscow, 1956.

[2] Kh. U. Usmanov and V. A. Kargin, J. Phys. Chem. 28, 224 (1954).

[3] S. Brunauer, The Adsorption of Gases and Vapors (in Russian), Foreign Lit. Press, 1948.*

[4] A. A. Tager, Solutions of High-Molecular Compounds (in Russian) 1951.

[5] E. A. Guggenheim, Trans. Farad. Soc. No. 15, 24 (1953).

[6] M. M. Dubinin, E. D. Zaverina and L. V. Radushkevich, J. Phys. Chem. 21, 1351 (1947); M. M. Dubinin and E. D. Zaverina, J. Phys. Chem. 23, 469 (1949).

[7] A. V. Kiselev and V. V. Kulichenko, J. Phys. Chem. 29, 663 (1955); A. V. Kiselev and Iu. A. El'tekov, J. Phys. Chem. 29, 904 (1955).

[8] A. V. Kiselev, Methods of Investigating Highly Dispersed and Porous Bodies (in Russian) Acad. Sci. USSR Press, 1953.

[9] A. V. Kiselev, J. Phys. Chem. 23, 452 (1949).

[10] A. A. Tager and Zh. Dombek, Colloid. J. 15, 69 (1953).**

[11] A. A. Tager, and V. A. Kargin, Colloid J. 14, 367 (1952).

[12] A. A. Tager, R. V. Krivokorytova and P. M. Khodorov, Proc. Acad. Sci. USSR 100, 741 (1955).

[13] C. Brunauer, P. H. Emmett and E. Teller, J. Am. Chem. Soc. 60, 309 (1938).

Received December 25, 1957

*Russian translation.

**Original Russian pagination. See C. B. Translation.

A CONTRIBUTION TO THE THEORY OF THE SURFACE TENSIONS OF SOLUTIONS OF STRONG ELECTROLYTES

V. E. Bravina

(Presented by Academician A. N. Frumkin, January 10, 1958)

Wagner [4] was the first to suggest that the enhanced surface tensions of aqueous solutions of inorganic salts [1, 2] arise as the result of electrostatic repulsion of ions by the solution surface. Having simplified Wagner's differential equations, Onsager and Samaras [5] then considered the case of solutions of strong uni-univalent electrolytes in which the dielectric constant, ϵ', of the external medium was assumed to be much less than the dielectric constant, ϵ, of the solvent. In the present work, the results of Onsager and Samaras will be extended in two directions: first, the case of solutions of unsymmetric polyvalent electrolytes will be considered, the supposition being made that $\epsilon' \gg \epsilon$; and, second, ϵ' will be taken into account in the treatment of solutions of uni-univalent electrolytes.*

1. In an unsymmetric polyvalent electrolyte the potential energy of an ion of the i-th type can be represented as

$$U_i = W_i + z_i e\varphi = \frac{z_i^2 e^2}{4\varepsilon x} e^{-2\varkappa x} + z_i e\varphi, \tag{1}$$

W_I being the adsorption potential due to the interaction of the ion with its electrostatic image when account is taken of the screening effect of the neighboring ions, and φ, the potential due to the lack of electrostatic symmetry and to the breakdown in the electrical neutrality of the various volume elements. The Debye-Huckel [3] theory, which is valid for electrolytes of any type, shows the Onsager and Samara [5] expression for W_I for the monovalent electrolytes to be also applicable to the polyvalent case. The potential φ satisfies the equation

$$\Delta\varphi = -\frac{4\pi}{\varepsilon}\sum_i z_i e n_i, \tag{2}$$

where

$$n_i = n_{0i} e^{-U_i/kT}. \tag{3}$$

Limiting ourselves to solutions of sufficiently low concentration, i.e., supposing that $\kappa q \ll 1$ ($1/\kappa$ is the Debye-Huckel radius and $q \sim e^2/\epsilon\, kT$, the distance at which the coulombic interaction becomes comparable to the mean thermal energy of translation) it is possible to divide the surface into two regions $x \lesssim x_0$ where $q \ll x_0 \ll 1/\kappa$. In region I ($x \leq x_0$), it can be assumed that $e^{-2\kappa x} \simeq 1$ and that the term $z_I \cdot e \cdot \varphi$ is negligible in the expression for U_I, the action of the image forces considerably exceeding that of the other ions in this region (the image is at a distance $x \ll 1/\kappa$, and the effective charge of the ion atmosphere, at a distance $\sim 1/\kappa$). The potential $\varphi_I(x)$ is to be found from the equation

*Just as in [5], specific adsorption will not be taken into account here.

$$\frac{d^2\varphi_I}{dx^2} = -\frac{4\pi}{\varepsilon}\sum_i z_i e n_{0i}\left(\exp\left[-\frac{z_i^2 e^2}{4\varepsilon kTx}\right]-1\right) \qquad (4)$$

with the boundary condition $(d\varphi_I/dx)_{x=0} = 0$ (continuity of the normal component of the electrostatic induction, supposing $\varepsilon' = 0$). In region II, ($x \geq x_0$), W_I/kT is small, since $x \gg q$. Remembering that $z_i e\varphi \ll kT$, (3) can then be expanded in a series in terms of U_I/kT. In region II, the potential is to be found from the equation

$$\frac{d^2\varphi_{II}}{dx^2} - \varkappa^2\varphi_{II} = \frac{\pi}{\varepsilon^2 kT}\sum_i (z_i e)^3 n_{0i}\frac{e^{-2\varkappa x}}{x} \qquad (5)$$

with the boundary condition $\varphi_{II}(\infty) = 0$.

In this case, an argument similar to that of Onsager and Samaras [5] shows that κ can be considered as independent of x.

The solutions of the Equations (4) and (5), joined smoothly at the point $x = x_0$, uniquely determine the potential φ in the region from 0 to ∞.

For a study of the structure of the surface layer, we will introduce the quantity $\Delta n_i = n_i(x) - n_{0i}$, which differs from zero only in this layer. It is also convenient to introduce the following parameters: $p_i = n_{0i}/n$, the number of ions of the i-th type which are formed on the dissociation of one molecule; u, the distance measured in the units $1/\kappa$; $h = e^2\kappa/4\varepsilon kT$, a small parameter of the theory, and $\ln z^* = \sum_i z_i^3 p_i \ln|z_i| \Big/ \sum_i z_i^3 p_i$. In these terms

$$\frac{\Delta n_i}{n} = p_i\left(\exp\left[-\frac{z_i^2 h}{u}\right]-1\right) \qquad \text{when } u \leqslant u_0;$$

and

$$\frac{\Delta n_i}{n} = -p_i z_i^2 h\frac{e^{-2u}}{u} - \frac{z_i p_i}{2} h\frac{\sum_k z_k^3 p_k}{\sum_k z_k^2 p_k}\left[e^{-u}\int_u^\infty \frac{e^{-v}}{v}dv - \right. \qquad (6)$$

$$\left. - e^{-u}\int_{3u}^\infty \frac{e^{-v}}{v}dv - 2e^{-u}\left(\ln\frac{1}{\sqrt{3}hz^{*2}} - 1 + 2\gamma\right)\right] \qquad \text{when } u \geqslant u_0.$$

For the distribution of the charge density we find:

$$\frac{\rho}{en} = \sum_i z_i p_i\left(\exp\left[-\frac{z_i^2 h}{u}\right]-1\right) \qquad \text{when } u \leqslant u_0;$$

and

$$\frac{\rho}{en} = -\sum_i z_i^3 p_i h\frac{e^{-2u}}{u} - \frac{h}{2}\sum_i z_i^3 p_i\left[e^{-u}\int_u^\infty \frac{e^{-v}}{v}dv - e^{-u}\int_{3u}^\infty \frac{e^{-v}}{v}dv - \right. \qquad (7)$$

$$\left. - 2e^{-u}\left(\ln\frac{1}{\sqrt{3}hz^{*2}} + 1 - 2\gamma\right)\right] \qquad \text{when } u \geqslant u_0,$$

γ being Euler's constant, 0.577... .

In distinction to the case of the uni-univalent electrolytes, the charge density is here not identically equal to zero, although it can be shown that the surface layer as a whole is electrically neutral.

For solutions of electrolytes of the type of MgI_2, the functions ρ/en and $\Delta n_i/n$ are represented in Figs. 1 and 2.

The change in the surface tension is related in the following way to the value of the adsorption, Λ, [6]:

$$\Delta\sigma = -kT\sum_i \int \Lambda_i d\ln a_i. \qquad (8)$$

Calculation gives the following results:

$$\Lambda_i = -\frac{n_{0i}(z_i e)^2}{4\varepsilon kT}\left(1 - 2\gamma + \ln\frac{2\varepsilon kT}{z_i^2 e^2 \varkappa}\right) + \\ + \frac{\pi n_{0i} z_i e}{\varepsilon^2 (kT)^2 \varkappa^2}\sum_h (z_h e)^3 n_{0h}\left(1 - 2\gamma + \ln\frac{2\varepsilon kT}{\varkappa (z_h e)^2}\right); \qquad (9)$$

$$\Delta\sigma = \frac{kT\varkappa^2}{16\pi}\left(\frac{3}{2} - 2\gamma + \ln\frac{2\varepsilon kT}{e^2\varkappa}\right) - \frac{kT\varkappa^2}{16\pi}\,\frac{\sum_i (z_i e)^2 n_{0i} \ln (z_i e)^2}{\sum_i (z_i e)^2 n_{0i}}. \qquad (10)$$

A convenient working form of Equation (10) is

$$\Delta\sigma = 39{,}7\left(\sum_i z_i p_i\right)\frac{m}{\varepsilon}\log\left[2{,}28\cdot 10^{-13}\,\frac{(\varepsilon T)^3}{z_0^4 \sum_i z_i^2 p_i m}\right], \qquad (11)$$

in which m is the concentration in moles per liter.

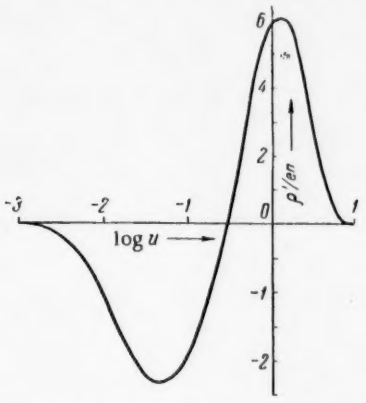

Fig. 1. $\rho\, du = \rho'\, d\log u$.

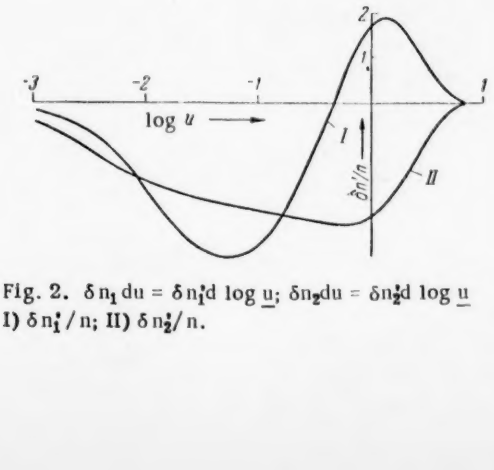

Fig. 2. $\delta n_1\, du = \delta n_1'\, d\log u$; $\delta n_2 du = \delta n_2'\, d\log u$ I) $\delta n_1'/n$; II) $\delta n_2'/n$.

In the case of the uni-univalent electrolytes, this result agrees with the limiting law of Onsager and Samaras [5]. It can be shown that the general equation obtained by these authors is without significance, the corrections to the limiting law which it contains being of the same order as terms which were neglected.

2. Let a certain ion of charge e be located at the origin of coordinates. The interface between the electrolyte and the external medium will be taken to be the plane $z = z_0 > 0$. The potential φ which arises from the ion and its atmosphere in a medium of dielectric constant ϵ and with a potential φ' in the external medium, is to be determined from the following equation and boundary conditions:

$$\Delta\varphi = -\frac{4\pi}{\varepsilon}\rho; \qquad \Delta\varphi' = 0; \qquad (12)$$

$$[\varphi - \varphi']_{z=z_0} = 0; \qquad \left[\varepsilon\frac{\partial\varphi}{\partial z} - \varepsilon'\frac{\partial\varphi'}{\partial z}\right]_{z=z_0} = 0. \qquad (13)$$

The charge density can be written as $\rho = e\,\delta(r) + \sum e_i n_i$, $\delta(r)$ being the delta function. Following the Debye-Huckel method, we will bring Equation (12) into the form

$$(\Delta - \varkappa^2)\varphi = -\frac{4\pi}{\varepsilon}e\delta(r). \qquad (12')$$

We will now carry out a Fourier transform on the variables $\underline{x}$ and $\underline{y}$. For the Fourier components $\varphi_k(z)$, we obtain the following equation

$$\left(\frac{d^2}{dz^2} - k_1^2 - k_2^2 - \varkappa^2\right)\varphi_k =$$

$$= -\frac{e}{\varepsilon\pi}\,\delta(z).$$

The presence of the δ-function results in the fact that for $z = 0$

$$\frac{d^2\varphi_k}{dz^2} - (k^2 + \varkappa^2)\,\varphi_k = 0 (k^2 = k_1^2 + k_2^2), \tag{14}$$

the first derivative has a discontinuity at the point $z = 0$

$$\left.\frac{d\varphi_k}{dz}\right|_{-0}^{+0} = -\frac{e}{\varepsilon\pi}. \tag{15}$$

The function $\varphi_k(z)$ is itself continuous at zero.

Similarly, we find for $\varphi'_k(z)$:

$$\frac{d^2\varphi'_k}{dz^2} - k^2\varphi'_k = 0. \tag{16}$$

The boundary conditions are

$$[\varphi_k - \varphi'_k]_{z=z_0} = 0, \quad \left[\varepsilon\frac{d\varphi_k}{dz} - \varepsilon'\frac{d\varphi'_k}{dz}\right]_{z=z_0} = 0. \tag{17}$$

Taking screening into account, the potential at the position of the ion due to the ion image, φ_e, is equal to

$$\varphi_e = [\varphi - (\varphi)_{z_0=\infty}]_{x=0,\ y=0,\ z=0}. \tag{18}$$

The term $(\varphi)_{z_0=\infty}$ represents the potential due to the ion and its atmosphere at a great distance from the surface.

Expressing φ and $(\varphi)_{z_0=\infty}$ through the Fourier components, we obtain

$$\varphi_e = \left[\int_{-\infty}^{+\infty}\int \varphi_k(z)\,e^{i(h_1x+h_2y)}\,dk_1dk_2 + \right.$$
$$\left. + \int_{-\infty}^{+\infty}\int \{-[\varphi_k(z)]_{z_0=\infty}\,e^{i(h_1x+h_2y)}\,dk_1dk_2\}\right]_{x=0,\ y=0,\ z=0} \tag{19}$$

It is to be noted that it is impossible to here suppose $\underline{x}$, $\underline{y}$, and $\underline{z}$ to be equal to zero in both members of the sum, since these members would then become infinite. This can be done, however, after the expressions under the integral sign have been added. Finally, after certain rearrangements, we find

$$\varphi_e = \frac{e}{\varepsilon}\int_{\varkappa}^{\infty} \frac{\lambda\varepsilon - \varepsilon'\sqrt{\lambda^2 - \varkappa^2}}{\lambda\varepsilon + \varepsilon'\sqrt{\lambda^2 - \varkappa^2}}\,e^{-2\lambda z_0}\,d\lambda \quad (\lambda = \sqrt{\varkappa^2 + k^2}). \tag{20}$$

The adsorption potential, $W(z) = e\,\varphi_e/2$, cannot be expressed in terms of elementary functions. If, in evaluating the adsorption Λ, account is taken of the fact that the parameter $\varkappa q$ is very small in the region

$z \ll 1/\kappa$, it is then possible to simplify considerably the function $W(z)$; over the region in which $z \gg q$, the exponent containing $W(z)$ can be developed in a series. This opens the way to expressing Λ in terms of elementary functions.

Calculation gives:

$$\Delta\sigma = \frac{e^2(\varepsilon-\varepsilon')n}{2\varepsilon(\varepsilon+\varepsilon')}\left[\ln\frac{2\sqrt{2\varepsilon kT(\varepsilon+\varepsilon')}}{\varkappa e^2(\varepsilon-\varepsilon')} + \right.$$
$$\left. + \frac{3}{2} - 2\gamma - \frac{1}{2}\left(\frac{\varepsilon+\varepsilon'}{\varepsilon-\varepsilon'}\right)\ln 2 + \frac{2\varepsilon^2}{(\varepsilon-\varepsilon')^2}\ln\frac{\varepsilon+\varepsilon'}{\varepsilon^2}\right]. \qquad (21)$$

When $\varepsilon' = 0$, this is in complete agreement with the results of Onsager and Samaras [5].

In conclusion, I would like to express my thanks to Prof. V. G. Levich for having set up this problem and to Prof. E. M. Lifshits for a number of valuable suggestions.

LITERATURE CITED

[1] A. Heydweiller, Ann. Phys. 33, 145 (1910).

[2] G. Schwenker, Ann. Phys. 11, 525 (1931).

[3] P. Debye and E. Hückel, Phys. Zs. 24, 185 (1923).

[4] G. Wagner, Phys. Zs. 25, 474 (1924).

[5] L. Onsager and N. T. Samaras, J. Chem. Phys. 2, 528 (1934).

[6] G. Harned and B. Owen, The Physical Chemistry of Solutions of Electrolytes (in Russian), Foreign Lit. Press, 1952.*

The M. V. Lomonosov State University,
Moscow

Received January 9, 1958

*Russian translation.

THE ENERGY OF ACTIVATION FOR DIFFUSIONAL CREEP IN METALLIC DISORDERED SOLID SUBSTITUTION SOLUTIONS

Ia. E. Geguzin

(Presented by Academician G. V. Kurdiumov, January 15, 1958)

1. The experimental results which have been accumulated through the study of the irreversible deformation of highly stressed metals at high temperatures, where the extension rate is proportional to the load ($\dot{\varepsilon} \sim P$), are quite satisfactorily described within the framework of the diffusional theory of these phenomena [1-3]. The basic assumption of this theory is that macroscopically observable creep results from a directed self-diffusional flow of vacancies under a vacancy concentration gradient which is proportional to the externally applied load. The coefficient of proportionality between the rate of extension and the applied load, the so-called coefficient of flow, ($\kappa = 1/\eta$, where η is the coefficient of viscosity) proves to be proportional to the product of the concentration of the vacant lattice positions (ξ) and the coefficient of self-diffusion of the vacancies, D_b^s, at the working temperature:

$$\varkappa = \frac{1}{\eta} \sim \xi D_b^s. \tag{1}$$

Speaking in general, Equation (1) should be equally applicable to a single component material and to a material involving atoms of several types in the form of disordered solid substitution solution (dsss).

2. The following relation is known [4] to hold between the coefficients of self-diffusion of vacancies, and of atoms (D_a^s):

$$\xi D_b^s = D_a^s. \tag{2}$$

A similar relation can be written as:

$$\xi D_b^s = C D_A^s + (1 - C) D_B^s \tag{3}$$

in the case of a solution of two components, or as

$$\xi D_b^s = \sum_{i=1}^{n} C_i D_i^s. \tag{4}$$

in the general case of a solution of n components. In these relations, D_I^s is the coefficient of self-diffusion of the n-th component in a solution in which its concentration is C_I. In (2) – (4), account has been taken of the fact that the concentration of the vacancies is negligibly small in comparison with the total concentration of the atoms, $\xi \ll \sum_{I=1}^{n} C_I = 1$.

The relations (2) – (4) follow naturally from the theory of the vacancy mechanism of self-diffusion and represent a formulation of the following obvious statement: the probability of an elementary act of self-diffusional transfer of one of the atoms of a solid solution (regardless of the type of this atom!) is equal to the probability of an elementary act of self-diffusional transfer of a vacancy.

If we limit ourselves in what follows to two component solid solutions, and take account of (1) and (3) and of the fact that the coefficient of viscosity of a solution alters with temperature according to an exponential law, it is then possible to write the following relation:

$$\frac{1}{\eta} \sim CD_A^s + (1-C)\, D_B^s \sim e^{-\theta(C)/RT}, \tag{5}$$

in which θ (C) is the energy of activation for diffusional creep of the solution, a quantity which varies with the concentration. An expression fixing the value of θ (C) follows naturally from Equation (5):

$$\theta(C) = R\,\frac{\Delta\left[\ln\left(CD_A^s + (1-C)\, D_b^s\right)\right]}{\Delta\,(1/T)}. \tag{6}$$

The quantity θ (C) can be determined from (6) if it is known how the coefficients of self-diffusion of the components of the solution vary with temperature and concentration. These functions can be evaluated in experiments using radioactive isotopes.

3. The quantity θ (C) can be determined by another method which differs from that described above in that it is based on a knowledge of the constants characterizing the phase diagram. It is known that the entropy of melting (ΔS) is practically the same for all metals having the same type of crystal lattice. In the case of solid substitution solutions of fixed base, it is natural to suppose* that ΔS will be independent of the nature of the dissolved atoms and their concentration, its value being fixed by the crystal lattice of the base metal. Presuming ΔS to be independent of C, it is possible to introduce the concept of the effective temperature of melting (T_s (C)), of an alloy which has the form of a dsss:

$$T_s(C) = T_s(O)\,\frac{Q_k(C)}{Q_k(O)} = \frac{Q_k(C)}{\Delta S}, \tag{7}$$

where, T_s (O) is the temperature of melting of the base metal and Q_k (C), the "configurational" heat of melting of a solution of concentration C. It is to be recalled that the "configurational" heat of melting of an alloy is the heat required for changing its phase, and is equal to the total experimentally measured heat of fusion diminished by the heat needed for warming the alloy in the region of stratification [7].

In characterizing the melting of the dsss by a definite temperature, we are at the same time comparing it with a certain pure metal which has the same lattice type as the solution and a heat of melting equal to Q_k (C). Taking account of the well known [7] expression defining Q_k (C), and applying to the case of the dsss the relation between the energy of activation of self-diffusion (and of viscous flow, as well – see above) and the melting temperature of the metal ($\theta = 20\,RT_s$) which has been developed by V. Z. Bugakov [8], it is possible to write:

$$\theta(C) = \frac{20R}{\Delta S}\left[Q_A(1-C) + Q_B C + NC(1-C)\left(u_0^{I} - u_0^{II}\right)\right]. \tag{8}$$

Here Q_A and Q_B are the heats of melting of the components, per mole; u_0^{I} and u_0^{II} are the respective energies of mixing, per particle, in the liquid and solid phases; and N is the Avogadro number. Equation (8) makes it possible to evaluate Q (C) if the heats of melting of the components and the difference between the energies of mixing in the liquid and in the solid phases are known. This difference can be determined from the phase diagram [5, 6, 9].

4. Thus there are three independent methods for finding the value of the energy of activation of diffusional creep in a dsss:

a) From data on the temperature dependence of the coefficients of self-diffusion of the components in a solution of the given concentration (see Equation (6)).

* The assumption that the entropy of melting of the dsss is independent of the concentration was introduced earlier by B. Ia. Pines [5, 6] and was employed by him in developing the simplest phase diagrams for binary alloys and in evaluating certin physical characteristics of solid solutions.

b) From data on the heats of melting of the components and the value of $\Delta u_0 = u_0^I - u_0^{II}$, as determined from the phase diagram (see Equation (8)).

c) Experimentally, from data on the temperature dependence of the rate of diffusional creep of the dsss at the given concentration.

All three of these methods can be tested on the Au–Ni system. In applying the first method we will make use of the data contained in [10, 11] where by the method of radioactive isotopes the dependence of the coefficients of self-diffusion of the atoms of gold and nickel on temperature and concentration was studied over the entire range of the concentrations. Calculation of θ (C) with the aid of Equation (6) led to the results which are shown in Fig. 1.

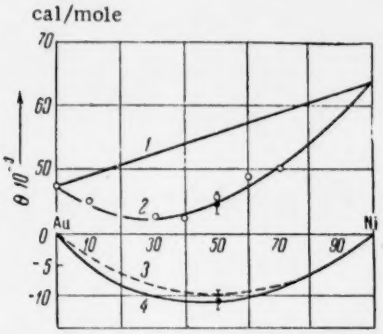

Fig. 1. 1,2) The function θ (C): 1) supposing the validity of the law of additivity ($\Delta u = 0$, see Equation (8)), 2) according to Equation (6); 3,4) departure of θ (C) from additivity: 3) found from Equation (8), 4) found by subtracting Curve 1 from Curve 2.

In evaluating θ (C) by the second of the above methods, the value of Δu_0 was determined from the positions of the points corresponding to various concentrations, use being made of the equations of [9] which show that $\Delta u_0 = -1.2 \cdot 10^{-13}$ ergs/particle = -1.75 kcal/mole, and the assumption being made that $\Delta S = 2.3$ cal/g·deg. In comparing the results of the calculations of θ (C) from Equation (6), and from Equation (8), it is useful to compare the deviations of the θ (C) curves from the straight line connecting the values of the energies of activation for diffusional creep in the solution components.* In the case of Equation (8), this deviation is covered by the relation: $L(C) = \frac{2O}{\Delta S} NC(1-C)\Delta u_0$ which is represented by the dotted curve in Fig. 1. From Fig. 1 it follows that concordant results are obtained by applying these two methods.

TABLE 1

Alloy	Type of phase diagram	Δ_{u_0}, ergs/particle	θ, kcal/mole		
			acc. to (6)	according to (8)	experimental
Cu	"Cigar"	0	—	53,4	54±1,6
Cu — Ni (75%—25%)			—	57,0	56,9±1,6
Cu — Ni (50%—50%)			—	58,9	59±1,6
Pb	Eutectic with limited solubility	$-3 \cdot 10^{-14}$	—	24,0	25,2±1,8
Pb — Sn (85%—15%)			—	21,7	21,1±1,8
Pb — Sn (75%—25%)			—	19,9	21,2±1,8
Au — Ni (50%—50%)	Minimum at the point of equal concentrations	$-1,2 \cdot 10^{-13}$	44,5	46,0	45±2

In order to determine experimentally the quantity θ (C), we have carried out creep experiments on specimens of an Au–Ni alloy (50 – 50 at. %) at temperatures of 800, 860 and 920°. These measurements were performed in the quartz apparatus which has been described earlier [13]. To insure a trustworthy value of θ which would not be distorted by differences in the grain dimensions [15] of the various specimens, series of measurements were made on the individual samples. The value of $\theta_{C=1/2}$ resulting from these experiments proved to be equal to $45 \pm 2 \cdot 10^3$ cal/mole. In Fig. 1, this value is designated by the black point; the agreement with the values obtained from Equations (6) and (8) is completely satisfactory.

* The value of θ_{Ni} has been taken out of [14].

5. Experiments were also undertaken with alloys from the systems Cu–Ni and Pb–Sn. Information on the D_i^s values for these systems is lacking, and for this reason $\theta(C)$ was determined experimentally and through Equation (8). The values of Δu_0 for these systems have been determined earlier [9, 12] and are equal, respectively, to $\Delta u_0^{Cu-Ni} = 0$ and $\Delta u_0^{Pb-Sn} = -3 \cdot 10^{-4}$ ergs/particle (it is the α-solution of tin in lead which is under consideration). Measurements of the rate of diffusional creep were carried out on the pure metals and on alloys of two different concentrations. The calculated and the experimentally determined values of θ are compiled in Table 1.

LITERATURE CITED

[1] C. Herring, J. App. Phys. 21, No. 5 (1950).

[2] Ia. E. Geguzin, L. O. Maron and B. Ia. Pines, Proc. Acad. Sci. USSR 87, No. 4 (1952).

[3] B. Ia. Pines, Prog. Phys. Sci. 52, vol. 4 (1954).

[4] Ia. I. Frenkel', Introduction to the Theory of Metals (in Russian), Moscow, 1948.

[5] B. Ia. Pines, Bull. Sect. Phys. Chem. Anal. 16, vol. 1 (1943).

[6] B. Ia. Pines, J. Exp. Theo. Phys. 13, vol. 11-12 (1943).

[7] Ia. E. Geguzin and B. Ia. Pines, Proc. Acad. Sci. USSR 85, No. 3 (1950).

[8] V. Z. Bugakov, Diffusion in Metals and Alloys (in Russian), Moscow–Leningrad, 1948.

[9] Ia. E. Geguzin and B. Ia. Pines, Proc. Acad. Sci. USSR 85, No. 4 (1950).

[10] A. D. Kurtz, B. L. Averbach and M. Cohen, Acta Metall. 3, 442 (1955).

[11] J. E. Reinolds, B. L. Averbach and M. Cohen, Acta Metall. 5, 29 (1957).

[12] Ia. E. Geguzin and B. Ia. Pines, J. Phys. Chem. 25, vol. 10 (1951).

[13] Ia. E. Geguzin and V. I. Kudrik, Phys. Met. and Metallography 7, 19 (1958).

[14] J. Weertman and P. Shahinian, J. Metals 10, 1223 (1956).

[15] Ia. E. Geguzin and V. Z. Bengus, Phys. Met. and Metallography 1, vol. 2 (1955).

The A. M. Gorky State University,
Kharkov

Received January 10, 1958

AN INVESTIGATION OF THE FILMS ON A MERCURY ELECTRODE

A. Ia. Gokhshtein and Ia. P. Gokhshtein

(Presented by Academician A. N. Frumkin, February 1, 1958)

In addition to the determination of capacities [1-3], and surface tensions [4, 5], the method which is described below can prove to be useful in studying anodic and cathodic films.

An electrolyzer containing the test solution is connected in an ordinary polarographic circuit. Keeping the potential of the dropping mercury electrode constant, certain discreet changes take place in the current flowing in the circuit. These changes can be observed on an oscillographic polarograph. The current rises sharply to a definite value and then falls smoothly to zero (Fig. 1). The interval of potentials over which this effect is observed, and the form and size of the impulses, differs for the various substances: a number of solutions do not give impulses, with many others the impulses are observed in the anode region, and, finally, still other solutions show such impulses in both the anode and the cathode regions (Table 1).

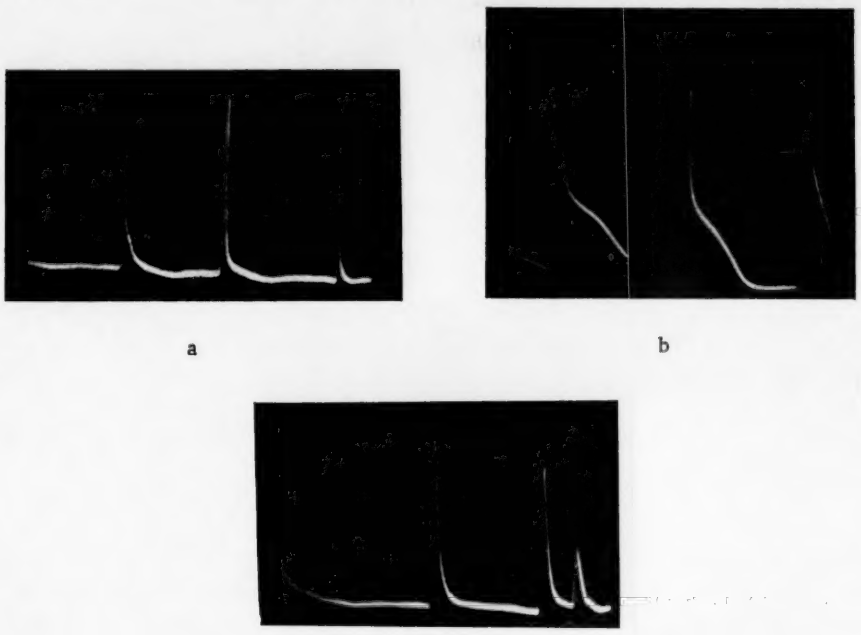

a b c

Fig. 1. Oscillograms of the solutions: a) 0.1 N KCl, b) 0.1 N KI, c) 0.1 N Na_2S. Potential of the dropping electrode, U = + 0.6 v with respect to Hg.

The potentials corresponding to the appearance and the disappearance of the impulses are not the same. In both cases, there is a certain retardation in the change. With $KHSO_4$, for example, the impulses appear at U = 3.7 v as the positive potential is increased and fall off at U = 1.5 v when this potential is diminished. In a number of solutions, as many as 10,000 impulses are observed during the life of a single drop. The amplitude and the duration of the impulses increase as the drop grows.

Despite the fluctuations, particularly in the frequency and the number of impulses, the time dependence of these quantities in our experiments was in every case reproducible to within the coefficient of the scaler, which was 64. That is to say, that in comparing the numbers of impulses obtained in two similar experiments the differences which appeared were less than 64, in a total number of impulses amounting to several thousand. This good reproducibility pointed to a statistical regularity in the process of breakdown of the film.

In Fig. 1 there are to be seen the different forms of the impulses in various solutions. Although the concentration and the potential profoundly affect the forms of these curves, and although differences are maintained over the greater portion of the interval of potentials, there are certain regions over which similarities are to be observed. From this it can be concluded that the processes traced out in the various solutions are similar in regard to the time factor.

These current impulses arise from the formation and breakdown of a film on the growing mercury drop. After being formed on the fresh electrode surface, the film deforms and then breaks, once a certain critical tension has been reached.

From the dimensions of the drop and the number of impulses during the period of its growth, it is possible to evaluate the freshly liberated surface as a quantity of the order of 10^{-4} mm^2. Combining the frequency of the process with certain other data, the degree of deformation of the film and its mechanical properties can be determined. The quantitative calculations are made complicated, however, by the lack of symmetry. In actuality, the spherical symmetry of the drop can not be used here, since the ruptured portion of the drop represents only a very small fraction of the drop surface. This, in its turn, leads to local irregularities in the growth of the drop, with various portions of the surface growing alternately. Under the microscope, these nonuniformities have the appearance of surface agitations. The fact that the current impulses are not superposed on one another indicates that only one section of the drop is involved in the growth at any given instant. The persistence of unilateral growth shows the freshly formed film to have lower stability and hence to be thinner. Rupture therefore occurs on one section of the surface as long as the tension in the film at this position does not diminish. At constant pressure of the mercury, a cause for the diminution of this tension is to be found in the decreasing radius of curvature of the growing section. Actually, by considering equilibrium in the film section (in the cracking of the film it is possible to limit oneself to the two-dimensional case), we obtain (Fig. 2):

$$\Sigma_y = -2Py + 2T(x)\frac{1}{\sqrt{1+y'^2}} = 0.$$

From this it follows that

$$T(x) = Py\sqrt{1+y'^2}$$

$$T(0) = P\lim\frac{y'}{\left(\frac{1}{\sqrt{1+y'^2}}\right)'} = -\frac{P}{\frac{y''}{(1+y'^2)^{3/2}}} = -PR.$$

Here, T is the tension, P is the pressure, and R is the radius of curvature. The fact that the film is of different thicknesses in two points of the surface shows that the growth of the surface continues even after it has become monomolecular. This is also indicated by the amount of percipitated material which is equivalent to the current of one impulse.

We will now turn to those quantities which might be used to characterize this process. Experimentally, it is possible to determine the following as functions of time: the amplitude and duration of the impulses (oscillographic polarograph), the number and frequency of these impulses (scaler), and their distribution over amplitudes (pulse analyzer). The variation of the number of impulses with time is quite reproducible from drop to drop, and quantitative calculations,can, therefore, be based on this quantity. Graphs showing the number of impulses and their distribution over amplitudes are given in Fig. 3 for the case of $KHSO_4$.

At small film thicknesses, the rate of growth of the drop remains constant. We will introduce the following symbolism: S_0 and S, the areas of the section before and after deformation; σ_0, the critical film tension; N, the number of impulses, counted from the instant of appearance of the drop; τ the duration of the impulse; t, the time and i_0, the amplitude of the impulse. Then $S \sim t^{2/3}$.

TABLE 1

Electrolyte, 0.1 N	U_2, v (relative to Hg)	U_1, v (relative to Hg)
NH_4F	+ 1.9	+ 2.4
KCl	+ 0.02	+ 0.03
KBr	+ 0.02	+ 0.6
KI	+ 0.13	+ 1.5
$KHSO_4$	+ 1.5	+ 3.7
Na_2S	above + 3.5 and from −0.1 to −0.9	−

In order to make a first approach to the theoretical determination of $\frac{dN}{dt}(t)$, i_0 and τ, we will suppose the deformation of the film to be elastic and the thickness to be the same over the entire surface.

Then $\sigma = k\frac{S-S_0}{S_0}$ or $\frac{d\sigma}{dt} = \frac{k}{S_0}\frac{dS}{dt}$; $\frac{dN}{dt} = \frac{1}{\sigma_0}\frac{d\sigma}{dt} = \frac{k}{\sigma_0 S_0}\frac{dS}{dt}$.

Taking into account the fact that $S_0 \approx S \sim t^{2/3}$, we obtain

$$\frac{dN}{dt} = \frac{2}{3}\frac{k}{\sigma_0}\cdot\frac{1}{t}; \quad \tau = \frac{dt}{dN} = \frac{3}{2}\frac{k}{\sigma_0}t.$$

The magnitude of the surface which is freed by rupture of the film is

$$\delta = \frac{dS}{dt}\tau \sim t^{1/3}.$$

Since the current i_0 is proportional to the free surface, it follows that $i_0 \sim t^{2/3}$. According to the experimental data

$$\frac{dN}{dt} \sim t^{-1/3}; \quad i_0 \sim t^{1/3}.$$

Thus these simplified calculations permit a qualitative explanation of the variation of the amplitude and the frequency of the impulses with time. For exact quantitative comparisons, the residual deformation of the film, the distribution of thickness over the film, and the radius of curvature should be taken into account. This problem is made difficult by fluctuations.

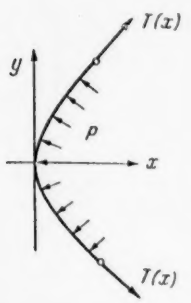

Fig. 2. The relation between the time, and the number of impulses, N, and the amplitude, (A_0), expressed in arbitrary units.

From the kinetic point of view, however, much interest attaches to a consideration of the single impulse, or process, which takes place on the freshly liberated electrode surface. Since this surface represents about 0.0001-th part of the mean surface of the drop, this section can be considered as a plane. The monotonic fall in the current which is observed on the oscillograms for 0.1 N KCl and 0.1 N Na_2S is readily explained if it is supposed that the defining stage of the process is an electrochemical reaction rather than diffusion. In this case the current i(t) is proportional to the concentration, C_0, of the solution and to the active surface of the electrode $S_0 - S(t)$:

$$i(t) = kC_0[S_0 - S(t)], \qquad (1)$$

k being a coefficient of proportionality, S_0, the fresh surface and S(t), the surface of the film:

$$S(t) = \frac{m}{lhd}\int_0^t i(t)\,dt. \qquad (2)$$

Here, m is the electrochemical equivalent of one of the ions which participates in the formation of the film, l is the amount of this ion in the film, d is the specific gravity and h is the film thickness.

Setting (2) into (1) and solving the resulting equation for i(t), we are led to an expression for the current of a single impulse:

$$i(t) = i(0) \exp\left[-\frac{km}{lhd} C_0 t\right]. \qquad (3)$$

From (2) we have S(0) = 0, and thus from (1) there follows:

$$i(0) = kC_0 S_0.$$

The existence of a proportionality between the initial concentration C_0 and the maximum impulse current i(0) is well confirmed by experiments at concentrations below 0.1 N.

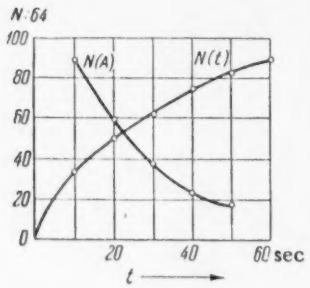

Fig. 3

The similarity between the oscillograms of 0.1 N KCl and 0.1 N Na_2S at U = 0.6 v does not, however, justify the conclusion that the assumptions adopted in the derivative of (3) are absolutely valid. Actually, the exponential law for the diminution of the current breaks down at lower potentials in solutions of KCl and Na_2S. For 0.1 N KI, this law is not valid at any potential; from Fig. 1b it is to be seen that the current falls at a markedly diminished rate in the middle of the impulse and then once more rises. The cause of the appearance of this wave in the central part of the impulse is still not sufficiently clear. It can be supposed that there is reflected here the influence of a nonstationary diffusion, i.e., of an increased flow of matter to the electrode with the passage of time. It is also possible that other phenomena, such as crystallization of the film [6] with an accompanying increase of the porosity, come into play.

The authors express their thanks to Academician A. N. Frumkin for his help in this work.

LITERATURE CITED

[1] A. N. Frumkin, V. S. Bagotskii, Z. A. Iofa and B. N. Kabanov, The Kinetics of Electrode Processes (in Russian), Moscow, 1952, pp. 44-57.

[2] S. E. S. El. Wakkad and T. M. Salem, J. Chem. Soc. 1955, 1489.

[3] L. Young, Trans. Farad. Soc. 53, 6, 841 (1957).

[4] A. N. Frumkin and A. V. Gorodetskaia, Zs. phys. Chem. 136, 451 (1928).

[5] C. C. Addison, W. E. Addison and D. H. Kerridge, J. Chem. Soc. 1955, 3047.

[6] H. R. Thirsk, Proc. Phys. Soc. B, 66, 129 (1953).

Received January 22, 1958

THE EFFECT OF POLARIZATION ON THE MECHANICAL PROPERTIES OF STEEL

G. V. Karpenko and R. I. Kripiakevich

(Presented by Academician P. A. Rebinder, January 24, 1958)

We have carried out experiments with a view to determining how the mechanical properties of a steel are effected by its polarization in various electrolytes. A standard IM-12 tensile strength machine with a special attachment made possible the rupture of a steel specimen in an electrolyte during anodic or cathodic polarization by an external current and thereby permitted the determination of the mechanical characteristics of the steel in the course of its polarization.

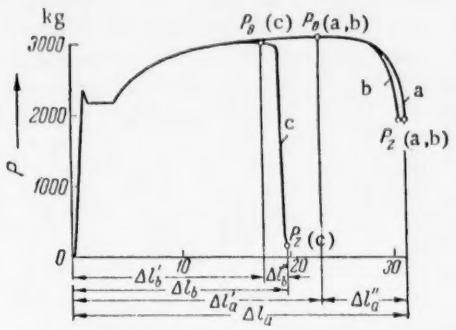

Fig. 1. A strain diagram for the annealed steel-3 at various polarizations: a) in air; b) at an anodic polarization of D_a = 10 amp/dm^2; c) at a cathodic polarization of D_c = 10 amp/dm^2. The electrolyte was acidic; the anode and cathode were iron.

In order to be able to observe the effect of diminishing plasticity, our experiments were carried out with a soft annealed steel-3 of perlite – ferrite structure. Specimens of this steel, 10 mm in diameter at a working length of 100 mm, were washed with aviation gasoline prior to experiment and desorbed by an activated silica gel. In the cathodic polarization of the steel, the anode was of this same soft steel-3, lead, copper or graphite. The electrolyte was an aqueous solution, 26% in sulfuric acid, or 18% in sodium hydroxide, or 3 % in NaCl. The current density at polarization was varied from 0 to ± 60 amp/dm^2; in certain cases the density was altered in steps of 0.005 amp/dm^2 in the neighborhood of zero.

The rupture experiments were performed at a constant rate of extension, V = 2 mm/min, the electrical circuit being closed at the instant the tensile strength machine was put into operation. The electrolyte was introduced just before beginning the experiment. Each experiment lasted 10-15 minutes. It was the aim of these experiments to determine the maximum breaking strength, σ_{mbs}, the flow limit, σ_f, the true stress at rupture, σ_{true}, (all in kg/mm^2), and the relative elongation, δ_{10}, and the relative contraction, ψ, (in percentage) of the steel at rupture, during the polarization process, each value being taken as the mean of these measurements.

During its loading in air, the soft annealed steel-3 showed a clearly expressed region of flow, and there was a pronounced elongation and transverse contraction (Fig. 1, a) which was accompanied by the appearance of flow figures. Similar effects were observed on loading a specimen in an electrolyte at this same rate either without polarization or with anodic polarization from an external current; here the specimen became covered with a thin oxide scale and the plasticity of the steel was altered only insignificantly (Fig. 1, b). In each case the ratio of the concentrated deformation, Δl^*, to the total deformation, Δl, amounted to ~ 25-30%.

The results of loading cathodically polarized specimens were quite different. These specimens ruptured brittlely, rupture occurring essentially across planes of maximum tangential stress (according to the flow figures).

In the cathodic polarization of a specimen, there was a marked decrease in δ_{10} and ψ, the indices of plasticity, and in σ_t, the true stress at rupture, the maximum breaking strength and flow limit remaining unaltered. The ratio of the concentrated deformation to the full deformation diminished strongly and amounted to only 9-12% (Fig. 1, c).

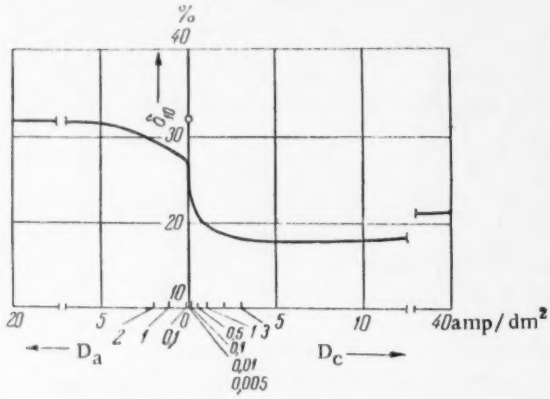

Fig. 2. The relation between the relative elongation, δ_{10}, of the annealed steel-3 and the magnitude and sign of the polarization. The electrolyte was acidic; the anode and the cathode were of Fe. The point A designates the value of δ_{10} in air.

In Fig. 2 there are shown curves indicating the alteration of the relative elongation, δ_{10}, of the annealed steel-3, and its dependence on the sign of the polarization and the current density, the anode in the cathodic polarization and the cathode in the anodic polarization being iron, and the electrolyte, acidic. Similar curves were obtained for the relative contraction and the true strain at rupture.*

It is to be seen from the curves (Fig. 2) that anodic polarization at high current densities was without effect on the mechanical properties of the steel. In anodic polarization at low current densities, there was observed a certain diminution in the plasticity and the true strain at rupture, comparison being with the values which had been obtained in air (point A). Experiments carried out in the electrolyte but without the application of an external current, i.e., under the conditions which prevail during the ordinary electrochemical corrosion, when microcathodic and microanodic regions appear on the steel speciment, gave a decrease in plasticity (by 26%) and in the true strain at rupture, although rupture was accompanied by cracking just as in air. On applying a cathode potential, the specimen fractured brittlely along the flow figures at even the lowest current densities (0.005 amp/dm^2), the maximum effect being observed at the very lowest current density; this effect varied somewhat depending on the anode metal and the electrolyte, (see Fig. 3). The effect of decreasing plasticity and true stress at rupture after passing through the maximum was less and less marked as the anodic current density increased (see Fig. 3).

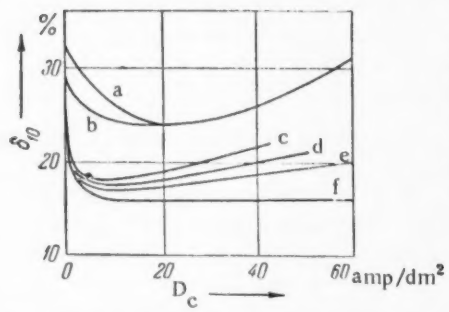

Fig. 3. The relation between the relative elongation, δ_{10}, of the annealed steel-3 and the magnitude of the cathodic polarization. a) electrolyte, 3% NaCl; anode, steel; b) 18% NaOH; anode, copper; c) 26% H_2SO_4; anode, steel; d) 26% H_2SO_4; anode, graphite; e) 26% H_2SO_4; anode, copper; f) 26% H_2SO_4; anode, lead.

In Table 1 there are presented the mechanical characteristics of steel-3 as obtained through experiments in air, in electrolytes without polarization of the specimen, and with cathodic polarization at that optimal value of the current density corresponding to the greatest alteration of these properties. The mechanical characteristics of the steel are given both in absolute units and relative to the data from the experiments in air.

The effect which was observed in cathodic polarization is explained in terms of the formation of a hydride film leading to the embrittlement of the stressed steel specimen. The formation of this hydride coating proceeds with high velocity and predominately along the lines of shear, i.e., in the zone of aggregation of the vacancies and dislocations, where concentration of the deformation energy is at a maximum. From the strain curves (Fig. 1) it is to be seen that the formation of a hydride coating did not occur up to the beginning of plastic shear, (i.e., up to the flow limit), the reason for this being that the experiments were of short duration.

*The determination of the relative elongation, δ_{10}, was much more accurate than that of ψ and σ_{true}, due to the fact that the ruptured cathode-polarized sample has lost its round shape (in the process of stretching).

TABLE 1

Anode	Electrolyte	Current density	ψ		δ_{10}		σ_{true}		σ_T		σ_{mbs}	
			abs. %	relative %	abs. %	relative %	abs. kg/mm	relative %	abs. kg/mm	relative %	abs. kg/mm	relative %
Fe	NaCl (3%)	O	69	98,5	32	100	80	92	28	100	39,5	98,7
		optimum	45	64,3	26	81	46	53,5	28,2	100,5	40	100
Cu	NaOH (18%)	O	68	97,2	31	97	75	86,3	28	100	40	100
		optimum	28	40,0	24	75	33	48,0	28	100	39	97,5
Cu	H_2SO_4 (26%)	O	48	68,6	28	87,6	48	55,2	29	103,5	40	100
		optimum	21	30,0	17	53,2	17	19,5	26,5	94,5	39	97,5
Pb	H_2SO_4 (26%)	O	46	65,7	27	84,5	53	61,0	28,5	101,7	40,5	101
		optimum	20	28,6	16	50	2	2,3	28,5	101,7	38,0	95
Fe	H_2SO_4 (26%)	O	42	60	27	84,5	41	47,2	28	100	39,5	98,7
		optimum	25	35,7	18	56,3	15	17,3	27,5	98,2	37,5	93,8
C	H_2SO_4 (26%)	O	43	61,4	26,5	83	42	48,4	28,5	101,7	39,5	98,7
		optimum	26	37,2	17,5	54,7	25	28,7	28,5	101,7	37,5	93,8
			70	100%	32	100	87	100	28	100	40	100

During the loading in an electrolyte when there is no polarization from the external current and microcathodic and microanodic regions appear on the strained specimen, it is clear that the decrease in the plasticity is also to be explained in terms of the embrittlement of the cathodic segments because of hydrogen. In anodic polarization these cathodic segments are gradually suppressed and, at a certain value of the current density, the whole specimen becomes anodic and there is then no longer any evolution of hydrogen on any one of its segments. It is clearly due to the briefness of the experiments, that no softening of the anodic portions of the steel resulted from the corrosional attack.

The Institute of Mechanisms and Automata of the
Academy of Sciences of the USSR

Received January 23, 1958

THE CHEMICAL ADSORPTION AND CATALYTIC OXIDATION OF CO ON ZnO, AND ON VARIOUS SOLID SOLUTIONS OF THE LATTER WHICH DIFFER IN CONDUCTIVITY

N. P. Keier and G. I. Chizhikova

(Presented by Academician A. N. Frumkin, February 19, 1958)

One of the principal problems of the electronic theory of catalysis is that of relating the electronic characteristics of semi-conductors and their catalytic properties. The present work is a continuation of an investigation of oxide systems with regular electronic properties [1-4]. Study has been made of zinc oxide, and of solid solutions of zinc oxide with the oxides of lithium and gallium, the conductivities of these substances differing by many orders (see Table 2). The chemical adsorption of the reaction components was studied in parallel with the catalytic activity, so that it was possible to deduce the changes occurring in the active surface as a result of variation of the electrical characteristics, and to make a more clear-cut interpretation of the physical nature of the relation between the conductivity and the catalytic activity. Zinc oxide was prepared by decomposing zinc carbonate in air at 850° for 6 hours. Solid solutions with lithium oxide were obtained under similar conditions by decomposing a zinc carbonate which had been impregnated with a solution containing the calculated amount of lithium carbonate. The solid solutions with gallium oxide were prepared from zinc carbonate which had been impregnated with a solution of gallium nitrate. In this case, the heating at 850° was continued for 30 hours. Values of the specific surfaces of these materials, as determined by the BET method from the adsorption isotherms of krypton at −195°, are shown in Table 1.

TABLE 1

The Specific Surfaces of the Experimental Specimens

Specimen	Specific surface, m^2/g
ZnO (6 hours and 30 hours)	1.5
ZnO (0.5 at. % Li)	0.2
ZnO (0.7 at. % Li)	0.2
ZnO (0.9 at. % Li)	0.2
ZnO (1.2 at. % Li)	0.1
ZnO (1.0 at. % Ga)	1.7

The addition of lithium oxide sharply diminished the specific surface. In Table 2, values are given for the electrical conductivity at 25° of specimens which had been prepared in vacuum at 350° and for the energy of activation for conduction.

Using a stoichiometric mixture at pressures below 2 mm of Hg, the catalytic reaction was studied in a vacuum system under static conditions. The product CO_2 was frozen out in a liquid nitrogen trap. Prior to experiment, the catalyst was degassed at 500°,. The adsorption was studied from the pressure drop under similar conditions, this drop being less than 10% of the initial pressure. The catalyst was protected from vapors of mercury and grease by a system of traps which were immersed in liquid nitrogen, one of these traps being on the quartz reactor to prevent the intrusion of grease vapors from the stop-cock trhough which the reactor was connected to the apparatus.

Catalytic activity. It was only at temperatures in excess of 250° that the oxidation of CO proceeded with measurable velocity. For each specimen, the kinetics of the oxidation proved to be of first order. In

Fig. 1 there is shown the temperature dependence of the velocity constants for the oxidation of CO on the experimental specimens. From this figure it is clear that the velocity constant was affected very little by adding lithium oxide up to 0.5 at. % Li; at higher concentrations of lithium oxide, this constant diminished precipitately and its measurement was then possible only in the region of higher temperatures. With increasing percentage of lithium oxide, there was an increase in the energy of activation, and in the constant multiplying the exponential term in the expression for the velocity constant. Here the equation $E = E_0 + \gamma \log k_0$ was followed (Fig. 2).

TABLE 2

The Electrical Conductivity and the Energy of Activation for Conduction of ZnO and its Solid Solutions

Specimen	σ (ohm · cm)$^{-1}$ (25°)	σ_0(ohm · cm)$^{-1}$	E_0, kcal/mole
ZnO (1 at % Ga)	$6{,}3 \cdot 10^{-4}$	$3{,}3 \cdot 10^{-3}$	2
ZnO at	$1{,}6 \cdot 10^{-5}$	$6{,}8 \cdot 10^{-2}$	10
ZnO (0,5at. % Li)	$2{,}5 \cdot 10^{-7}$	$3{,}0 \cdot 10^{-2}$	14
ZnO (0,9at. % Li)	$4{,}5 \cdot 10^{-9}$	$3{,}4 \cdot 10^{-2}$	19
ZnO (1,2at. % Li)	$4{,}5 \cdot 10^{-10}$	$1{,}9 \cdot 10^{-2}$	21

In Table 3 there are given values of the energy of activation and the constant multiplying the exponential term in the expression for the velocity constant. The addition of gallium oxide slightly diminished the energy of activation for the oxidation of CO, but at the same time markedly lowered the constant multiplying the exponential term. On the whole, the rate of oxidation diminished over the observed temperature interval.

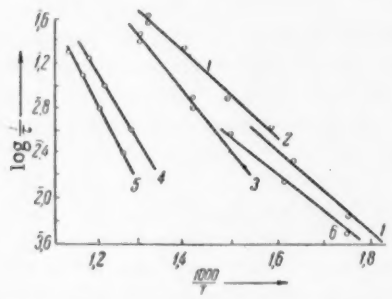

Fig. 1. The temperature dependence of the catalytic activity of ZnO and its solid solutions in the oxidation of CO. 1) ZnO (pure), 2) ZnO (0.5 at. % Li), 3) ZnO (0.7 at. % Li), 4) ZnO (0.9 at. % Li), 5) ZnO (1.2 at. % Li), 6) Zn (1 at. % Ga).

Adsorption measurements. a) The adsorption of oxygen lowered the electrical conductivity of each of the specimens, this showing the adsorption to be accompanied by a decrease in the concentration of free electrons. The adsorption was measured in the interval of temperatures from 300 to 500°. The addition of lithium oxide very markedly increased the rate of oxygen adsorption, the acceleration being much more pronounced at 0.5 at. % Li than at 1.2 at. %. In Fig. 3 there are shown the kinetic isotherms for adsorption at 400° on ZnO, ZnO (0.5 at. % Li), and ZnO (1.2 at. % Li). In each case the adsorption was less than would have corresponded to a monolayer. The increase in velocity was accompanied by a decrease in the energy of activation for adsorption from 36 kcal/mole for ZnO at a coverage of 0.01 cm^3/m^2 to 7 kcal/mole for ZnO containing 1.25 at. % Li, and even lower for the specimen containing 0.5 at. % Li. In the adsorption of oxygen on the specimen of ZnO (0.5 at. % Li), 40% of the Zn^{2+} cations on the surface were covered in the neighborhood of the maximum. This value was 16 times greater than for ZnO and 4 times greater than for ZnO (1.2 at. % Li).

b) The adsorption of CO was measured on ZnO and on solid solutions containing 0.5 and 1.25% Li. Two types of adsorption of CO on ZnO are known from the literature: a reversible adsorption at lower temperatures, and an irreversible adsorption at higher temperatures [5]. The adsorption of CO was investigated in the interval of temperatures from 0 to 300°. At room temperature, the adsorption of CO proceeded at a high rate. Here a part of the gas was adsorbed reversibly and could be removed from the surface by pumping.

On going above room temperature, the measured rate of gas adsorption diminished and became infinitesimally small at 200°, this being due to the high rate of desorption. Above 250°, the rate of adsorption began to

TABLE 3

Values of the Velocity Constants, Energies of Activation, and Multipliers for the Exponential Term in the Expression for the Velocity Constants for the Oxidation of CO

Specimen	K(t = 368°), $(min \cdot m^2)^{-1}$	K_0, $(min \cdot m^2)^{-1}$	E, kcal/mole
ZnO	$1,5 \cdot 10^{-1}$	$2,4 \cdot 10^{4}$	16,6
ZnO (0,5 at. % Li)	$1,9 \cdot 10^{-1}$	$5,7 \cdot 10^{5}$	19,3
ZnO (0,7 at. % Li)	$0,8 \cdot 10^{-1}$	$2,9 \cdot 10^{6}$	23,0
ZnO (0,9 at. % Li)	$0,9 \cdot 10^{-3}$	$1,1 \cdot 10^{5}$	28,0
ZnO (1,2 at. % Li)	$2,2 \cdot 10^{-4}$	$9,1 \cdot 10^{9}$	40,6
ZnO (1 at.% Ga)	$6,9 \cdot 10^{-2}$	$6,6 \cdot 10^{2}$	18,8

rise, but adsorption under these conditions was accompanied by a slow oxidation of CO by the oxygen of the zinc oxide. At 300°, 23% of the adsorbed CO was oxidized.

These two types of adsorption differently affected the electrical conductivity. Despite a higher degree of coverage, the adsorption of CO did not bring about any change in the electrical conductivity at room temperature. At 340°, the conductivity was increased by the adsorption of CO.

The addition of lithium oxide to the extent of 0.5 and 1.25 at. % Li completely suppressed the adsorption of CO at room temperature, and at higher temperatures as well.

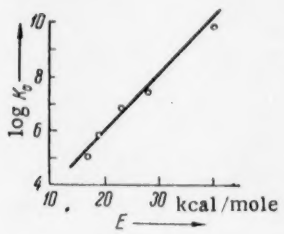

Fig. 2

DISCUSSION OF RESULTS

The marked effect of the addition of lithium oxide on the catalytic properties is due to a change in the active surface, as can be seen from the study of the chemical adsorption of the reaction components. The decrease in the energy of activation can not be explained in terms of a change in the level of the electronic chemical potential, since the latter diminishes on the addition of lithium oxide and this, according to Khauffe and Stone [6], should lead to a diminution of the heat of adsorption and, in view of the Bronsted rule, to an increase in the energy of activation for the adsorption of O_2. The inverse relation should hold for the adsorption of CO, an electron donor. The absence of any relationship between the rate of oxygen adsorption and the concentration of free electrons indicates that the latter cannot be the adsorption centers for the oxygen. The similarity between these results and those which have been obtained on the effect of dissolved lithium oxide on the chemical adsorption of oxygen by nickelous oxide, can be taken as indicating that the mechanism of the lithium oxide effect is the same in both substances although they belong to different classes of semi-conductors. The electrical conductivity of ZnO is related to the presence of excess zinc in the interstices, this zinc being easily ionized and the electrons transferred into the conduction zone. On the addition of lithium oxide to ZnO, there is formed a solid substitution solution in which a portion of the Zn^{2+} lattice positions are occupied by Li^+ cations. The diminished charge of these added cations is compensated for by the presence of interstitial cations (Zn^+_{inter}). The cation set, ($Li^+ Zn^+_{inter}$), is an acceptor of electrons. By interchange, this acceptor can take up an electron, and a neutral zinc (Zn^0_{inter}) will thus be formed near the lithium cation. Through the formation of the ($Li^+ Zn^0_{inter}$) set, the charge of the surrounding oxygen ions is left uncompensated. This must lead to the production of a strong electrostatic field around the cation set so that the work function for the escape of an electron to neighboring cation lattice positions will decrease. As a result, there must be a diminution in the energy of activation for the

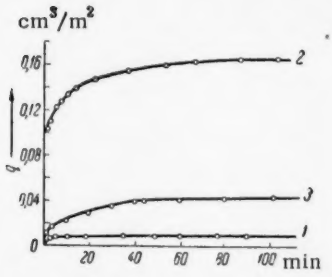

Fig. 3. The adsorption of oxygen at 400°. 1) on ZnO, 2) on ZnO (0.5 at. % Li), 3) on ZnO (1.2 at. % Li).

adsorption of electron acceptor gases on the neighboring cation lattice positions, when electrons are present there. With increasing concentration of lithium, the concentration of the free electrons falls, and on this basis the number of active centers for the adsorption of oxygen should pass through a maximum, as is actually observed experimentally.

The adsorption of CO diminishes with increasing concentration of lithium oxide, and this fact points to active centers of a different type for this substance. It is most probable that these are local donor levels (Zn^0_{inter}) which are free of electrons and which show a decrease in activity with increasing dissolved lithium. The transfer of an electron to a (Zn^+_{inter}) cation or to the neighboring Zn^{2+}, is favored energetically since this reestablishes the neutrality which was broken down locally at the given lattice position.

A comparison of the adsorption data with the results obtained on the oxidation of CO, leads to the conclusion that the oxidation rate cannot be determined from the adsorption of either oxygen or CO, the adsorption of the first markedly increasing at 0.5 at. % of Li while that of the second is equal to zero. With increasing concentration of lithium, there is a rise in the energy of activation for the oxidation of CO, but at the same time, the constant K_0 also markedly increases. Such relationship indicates that although the adsorption of oxygen is not the process which limits the oxidation rate, it still has a considerable influence on the step which determines this rate. This step could be either the adsorption of the CO or the interaction of the adsorbed oxygen with CO from the gaseous phase. In this latter case, an increase of the energy of activation of this interaction with increasing concentration of lithium would result in a diminution of the reaction rate.

Experiment proves that the oxygen adsorbed on a specimen of ZnO (0.5 at. % Li) reacts with high velocity with CO from the gaseous phase to form CO_2.

LITERATURE CITED

[1] G. M. Schwab and J. Block, Zs. Phys. Chem. 1, No. 4, 42 (1954).

[2] G. Parravano, J. Am. Chem. Soc. 75, 1448, 1352 (1952).

[3] N. P. Keier, S. Z. Roginskii and I. S. Sazonova, Bull. Acad. Sci. USSR 21, 2, 185 (1957).

[4] N. P. Keier and L. N. Kutseva, Proc. Acad. Sci. USSR 117, No. 2 (1957).

[5] E. W. Garner, J. Chem. Soc. 1947, 1239.

[6] F. S. Stone, Chemistry of Solid State, 1955, p. 367.

Received February 18, 1958

THE ENERGY OF COULOMBIC INTERACTION BETWEEN SILICA GEL HYDROXYL GROUPS AND BENZENE MOLECULES

A. V. Kiselev and D. P. Pashkus

(Presented by Academician A. N. Frumkin, January 18, 1958)

In a number of papers from our laboratory, it has been shown that the adsorption of benzene vapors on a silica gel whose surface is almost fully covered with hydroxyl groups is considerably greater than the adsorption on a silica gel whose surface has been partially freed of such groups by heating [1-3]. On a hydrated specimen of silica gel at a surface coverage of $\theta = 0.2$, the heat of adsorption of benzene vapors is larger by about 2-3 kcal/mole than the heat of adsorption on a strongly dehydrated specimen [2, 4]. The enhanced magnitude, and heat, of adsorption of benzene vapors for a hydrated silica gel as compared with a dehydrated specimen is to be explained by the formation of hydrogen bonds between the surface hydroxyl groups of the silica gel and the π-electrons of adsorbed benzene molecules [5]. Spectroscopic data [6-10] also point to the ability of the molecules of benzene, and other aromatic compounds, to form hydrogen bonds with acidic hydroxyl groups. According to the electrostatic theory, the energy of the hydrogen bond is largely determined by the electrostatic attraction of either the dipoles, or the residual charges of the interacting groups. In the present work, an attempt has been made to evaluate the energy of the coulombic interaction between the hydroxyl groups of silica gel and the adsorbed benzene molecules, the aim being to elucidate the role of this interaction in the formation of hydrogen bonds between these groups and the benzene molecules.*

The energy of coulombic interaction between two molecules has been evaluated by a number of authors [11-16]. An exact calculation of this energy must take into account the electrostatic interaction of the nuclei and of the electron clouds of all of the orbits of both molecules [16]. Such calculations are, however, quite involved, and it is customary in work of this kind to make use of various models which approximate the charge distribution in the interacting molecules.

The energy of coulombic interaction between the hydroxyl groups and the σ-electrons, and between these groups and the associated positive residual charges of the nuclei of the carbon and hydrogen atoms of the adsorbed benzene molecules, is small and can be neglected in a first approximation, since the density of the σ-electrons is concentrated in the plane of the nuclei of the carbon and hydrogen atoms of the benzene molecule while the hydroxyl groups of the silica gel (dipoles) are located beneath this plane.

According to quantum chemistry, the π-electron clouds in the benzene molecule extend along the whole perimeter of the benzene ring, going above and below it, and the distribution of the charge of these electrons and the residual positive charge of the carbon nuclei in the molecule can be crudely represented by the model which is shown in Fig. 1a. In this model, the regular hexagon of benzene ring is, for simplicity, replaced by a circle of radius R = 1.4 A, this being the approximate length of the C–C bond in benzene. The distance of the circles representing the π-electron clouds from the plane of the benzene ring is taken as the mean distance of the half p-electron cloud of the isolated carbon atom from the nucleus, $\bar{r} = 0.81$ A, as evaluated from the single electron atomic function for the $2p_Z$-electron

*A report of this work was made by D. P. Pashkus at the Leningrad Conference on Sorbents, December 6, 1957.

$$\psi_{2p_z} = \frac{1}{4\sqrt{2\pi}}\left(\frac{Z}{a_0}\right)^{3/2} re^{-\frac{Zr}{2a_0}}\cos\theta$$

through the relation:

$$\bar{r} = \int \psi^2_{2p_z} r^3 \sin\theta\, dr\, d\theta\, d\varphi,$$

a_0 being the radius of the Bohr orbit, 0.529 A, and Z = 3.25, the effective nuclear charge calculated according to the method of Slater [17]. It is assumed that the charge of the π-electrons, 6e, (e is the charge of the electron), is uniformly distributed over the circle so that its density is $\sigma = \frac{3e}{2\pi R}$. The residual positive charges of the carbon nuclei, which are associated with the π-electrons, are each equal in absolute magnitude to the electronic charge, e, and are designated in the figure by black dots.

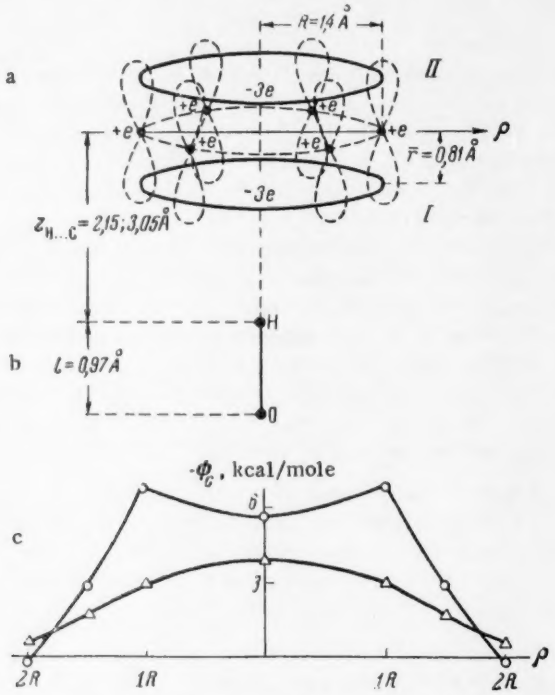

Fig. 1. A model of the distribution of the electrical charge in the benzene molecule (a), and in the hydroxyl group (b), and the dependence of the coulombic interaction between the benzene molecule and the hydroxyl group, Φ_c, on the mutual positions (c): the circles are for $z_{H...C}$ = 2.15 A; the triangles, for $z_{H...C}$ = 3.05 A.

In our calculations, the hydroxyl group has been considered as a system of two point charges at positions approximately coinciding with those of the nuclei of the oxygen and hydrogen atoms (Fig. 1b), the effective charges of the hydrogen atom, q_H, and of the oxygen atom, q_O being determined from the relation $\mu = ql$, where μ is the dipole moment of the hydroxyl group and l is the internuclear distance. Since the electronegativities of the hydrogen and silicon atoms are about the same (2.1 and 1.8, respectively [19]) and l = 0.97 A, a value approximately equal to the dipole moment of the hydroxyl group in the water molecule μ = 1.6 D, [18] was adopted for the hydroxyl groups on the silica gel surface. From this it follows that $q_H \approx q_O = 1.6 \cdot 10^{-10}$ esu.

When the actual charge distribution is replaced by the model which has been accepted above, the energy of coulombic interaction between the hydroxyl group and the benzene molecule is given by the following expression:

$$-\Phi_C = \sum_{i=H;\,O} \sum_{j=I;\,II} \sigma q_i \int \frac{ds}{r_{i-j}} + \sum_{i=H;\,O} \sum_{k=1}^{k=6} e q_i \frac{1}{r_{i-k}},$$

where the first member on the right expresses the coulombic interaction between the effective point charges of the hydroxyl group, q_H (the effective positive charge of the hydrogen atom), and q_O (the effective negative charge of the oxygen atom), and the charge of the π-electrons of the benzene molecule, which is uniformly distributed over the upper circle (I) and the lower circle (II); the second member is the energy of coulombic interaction between these same effective point charges of the hydroxyl group and the residual positive charges of the carbon nuclei (k = 1, ..., 6); ds is the differential arc of the circumference; and r_{i-j} and r_{i-k} are respectively the distance between the effective point charges of the hydroxyl group, $\underline{i}$ (i = H; O) and some point on a circle, $\underline{j}$, (j = I; II), and the distance between these point charges and the effective positive charge of the nucleus of a carbon atom, C. The first member is readily reduced to an elliptic integral and the second can be evaluated by numerical summation.

With the hydroxyl group directed perpendicularly to the plane of the benzene ring (the energetically preferred orientation), the energy of coulombic interaction was evaluated at the following positions measured along a radius ρ passing through the nucleus of a carbon atom; at the center of the benzene ring, $\rho = 0$; at the center of a carbon atom, $\rho = R$; and at points located outside of the benzene ring at distances $\rho = 1.5\,R$ and $\rho = 2R$ from its center. The equilibrium distance, $z_{H...C}$, from the nucleus of a hydrogen atom of the hydroxyl group to the plane of the ring of carbon atoms of the benzene molecule, is unknown. For this reason, the evaluation of Φ_C was carried out for the two extreme values of $z_{H...C}$: 2.15 A and 3.05 A, these being the sum of one half of the van der Waals thickness of the benzene molecule (1.85 A) and either the covalent radius (0.3 A), or the van der Waals radius (1.2 A), of the hydrogen atom. The resulting values of the energy of the coulombic interaction between the hydroxyl group and the benzene molecule at various positions are represented graphically in Fig. 1c.

For displacement of the hydroxyl group within the limits of the benzene ring, Fig. 1c shows the energy of coulombic interaction to depend but slightly on the relative positions and to amount to about 4-6 kcal/mole This interaction energy diminishes rapidly beyond the limits of the benzene ring.

A provisionary evaluation of the energies of the two types of interaction, the polarizational and the dispersive, shows that each amounts to about 2 kcal/mole. In all likelihood, the repulsive energy is of the same order. When the actual charge distribution in the molecule is taken into account, these results indicate that the energy of the coulombic interaction of the polar hydroxyl groups with the nonpolar benzene molecules is high and that it plays a determining role among the other types of interaction (polarizational-aceptor-donor, dispersive and repulsive) in establishing hydrogen binding in this system, especially since these latter interactions must partially compensate one another.

A molecule of benzene which is adsorbed on the surface of a fully hydrated silica gel will, on the whole interact with one or several hydroxyl groups, the area per hydroxyl group on the fully hydrated surface being approximately equal to 13 A^2 [20] which is, in turn, nearly equal to the area of that part of the benzene molecule within whose limits the energy of the coulombic interaction with the hydroxyl groups falls to one half of the maximum value.

In addition to its interaction with the hydroxyl groups, a molecule of benzene which is adsorbed on a hydroated silica gel surface will also interact (principally by dispersive interaction and by repulsion) with the remaining atoms which form parts of the silica gel structure. The removal of hydroxyl groups from the silica gel surface must lead, on the one hand, to a diminution of the heat of adsorption of the benzene molecule as compared with the value on the hydrated surface, this being due to the elimination of the interaction between the hydroxyl groups and the benzene molecules and give rise, on the other, to an increase in the energy of interaction of the adsorbed benzene molecules with the bulk silica gel , since by removing the hydroxyl groups from the surface the benzene molecules approach to a certain extent the surface of the particles in the silica gel structure. Thus, the experimentally determined difference between the heats of adsorption of benzene vapors

on hydrated, and on dehydrated, silica gels must be less than the energy of interaction of the benzene molecules with the hydroxyls of the latter. In addition, the hydroxyl groups on the surface of a silica gel must be variously oriented with respect to the plane of the ring of the adsorbed benzene molecule, and this will result in a certain decrease in the energy of interaction in comparison with that corresponding to perpendicular arrangement. For example, a rough calculation shows that the energy of coulombic interaction is diminished by approximately 30% when the hydroxyl groups are inclined at an angle of 45° to the plane of the benzene ring.

Considering what has been said, and taking account of the crudeness of the accepted model for the distribution of the electric charges in both the benzene molecule and in the hydroxyl group, and the indefiniteness in the value of the equilibrium distance $z_{H...C}$, it can be concluded that the calculated energy of the coulombic interaction (about 4-6 kcal/mole) is in satisfactory agreement with the experimentally determined decrease (2-3 kcal mole) in the heat of adsorption of benzene which results from the dehydration of the silica gel surface.

LITERATURE CITED

[1] A. V. Kiselev, K. G. Krasil'nikov and L. N. Soboleva, Proc. Acad. Sci. USSR 94, 85 (1954).

[2] A. A. Isirikian and A. V. Kiselev, Proc. Acad. Sci. USSR 115, 343 (1957). •

[3] L. D. Beliakova and A. V. Kiselev, Proc. Acad. Sci. USSR 119, 298 (1958). •

[4] A. V. Kiselev, The Structure of Certain Corpuscular Adsorbents and its Influence on their Adsorptive Properties, Colston Papers, 10, Bristol, 1958.

[5] A. V. Kiselev, Proc. Acad. Sci. USSR 106, 1046 (1956).

[6] M. L. Josien, Compt. rend. 237, 175 (1953).

[7] W. Lüttke and R. Mecke, Zs. Elektrochem 53, 241 (1949).

[8] M. Tamres, J. Am. Chem. Soc. 74, 3375 (1951).

[9] A. N. Terenin, Sympos., The Surface Chemical Compounds and their Role in Adsorption Phenomena (In Russian), Moscow, 1957, p. 206.

[10] R. S. McDonald, J. Am. Chem. Soc. 79, 850 (1957).

[11] M. Davies, J. Chem. Phys. 15, 739 (1947).

[12] M. M. Jones, W. R. Gilkerson and G. A. Gallup, J. Chem. Phys. 20, 1048 (1952).

[13] J. E. Lennard-Jones and J. A. Pople, Proc. Roy. Soc. A, 205, 155 (1951).

[14] J. A. Pople, Proc. Roy. Soc. A, 205, 163 (1951).

[15] W. S. Fyfe, J. Chem. Phys. 21, 2 (1953).

[16] W. G. Schneider, J. Chem. Phys. 23, 26 (1955).

[17] J. C. Slater, Phys. Rev. 36, 57 (1930).

[18] H. Landolt – R. Börnstein Tabellen, Aufl. 6, 1, Teil 3, S. 506.

[19] M. V. Vol'kenshtein, The Structure and Physical Properties of Molecules (In Russian), Moscow – Leningrad, 1955.

[20] S. P. Zhdanov and A. V. Kiselev, J. Phys. Chem. 31, 2213 (1957).

The M. V. Lomonosov State University,
Moscow
The Institute of Physical Chemistry of the
Academy of Sciences of the USSR

Received January 18, 1958

• Original Russian pagination. See C. B. Translation.

THE CHEMICAL REACTIONS OF ATOMS WITH ENERGIES COMPARABLE TO THE ENERGY OF ACTIVATION

B. N. Provotorov

(Presented by Academician V. N. Kondrat'ev, January 24, 1958)

When the energy of the atom is comparable with the energy of activation of a chemical reaction, the probability of this reaction is expressed by the specific rate constant. The specific rate constant for the reaction can be calculated by the method of activated complexes or, it can be determined experimentally.

The number of molecules of C, or of D, which are formed per unit time per unit volume by the reaction $A + B \longrightarrow C + D$, is equal to $K(T)\, n_A n_B$, n_A being the concentration of the atoms of the gas A, and n_B, the concentration of the molecules of the gas B.

On the other hand, this number can be expressed through the reaction cross-sections, $\sigma_n(v)$, as

$$K(T)\, n_A n_B = n_A n_B \left(\frac{\mu}{2\pi kT}\right)^{3/2} 4\pi \int_0^\infty \exp\left(-\frac{\mu v^2}{2kT}\right) \frac{\sum_n \omega_n \sigma_n(v) \exp\left(-\frac{\varepsilon_n}{kT}\right)}{\sum_n \omega_n \exp\left(-\frac{\varepsilon_n}{kT}\right)} v^3 dv, \qquad (1)$$

if it is supposed that there is a Maxwellian distribution of velocities over the particles A and B. Here m_A is the mass of the atom A, m_B is the mass of the molecule B, $\mu = \dfrac{m_A m_B}{m_A + m_B}$, ϵ_n, and ω_n are the energy, and the statistical weight, of the n-th quantum state of the molecule B and $\sigma_n(v)$ is the cross-section for chemical reaction when the molecule is in the quantum state n, this value to be averaged over all directions of the relative velocity. The atoms will be considered as in the ground quantum state, this being in keeping with the high energy required for excitation of the electronic levels of the individual atom.

In general, the reaction threshold energies in Equation (1) will differ for each reaction path. This difference must be of the order of ϵ_n. In this case, when $\epsilon_n \gg kT$, practically none of the gas molecules will possess excitation energy. On the other hand, this difference can be neglected when $\epsilon_n \leq kT$, since $E_0 \gg kT$, and it can then be considered that the threshold energy is the same for all paths. Expression (1) can then be rewritten as

$$K(T) = \left(\frac{\mu}{2\pi kT}\right)^{3/2} 4\pi \frac{\sum_n \omega_n \exp\left(-\frac{\varepsilon_n}{kT}\right) \int_{v_0}^\infty \sigma_n(v) \exp\left(-\frac{\mu v^2}{2kT}\right) v^3 dv}{\sum_n \omega_n \exp\left(-\frac{\varepsilon_n}{kT}\right)}. \qquad (2)$$

Here $v_0 = \sqrt{\dfrac{2E_0}{\mu}}$ is the reaction threshold energy. $K(T)$ can usually be expressed as $A(T) \exp\left(-\dfrac{E_0}{kT}\right)$, where $A(T)$ is a quantity which alters slowly with the temperature. This indicates that the functions $\sigma_n(v)$ also changes slowly in the interval $v - v_0 \sim \sqrt{\dfrac{2kT}{\mu}}$.

Taking $\sigma_n(v)$ out from under the sign of integration and considering that $E_0 \gg kT$, we obtain

$$\frac{\sum_n \omega_n \exp\left(-\frac{\varepsilon_n}{kT}\right)\sigma_n(v_0)}{\sum_n \omega_n \exp\left(-\frac{\varepsilon_n}{kT}\right)} = \left(\frac{\pi kT}{2\mu}\right)^{1/2} \frac{k(T)}{v_0^2} \exp\left(\frac{E_0}{kT}\right). \tag{3}$$

Because of the presence of the multiplying term $\exp\left(-\frac{\mu v^2}{2kT}\right)$ in the integral of Equation (3), it is to be seen that K(T) will be determined by the cross-sections $\sigma_n(v_0)$.

Below, we will show the probability of chemical reaction can be expressed through these same quantities, $\sigma_n(v_0)$, even when the atom A has a definite velocity $v_A \leq v_0$.

In terms of relative velocities, the distribution is of the form

$$w(v) = \left(\frac{m_B}{2\pi kT}\right)^{3/2} \exp\left(-\frac{m_B (v - v_A)^2}{kT}\right).$$

Making use of this expression, we obtain for the probability of chemical reaction in unit time

$$\alpha(v_A) = n_B \int_{v_0}^{\infty} w(v)\, v \, \frac{\sum_n \omega_n \exp\left(-\frac{\varepsilon_n}{kT}\right)\sigma_n(v)}{\sum_n \omega_n \exp\left(-\frac{\varepsilon_n}{kT}\right)} dv$$

or, after averaging over the angle between the direction of the relative velocity $\underline{v}$ and the velocity v_A,

$$\alpha(v_A) = \left(\frac{m_B}{2\pi kT}\right)^{3/2} n_B 4\pi \exp\left(-\frac{m_B v_A^2}{2kT}\right) \int_{v_0}^{\infty} \exp\left(-\frac{m_B v^2}{2kT}\right) \frac{\operatorname{sh}_1 \frac{m_B v_A v}{kT}}{\frac{m_B v_A v}{kT}} \times$$
$$\times \frac{\sum_n \omega_n \exp\left(-\frac{\varepsilon_n}{kT}\right)\sigma(v)}{\sum_n \omega_n \exp\left(-\frac{\varepsilon_n}{kT}\right)} v^3 dv. \tag{4}$$

When $v_A \leq v_0$, the region of velocities making the principal contribution to the value of the integral will be determined by the coefficient $\exp\left(-\frac{m_B v^2}{2kT} + \frac{m_B v_A v}{kT}\right)$, i.e., as before, the width of this region will be of the order of $\sim \sqrt{\frac{2kT}{m_B}}$: thus we can again take the cross-sections out from under the integral sign and, after taking (3) into account, obtain

$$\alpha(v_A) = K(T) \exp\left(\frac{E_0}{kT}\right) n_B \left(\frac{m_A + m_B}{m_B}\right)^{1/2} \frac{\exp\left(-\frac{m_B v_A^2}{2kT}\right)}{v_0^2 v_A} \times \tag{5}$$
$$\times \int_{v_0}^{\infty} \exp\left(-\frac{m_B v^2}{2kT}\right)\left(\operatorname{sh} \frac{m_B v_A v}{kT}\right) v^2 dv.$$

Consequently, $v_0 \gg \sqrt{\frac{2kT}{m_B}}$ for $\left(\frac{2kT}{m_B}\right)^{1/2} < v_A \ll v_0$

$$\alpha(v_A) = K(T) \exp\left(\frac{E_0}{kT}\right) n_B \left(\frac{m_A + m_B}{m_B}\right)^{1/2} \frac{kT}{m_B v_A v_0} \exp\left(-\frac{m_B v_0^2}{2kT}\right) \operatorname{sh} \frac{m_B v_A v}{kT}. \qquad (6)$$

It is to be seen from Equation (6), that with increasing v_A, $\alpha(v_A)$ increases as $\exp\left(\frac{m_B v_A v}{kT}\right)$. When $v_A = v_0$,

$$\alpha(v_0) = K(T) \exp\left(\frac{E_0}{kT}\right) n_B \left(\frac{m_A + m_B}{m_B}\right)^{1/2} \frac{kT}{m_B v_0^2}.$$

can be easily obtained from (4).

With further increase in v_A, the function $\alpha(v_A)$ will be determined by the dependence of the cross-section $\sigma_n(v)$ on the velocity and for its evaluation it is necessary to know the exact form of this function.

Received January 21, 1958

THE EFFECT OF CONCENTRATION ON THE CRITICAL DEFORMATION AND THE ASSOCIATED STRUCTURAL STRENGTH OF ALUMINUM NAPHTHENATE OLEOGELS

V. A. Fedotova and A. A. Trapeznikov

(Presented by Academician P. A. Rebinder, February 7, 1958)

For the general theory of the deformation – strength characteristics and, in particular, for an interpretation of the high-elastic properties of colloidal systems, much interest attaches to the study of the relationship which exists between the value of the critical deformation at rupture, ϵ_r, determined from the maximum, P_r, on the $P(\epsilon)$ curve (P is the stress, and ϵ, the deformation), and the associated shear stress, P_r [1]. In the aluminum naphthenate oleogels, the critical shear deformation at rupture is quite clearly marked out and reaches values of several thousand percent, so that there is ground for considering these systems to be similar to super-elastic high polymers.

The ϵ_r, P_r relation has been investigated for 2-20% aluminum naphthenate oleogels in decalin,* the aim being to study the relation between the gel concentration and the physicomechanical characteristics which fix the high-elastic properties of this system.

From the $\epsilon_r(P_r)$ curves which have been obtained on the complex elastoviscosimeter,** (some of these curves are shown in Fig. 1), it is possible to determine the critical deformation, ϵ_{rm}, at each concentration of the oleogel, this being the value which corresponds to constancy of ϵ_r under continually increasing P_r and indicates the maximum possible elastic deformation in the system as a whole.*** From these same curves there can be found the values $P_r = P_{r_2}$, at which ϵ_{rm} is first reached (Fig. 1, the values of P_{r_2} are indicated by arrows).

Values of ϵ_{rm} and P_{r_2}, determined from the $\epsilon_r(P_r)$ curves at various C's, are presented in Table 1.

From the data of Table and Fig. 1, it follows that ϵ_{rm} diminishes with increasing C. This indicates a diminution in the elasticity, i.e., in the critical deformation, of the oleogel with increasing concentration.

This decrease in the elasticity of the system with increasing content of the dispersed phase (the aluminum naphthenate) in the oleogel might be explained as follows. The presence (at low concentrations of the thickener) of a small number of local, possibly very labile, bonds, which fill, as it were, the role of junctions (cross bonds) binding the structural net together, is no very great impediment to the deformation of those intermediate chain segments which are included between them. In this case, the local bonds are distributed so sparsely that large flexible segments of the molecular chains can exist between them, and these are in a position to give high reversible deformations. This results in the high elasticity of the net at small concentrations

---

* These oleogels were studied 20 days after their preparation. An aluminum naphthenate which had been prepared according to the procedure of [2] by precipitation at pH 5 with 36% free alkali, was used as a thickener of the decalin.

** A detailed description of the technique of determining ϵ_r and P_r on the complex elastoviscosimeter, is given in [3].

*** In certain cases, the actually determined value of the elastic deformation, ϵ_e, (elastic yield) can be less than those of ϵ_{rm} [4].

TABLE 1

C, %	ϵ_{rm}, %	$P_{r_2} \cdot 10^{-3}$, dynes · cm^{-2}	$A_{r_2} \cdot 10^{-4}$, ergs · cm^{-3}
2	7600	1,0	3,80
3	5000	3,0	7,50
4	4200	4,5	9,45
6	2660	7,0	9,31
8	2420	11,5	13,91
10	1960	15,0	14,70
15	1030	24,0	12,36
20	540	32,0	8,64

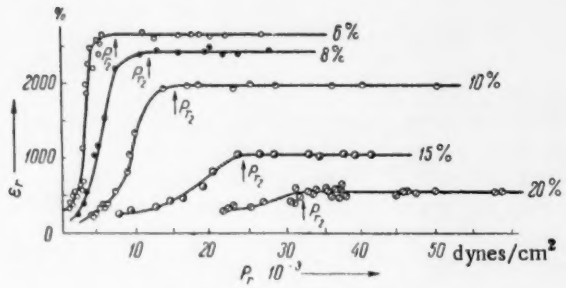

Fig. 1.

of the aluminum naphthenate in the oleogel (in the case of a gel of 2-4% concentration, for example, where ϵ_{rm} reaches values of the order of 4000-7000%).

The longer such intermediate chain segments are, the higher must be the elasticity of the system. With increasing concentration of the gel, the formation of additional cross bonds between the chains must lead to an increase in the total number of bonds per unit volume of the system with a simultaneous decrease in the lengths of the intermediate chains segments which are located between the junction points. This leads to a diminution in the system's elasticity, as could be surmised from the maximum deformation at rupture. In such a netted colloidal structure, an increase in the number of cross bonds is equivalent to "spatial polymerization." The existence of this latter does not, of course, exclude the possibility of a simultaneous "linear polymerization," i.e., the possibility of increase in the particle length, on increasing the gel concentration. In the region of high gel concentrations, however, such a lengthening of the particles probably plays a secondary role.

A diminution of the elasticity of a colloidal system with increasing concentration has also been noted in work on the elastoviscous properties of calcium stearate in soap [5]. The quantity $\lambda = \frac{E_1}{E_1 + E_2}$ which expresses the ratio of the shear moduli as measured at low shear stress was there used to characterize the elasticity of the system. The quantity λ does not give the maximum high-elastic deformation at rupture, which appears quite clearly in the liquid systems which we have studied. The systems with calcium stearate show solid plasticity and are similar to high concentration, consistent, greases with comparatively low ultimate shear deformations [6].

The P_{r_2}, C relation, which shown in Fig. 2, is adequately represented by a straight line. This indicates that the value of $P_r = P_{r_2}$, at which the rupture deformation ϵ_r reaches its maximum of ϵ_{rm} (with increasing rate of deformation) increases in proportion to the system concentration, being, as it were, a linear function of the number of local (cross) bonds which are formed between the separate chains. According to the equation

$$P_{r_2} = K (C - C_0) \qquad (1)$$

the intersection of the line $P_{r_2}(C)$ (Fig. 2) with the axis of abcissas gives the value $C = C_0$ (equal, in this case, to $\approx 1.43\%$) at which P_{r_2} becomes equal to zero, and below which, i.e., with $C < C_0$, the system loses that structure which determines P_{r_2}. This loss could have two causes: either the chain-like macromolecules of aluminum naphthenate are so far apart at these low concentrations that they cannot be bound into a single structural net, or there is a dissociation of the polymer particles with a resulting decrease in the "molecular" weight.

The curve of Fig. 3a shows the dependence of the critical deformation, ϵ_{rm}, on the concentration of the oleogel. This same relation is given in logarithmic coordinates in Fig. 3b. The angle of inclination of the straight line of Fig. 3b is 45° and from this it follows that the ϵ_{rm}, C relation corresponds to a hyperbola of the first degree with the equation:

$$\epsilon_{rm} C = B \qquad (2)$$

in which the constant B has physical meaning when $C \geq 1.43\%$.

From the values of P_{r_2} and ϵ_{rm}, the work of deformation of the gel can be roughly calculated as $A_{r_2} = \frac{1}{2} P_{r_2} \epsilon_{rm}$, if it is provisionally assumed that the increase in P along the deformation curve $P(\epsilon)$ is linear up to $P = P_r = P_{r_2}$. In this case, we find from Equations (1) and (2) that:

$$A_{r_2} = \frac{1}{2} P_{r_2} \varepsilon_{rm} = q\left(1 - \frac{C_0}{C}\right); \qquad (3)$$

where $q = \frac{1}{2} BK = 14.35 \cdot 10^4$ ergs $\cdot$ cm^{-3} and $C_0 = 1.43\%$.

The curve corresponding to Equation (3) is shown by the full line in Fig. 4. The points in this figure mark the experimental values of A_{r_2} which are given in Table 1. It is to be seen from this curve that the maximum work of deformation, A_{r_2}, corresponding to $P = P_{r_2}$ falls rapidly at low gel concentrations and tends toward a practically constant value at higher concentrations, $C \approx 6$-8%. The observed distribution of the experimental points results principally from the fact that not all of the values of ϵ_{rm}, fall exactly on the hyperbola (Fig. 3).

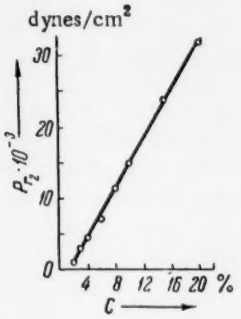

Fig. 2

The relative constancy in the work of structural breakdown per unit volume of gel, A_{r_2}, over the region of high C values indicates that although the increase in the number of bonds (junctions, cross bonds) calls for an increase in the rupture stress, it is, to a certain degree, compensated by a diminution in the critical rupture deformation of the system.

It should be pointed out that with increasing rate of deformation, $\dot{\epsilon}$, in the region $\dot{\epsilon} > \dot{\epsilon}_{r_2}$, the value of P_r continues to rise at constant ϵ_{rm}, so that the work of rupture $A_r = \frac{1}{2} P_r \epsilon_{rm}$, will also increase. For this reason, the values of A_{r_2} which have been calculated above are not maximum values of the work of rupture of the system but only certain limiting values corresponding to the instant at which the value ϵ_{rm} is reached.

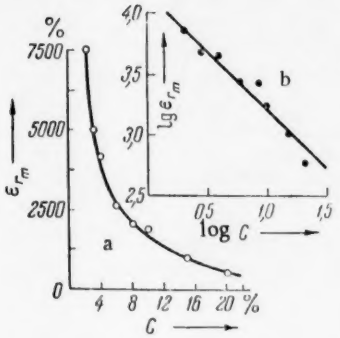

Fig. 3

The value of ϵ_{rm} for pure aluminum naphthenate is found by extrapolating Equation (2) to $C \approx 100\%$, and proves to be equal to $\sim 160\%$. This indicates that such a system (a "dry" soap) can experience under shear a deformation which does not exceed one and a half fold and that there is thus an almost complete loss of high elasticity in comparison with the dissolved (gel-like) state. (Externally, the dry aluminum naphthenate resembles a resinous powder, and for such, so low a deformability is quite reasonable).

In the systems which are under consideration, the structure which is taken on by the aluminum soap can arise through the formation of bonds of the coordination type between the aluminum atoms of the one molecule and the oxygen atom of the other, or as the result of hydrogen bonding between hydroxyl groups, or between the hydroxyl and carboxyl groups of different molecules, or between hydrating water molecules. The existence of bonds of the cross linked type in the gels of aluminum soaps has been considered by many investigators [2, 3, 7-12] and has recently been directly confirmed in certain cases [13].

In the above papers, the gels of the aluminum soaps were treated as high molecular compounds. In actuality, all of the high-elastic properties which we have studied point to a very close similarity between the gel-like solutions of aluminum naphthenate and the typical high polymers in the dissolved condition or in the

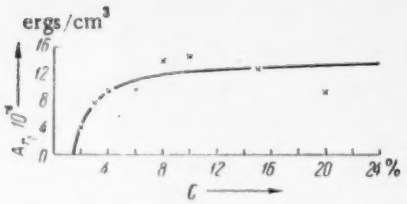

Fig. 4

initial condition without the solvent. The difference appears, in all likelihood, in a more gradual weakening of the interaction between the particles of the naphthenate under the influence of additions of polar substances, and this points to the great role of weak associating bonds in the naphthenates.

LITERATURE CITED

[1] A. A. Trapeznikov and V. A. Fedotova, Proc. Acad. Sci. USSR 81, 1101 (1951); 82, 97 (1952).

[2] A. A. Trapeznikov and G. V. Belugina, Proc. Acad. Sci. USSR 87, 635, 825 (1952); 94, 97 (1954).

[3] A. A. Trapeznikov and V. A. Fedotova, Proc., Third All-Union Conference on Colloid Chemistry (in Russian), Acad. Sci. USSR, Press, 1956.

[4] A. A. Trapeznikov, Colloid J. 20, No. 4 (1958).*

[5] E. E. Segalova and P. A. Rebinder, Colloid J. 10, 223, (1948); E. E. Segalova, P. A. Rebinder and L. N. Sentiurikhina, Colloid J. 13, 461 (1951).

[6] A. A. Trapeznikov and S. Kh. Zakieva, Proc. Acad. Sci. USSR. 73, 519 (1950); Proc. Second All-Union Conference on Colloid Chemistry (in Russian) Kiev, 1952; A. A. Trapeznikov and E. M. Shlosberg, Sympos., New Methods in the Physical-Chemical Investigation of Surface Phenomena (in Russian), vol. 1, 1950, p. 39.

[7] V. R. Gray, Trans. Farad. Soc. 42B, 196 (1946); V. R. Gray and A. E. Alexander, J. Phys. and Coll. Chem. 53, 9, 23 (1949); A. E. Alexander and V. R. Gray, Proc. Roy. Soc. A, 200, 162 (1950).

[8] A. A. Trapeznikov and E. M. Shlosberg, Colloid J. 8, 421 (1946).

[9] E. P. Marion and A. W. Thomas, J. Coll. Sci. 1, 221 (1946).

[10] T. S. McRoberts and J. H. Schulman, Nature 162, 101 (1948); Proc. Roy. Soc. A, 200, 136 (1950).

[11] H. Sheffer, Canad. J. Res. 26, 481 (1948).

[12] C. G. McGee, J. Am. Chem. Soc. 71, 278 (1949).

[13] W. W. Harple, S. E. Wiberley and W. H. Bauer, Anal. Chem. 24, 635 (1952); F. A. Scott, J. Goldenson, S. E. Wiberley and W. H. Bauer, J. Phys. Chem. 58, 61 (1954).

Received February 1, 1958

*Original Russian pagination. See C. B. Translation.

EFFECT OF NICKEL ON THE ELECTROCHEMICAL AND CORROSION BEHAVIOR OF STEEL

G. M. Florianovich, Ia. M. Kolotyrkin and N. K. Smirnova

(Presented by Academician A. N. Frumkin, January 1, 1958)

The corrosion resistance of metal construction materials depends essentially on their capacity for passivation and preservation of the passive state under working conditions. We have shown earlier [1] that the most important characteristic of the electrochemical and corrosion behavior of metals under passivating conditions is represented by the curve expressing the variation of the stable solution rate as the function of the potential within a wide range of values of the potential. Such a curve, obtained by the potentiostatic method, allows one to determine the polarization limits of the stable passive state and the amount of metal lost by corrosion within the passivation area. It appeared of interest to apply the potentiostatic method to the investigation of the effect of the chemical composition of steels on their electrochemical and corrosion behavior under passivating conditions.

As we have shown earlier [1], passivation or activation of metal results from the change of its surface. The degree of passivity of a metal surface depends on the electrode potential and, for a constant potential, it varies as the function of time, tending toward a stationary state. The variation of the electrode surface with time and potential is apparently due to the adsorption of different components of the solution on the surface; among these components are, for example, the anions of the electrolyte or the OH^- and O^{-2} ions; the latter may be adsorbed as the result of interaction of the surface atoms of the metal with water molecules.

It would be natural to assume that the variation of the chemical composition of steel will lead to the variation of its adsorptional properties and consequently to the variation of the electrochemical and corrosion properties within the region of passivity; these results would be observable by comparing the potentiostatic curves of steels of different compositions.

In our present work we used the potentiostatic method of measurement of polarization curves to investigate the effect of nickel on the behavior of steel in the region of passivity.* We investigated the following steels: Cr22Ti, Cr22Ni14Ti and Cr20Ni6C2Ti; the composition of these steels is described in Table 1.

TABLE 1

Number of steel	Chemical composition in %							
	C	Cr	Ni	Ti	Si	S	P	Mn
Cr22Ti	0,16	22,50	—	0,55	0,47	0,013	—	—
Cr20Ni6C2Ti	0,15	19,42	5,89	0,54	2,12	0,013	0,008	0,83
Cr22Ni14Ti	0,14	22,45	14,41	0,72	0,45	0,010	—	—

The measurements were performed in a 0.1 N H_2SO_4 solution in an atmosphere of nitrogen at 20°. The electrodes were first cleaned mechanically and chemically and then submitted to a preliminary cathodic polarization prior to measurements.

* L. N. Belogurova collaborated in this work.

For potentials for which, aside from the dissolution of steel, other electrode reactions such as evolution of hydrogen or oxygen could take place, the real solution rate of steel was determined by using photocolorimetric analysis of the solution for Fe, Cr, and Ni after the sample was maintained in the solution for a given time.

The results obtained (Fig. 1) show that the variation of the stable solution rate of Cr22Ti steel as the function of the potential is characterized by a relatively complicated curve (Curve I). For potentials more negative than -0.43 volt the solution rate increases systematically with the value of potential according to a straight line relationship. Within the interval of potentials from -0.430 to -0.270 volt the polarization curve changes its direction several times, while the stable solution rate remains within the limits of $1 \cdot 10^{-4} - 1 \cdot 10^{-3}$ amp/cm^2. Further displacement of the potential toward positive values up to -0.16 volt is accompanied by a systematic decrease of the solution rate down to $5 \cdot 10^{-7}$ amp/cm^2. Within the area of potentials from -0.160 to -0.010 volt the direction of the curve changes again but the value of the solution current remains about 1000 times smaller than that within the area of potentials preceeding the beginning of deep passivation.

The minimum solution rate of Cr22Ti steel occurs within the area of potentials extending from 0.0 to + 0.500 volt. Within this area the solution rate is independent of the potential and is equal to $3.2 \cdot 10^{-7}$ amp/cm^2. For potentials more positive than + 0.500 volt the solution rate increases with the potential and for the value of the potential equal to + 0.850 volt reaches $1 \cdot 10^{-5}$ amp/cm^2; beyond this point passivation takes place again, preceeding a new area of active solution – the so-called area of overpassivation – within which steel dissolves with the appearance in the solution not only of tri-but also of six-valent chromium. Within this area the solution current increases up to $1.5 \cdot 10^{-3}$ amp/cm^2 when the potential is equal to + 1.450 volts and remains approximately constant* up to the potential values of + 1.800 volts; when this value is reached the evolution of oxygen becomes visible.

Figure 1 shows that an analogous variation of the stable solution rate with potential also takes place for the other steels investigated. The difference in the behavior of these steels is essentially qualitative. The introduction of nickel leads first of all to the decrease of the stable solution rate for all potentials more negative than + 1.200 volts. Within the passivity area the solution rate decreases systematically with the concentration of nickel in the steel.

Thus when the potential varies from 0.0 to + 0.500 volt the solution rate, equal to $3.2 \cdot 10^{-7}$ amp/cm^2 for Cr22Ti steel, becomes equal to $1 \cdot 10^{-7}$ amp/cm^2 for Cr20Ni6C2Ti steel, and $4.8 \cdot 10^{-8}$ amp/cm^2 for Cr22Ni14Ti steel. The most significant effect, however, is observed within the polarization areas preceeding deep polarization. Thus, for example, when the potential is equal to -0.400 volt the solution rate of Cr22-Ni14Ti steel is almost 1000 times smaller than the solution rate of Cr22Ti steel. This means that the presence of nickel affects not only the electrochemical behavior of steel in the passivity region but also leads to a significant increase of overpotential of the anodic reaction within that polarization region, where the active state is the stable state. This result is reflected in the value of the anodic current necessary to induce the passive state in steel. This current is equal to $1 \cdot 10^{-3}$ amp/cm^2 for Cr22Ti steel and $3 \cdot 10^{-6}$ amp/cm^2 for Cr22Ni14Ti steel.

The results of Fig. 1 show that the introduction of nickel hardly affects the position of the curve characterizing the hydrogen overpotential. This indicates that the observed difference between the values of stationary potentials and the free solution rate of the different steels in sulfuric acid is completely determined by the difference in the slopes of the anodic curves.

In the case of Cr22Ti steel the hydrogen evolution rate under the condition of deep passivity (potential equal to -0.27 volt) is smaller than the corresponding passivating current. As the result, in this case, the curve of hydrogen overpotential intersects the anodic curve when the potential is equal to $\varphi'_{st} = -0.29$ volt, i.e., within the polarization region preceeding the passage of the alloy into the passive state. The free solution rate of this steel in sulfuric acid, taking place with hydrogen depolarization proceeds therefore at a considerable rate, equivalent to the density of current $i'_0 = 3.5 \cdot 10^{-4}$ amp/cm^2.

* The nature of the limit current within the region of potentials from + 1.450 to + 1.800 will be discussed separately. For the present one must note that according to our results, obtained with rotating Cr18Ni9 steel electrodes (up to 1500 rpm), the magnitude of this current was independent of the rotation speed.

In the case of Cr22Ni14Ti steel the relationship between the rates of the anodic and the cathodic reaction is different. In this case the hydrogen evolution rate under the condition of passivity is considerably higher than the solution rate of the alloy. As the result, the exclusion of cathodic polarization leads to self-passivation of the steel: the stationary potential $\varphi_{st}^{''}$ becomes close to the potential of the reversible hydrogen electrode in the same solution; to this value of the potential corresponds the passive state of the metallic surface and a low solution rate equivalent to the density of current $i_0^{''} = 2.8 \cdot 10^{-7}$ amp/cm^2.

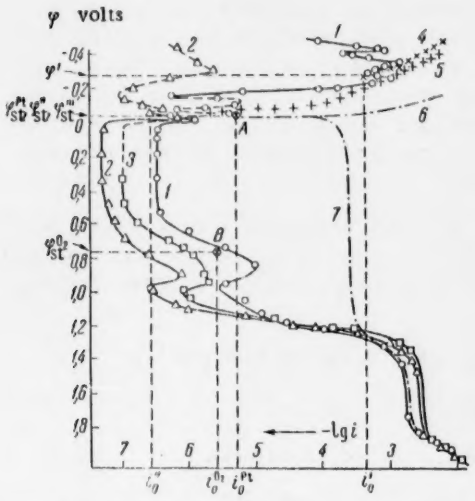

Fig. 1. Polarization curves of the real solution rate of Cr22Ti (1), Cr22Ni14Ti (2), and Cr20Ni6C2Ti (3) steel in 0.1 N H_2SO_4 solution. The curves 4 and 5 represent hydrogen overpotential curves for the Cr22Ti and Cr22Ni14Ti steels. Curves 6 and 7 represent the cathodic and anodic curves of Cr22Ti steel in the presence of platinum, in an atmosphere of hydrogen, measured by the current intensity.

The stabilization of $\varphi_{st}^{''}$ within the region of zero hydrogen is due to the fact that in this case the ionization rate of hydrogen (if hydrogen is present in the solution after the preliminary cathodic polarization) is considerably higher than the solution rate of steel. This potential is unstable, however; as the solution becomes saturated with nitrogen, and consequently the dissolved hydrogen is being removed from the layer close to the electrode, it shifts toward more positive values, where the dissolution of the alloy is compensated by the restitution of traces of oxygen present in nitrogen.

Cr20Ni6C2Ti steel behaves in an analogous manner; for this steel the stationary potential is equal to $\varphi_{st}^{'''} = 0$.

The results obtained allow us to conclude that in order to induce passivity in a steel, and consequently to increase its corrosion resistance in the absence of outside polarization, it is necessary to ensure a shift of the stationary potential toward more positive values, i.e., more positive than the passivation potential (but not higher than the potential of the beginning of overpassivation). Such a shift can be created not only by the increase of the overpotential of the anode reaction, as was the case in our investigation, but also by increasing the sum total of all the depolarizing reaction rates. Our experiments with Cr22Ti steel have shown that the increase of the depolarization rate of all the cathodic reactions can be achieved either by decreasing the hydrogen overpotential or by introducing into the solution a new oxidizing agent capable of being restored on the surface of the alloy within the polarization region studied.

In our experiments the decrease of the hydrogen overpotential was achieved by precipitating a small amount of platinum on the surface of the steel. Figure 1 shows that this precipitation displaces the hydrogen overpotential curve from position 4 to position 6; this displacement shifts the stationary potential φ_{st}^{Pt} toward more positive values (up to the point close to the potential of the reversible hydrogen electrode in the same solution) and considerably decreases the solution rate, down to the value equivalent to the current density $i_0^{Pt} = 4.9 \cdot 10^{-6}$ amp/cm^2. This value (point A on Curve 1) is almost precisely equal to the stable solution rate of steel at the corresponding potential determined by the potentiostatic curve.

Analogous results were also obtained by introducing oxygen from the air into the solution. In this case the stationary potential of steel was displaced down to the values $\varphi_{st}^{O_2} = +0.740$ volt and the stable solution rate decreased simultaneously down to the value equivalent to the current density $i_0^{O_2} = 2.5 \cdot 10^{-6}$ amp/cm^2 (point B, Fig. 1) which also corresponds to the potentiostatic curve of solution of steel obtained by an independent method. These results confirm our previous assumption that the effect of passivating agents such as cathodic additions and oxidizers is not necessarily connected with their direct formation of passivating layers on the metal surface. It seems that an analogous explanation can be given to the passivating action of other oxidizing agents such as, for example, Fe^{+3} ions, etc. [2-4].

On the basis of the results obtained one can assume that measurements of the potentiostatic polarization curves of different steels may represent a rational method for choosing an optimum qualitative and quantitative composition of steels from the point of view of their corrosion resistance.

Furthermore, the curves obtained can be used to choose the conditions decreasing the solution rate of steel of a given composition, either with or without supply of current. One must take into account the fact that the capacity of steel for self-passivation is determined by the relation between the sum of all the anodic and cathodic reaction rates taking place, and also by the real solution rate of steel under each given potential. If the sum of all the cathodic and anodic reactions is equal when the potential is located within the passivity region of a given steel, then the steel, in the absence of an external current, will be self-passivating. In this case the cathodic polarization of steel may lead not to protection but to an increase of the corrosion rate in accordance with the potentiostatic polarization curve of steel.

The results obtained show that the degree of passivity of the surface of a steel of a given composition is the function of the potential and, in the cases described, does not depend on the way its potential is maintained. The displacement of the potential by the chemical composition of the steel may lead to a significant change in the degree of its passivity for a given potential.

We wish to express our gratitude to A. A. Babakov for the steel samples used in this work.

LITERATURE CITED

[1] Ia. M. Koltyrkin and V. M. Kniazheva, J. Phys. Chem. USSR 30, 1990 (1956).

[2] N. Ia. Bune and Ia. M. Kolotyrkin, Proc. Acad. Sci. USSR 111, 1050 (1956).*

[3] H. C. Gatos, J. Electrochem. Soc. 103, 286 (1956).

[4] V. P. Batrakov, Proc. Acad. Sci. USSR 111, 845 (1956).*

Received October 9, 1957

*Original Russian pagination. See C. B. Translation.

EFFECT OF HIGH PRESSURES ON SELF-ADHESION (AUTOHESION) OF HIGH-POLYMERS

L. A. Igonin, Iu. V. Ovchinnikov and S. A. Arzhakov

(Presented by Academician V. A. Kargin, February 25, 1958)

The phenomena of self-adhesion of high-polymers represent one of the characteristics of these materials that are very important in practice, but which have received little study. The self-adhesion of rubberlike polymers was studied in a number of papers [1-4], and only a very few papers exist on the subject of the self-adhesion of thermoplasts. However, no doubt exists as to the important role played by self-adhesion phenomena in processes for the molding of articles from powdered and granulated thermoplasts.

In this paper we investigated the effect of temperature and pressure on the self-adhesion of some powdered thermoplasts. We investigated the conditions for the formation of a clear specimen when powdered material was molded in a heated cylindrical press-mold. The molded specimens had a diameter of 10 mm and a length of 4-5 mm, in which connection both the temperature and pressure of molding were varied in a wide interval.

The following regime was used to mold the specimens: a weighed amount of polymer was placed in the cold press-mold and a certain pressure was applied; after this the temperature of the press-mold was raised to the desired temperature and the specimen kept at this temperature for 15 minutes. After cooling the press-mold to 50-60° the pressure was released, the specimen was removed from the press-mold, and then it was visually inspected for degree of transparency to ordinary light.

In the case where the molding of a powdered thermoplast under pressure yields a transparent specimen, there occurs either partial or complete coalescence of the grains of the material and the disappearance of the boundaries between them. Here the strength of a transparent specimen does not necessarily reach the cohesion strength of the material, as is sometimes assumed [5]. The change in the thickness of transparent specimens of polyvinyl chloride when annealed at 100° for 15 minutes is shown in Fig. 1. The curve was taken using a dynamometric scales, which in the present case served as a thickness meter.

The specimens were molded under pressure at various temperature. The pressure was 400 kg/sq cm, and the compression time was 15 minutes. From Fig. 1 it follows that specimens, pressed at temperatures up to 130° show substantial change in their dimensions on annealing. Here they also lose their transparency and turn white.

Specimens, pressed at higher temperatures, are stable when annealed, retaining both their dimensions and transparency.

Consequently, only partial coalescence of the polymer grains occurs at temperatures up to 130°, and it is only at higher press-mold temperatures that the strength of the specimens reaches the cohesion strength of the material. In the case where pressing of a polymer powder yields opaque specimens, self-adhesion of the grains fails to occur.

The P—T curve for polyvinyl chloride is shown in Fig. 2, defining the region of temperatures and pressures where transparent specimens are formed. From these data it follows that self-adhesion of polyvinyl chloride begins at temperatures that are about 5 to 10° above its glass transition temperature. In this connection the limit, separating the region of forming opaque specimens from that in which transparent specimens are formed, lies in the interval 100-150 kg/sq cm.

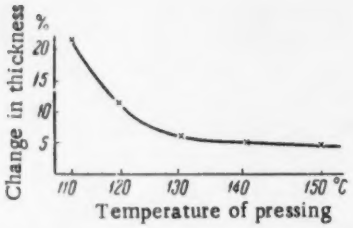

Fig. 1. Change in the thickness of transparent polyvinyl chloride specimens when annealed.

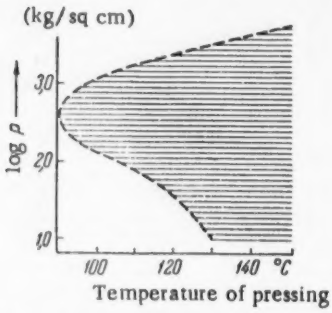

Fig. 2. Region in which transparent specimens of polyvinyl chloride are formed.

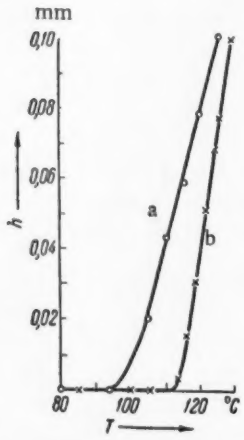

Fig. 3. Change in the volume of polyvinyl chloride in a press-mold with elevation of the temperature. a) Pressure 1100 kg/sq cm, b) pressure 2400 kg/sq cm.

As a result, increasing the compression pressure at a constant temperature at first yields opaque specimens, clear up to the pressure defined by the lower curve. This region corresponds to a growth in the total area of contact of the grains of the material with increase in the pressure, which is a necessary condition for the creation of self-adhesion. Further increase in the pressure leads to the formation of transparent specimens, i.e., to a disappearance of the boundaries between the grains of the material as the result of either complete or partial coalescence. As had already been indicated above, complete coalescence for polyvinyl chloride under the adopted time of holding occurs at temperatures that exceed T_g by 50°, i.e., at temperatures above 130°.

The upper branch of the curve defines the compression pressures above which only opaque specimens are formed again, i.e., the material fails to show self-adhesion at these pressures. The existence of the upper branch is to be explained as being due to an increase in the stiffness of the polymer chain of polyvinyl chloride, which becomes noticeable at pressures exceeding 1000 kg/sq cm. Here the glass transition temperature of the polymer increases, approaching the temperature of compression, which limits self-adhesion and leads to the formation of opaque specimens.

This situation is illustrated by the data shown in Fig. 3. In this experiment the die of the mold was connected to an indicator, showing the change in the volume of the polymer powder placed in the mold when the temperature of the mold was raised at a rate of 1° per minute. Before starting to heat the mold a pressure, corresponding to one of the values found on the upper branch of the curve, was applied to the material, and this pressure was maintained constant during the whole experiment. In this case, it could be expected that a sharp change in the volume of the material will take place in the T_g region of the polymer due to its being squeezed into the empty spaces in the mold. From Fig. 3 it can be seen that for pressures of 1100 kg/sq cm and 2400 kg/sq cm a sharp change in the volume was observed at 100 and 115°, respectively, which coincides closely with the shape of the upper branch of the curve in Fig. 2 for these pressures.

The above indicated relation between the glass transition temperature of polyvinyl chloride and the pressure was also observed for several other polymers. The P–T curves for polyvinyl chloride, polystyrene and polymethylmethacrylate are shown in Fig. 4.

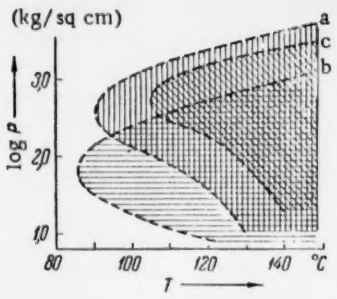

Fig. 4. Region of formation of transparent specimens: a) Polyvinyl chloride (T_g = 80°), b) block polystyrene (T_g = 80°), c) polymethylmethacrylate ST-1 (T_g = 115°).

These relationships can be seen more clearly if two specimens of the polymer, cut from a sheet, are subjected to compression under the above indicated regime. In this case monolithic transparent specimens are obtained only at the pressures circumscribed by the upper and lower curves.

LITERATURE CITED

[1] S. S. Voiutskii and B. V. Shtarkh, Proc. Acad. Sci. USSR 90, 573 (1953).

[2] B. V. Deriagin and N. A. Krotova, Adhesion [in Russian] (Izd. AN SSSR, 1949).

[3] B. V. Deriagin, S. K. Zherebkov and A. M. Medvedeva, Proc. Acad. Sci. USSR 111, 1267 (1956).

[4] S. S. Voiutskii, A. I. Shapovalova and A. P. Pisarenko, Proc. Acad. Sci. USSR 105, 1000 (1955).

[5] H. P. Meissner and E. W. Merrill, Mod. Plastics 26, No. 8, 104 (1949).

MECHANISM OF THE PROTECTIVE ACTION OF COLORED LACQUER COATINGS

Academician V. A. Kargin, M. I. Kariakina and Z. Ia. Berestneva

In discussing the anticorrosion action of colored lacquer coatings it is usually assumed that corrosion of a metal is determined by the rate with which the attacking substances penetrate through the film, and in connection with this a choice of coatings is made by selecting the film with the least permeability. There is no doubt about the fact that preventing or retarding the penetration of attacking substances through a film plays an important role. However, it is known from the literature, and also from practice, that films frequently permit the passage of substantial amounts of water, acids, oxygen, etc., and still possess sufficiently high protective properties [1-3].

It could be assumed that, together with the ability of a film to prevent the penetration of attacking substances, still other phenomena exist, which determine the corrosion properties of a metal after a colored lacquer film had been deposited on it. Their influence should be revealed in the case where a constant amount of attacking substance is applied to the surface of a metal in a constant length of time, i.e., where the influence of diffusion through a film is excluded.

The problem reduces to being able to apply the attacking substance to the surface of a corroding metal in the presence of a film as though the film had ideal diffusion properties in the sense of being completely void and does not retard the process of the penetration of this substance to the metal, i.e., it reduces to being able to create such conditions where the penetration of the attacking substance is the same whether the metal is coated or not coated with a film, and where the penetration is also independent of both the composition and the thickness of the lacquer coating.

The most convenient study method here, which permits excluding the effect of diffusion through a film, is the electrochemical method.

Experimentally, the problem reduces to maintaining a constant amperage in a system with variable resistance, for the amount of corroded iron or the amount of oxide formed will be proportional to the amount of electricity passed, or to the product of amperage by time, and is determined directly using Faraday's law.

Since colored lacquer films have a high electrical resistance, the tests were run with a large difference in the potentials. For this we built an apparatus with a maximum voltage of 3000 v, equipped with an automatic regulator which permitted maintaining a constant amperage with an accuracy of 10 ma.

As electrolyte we used 0.01 N sodium carbonate solution; as electrodes we used a platinum sheet as the cathode and an iron rod, coated with the colored lacquer material being studied, as the anode.

The specimens were tested for 2 hours and were examined every 15-30 minutes. The current density was maintained constant in all of the experiments and was equal to 1.8 ma/sq cm [4].

Consequently, the amount of attacking substance, penetrating to the surface of the metal in a given length of time, should remain constant; if corrosion of the metal was determined only by the permeability of the film, then both the lacquer-coated and the bare electrodes would be corroded to the same extent. However, the very first experiments revealed that both the time required and the character of the corrosion are different for specimens not coated and those coated with a protective lacquer, despite the fact that the amount of attacking substance applied was the same in both cases. In the case of the uncoated specimen the corrosion was rapid and

spread over the whole surface. In the case of the lacquer-coated specimen only localized corrosion spots appeared, in which connection the time required for their formation was many times greater than in the first case. As a result, with the same amount of surface exposed, the amounts of oxides (from the electrochemical corrosion of iron) formed on a base surface and on a surface protected by a colored lacquer film are different.

Consequently, other factors besides the diffusion properties of films affect the corrosion of a metal protected by a colored lacquer coating.

Corrosion is the transition of a metal into some chemical compounds, which arise at the metal–film interface, and the separation of which denotes the appearance of a new phase.

To form this new phase arising at the metal–film interface, it is necessary to complete the activation work, which will correspond to the energy required to cleave the film from the surface of the metal. This phenomenon is completely analogous to any process for the formation of a new phase inside a solid (for example, the formation of gas bubbles inside of metals, etc.), and it is well known that such processes proceed with large activation heats. In the case where the separation of these substances as a new phase proceeds with large activation heats it is possible for substantial supersaturation to arise; it is possible for the formed oxides to dissolve in the film substance, forming solutions with enormous degrees of supersaturation. And actually, investigations of coatings with a high diffusion permeability, which also swell readily in water (gelatin and polyvinyl alcohol), proved that iron oxide is formed, not on the surface of the metal, but instead on the external surface of the film, clear up to the formation of a copious precipitate of iron hydroxide in the solution without any destruction of the protective films. This indicates that conditions do not exist at the metal surface–film interface for the formation of a new phase as the result of these films having a high adhesion capacity, while the formed oxides dissolve in the film substance and, diffusing through it, separate there, where the formation of a new phase proceeds without any difficulties, i.e., at the interface of protective film and solution.

Colored lacquer coatings were also investigated by the method of cathodic polarization, i.e., the investigated lacquer-coated iron rod served as the cathode, while a platinum sheet served as the anode. Hydrogen was evolved when an electrical field was applied to the cathode, which with good adhesion between the film and the metal diffused into solution. Hydrogen could accumulate at the spots of least adhesion, creating a pressure on the film, which made it possible for the film to break away from the surface of the metal.

Actually, with this method of investigation the film peeled away from the surface of the metal at the points of least adhesion, forming bubbles; here the film itself remained intact. Then the specimen was subjected to anodic polarization and here corrosion first appeared at the points of film separation. These experiments show very clearly the important part played by the adhesion properties of colored lacquer coatings.

Since internal strains [5, 6] arise in colored lacquer coatings, which, depending on the conditions under which the relaxation processes are run, may be retained for a long time and facilitate premature destruction of the coating, we made a study of the effect of these strains on the adhesion properties of films, and it was established that increasing the strains leads to a reduction in the adhesion properties of films.

Consequently, the method developed by us permits (having eliminated the phenomenon of film permeability) evaluating the protective properties of coatings either from the time required for corrosion to appear in the case of anodic polarization, or from the appearance of bubbles in the case of cathodic polarization; at the same time it clearly shows the important role played by the adhesion properties of films in the protective action of coatings.

As a result, in contrast to the existing theory that film permeability is the main factor in determining the protective properties of colored lacquer coatings, it was shown in the present study that the adhesion properties of coatings play an equal, and at times even a greater role, since adhesion properties possess importance not only as a factor determining the adhesion of the film to the base but also as a factor that prevents the formation of a new phase at the metal–film interface.

LITERATURE CITED

[1] J. E. O. Mayne, J. Oil and Colour Chem. Ass. 32, No. 352, 481 (1949).

[2] R. Ledwith and J. Lewin, J. Oil and Colour Chem. Ass. 29, No. 360, 67 (1946).

[3] S. Finn and G. Lewis, J. Oil and Colour Chem. Ass. 34, No. 372, 266 (1951).

[4] V. A. Kargin, M. I. Karlakina and Z. Ia. Berestneva, J. Chem. Industry (USSR) No. 5, 20 (1956).

[5] V. A. Kargin, T. I. Sogolova and M. I. Karlakina, J. Chem. Industry (USSR) No. 7, 8 (1955).

[6] M. I. Karlakina, V. A. Kargin and T. I. Sogolova, J. Chem. Industry (USSR) No. 5, 9 (1957)

L. Ia. Karpov Physicochemical
Research Institute

Received March 1, 1958

THE QUASI-STATIONARY THERMAL REGIME IN EXPLOSION REACTIONS

A. G. Merzhanov and F. I. Dubovitskii

(Presented by Academician V. N. Kondrat'ev, February 3, 1958)

The nonstationary system of equations describing the thermal explosion in terms of dimensionless variables* has the form:

$$\gamma \frac{d\theta}{d\tau} = e^{\theta}\varphi(\eta) - \frac{1}{\varkappa}\theta, \tag{1}$$

$$\frac{d\eta}{d\tau} = e^{\theta}\varphi(\eta). \tag{2}$$

The initial conditions are: $\tau = 0$, $\eta = 0$ and $\theta = 0$, where $\eta = (C_0 - C)/C_0$, is the degree of reaction; $\theta = \frac{E}{RT_0^2}(T - T_0)$, is the heat-up; $\tau = k_0 e^{-E/RT_0} t$, is the time; and

$$\varkappa = \frac{1}{4e\delta_{crit}} \frac{Q}{\lambda} \frac{E}{RT_0^2} d^2 k_0 e^{-E/RT_0}; \quad \gamma = \frac{c\rho}{Q} \frac{RT_0^2}{E};$$

$\varphi(\eta)$ being a function which expresses the law covering the course of the reaction under isothermal conditions.

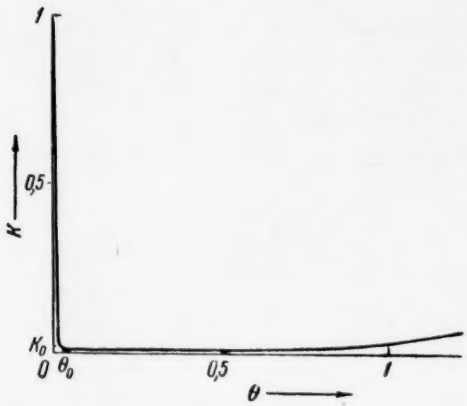

Fig. 1. The K, θ relation for $\gamma = 0.005$, $\eta_0 = 0.01$, $\kappa = 1.55$.

The criterion κ gives the relation between the constants and the reaction conditions. The criterion γ characterizes the explosive properties of the reaction. The smaller γ, the more clearly are these explosive properties expressed.

The following symbolism will be employed: C, the concentration of the initial products; C_0, the initial concentration of the initial products; T, the temperature (deg); T_0, the initial value of the temperature (deg); t, the time (sec); d, the diameter of the reaction vessel (cm); E, the energy of activation (cal/mole); k_0, the multiple of the exponential in the expression for the velocity constant (sec^{-1}); Q, the heat of reaction (cal/cm^3); λ, the thermal conductivity (cal/cm·sec·deg); c, the specific heat capacity (cal/g·deg); ρ, the density (g/cm^3); and, δ_{crit}, the critical value of the Frank – Kamenetskii constant [1] (equal to 0.88 for a plane – parallel, to 2.00 for a cylindrical, and to 3.32 for a spherical, vessel).

*In converting to dimensionless variables, use has been made of the technique proposed by Frank – Kamenetskii for decomposing exponents [1].

A general investigation of such systems has been carried out by Todes [2-4]. This author treated the reaction kinetics and the heat-up through a method of numerical integration and obtained an expression for the explosion limit. Analyzing his results and our own experimental data, we have come to the conclusion that a quasi-stationary reaction regime can be set up under certain conditions, in which the rate at which heat accumulates is so small in comparison with the rate at which heat is delivered (almost all of the evolved heat being carried out of the reaction zone) that the accumulation can be neglected. Such a reaction process consists, as it were, of a series of stationary, equilibrium positions. The passage from one of these positions to another, is brought about by an isothermal alteration in the reaction rate, and in the associated rate of delivery of heat. That is to say that in the quasi-stationary regime, the principal role in the non-isothermal reaction process is played by the isothermal alteration in the velocity,* rather than the accumulation of heat. Such a process becomes possible when the time for establishing thermal equilibrium is much less than the time of reaction, i.e., when the point of equilibrium shifts only insignificantly while equilibrium is being established.

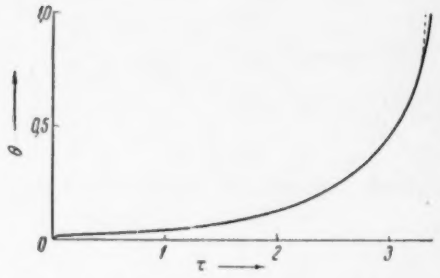

Fig. 2. Curves showing the θ, τ relation as obtained by solving the nonstationary system (full line), and the quasi-stationary system (dotted line). The values of the parameters are the same as in Fig. 1.

For reactions showing auto-acceleration under isothermal conditions, a study of the quasi-stationary regime makes it possible to obtain all of the fundamental characteristics of the thermal explosion; the critical condition (the explosion limit), the extent of the pre-explosion reaction and the induction period.

Without diminishing the generality of the conclusions, we will consider the simplest type of auto-accelerating reaction; namely, that of an auto-catalytic reaction of the first order.

$$\varphi(\eta) = (\eta + \eta_0)(1 - \eta),$$

here η_0, the criterion for auto-catalysis, is an essentially small quantity ($10^{-1} - 10^{-3}$). Speaking in general, the criterion η_0 depends on T, but it can be considered as constant in integration [4].

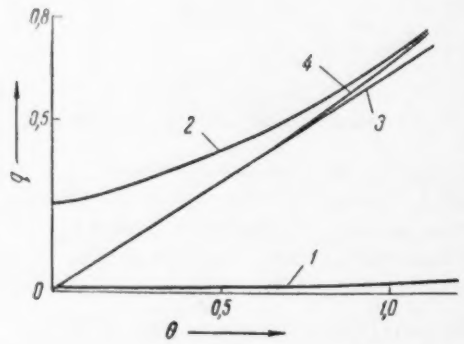

Fig. 3. A graphical interpretation of the heat balance equation: 1 and 2) curves for the heat delivery at the initial, and at the maximum, velocity; 3) direct transport of heat; 4) integral curve for the heat delivery. The values of the parameters are the same as for Fig. 1.

The quasi-stationary system of equations has the form

$$e^{\theta}(\eta + \eta_0)(1 - \eta) - \frac{1}{\varkappa}\theta = 0, \qquad (3)$$

$$\frac{d\eta}{d\tau} = e^{\theta}(\eta + \eta_0)(1 - \eta). \qquad (4)$$

When $\tau = 0$, $\eta = 0$.

Equation (3) expresses the equilibrium relation between the heat-up and the extent of reaction. An analysis of this relation shows that the quasi-stationary regime can exist above the explosion limit in the interval $\theta_0 < \theta < 1$ for the values $\kappa < 1/e\eta_0$. The minimum quasi-stationary heat-up, θ_0, can be found from the equation

$$\theta_0 e^{-\theta_0} = \varkappa\eta_0.$$

The quasi-stationary regime has not yet been established when $\theta < \theta_0$ and has already broken down when $\theta > 1$. The specific properties of the auto-accelerating reaction do not come into play when $\kappa > 1/e\eta_0$ (the

*In contrast, the accumulation of heat plays the principal role under adiabatic conditions.

initial rate satisfies the condition for explosion) and, in principle, a quasi-stationary reaction process is then impossible.

By solving the system of equation (3) – (4), expressions are obtained for: the critical condition

$$\varkappa = \frac{4}{e(1+\eta_0)^2};$$

the extent of the preliminary reaction

$$\eta_{exp} = \frac{1-\eta_0}{2} - \sqrt{\left(\frac{1+\eta_0}{2}\right)^2 - \frac{1}{e\varkappa}};$$

and, the induction period

$$\tau_{ind} = \frac{1}{2}\int_0^1 \frac{(1-\theta)\,e^{-\theta}\,d\theta}{\theta\sqrt{\left(\frac{1+\eta_0}{2}\right)^2 - \frac{1}{\varkappa}\,\theta e^{-}}}.$$

The induction period (dimensional) at the explosion limit is equal to

$$t_{crit} = \frac{1}{k_0(1+\eta_0)}\,e^{E/RT}\int_{\theta_{(\eta_*)}}^1 \frac{(1-\theta)\,e^{-\theta}\,d\theta}{\theta\sqrt{1-\theta e^{(1-\theta)}}}$$

It is to be seen from this expression that t_{crit} is determined by the rate constants for the isothermal reaction alone, and is independent of such quantities as Q, λ, etc., which are essential to the thermal explosion, but here serve only to fix the position of the explosion limit. This property can be utilized for determining the rate constant from the experimental data on the thermal explosion.

The reaction time can be conveniently determined from the equation

$$\tau = \varkappa\int_0^{\eta} \frac{d\eta}{\theta(\eta, \varkappa, \eta_0)}.$$

$\theta(\eta, \kappa, \eta_0)$ is to be found from Equation (3).

In treating the problem of the conditions required for the existence of the quasi-stationary regime, we will introduce the quantity

$$K = \gamma\frac{d\theta}{d\eta}.$$

into the discussion. This represents the ratio between the rates of accumulation, and of delivery, of heat and characterizes the reaction regime. For an adiabatic regime, K = 1; for a stationary regime, K = 0 and for a quasi-stationary, K << 1.

Figure 1 represents the K, θ relation as obtained by numerical integration. As a criterion for the quasi-stationary regime there can be selected the value of K at the point θ_0. An approximation (valid for small values of K) gives

$$K_0 \simeq \frac{\varkappa\gamma}{(1-\theta_0)\,e^{-\theta_0}}. \qquad (5)$$

The quasi-stationary regime can be considered as the limiting form of the nonisothermal reaction process when $K_0 \to 0$. The value of K_0 can be low either because κ is small (conditions approaching isothermal) or because γ is small. For reactions leading to thermal explosion, γ is of the order $10^{-2} - 10^{-3}$. Thus, for autocatalytic reactions, a quasi-stationary regime always exists above the explosion limit (when κ is not small).

The width of the region for a quasi-stationary process in the pre-explosion reaction (in terms of κ) depends on the degree of auto-acceleration. For reactions with normal kinetics, the quasi-stationary regime exists above the explosion limit only beyond the maximum in the heat-up, and is, naturally, without interest.

The process of establishing the quasi-stationary regime can be investigated by solving the system of equations (1) and (2) when $0 < \theta < \theta_0$ and $0 < \eta < \eta_{est}$. The condition for the quasi-stationary regime corresponds to $\eta_{est} \ll \eta_0$. Through an approximate solution for small values of θ_0 (which satisfy the representation $e^{\theta_0} \approx 1 + \theta_0$), expressions for η_{est} and τ_{est} are obtained:

$$\ln\left(\frac{1}{1-\varkappa\eta_0}\frac{\eta_{est}}{\eta_0}\right) + \varkappa\eta_0 = -\frac{(1-\varkappa\eta_0)^2}{\varkappa\gamma}\frac{\eta_{est}}{\eta_0},$$

$$\tau_{est} = -\frac{\varkappa\gamma}{1-\varkappa\eta_0}\ln\left(\frac{1}{1-\varkappa\eta_0}\cdot\frac{\eta_{est}}{\eta_0}\right).$$

Figure 2 represents $\theta(\tau)$ curves which have been obtained by numerical integration of the system (1) – (2), and by solving the system (3) – (4) with a correction for the establishment of the regime.

If the reaction is quasi-stationary because of the excessively low value of γ, the following evaluation can be set up for τ_{ind}:

$$\varkappa\int_0^{\eta_{exp}}\frac{d\eta}{0(\varkappa,\eta)} < \tau_{ind} < \int_0^{\eta_{exp}}\frac{d\eta}{\varphi(\eta)}.$$

The lower evaluation is obtained by supposing η_{exp} to reach the quasi-stationary value; the upper, by assuming it to reach the isothermal value.

The quasi-stationary regime can be conveniently observed in the diagram (Fig. 3) as the approach of the integral curve for the heat delivery to the straight line for the heat transport.

The authors express their thanks to N. N. Semenov, Academician, and to Ia. B. Zel'dovich, Corresponding Member, of the Academy of Sciences of the USSR for valuable consultations during the course of this work.

LITERATURE CITED

[1] D. A. Frank-Kamenetskii, J. Phys. Chem. 13, 738 (1939).

[2] O. M. Todes, J. Phys. Chem. 13, 868 (1939).

[3] O. M. Todes and P. V. Melent'ev, J. Phys. Chem. 13, 1594 (1939).

[4] O. M. Todes and P. V. Melent'ev, J. Phys. Chem. 14, 1026 (1940).

Received February 3, 1958

STUDY OF THE ADSORPTION OF CATIONS ON PLATINIZED PLATINUM BY THE METHOD OF MEASURING THE ADSORPTION POTENTIALS

A. D. Obrucheva

(Presented by Academician A. N. Frumkin, March 4, 1958)

In an earlier paper [1] the specific adsorption of chlorine, bromine and iodine ions and of the thallium cation on a platinized platinum electrode was studied by the method of direct determination of the shift in the adsorption potential. Some electrolyte, for example 1 N H_2SO_4, washing an electrode depolarized down to a potential range of 0.3 v to 0.7 v (with the normal hydrogen electrode as reference standard), was displaced in a nitrogen atmosphere by an electrolyte containing the adsorbed ion after which the shift in the potential with time was determined, until the potential assumed a new constant value. The shift in the potential can serve as an approximate measure of the specific adsorption. In addition, as had been described earlier for the adsorption of thallium [1], a determination of the change in the shape of the anodic load curves served as a measure of the adsorption and degree of desorption of the cations.

Using these methods we investigated in the present study the specific adsorption of lead, zinc and cadmium ions, all shifting the electrode potential toward the positive side. Lead was adsorbed from 0.1 N $Pb(ClO_4)_2$ on a ground of $HClO_4$, zinc was adsorbed from 0.1 N $ZnSO_4$ on a ground of 1 N H_2SO_4, and cadmium was adsorbed from cadmium sulfate, the chloride or the iodide on the same ground of 1 N H_2SO_4. Adsorption equilibrium was achieved for all practical purposes in 20 to 60 minutes.

In the case of lead adsorption the shift in the potential with an initial potential value of 0.3 v was 0.46 v. The anodic load curve, taken in lead perchlorate solution after the electrode, the initial potential of which was 0.3 v, had remained in it for 24 hours, does not show separation into a hydrogen and an oxygen region (Figs. 1 and 2). After repeated rinsing of the perchloric acid from the electrode with simultaneous anodic polarization to a potential of 1.6 v the shape of the load curve is restored almost to normal, but the hydrogen portion remains somewhat abridged, while the start of oxidation is shifted to less positive values of the potential (Figs. 1 and 3). When such a rinsed electrode is allowed to stand in perchloric acid, void of lead ions, for 20 hours in a nitrogen atmosphere, the hydrogen portion of the anodic curve is diminished even more and the start of oxidation is shifted even more strongly toward smaller anodic potential values (Figs. 1 and 4). This last indicates that when platinum is in contact with $Pb(ClO_4)_2$ solution the lead shows partial penetration into the platinum interior and then gradually emerges again to the surface after its purification. A similar effect of anions penetrating into the interior of platinum was first observed by N. A. Balashova, who used the method of radioactive indicators [2], and was confirmed by the present method for the case of iodine and thallium [1]. A shift of the start of oxidation toward greater cathodic potential values when a lead salt is added to the chloroplatinate during platinization was already described earlier [3].

The experiments on adsorption from 0.1 N $CdSO_4$ solution were run at initial potential values of 0.3 v and 0.6 v. In the first case the adsorption shift of the potential was + 0.32 v. The anodic load curve in $CdSO_4$ solution (Fig. 2, 2) has an unusual shape, indicating substantial strengthening of the hydrogen bond with the metal; however, this distorted anodic curve, in contrast to what is observed in the majority of cases where substantial adsorption effects are present, is not abridged and practically merges with the initial curve at 0.9 v. The initial shape of the anodic load curve can be restored by rinsing in sulfuric acid with simultaneous anodic polarization to 1.6 v (Fig. 2, 3). An earlier oxidation of the platinum is observed in the case of cadmium

adsorption, which was also observed in the adsorption of thallium and of lead, and also the emergence of cadmium from the deeper layers of the metal to the rinsed platinum surface. However, the last phenomenon is much more weakly expressed than in the case of Pb. With an initial potential of 0.6 v the adsorption shift of the potential was a total of only 0.085 v and penetration of cadmium into the interior of the metal was not observed.

We also examined the behavior of a Pt-electrode in solutions of cadmium chloride and iodide. Since both the anion and the cation are active in these salts, then the sign of the adsorption shift of the potential in the presence of these salts depends on the values of the initial potential. The values of the adsorption shifts of the potential in solutions of the sulfate, chloride and iodide of cadmium are given in Table 1, and for comparison, also the absorption shifts of the potential in solutions of the chloride and iodide of potassium in a certain interval of initial potentials.

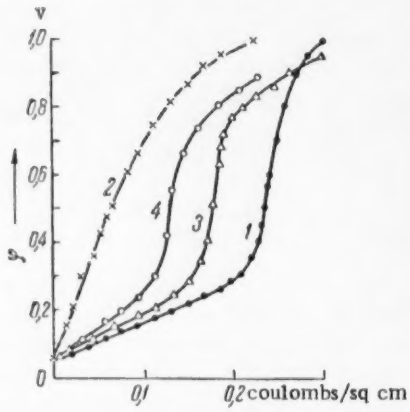

Fig. 1. Effect of adsorption of lead ions on the anodic load curves of platinized Pt. 1) in 1N $HClO_4$; 2) in 1N $HClO_4$ + 0.1N $Pb(ClO_4)_2$; 3) after repeated rinsing of the $HClO_4$ with simultaneous anodic polarization; 4) after remaining in $HClO_4$ for 20 hours.

As can be seen from Table 1, a shift of the initial potential in the anodic direction is accompanied by a decrease in the positive shift of the potential in the case of $CdSO_4$, by a transition from positive to negative values in the case of $CdCl_2$, and by an increase in the absolute value of the negative shift of the potential in the case of CdI_2. As a result, in all cases more positive values of the initial potential favor adsorption of the anion and impede adsorption of the cation. The shifts of the potential, observed in solutions of cadmium salts, have in all cases either a more positive or a less negative value than is the case with solutions of potassium salts having the same anion, which is due to superimposition of the adsorption effect of the cation Cd^{2+} on the adsorption effect of the anion. For the case of the solution–air interface, where the specific adsorption of cations is absent, A. N. Frumkin [4] observed a more negative value for the adsorption shift of the potential in the presence of CdI_2 when compared with KI solutions of the same concentration, which he associated with the presence of complex anions of the type CdI_3^-, having a high adsorbability, in the CdI_2 solution.

The anodic load curves, obtained in the presence of $CdCl_2$ (Fig. 3, 2), indicate that firmly bound hydrogen is present and that the start of oxidation is shifted toward more anodic values. The latter must evidently be regarded as being due to the influence of the chlorine ion, making a shift of the start of oxidation in the cathodic direction, caused by the adsorption of cadmium. Repeated rinsing of the sulfuric acid restores the anodic load curve to its original shape (Fig. 3, 3), after which the appearance of cadmium on the surface of the electrode can again be shown after the electrode has remained in sulfuric acid for 20 hours (Fig. 3, 4).

The anodic load curve in CdI_2 solution (Fig. 4, 2) was taken only up to 0.55 v due to the oxidation that set in at greater anodic potentials. A load curve (Fig. 4, 3) characteristic for iodine is obtained after CdI_2 adsorption at a potential of 0.3 v and rinsing in H_2SO_4. With further rinsing and alternate anodic and cathodic polarization the shape of the load curve approaches that of the original, but the hydrogen region remains contracted and the start of oxidation is shifted toward more positive potentials, the same as was observed after the adsorption of iodine from KI solutions. Suppression of the start of oxidation after adsorption from CdI_2 solution was expressed more weakly than in the case of adsorption from KI solution. The influence of the Cd ions is responsible for this. The influence of iodine ion on the shape of the load curve is expressed more strongly after Cd adsorption at an initial potential of 0.6 v; the start of oxidation in this case is shifted toward greater anodic potentials.

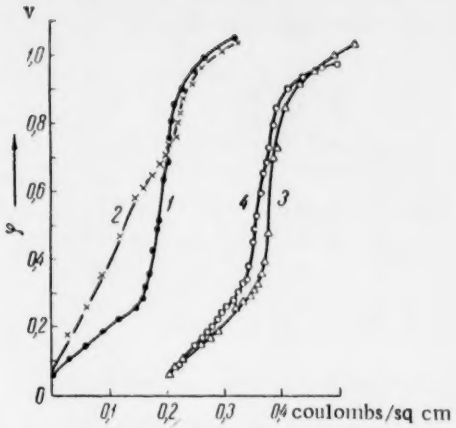

Fig. 2. Effect of the adsorption of Cd ions from cadmium sulfate solution on the anodic load curves of platinized Pt. 1) in 1 N H_2SO_4; 2) in 1 N H_2SO_4 + 0.1 N $CdSO_4$; 3) after adsorption for 20 hours from 1 N H_2SO_4 + 0.1 N $CdSO_4$ with an initial potential of 0.3 v and repeated rinsing in 1 N H_2SO_4; 4) after remaining in H_2SO_4 solution for 80 hours. The start of Curves 3 and 4 is shifted by 0.2 v on the abscissa.

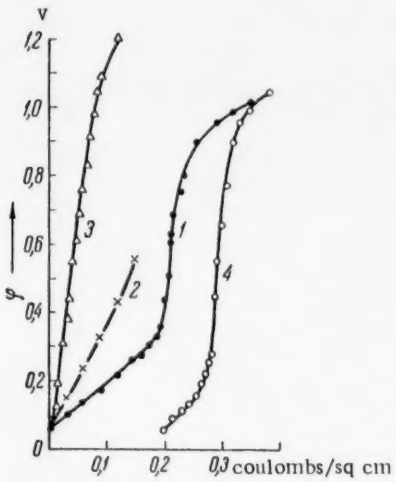

Fig. 4. Effect of CdI_2 adsorption on the anodic load curves of platinized Pt. 1) in 1 N H_2SO; 2) in a solution of 1 N H_2SO_4 + 0.1 N CdI_2; 3) after CdI_2 adsorption at an initial potential of 0.3 v, rinsing in H_2SO_4 and a single cathodic polarization; 4) after further repeated rinsing in 1 N H_2SO_4 with alternate anodic and cathodic polarization. The origin of Curve 4 is shifted by 0.2 v on the abscissa.

Fig. 3. Effect of $CdCl_2$ adsorption on the anodic load curves of platinized Pt. 1) in 1 N H_2SO_4; 2) in 1 N H_2SO_4 + 0.1 N $CdCl_2$; 3) in 1 N H_2SO_4 after adsorption from 1 N H_2SO_4 + 0.1 N $CdCl_2$ at 0.3 v and repeated rinsing in H_2SO_4; 4) in 1 N H_2SO_4 after remaining in solution for 20 hours. The origin of Curves 3 and 4 is shifted by 0.05 v on the abscissa.

The adsorption shifts of the potential in the case of Zn^{2+} were expressed more weakly than was the case for the other cations investigated in the present study, and on a ground of 1 N H_2SO_4 at an initial potential of 0.3 v were 0.12 v for 0.1 N $ZnSO_4$ and 0.31 v for 1 N $ZnSO_4$.

The adsorption of Li^+, Cs^+, Sr^{2+} and Ba^{2+} could not be shown, either by a distortion of the shapes of the anodic load curves or by a shift of the potential. A similar result had been obtained earlier [1] in the case of lanthanum and thorium sulfates. The fact that these high-charge ions fail to show noticeable specific adsorption may be due to their greater energy of hydration.

The presented results, together with the data obtained earlier for the adsorption of thallium on platinum [1] and mercury [5], do not leave any doubt but that cations, the electron clouds of which do not have the configuration of the noble gases, can show a specific adsorption on metal surfaces that is just as strongly expressed as that of iodine, a typical surface-active anion. A comparison of the data, obtained in the present study for the case of cadmium, with the data relating to the adsorption of Cd on mercury [5], lead to the postulation that these phenomena are much more strongly expressed in the case of adsorption on platinum.

TABLE 1

Adsorption Shifts of the Potential (v) of a Platinized Pt-Electrode in the Adsorption of $CdSO_4$, $CdCl_2$, CdI_2, KCl and KI. In a solution of 1N H_2SO_4

Expt. No.	Initial potential, v	0.1 N $CdSO_4$	0.1 N $CdCl_2$	0.1 N KCl	0.1 N KCl	0.1 N KI
1	0.3	0.32	0.177	−0.06	−0.06	−0.27
2	0.4		0.146		−0.12	
3	0.5		0.085			
4	0.6	0.085	−0.015	−0.3		
5	0.65		−0.085			−0.46

I wish to express my deep gratitude to Academician A. N. Frumkin for his valuable counsel when the results of the present study were discussed.

LITERATURE CITED

[1] A. D. Obrucheva, J. Phys. Chem. (USSR) 32 (in press).

[2] N. A. Balashova, J. Phys. Chem. (USSR) 32 (in press); Proc. Acad. Sci. USSR 115, 336 (1957);* Z. physik. Chem. 207, 340 (1957).

[3] A. I. Shlygin, Sci. Reports Kishinev Univ. 8, 3 (1953).**

[4] A. N. Frumkin, Z. physik. Chem. 109, 34 (1924).

[5] A. N. Frumkin and A. S. Titievskaia, J. Phys. Chem. (USSR) 31, 485 (1957); A. N. Frumkin and N. S. Poilanovskaia, J. Phys. Chem. (USSR) 32, 157 (1958).

M. V. Lomonosov
State University (Moscow)

Received February 19, 1958

*Original Russian pagination. See C. B. Translation.

**In Russian.

X-RAY DIFFRACTION FROM REGIONS COMPOSED OF LONG MOLECULES

D. Ia. Tsvankin

(Presented by Academician V. A. Kargin, January 8, 1958)

A review of recent data on the structure of linear polymers leads to the conclusion that the structural unit in many such polymers is a set, or bundle, or variously arranged chains simultaneously passing through a single region [1]. From the point of view of this model, it is of interest to calculate the diffraction from regions consisting of long molecules whose axes are arranged parallel to one another. It is possible to imagine various packings of parallel molecular chains which would differ in their degree of order. One such case, that of diffraction from a "textured liquid," has been considered by N. S. Andreeva and V. I. Iveronova [2].

In the present work, calculations will be carried out on the diffraction from a collection of regions which give rise to an axial texture. These regions are similar to one another, being built up from long molecules whose axes are parallel to the texture axis. We will consider the following cases:

I. Full three-dimensional order exists within each of the regions. The chain axes form a true lattice. The azimuthal rotation of the chains around their axes, and the displacement of the chains along these axes, are strictly regular.

II. There is free rotation and regular chain displacement, the chains rotating freely around their axes while the displacement along the axes remains regular.

III. There is free rotation and irregular displacement, this being the case of one-dimensional diffraction, in which both the azimuthal rotation and the displacement along the axes are irregular. The case of irregular displacement and regular azimuthal order will not be considered, since it is clearly not realizable.

I. We will suppose that there are Z regions, each consisting of n chains. The chain, in its turn, will consist of N identical atomic groups, N being a large number. This repeating group of P atoms will be designated as the cell of the chain. It has been shown in [3] that there are only two possible types of arrangement of the chain projections in the equatorial plane. In the one case all of the chains are translationally identical; in the other, there are two groups of translationally identical chains. The chains are related translationally if they can be transformed into one another with the aid of a vector which is perpendicular to the chain axis, i.e., lying in the equatorial plane. The chains which are unrelated translationally are ones which are distinguished by translation along the texture axis and rotation around this same axis.

In considering the general case, we will suppose that the region can be divided into two groups of translationally identical chains. The scattering intensity of a single region, in electron scattering units, is:

$$I = \sum_{kk'} f_k f_{k'} \exp\,(is\mathbf{R}_{kk'}),$$

where f_k is the atomic factor, $s = 4\pi \sin\theta/\lambda$ and $\mathbf{R}_{kk'}$ is the interatomic vector.

We will divide I into two parts: $I = I' + I''$. I' will include all of those members which involve summation over the atoms of translationally related chains, and I'', all of those members involving pairs of atoms of translationally unrelated chains.

We will consider I''. Any interatomic vector, $R_{kk'}$, can represented as:

$$R_{kk'} = \vec{\rho}_{mm'} + l_{kk'}b + \eta_{mm'}b + r_{kk'}.$$

The chains are enumerated by m and m', and the atoms, by k and k', $\vec{\rho}$ is the interchain vector in the equatorial plane; b is a vector along the axis, of magnitude equal to the chain period, l is an integer and $|\eta_{mm'}| < 1$. The component of s along the axis of the molecule will be designated as s_b and the component in the equatorial plane as s_r: $s = s_b + s_r$; in a similar fashion, the component of $r_{kk'}$ along the axis will be $\eta_{kk'}b$ and the component in the plane, $\vec{\rho}_{kk'}$: $r_{kk'} = \vec{\rho}_{kk'} + \eta_{kk'}b$, $\vec{\rho}_{mm'kk'} = \vec{\rho}_{mm'} + \vec{\rho}_{kk'}$ and $\eta_{mm'kk'} = \eta_{mm'} + \eta_{kk'}$. Since the same set $r_{kk'}$ is obtained for each pair of cells it follows that the summations over mm' and kk' can be separated, so that after rearranging, we obtain (ξ is the layer number):

$$I'' = N^2 \sum_{mm'} \sum_{kk'} f_k f_{k'} \exp\left[i\left(s_r \vec{\rho}_{mm'kk'} + 2\pi\xi\eta_{mm'kk'}\right)\right].$$

For chains which are translationally identical, $\eta_{mm'} = 0$, and

$$I' = N^2 \sum_{mm'} \sum_{kk'} f_k f_{k'} \exp\left[i\left(s_r \vec{\rho}_{mm'kk'} + 2\pi\xi\eta_{kk'}\right)\right].$$

The rotation of the regions with respect to the texture axis is irregular. The average intensity of scattering from all of the regions is: $\overline{I} = \overline{I'} + \overline{I''}$; φ being the azimuthal angle in the equatorial plane. Since

$$\frac{1}{2\pi}\int_0^{2\pi} \exp\left[is_r \vec{\rho}_{mm'kk'}\right] d\varphi = J_0(s_r\rho_{mm'kk'}) \quad (J_0 \text{ is a Bessel function}),$$

the result of averaging is

$$\overline{I''} = N^2 Z \sum_{mm'} \sum_{kk'} f_k f_{k'} J_0(s_r\rho_{mm'kk'}) \exp\left[i2\pi\xi\eta_{mm'kk'}\right]; \qquad (1)$$

$$\overline{I'} = N^2 Z \sum_{mm'} \sum_{kk'} f_k f_{k'} J_0(s_r\rho_{mm'kk'}) \exp\left[i2\pi\xi\eta_{kk'}\right]. \qquad (2)$$

Interest attaches to a reformulation of (1) and (2) with the aid of the well known development of J_0.

$$\rho_{mm'kk'} = \sqrt{\rho_{mm'}^2 + \rho_{kk'}^2 - 2\rho_{mm'}\rho_{kk'}\cos\varphi_{mm'kk'}},$$

and if $\alpha_{mm'kk'}$ is the angle between $\vec{\rho}_{mm'}$ and $\vec{\rho}_{kk'}$, $\varphi_{mm'kk'} = 180° - \alpha_{mm'kk'}$; then

$$J_0(s_r\rho_{mm'kk'}) = J_0(s_r\rho_{mm'})J_0(s_r\rho_{kk'}) + 2\sum_{n=1}^{\infty} J_n(s_r\rho_{mm'})J_n(s_r\rho_{kk'})\cos n\varphi_{mm'kk'}. \qquad (3)$$

Using (3), we will first rearrange $\overline{I}$: Since for the transplationally identical chains $\rho_{kk'}^{k} = \rho_{k'k}$ and $\eta_{kk'} = -\eta_{k'k}$, it follows that

$$\sum_{mm'} \sum_{kk'} f_k f_{k'} J_0(s_r\rho_{mm'}) J_0(s_r\rho_{kk'}) \exp\left[i2\pi\xi\eta_{kk'}\right] =$$

$$= \left[n + 2\sum_{mm'}^{m'>m} J_0(s_r\rho_{mm'})\right]\left[\sum_{k=1}^{p} f_k^2 + 2\sum_{kk'}^{k'>k} f_k f_{k'} J_0(s_r\rho_{kk'})\cos 2\pi\xi\eta_{kk'}\right].$$

$\varphi_{mm'kk'} = 180° - \varphi_{mm'k'k}$, so that the sum $\cos n\varphi_{mm'kk'} + \cos n\varphi_{mm'k'k}$ is equal to zero when n is odd and to $2\cos n\varphi_{mm'kk'}$ when n is even. Thus summation over the translationally related chains gives:

$$\overline{I'} = N^2 Z\left\{\left[n + 2\sum_{mm'}^{m'>m} J_0(s_r\rho_{mm'})\right]\left[\sum_{k=1}^{p} f_k^2 + 2\sum_{kk'}^{k'>k} f_k f_{k'} J_0(s_r\rho_{kk'})\cos 2\pi\xi\eta_{kk'}\right] + \right.$$
$$\left. + 8\sum_{mm'}^{m'>m}\sum_{kk'}^{k'>k}\sum_{n\ \text{even}} f_k f_{k'} J_n(s_r\rho_{mm'}) J_n(s_r\rho_{kk'})\cos 2\pi\xi\eta_{kk'}\cos n\varphi_{mm'kk'}\right\}. \quad (4)$$

We will now consider $\overline{I''}$. Into (1) there enters a summation over translationally unrelated chains, so that, speaking in general $\rho_{kk} \neq 0$, $\eta_{kk} = 0$ and $m \neq m'$, but $\rho_{mm'kk'} = \rho_{m'mk'k}$ and $\eta_{mm'kk'} = -\eta_{m'mk'k}$.

Summing all members over the pairs $mm'kk'$ and $m'mk'k$, and expanding $J_0(s_r\rho_{mm'kk'})$ in a series according to (3), we obtain

$$\overline{I''} = 2N^2 Z\left[\sum_{mm'}^{m'>m}\sum_{kk'} f_k f_{k'} J_0(s_r\rho_{mm'}) J_0(s_r\rho_{kk'})\cos 2\pi\xi\eta_{mm'kk'} + \right.$$
$$\left. + 2\sum_{mm'}^{m'>m}\sum_{kk'}\sum_{n} f_k f_{k'} J_n(s_r\rho_{mm'}) J_n(s_r\rho_{kk'})\cos 2\pi\xi\eta_{mm'kk'}\cos n\varphi_{mm'kk'}\right]. \quad (5)$$

In the general form, it is not possible to carry out on $\overline{I''}$ a simplification of the same type as that used for $\overline{I'}$, since if $\eta_{kk'} = -\eta_{k'k}$, then $\rho_{kk'} \neq \rho_{k'k}$ and similarly for $\eta_{mm'}$ and $\rho_{mm'}$.

II. In this case, $\rho_{mm'}$, $\eta_{mm'}$, and $\eta_{kk'}$, among the quantities characterizing the interchain and interatomic distances, remain unaltered, while $\varphi_{mm'kk'}$ and $\rho_{kk'}$ will be changed.

In dealing with the case of free rotation and uni-dimensional diffraction, we will not consider the effect on the intensity of a variation in the location of the chain centers in the equatorial plane. We note that the equations which are obtained below remain valid when the chain axes are displaced from their proper positions. $\varphi_{mm'kk'}$ takes any value in the range from 0 to 2π. In the average $\overline{\cos n\varphi_{mm'kk'}} = 0$. We will separate out the components for which $m = m'$. Then

$$\overline{I'} = n\left[\sum_{k=1}^{p} f_k^2 + 2\sum_{kk'}^{k'>k} f_k f_{k'} J_0(s_r\rho_{kk'})\cos 2\pi\xi\eta_{kk'}\right] +$$
$$+ 2\sum_{mm'}^{m'>m}\sum_{kk'} f_k f_{k'} J_0(s_r\rho_{mm'}) J_0(s_r\rho_{kk'})\cos 2\pi\xi\eta_{kk'},$$
$$\rho_{kk'} = \sqrt{\rho_k^2 + \rho_{k'}^2 - 2\rho_k\rho_{k'}\cos\psi_{kk'}},$$

in which $\vec{\rho}_k$ and $\vec{\rho}_{k'}$ are the projections of r_k and $r_{k'}$ on the equatorial plane, and $\psi_{kk'} = 180° - \gamma_{kk'}$, $\gamma_{kk'}$ being the angle between $\vec{\rho}_k$ and $\vec{\rho}_{k'}$. $\rho_{kk'}$ is the constant, since for independent rotation of the chains, $\psi_{kk'}$ goes from 0 to 2π, when the atoms k and k' belong to different chains. Thus each $J_0(s_r\rho_{k'})$ entering into the sum

$$\sum_{mm'}^{m'>m}\sum_{kk'} f_k f_{k'} J_0(s_r\rho_{mm'}) J_0(s_r\rho_{kk'})\cos 2\pi\xi\eta_{kk'}\ \overline{J_0(s_r\rho_{kk'})} = J_0(s_r\rho_k) J_0(s_r\rho_{k'}).$$

must be averaged.

As a result, for the case of free rotation we obtain

$$\overline{I'} = N^2 Z \left\{ n \left[\sum_{k=1}^{p} f_k^2 + 2 \sum_{kk'}^{k'>k} f_k f_{k'} J_0 (s_r \rho_{kk'}) \cos 2\pi \xi \eta_{kk'} \right] + \right.$$
$$\left. + 2 \sum_{mm'}^{m'>m} J_0 (s_r \rho_{mm'}) \sum_{kk'} f_k f_{k'} J_0 (s_r \rho_k) J_0 (s_r \rho_{k'}) \cos 2\pi \xi \eta_{kk'} \right\}. \quad (6)$$

Reasoning in a similar fashion, we have for $\overline{I''}$:

$$\overline{I''} = 2N^2 Z \sum_{mm'}^{m'>m} \sum_{kk'} f_k f_{k'} J_0 (s_r \rho_{mm'}) J_0 (s_r \rho_k) J_0 (s_r \rho_{k'}) \cos 2\pi \xi \eta_{mm'kk'}. \quad (7)$$

III. Since averaging has been carried out for the case of free rotation, it remains to consider how the Equations (6) and (7) will be changed under irregular displacement along the axis. The results of averaging will be different for $\xi = 0$ and $\xi \neq 0$. It is clear that $\overline{I''} = 0$ when $\xi \neq 0$, since $\overline{\cos 2\pi \xi \eta_{mm'kk'}} = 0$.

$\overline{\cos 2\pi \xi \eta_{kk'}}$, if the atoms k and k' are from different chains and

$$\overline{I} = \overline{I'} = N^2 Z n \left[\sum_{k=1}^{p} f_k^2 + 2 \sum_{kk'}^{k'>k} f_k f_{k'} J_0 (s_r \rho_{kk'}) \cos 2\pi \xi \eta_{kk'} \right].$$

For $\xi = 0$,

$$\overline{I} = \overline{I'} + \overline{I''} = N^2 Z \left\{ n \left[\sum_{k=1}^{p} f_k^2 + 2 \sum_{kk'}^{k'>k} f_k f_{k'} J_0 (s_r \rho_{kk'}) \right] + \right.$$
$$\left. + 2 \sum_{mm'}^{m'>m} J_0 (s_r \rho_{mm'}) \sum_{kk'} f_k f_{k'} J_0 (s_r \rho_k) J_0 (s_r \rho_{k'}). \right.$$

Here all of the chains are on the same footing, and summation is extended over all of them.

In conclusion, we note a peculiarity of the expressions for $\overline{I'}$ and $\overline{I''}$ in the case of three-dimensional order. In Equations (4) and (5), the terms involving summation over n contain Bessel functions of high orders. It is well known that with an increase in the order, the first maximum diminishes and is displaced toward higher values of the argument. The first term involves functions of zero order and is independent of the azimuthal arrangement, and thus essentially characterizes the whole intensity curve for low values of s_r, i.e., for small θ's. The higher the number of any one of the remaining terms, the greater will be its contribution to the larger values of θ. The principal result of free rotation is found in the absence of terms in J_n for $n \geq 1$, i.e., in a limitation of the diffraction field. In the result, an averaging over the variation in $\rho_{kk'}$ will have little effect on the intensity curve. There will also be a limitation of the diffraction field due to vibrations of the chains over a certain interval of angles around the texture axis, since the larger n the more strongly will small changes in $\varphi_{mm'kk'}$ "neutralize" cos $n\varphi_{mm'kk'}$.

The interchain and interatomic distances must be known in order that calculations be carried out through the derived equations. When these quantities are known, a comparison of the calculated and the experimental results makes it possible to study the degree of order in the various regions of the polymer. This problem will be considered elsewhere.

This work was carried out under the direction of Professor A. I. Kitaigorodskii, to whom the author would like to express his deep thanks.

LITERATURE CITED

[1] V. A. Kargin, A. I. Kitaigorodskii and G. L. Slonimskii, Colloid J. 19, vol. 2, 131 (1957).*

*Original Russian pagination. See C. B. Translation.

[2] N. S. Andreeva and V. I. Iveronova, Biophysics 2, vol. 3, 281 (1957).

[3] A. I. Kitaigorodskii, Organic Crystal Chemistry (in Russian) Acad. Sci. USSR, Press, 1955.

Received January 6, 1958

[2] N. S. Andreev

THE EDGE PROBLEM IN THE THEORY OF HEAT EXPLOSION

V. V. Barzykin and A. G. Merzhanov

(Presented by Academician V. N. Kondrat'ev, February 26, 1958)

In studying theheat explosion of substances in a condensed phase we noticed that a constancy of the temperature at the interface of substance and surrounding medium* can be maintained only under special experimental conditions. Under ordinary conditions the heat exchange that prevails at the interface is more complex. This is possible for the reason that the heat capacity per unit volume of the substance in the condensed phase is either commensurate with the heat capacity per unit volume of the surrounding medium or is slightly greater than it. The heat liberated during reaction heats up the adjacent layer of the surrounding medium, and the temperature on the surface of the substance becomes different from the temperature of the medium at infinity.

In the present paper we discuss the critical conditions for heat explosion when such more complex heat exchange prevails. In such case the limiting conditions have the form:

$$\lambda\left(\frac{\partial T}{\partial n}\right)_S = -\alpha\,(T_S - T_0),$$

where λ is the heat conductivity coefficient of the exploding substance, T_0 is the temperature of the surrounding medium beyond the interface, α is the heat transfer coefficient, and $\underline{n}$ is the normal to the surface of separation S. The heat transfer coefficient α depends on the nature of the contacting surfaces, the character of the heat exchange with the surrounding medium, and the temperature of the surface (this last function is usually neglected), and is independent of the temperature distribution in the substance. The presence of a wall does not complicate the problem mathematically. In this case the total heat resistance $1/\alpha$ will include the heat resistance of the wall.

Todes and Kontorova [2] solved the problem relating to heat explosion using similar limiting conditions, but they failed to obtain a satisfactory solution. We will use the Frank-Kamenetskii method to solve the problem, making use of it by transposing the exponent into the Arrhenius law. In our case the equation of stationary heat conduction under the limiting conditions will have the form:**

$$\frac{d^2\theta}{d\xi^2} + \frac{m}{\xi}\frac{d\theta}{d\xi} = -\delta e^{\theta}, \tag{1}$$

$$\text{when } \xi = 1 \quad \left(\frac{d\theta}{d\xi}\right)_S = -\mathrm{Bi}\,\theta_S. \tag{2}$$

For an infinite parallel-walled vessel m = 0, for an infinite cylinder m = 1, and for a spherical vessel m = 2.

Analysis of the equation and limiting conditions reveals that at the explosion limit Frank-Kamenetskii's criterion δ is a function of the criterion $\mathrm{Bi} = \alpha r/\lambda$. When $\mathrm{Bi} \to \infty$, i.e., when the heat exchange between

*As was shown by Frank-Kamenetskii [1], in the case of heat explosion in a gas phase the temperature of the surrounding medium T_0 can be considered to be the same as that imparted to the inner wall surface of the reaction vessel.

**Using Frank-Kamenetskii's designations.

the surface of the substance and the surrounding medium is so intense that it does not permit the surface to become hotter than the medium, then $\theta_s \to 0$, and the problem reduces to Frank-Kamenetskii's problem. By varying Bi from infinity to zero, we thus embrace all of the possible cases of heat exchange, beginning with the ideal transfer of heat from a surface, and ending with heat exchange being absent (adiabatic case).

We will find the stationary distributions of the temperatures and the critical conditions for the vessel shapes indicated above.

For an infinite cylindrical vessel the problem is solved analytically to the end. The total integral of equation (1) at m = 1 was found by Lemke [3], and has the form:

$$\theta = \ln \frac{8-b}{\delta} - 2 \ln \left(a \xi^{k_1} + \frac{1}{a} \xi^{k_2} \right),$$

where a and b are integration constants, and k_1 and k_2 are roots of the equation:

$$k^2 - 2k + \frac{b}{8} = 0.$$

From the condition $d\theta/d\xi = 0$ when $\xi = 0$ we have $b = 0$, $k_1 = 2$, $k_2 = 0$. The form of the solution is simplified:

$$\theta = \ln \frac{8}{\delta} - 2 \ln \left(a \xi^2 + \frac{1}{a} \right). \tag{3}$$

Constant a is found from the transcendental equation

$$\mathrm{Bi} \left[\ln \frac{8}{\delta} - 2 \ln \left(a + \frac{1}{a} \right) \right] = \frac{4a^2}{a^2 + 1}, \tag{4}$$

which was obtained using the limiting conditions of (2). At the explosion limit this equation gives two values of a (δ, Bi), corresponding to two stationary distributions of the temperatures – a stable and an unstable distribution. At the explosion limit both distributions merge and a becomes a function of only one parameter

$$a_{cr} = \sqrt{\sqrt{\frac{4}{\mathrm{Bi}^2} + 1} - \frac{2}{\mathrm{Bi}}}. \tag{5}$$

The critical condition has the form:

$$\delta = \frac{8a_{cr}^2}{(a_{cr}^2 + 1)^2} \exp \left[- \frac{4a_{cr}^2}{(a_{cr}^2 + 1)\,\mathrm{Bi}} \right]. \tag{6}$$

It is easy to see that when $\mathrm{Bi} = \infty$, $a_{cr} = 1$, $\delta = 2$, and the distribution at the explosion limit appears as such:

$$\theta = \ln \frac{4}{(\xi^2 + 1)^2}.$$

As can be seen from equations (3), (5) and (6), the maximum heating up at the explosion limit decreases with decrease in Bi, which indicates that transposition of the exponent at any Bi is valid.

Knowing (3) and (4), it is possible to find all of the values associated with the distribution (average heat evolution, heat flow, etc.) at any heat exchange.

The total integral of Equation (1) for an infinite parallel-walled vessel is given by Frank-Kamenetskii. Employing the limiting conditions, we calculated the critical function δ (Bi).

We were unable to find the total integral of Equation (1) for a spherical vessel. It is possible that in general it does not exist. Substituting

$$x = \xi^2 e^{\theta}, \quad y = \xi \frac{d\theta}{d\xi}$$

Equation (1) reduces to a first order equation

$$\frac{dy}{dx} = -\frac{y + \delta x}{(y+2)x},$$

which is easily integrated numerically. The critical bond δ (Bi) is found from the condition of the integral curve being tangent to the curve $y = -\text{Bi} \ln x$, obtained from the limiting conditions.

It was observed that for the discussed vessel shapes the curves expressing the function δ (Bi) at the explosion limit are readily transformed into each other (with an accuracy of 1-2%) and can be depicted by the general formula

$$\delta = \delta_{\infty} \varphi(\text{Bi}),$$

where δ_{∞} is the critical value of parameter δ at Bi = ∞, and φ(Bi) is a universal function, not depending on the shape of the vessel, the form of which is evident from (6).

It should be mentioned that the critical function δ (Bi) may be obtained approximately within the confines of the nonstationary theory by adding the effective coefficient of heat transfer, determined by the Frank-Kamenetskii method, to the heat-exchange coefficient α. The equation obtained in this manner has the form:

$$\frac{1}{\delta} = \frac{1}{\delta_{\infty}} + \frac{e\beta}{\text{Bi}}$$

with β = 1 for the parallel-walled vessel, β = 1/2 for the infinite cylinder, and β = 1/3 for the sphere.

Comparison of this approximate equation with that obtained by exact solution reveals that the maximum divergence reaches 5% for the flat-walled vessel, 9% for the infinite cylinder, and 16% in the case of the sphere.

LITERATURE CITED

[1] D. A. Frank-Kamenetskii, J. Phys. Chem. (USSR) 13, 738 (1939).

[2] T. A. Kontorova and O. M. Todes, J. Phys. Chem. (USSR) 4, 81 (1933).

[3] H. Lemke, J. f. Math. 142, 118 (1913).

Institute of Chemical Physics
Academy of Sciences of the USSR

Received February 24, 1958

THE THERMODYNAMICS OF FORMATION OF THE HIGHER ANTIMONIDE OF IRON

V. A. Geiderikh, Corresponding Member Academy of Sciences, U.S.S.R.

Ia. I. Gerasimov and A. A. Vecher

The thermodynamics of the formation of the compound $FeSb_2$ from its elements according to the reaction:

$$Fe(s) + 2Sb(s) = FeSb_2 \qquad (1)$$

has been studied using the E.M.F. method.

A study has been made of the relationship between temperature and the E.M.F. of the cell

$$Fe\,|\,Fe^{2+},\ KCl + LiCl\ (melt)\,|\,FeSb_2 + Sb$$

within the temperature range 410-610°. Studies were made of 12 alloys of seven different compositions, lying within the heterogeneous region $FeSb_2$ + Sb in the diagram of state of the Fe–Sb system (see Fig. 1 [1]).

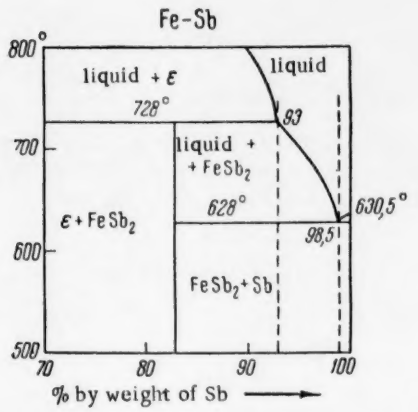

Fig. 1. Part of the fusion diagram for the Fe–Sb system.

The experimental procedure was similar to that described earlier. Oxidation of the electrodes was prevented by the passage of a slow current of nitrogen, previously passed through a layer of copper at 500-600° to remove all oxygen. The E.M.F. is established in 20-30 hours, after which it remains constant within 1 mv at a given temperature and is readily reproducible when the temperature range is traversed repeatedly in both directions. The potentials of the various alloy–electrodes relative to the same reference electrode differ by 0-3 mv.

The results of all the experiments were treated by the method of least squares. For the relationship E = f(T) the equation found is:

$$E = 0.1497 - 0.00004T\ (volt), \qquad (2)$$

by means of which it possible to calculate the isobaric–isothermal potential, enthalpy and entropy for the formation of $FeSb_2$ from iron and antimony according to reaction (1).

$$\Delta Z = -nFE = -6.9 + 0.0018T\ (kcal/mole). \qquad (3)$$

For T = 800°K, $\Delta Z_{800^\circ} = -5.4 \pm 0.1$ (kcal/mole) $= -1.8 \pm 0.03$ (kcal/g-atom).

From (3) and $\Delta Z = \Delta H - T\Delta S$ we obtain:

$$\Delta H = -6.9 \pm 0.4\ (kcal/mole) = -2.30 \pm 0.1\ (kcal/g\text{-}atom),$$

$$\Delta S = -1.8 \pm 0.4\ (cal/deg \cdot mole) = -0.6 \pm 0.1\ (cal/deg \cdot g\text{-}atom).$$

DISCUSSION OF RESULTS

Only one value of ΔH for the formation of $FeSb_2$ can be found in the literature, namely $\Delta H = -1.2$ kcal/g-atom, obtained by Korber and Oelsen [2, 3] by mixing the liquid metals in a calorimeter. This value differs from the value which we have obtained for the heat of formation of $FeSb_2$ by approximately 1 kcal/g-atom. The explanation of this discrepancy is probably as follows. Korber and Oelsen determined ΔH for the formation of the alloy as the difference between the heat evolved when liquid iron and antimony were mixed together and the resultant alloy cooled, and the heat evolved when the same quantities of the metals were cooled over the same temperature range without alloy formation. This difference amounted to only a small percentage of the quantities of heat measured and may be determined with a considerable error, as Oelsen himself points out [3]. On the other hand, Korber [4] points out that the method which they used admits an error due to insufficient homogenization of the alloy on rapid cooling. These errors in the mixing method may be particularly important in the determination of the heats of formation of compounds which melt incongruently, as has been pointed out by Wagner [5]. O. S. Ivanov [6] has noted the inaccuracy of Korber's data for the heats of formation of alloys in the systems Fe – Sb, Co – Sb and Ni – Sb, arising as a result of the over-rapid solidification of the alloys, which leads to the formation of a nonequilibrium mixture. Indeed, Kornakov and Konstantinov [7] have found that a melt of composition $FeSb_2$ solidifies in the form of a three-phase mixture of crystals of the compound $FeSb_2$, an ϵ-phase and antimony. Interaction of the ϵ-phase with antimony to form $FeSb_2$ is complete only after a 30-hour annealing process at a temperature of 710°. It is thus hardly possible that in Korber and Olesen's calorimeter the heat of formation of the $FeSb_2$ is completely evolved.

Theoretical calculation. If it is assumed that a dilute liquid solution of iron in antimony has the properties of an ideal solution, then it is possible to calculate $\Delta Z'$ for the formation of solid $FeSb_2$ from liquid iron and antimony, using the equation for part of the liquidus (bounded by broken lines in the Figure) in the fusion diagram for the Fe–Sb system (see Fig. 1) found by us from the data of Kurnakov and Konstantinov [7].

$$\log N_{Fe} = -7.023 + 6.135 \cdot 10^{-3} T \qquad (4)$$

$$\log N_{Sb} = 0.428 - 0.490 \cdot 10^{-3} T \qquad (5)$$

For the equilibrium between the liquid and solid phases we have:

$$\Delta Z'_{FeSb(s)} = \Delta\mu_{Fe(l)} + 2\Delta\mu_{Sb(l)} = 4.575\,T\,(\log N_{Fe} + 2 \log N_{Sb}).$$

Substituting from (4) and (5), we obtain: $\Delta Z' = -28.21\,T + 23.58 \cdot 10^{-3}\,T^2$. For 950°K $\Delta Z'_{950°} = -5.5$ kcal/mole.

In order to calculate ΔZ for the formation of solid $FeSb_2$ from solid iron and antimony, it is necessary to take into account ΔZ for the fusion of iron and antimony and for the phase changes of iron, which we may do using the values given in [8] for the heats of fusion of iron and antimony and for the heats of the phase changes in solid iron:

$$\Delta Z_{FeSb(s)} = \Delta Z'_{FeSb_2(s)} - \sum \Delta Z \text{ for the fusion and phase changes}$$

$$= -5.5 - 1.4 = -6.9 \text{ kcal/mole.}$$

The calculated value of ΔZ relates to approximately the same temperature range and is close to that found experimentally.

LITERATURE CITED

[1] M. Hansen, The Structure of Binary Alloys (1941) 2, p. 697.*

[2] F. Körber and W. Oelsen, Mitt. Kaiser Wilhelm Inst. Eisenforsch. Düsseldorf 19, 209 (1937).

[3] W. Oelsen, Z. Elektrochem. 43, 8, 530 (1937).

[4] F. Körber, Stahl u. Eisen. 56, 48, 1401 (1936).

[5] C. Wagner, The Thermodynamics of Alloys (1957) pp. 99, 102.*

[6] O. S. Ivanov, Izv. Akad. Nauk SSSR, Otdel Khim. Nauk 192 (1944).

*Russian translation.

[7] N. S. Kurnakov and N. S. Konstantinov, from the book: N. S. Kurnakov, Collection of Selected Works,* (1939) 2, p. 60.

[8] O. Kubaschevski and E. Evans, Metallurgical Thermochemistry,** (IL, 1954) p. 302.

M. V. Lomonosov State University, Moscow

Received March 1, 1958

*In Russian.

**Russian translation.

THE PROPERTIES OF GUTTAPERCHA IN THE AMORPHOUS STATE

Academician V. A. Kargin, T. I. Sogolova and B. I. Alkhodzhaev

When a crystalline polymer is melted and subsequently cooled, it crystallizes with the establishment of order in the relative position of the chain molecules. It is difficult to imagine that rapid cooling of a polymer in which the molecular chains are arranged in quite random fashion and are greatly entangled, can lead to rapid, complete and extensive crystallization.

It is evident that the way must be already paved in the amorphous state for the molecular order which can be readily detected in the crystalline polymer. We have suggested that if the relative position of the molecular chains is fixed in some way, then it is possible to detect any divergence in the properties of such amorphous polymers since the degree of order of amorphous polymers may vary within very wide limits and under certain conditions may reach high values [1-4]. It cannot be doubted that molecular order in polymers existing in the amorphous state is a prerequisite for rapid crystallization.

The fixation of the relative position of the molecular chains should also influence the rate and extent of the crystallization [5-8], and consequently the physical and mechanical properties of crystalline polymers.

The aim of the present study was the examination of the influence of the degree of order of the molecular chains on the properties of a polymer. The material chosen for study was guttapercha, a natural crystalline polymer, which changes readily from the crystalline to the amorphous state at 55° and crystallizes rapidly when the melt is cooled. Since the degree of order of the molecules is dependent to a considerable extent on the temperature, the process of fixing the different states of molecular order may be carried out by vulcanization at different temperatures.

Vulcanization was carried out at 143° with finely dispersed sulfur, at 70° and 20° in S_2Cl_2 vapor and at 20° by mixing a solution of guttaphercha in CCl_4 with a solution of S_2Cl_2 in ether. In the latter case vulcanization of the guttapercha took place in the process of formation of a film from the mixed solutions. The quantity of combined sulfur was determined chemically.

Table 1 and Fig. 1 show data obtained from the study of the original guttapercha and of specimens of guttapercha vulcanized under the different conditions but containing approximately the same quantities of combined sulfur. It was found that for a combined sulfur content of approximately 4%, the guttapercha became completely amorphous only when vulcanization was carried out at temperatures above the melting point of the crystals, i.e., at 143 and 70°.

In those cases where the processes of film formation and vulcanization are combined, the structural and mechanical properties of guttapercha provide evidence that it has become to a considerable extent amorphous, with some retention of the crystalline state. Evidently the reduction in the intensity of the thermal motion and the slow evaporation of solvent in the process of film formation create favorable conditions for the establishment of order in the molecular chain arrangement so that in spite of the vulcanization process, the crystalline structure is to a considerable extent retained.

An even greater difference in the properties of the guttapercha was observed when vulcanization of prepared films was carried out in S_2Cl_2 vapor at 70 and 20°. In the first case, with a combined sulfur content of 4%, the guttapercha remained amorphous and did not crystallize even when cooled to 20°, while in the second case, with a combined sulfur content of 4% and even of 5.6%, the guttapercha retained its crystalline structure (Table 1).

TABLE 1

The Relationship Between the Mechanical and Physical Properties of Guttapercha and the Vulcanization Conditions

Vulcanization conditions	Combined sulfur content, %	Phase state at 20°	Strength at 20°, kg/cm²*	Modulus of elasticity at 20°, kg/cm²	Relative elongation at rupture (20°), %	Vitrification temperature, °C
At 143°	4.2	At 20°, solution of guttapercha in CCl_4 with S_2Cl_2 solution	25	20	500	−40
At 70°, in S_2Cl_2 vapor	4.0	Amorphous, but crystallizes after storage for 6 months at 20°	20	65	60	0
At 20°, solution of guttapercha in CCl_4 with S_2Cl_2 solution	4.0	Retains slight crystalline structure	100	120	80	–
At 20°, in S_2Cl_2 vapor	5.6	Retains crystalline structure	180	2000	40	–
Original guttapercha	–	Crystalline	200	2000	350	–

*Calculated on the original cross-section.

Thus by fixing the particular state of the guttapercha at different temperatures we find it possible to examine the mechanical properties exhibited by the guttapercha in the change from the state of maximum order to the limiting ordered state.

It follows from the data presented that the degree of amorphous character of structured crystalline polymers depends not only on the number of cross-linkages formed but also to a considerable extent on the state in which the polymer existed during the process of structure-formation. The lower the degree of order of the polymer during structure-formation, the less the extent of the subsequent crystallization.

Particular attention must be paid to the interesting experimental fact that it is possible, for the same combined sulfur content, to obtain two types of amorphous guttapercha with completely different physical and mechanical properties (Table 1, Fig. 1).

The difference in properties of the two types of amorphous guttapercha is apparently related to the fact that as the temperature is increased, increase in the thermal motion leads to a reduction of order in the arrangement of the molecular chains so that at higher vulcanization temperatures fixation of a more disordered arrangement of molecular chains takes place.

It can be seen from an examination of the experimental data which we have obtained that increased deformability and lower values for the modulus of eleasticity and for the vitrification temperature are associated with the amorphous guttapercha vulcanized at the higher temperature (143°). Comparatively low deformation and higher values for the modulus of elasticity and vitrification temperature are associated with the guttapercha vulcanized at 70°, i.e., at a lower temperature, close to the melting point of the crystals.

It might be suggested that the difference in properties of the two types of amorphous guttapercha is caused by the fact that vulcanization with sulfur monochloride leads to the formation of monosulfide bonds [9, 10] while vulcanization with finely dispersed sulfur leads to the formation of polysulfide bonds [11]. The new experimental facts obtained, however, provide evidence that the difference in properties of the amorphous guttapercha results not merely from the presence of mono- and polysulfide bonds. The amorphous guttapercha vulcanized at 143° did not crystallize after storage for 10 months at 20°, while the amorphous guttapercha vulcanized at 70° became crystalline after storage for only six months.

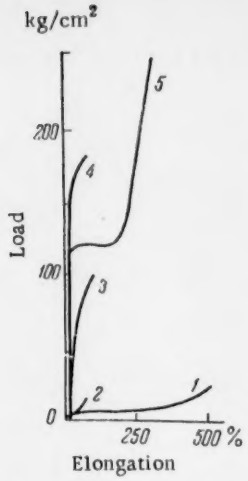

Fig. 1. The influence of vulcanization temperature on the mechanical properties of guttapercha at 20°. 1) vulcanized at 143° with finely dispersed sulfur, combined sulfur content 4.2%; 2) vulcanized at 70° in S_2Cl_2 vapor, combined sulfur content 4.0%; 3) vulcanized at 20° in mixture of solutions, combined sulfur content 4.0%; 4) vulcanized at 20° in S_2Cl_2 vapor, combined sulfur content 5.6%; 5) original guttapercha.

This phenomenon can only result from the greater order in the arrangement of the molecular chains in the guttapercha specimens vulcanized at 70° compared with the specimens vulcanized at 143°.

It thus follows from what has been said that the fixation of different degrees of order in the arrangement of the molecular chains of a polymer within the limits of the amorphous state leads to the formation of polymers exhibiting different mechanical and physical properties.

LITERATURE CITED

[1] V. A. Kargin, A. I. Kitaigorodskii and G. L. Slonimskii, Colloid J. 19, 1311 (1957).*

[2] A. V. Ermolina, G. S. Markova and V. A. Kargin, Crystallography 2, 623 (1957).**

[3] V. A. Kargin and G. S. Markova, Proc. Acad. Sci. 117, 427 (1957).*

[4] T. A. Koretskaia, Degree Thesis, L. Ia. Karpov Phys.-Chem. Inst. (Moscow, 1958).***

[5] J. M. Goppel and J. J. Arlman, Rubb. Chem. and Technol. 23, 310 (1950).

[6] A. W. Gent, J. Polym. Sci. 18, 321 (1955).

[7] T. I. Sogolova, B. I. Aikhodzhaev and V. A. Kargin, Zhur. Fiz. Khim. 31, 2340 (1957).

[8] B. I. Aikhodzhaev, T. I. Sogolova and V. A. Kargin, Zhur. Fiz. Khim. 31, 2551 (1957).

[9] J. Glaser and J. Shulman, J. Polym. Sci. 14, 169, 225 (1954).

[10] H. Mark, Ber. 61, 1948 (1928).

[11] B. A. Dogadkin and Z. N. Tarasova, Colloid J. 15, 343 (1953).*

L. Ia. Karpov Physicochemical Institute

Received March 4, 1958

*Original Russian pagination. See C. B. Translation.
**See English translation.
***Russian translation.

RELAXATION REACTION OF IMPACT WAVES WITH A ZONE OF COMBUSTION

S. M. Kogarko and V. I. Skobelkin

(Presented by Academician N. N. Semenov, March 6, 1958)

One of the authors had shown experimentally that in some explosive mixtures the passage of an impact wave through the zone of combustion results in the intensification of the latter. The relation between the intensification coefficient k^2 and the composition of a mixture is shown in Fig. 1 for a mixture composed of benzene and air.

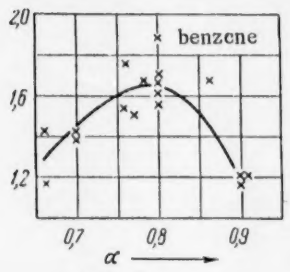

Fig. 1

We will investigate the manner in which the combustion kinetics affect the structure and power of an impact wave when it is passed through a combustion zone. We will define the structure of an impact wave by the wave width b, the amplitude of the pressure $\overline{\Delta p}$ and density $\overline{\rho}$ at the advancing front of the wave, the impulse I, and the propagation rate in the starting mixture D.

We will introduce into the discussion the term of a kinetic diffusion relaxation time t_r, i.e., the time during which momentary changes of the reaction conditions by the impact wave do not cause substantial changes in the diffusion and heat flows in the reaction zone. When the impact wave is disturbed by a statistical equilibrium the transition to a new equilibrium state occurs in finite time. The time of establishing a new temperature (relaxation energy of a forward motion of the molecules) is of the order of 10^{-9} sec, and the time of a macroscopic equalization of the temperature and concentration throughout the area as the result of motion, diffusion and heat conductivity is immeasureably greater. Incomplete statistical equilibrium is observed during this time.

Calculations reveal that t_r has the same order as the reaction time τ (10^{-3}–10^{-5} sec), defined as the ratio of the width of the combustion zone l to the normal rate of flame propagation λ.

As a result, in time t_r both the temperature and the pressure show an increase inside the reaction zone. Changes in the reaction zone cause corresponding changes (transmitted with the speed of sound) in the parameters of the gas in the vicinity of the combustion zone.

If the state of the reaction zone is characterized by variation of the impulse $I_r = \int_0^{\tau} \Delta p dt$, then the state of the gas near the combustion zone is determined by a corresponding variation in the amount of motion, here both the total impulse and the total amount of gas motion remain the same as before (external forces are absent).

At the end of the relaxation time the excess impulse in the reaction zone is converted into impulse of the impact wave, running ahead, and into the same, but of opposite sign, impulse of the impact wave, running behind.

If Q is the mass heat-generating capacity of a burning substance, expressed in mechanical units, w is

the reaction rate, referred to unit mass of the gas, and $\mathfrak{M}$ is the mass rate of heat-evolution, then $Q = \int_0^\tau \mathfrak{M}\, dt = Q \int_0^\tau w\, dt$, whence $\int_0^\tau w\, dt = 1$.

To describe the state in the impact wave we will consider the moment when the advancing front of the impact wave and the front of the flame coincide as the start of reading the time. Then any state in the impact wave behind the flame front is determined by two parameters: t and t'. The time t' is fixed as the moment when the flame front passes through the given state in the impact wave, while t is the time, beginning from the moment $t = t'$, when the given state changes into a process for propagation of the impact wave. As a result, $\rho = \rho(t, t')$, $p = p(t, t')$, $w = w(t, t')$, etc.

We will designate the excess density in the impact wave with respect to the starting gas by $\Delta\rho(t, t') = \rho(t, t') - \rho_0$. The excess mass of gas that passes through the flame front in time dt' is

$$\lambda \Delta\rho(t, t')\, dt'.$$

The amount of heat, liberated by this mass due to chemical reaction, occurring in time dt, will be

$$\Delta q = \lambda \Delta\rho(t, t')\, \mathfrak{M}(t, t')\, dt\, dt'.$$

The total amount of heat, liberated during the relaxation time in the reaction zone, is determined by the equation

$$q = \lambda \int_0^\tau dt' \int_{t'}^{\tau} \Delta\rho(t, t')\, \mathfrak{M}(t, t')\, dt = \lambda Q \int_0^\tau dt' \int_{t'}^{\tau} \Delta\rho(t, t')\, w(t, t')\, dt. \tag{1}$$

All of the excess heat, liberated during time τ in the reaction zone in the passage of the impact wave, goes to increasing the internal energy of the gas in the reaction zone

$$q = \lambda \int_0^\tau dt' \int_{t'}^{\tau} c_v \frac{\partial \Delta\rho T(t,t')}{\partial t}\, dt =$$
$$= \frac{\lambda}{\gamma - 1} \int_0^\tau dt' \int_{t'}^{\tau} \frac{\partial \Delta p(t, t')}{\partial t}\, dt = \frac{\lambda}{\gamma - 1} \int_0^\tau \Delta p(\tau, t')\, dt', \tag{2}$$

where $\gamma = C_p/C_v$; and ΔT and Δp are the changes in the temperature and pressure in the reaction zone. Substituting expression q from (1) in (2), and taking into consideration that $\int_0^\tau \Delta p\, dt' = I_r$ is an additional impulse of the impact wave, generated by the combustion, we obtain

$$Q(\gamma - 1) \int_0^\tau dt' \int_{t'}^{\tau} \Delta\rho(t, t')\, w(t, t')\, dt = I_r. \tag{3}$$

We will take as a first approximation the linear approximation of the explosion reaction rate with time. In the interval $t' \leq t \leq t' + \tau$, $w = \beta(t - t')$. At $t \leq t'$, i.e., up to the moment where the flame front passes through the state of the impact wave with density $\rho(t, t')$, the reaction rate w is equal to zero, then it constantly increases during time τ, and at $t = t' + \tau$ it instantly drops to zero. From the identity $\int_{t'}^{t'+\tau} w\, dt \equiv 1$ we determine $\beta = 2/\tau^2$. Consequently, $w = \frac{2}{\tau^2}(t - t')$.

If τ_b is the time that the combustion zone remains in the impact wave, then depending on whether $\tau \geq \tau_b$ or $\tau \leq \tau_b$, the rules for the liberation of heat in the impact wave will essentially differ. In the first case reaction does not succeed in reaching completion during the time that the wave passes through the flame front and the wave receives only part of the chemical energy, going to increase the impulse of the wave. In the second case the reaction is completely ended in time τ.

In accordance with these two cases, the total integral (3) breaks down into two integrals:

$$I_r = Q(\gamma - 1)\int_0^{\tau_b} dt' \int_{t'}^{\tau_b} \Delta\rho(t, t')\, w(t, t')\, dt; \quad \tau \geqslant \tau_b, \tag{4}$$

$$I_r = Q(\gamma - 1)\int_0^{\tau} dt' \int_{t'}^{\tau} \Delta\rho(t, t')\, w(t, t')\, dt; \quad \tau \leqslant \tau_b. \tag{5}$$

Substituting $w = \frac{2}{\tau^2}(t - t')$ and $\rho = \bar{\rho} + (\rho_0 - \bar{\rho})\frac{t'}{\tau_b}$ in (4) and (5) and integrating, we obtain

$$I_r = \frac{Q(\gamma - 1)(\bar{\rho} - \rho_0)\tau_b^3}{4\tau^2}; \quad \tau \geqslant \tau_b \qquad I_r = \frac{Q(\gamma - 1)(\bar{\rho} - \rho_0)}{3}\frac{\tau}{\tau_b}\left(\tau_b - \frac{1}{4}\tau\right). \quad \tau \leqslant \tau_b \tag{6}$$

After determining the impulse of the impact wave $I = \int_0^b \rho v\, dx$, where v is the natural rate of motion of the gas in the impact wave. We will substitute v and ρ in I. Then $I = {}^1/_2 D^2 \tau_b(\bar{\rho} - \rho_0)$. Expressing $\bar{\rho} - \rho_0$ from this by I, D and τ_b, and substituting in (6), we obtain

$$I_r = \frac{(\gamma - 1)Q}{2D^2}\frac{\tau_b^2}{\tau^2} I; \quad \tau \geqslant \tau_b \qquad I_r = \frac{2(\gamma - 1)Q}{3D^2}\frac{\tau^2}{\tau_b^2}\left(\frac{\tau_b}{\tau} - \frac{1}{4}\right) I. \quad \tau \leqslant \tau_b \tag{7}$$

The total impulse of wave I* after the impact wave has passed through the combustion zone is composed of the natural impulse I and the additional (relaxation) I_r

$$I^* = \left(1 + \frac{(\gamma - 1)Q}{2D^2}\frac{\tau_b^2}{\tau^2}\right) I, \quad \tau \geqslant \tau_b \qquad I^* = \left[1 + \frac{2(\gamma - 1)Q}{3D^2}\frac{\tau^2}{\tau_b^2}\left(\frac{\tau_b}{\tau} - \frac{1}{4}\right)\right] I. \quad \tau \leqslant \tau_b \tag{8}$$

In (8) I is the impulse of the impact wave after it has passed through the combustion zone. If ξ is the index of refraction, then $I = \xi I_0$, where I_0 is the impulse of the original wave. The impulse I' of the reflected wave is obviously equal to $(1 - \xi)I_0$. Consequently, for impact waves, passing through a combustion zone, we have: $I^* = k_i \xi I_0$, and for the reflected waves we have $I^{*\prime} = k_i(1 - \xi)I_0$, where k_i is the relaxation intensification coefficient of the impact wave impulse

$$k_i = 1 + \frac{(\gamma - 1)Q}{2D^2}\frac{\tau_b^2}{\tau^2}; \quad \tau \geqslant \tau_b \qquad k_i = 1 + \frac{2(\gamma - 1)Q}{3D^2}\frac{\tau}{\tau_b}\left(1 - \frac{1}{4}\frac{\tau}{\tau_b}\right). \quad \tau \leqslant \tau_b \tag{9}$$

The coefficient $k = \frac{\Delta p^*}{\Delta \bar{p}}$ of the relaxation intensification of the amplitude of the impact wave is determined in like manner by the equations

$$k = \frac{l^*}{l} = k_i; \quad k = 1 + \frac{l_r}{l}\frac{\tau_b}{\tau} = 1 + \frac{2(\gamma-1)Q}{3D^2}\left(1 - \frac{1}{4}\frac{\tau}{\tau_b}\right). \tag{10}$$
$$\tau \geqslant \tau_b \qquad \tau \leqslant \tau_b$$

For values $\overline{\Delta p}/p_0 \ll 1$ the intensification coeffficient is independent of the number of passages of the impact wave through the combustion zone:

$$k = 1 + \frac{(\gamma-1)Q}{2c_0^2}\frac{\tau_b^2}{\tau^2}; \quad k = 1 + \frac{2(\gamma-1)Q}{3c_0^2}\left(1 - \frac{1}{4}\frac{\tau}{\tau_b}\right), \tag{11}$$
$$\tau \geqslant \tau_b \qquad \tau \leqslant \tau_b$$

where c_0 is the speed of sound in the original medium. At $\tau/\tau_b \ll 1$ $k = k_{max} = 1 + \frac{2(\gamma-1)Q}{3c_0^2}$ and maximum intensification exists; if $\tau/\tau_b \gg 1$, then $k = k_{min} = 1$, and intensification is absent. The intensification coefficient of the impact wave impulse, as follows from (9), has a maximum at $\tau = \tau_b$, and is close to unity for both $\tau/\tau_b \gg 1$ and $\tau/\tau_b \ll 1$.

The phenomenon of a maximum intensification of the impact wave impulse when the condition $\tau = \tau_b$ (relaxation "embrace" of the combustion zone impact wave) is satisfied can be given the name of impulse resonance.

The refractive indices are determined from the conditions of the transition of the impact wave from a medium with temperature T_0, density ρ_0 and pressure p_0 into a medium with temperature T, density ρ and with the same pressure p_0, or the reverse. Here the surface separating the media is the contact explosion. If the temperature T of the medium is maintained by spreading of the flame, then T is determined from the condition $Q = C_p(T - T_0)$. In the absence of spreading of the flame the contact explosion dissipates due to heat conduction.

For weak impact waves, spreading from medium (T_0, p_0, ρ_0), the index of fraction is $\xi_- = \frac{2}{1+\sqrt{T/T_0}}$; for waves, spreading in the opposite direction, $\xi_+ = \frac{2\sqrt{T/T_0}}{1+\sqrt{T/T_0}}$.

For real exposive mixtures, in particular for benzene and air, the value $\xi_+\xi_- < 1$ is close to one. Consequently, if we designate by $k_\pm$ the intensification coefficient of an impact wave, running from the wall of a closed chamber to the other in one cycle, then $k_\pm = k^2\xi_+\xi_-$. Under resonance conditions the value $\xi_+\xi_-$ can be neglected and $k_\pm = k^2$. In the absence of resonance embrace and when $\tau \to 0$, and consequently the limiting zone of combustion becomes infinitely thin, $k_\pm = k_{max}^2$. In this case, as was to be expected, the amplitude of the impact wave shows maximum increase, while the impulse of the wave does not change.

It is of interest to discuss the relation between $\underline{k}$ and the coefficient α of an excess of air in the burning mixture. In this case the heat generating capacity of the mixture is $Q_{mix} = \frac{\alpha Q}{1+\alpha Z}$ if $\alpha \leq 1$ and $Q_{mix} = \frac{Q}{1+\alpha Z}$ if $\alpha \geq 1$, where Z is the amount of air required to completely burn 1 kg of fuel.

For a mixture of benzene and air, k_{max} varies within the limits of 2.5 to 2.8, and the corresponding variation in α ranges from 1.2 to 0.65. As is revealed by experiment (Fig. 1), for this mixture the maximum value $k^2 = 1.6$ is shifted toward richer mixtures ($\alpha = 0.8$), which corresponds to a faster reaction rate, i.e., to a smaller τ. Based on the calculations for a mixture of benzene and air at $\alpha = 0.8$, such a maximum $k^2 = 1.6$ is obtained at $\tau/\tau_b = 1$. Moving from point $\alpha = 0.8$ in the direction of either poorer or richer mixture, we obtain smaller values of $\underline{k}$.

Institute of Chemical Physics
Academy of Sciences of the USSR

Received February 25, 1958

VAPOR PRESSURE OF SATURATED SELENIUM VAPORS BELOW THE MELTING POINT

A. A. Kuliev and M. G. Shakhtakhtinskii

(Presented by Academician V. N. Kondrat'ev, March 1, 1958)

The use of radioactive isotopes makes it possible to study the vapor pressure of a substance below its melting point, which permits determining the importance of thermodynamic functions in this temperature range. In this communication we present the experimental results obtained when we studied the saturated vapor pressure of solid selenium in the temperature range 86-200°C. The Knudsen method was employed to make the measurements, using the radioactive isotope of selenium.

As is known [1], the Knudsen method is based on the effusion of a vapor through a small orifice in a vacuum.

The apparatus, used in our experiments to determine the vapor pressure of saturated selenium vapor, consisted (see Fig. 1) of a cylindrical glass flask 1, inside of which was placed furnace 2 for heating crucible 3 with investigated substance.

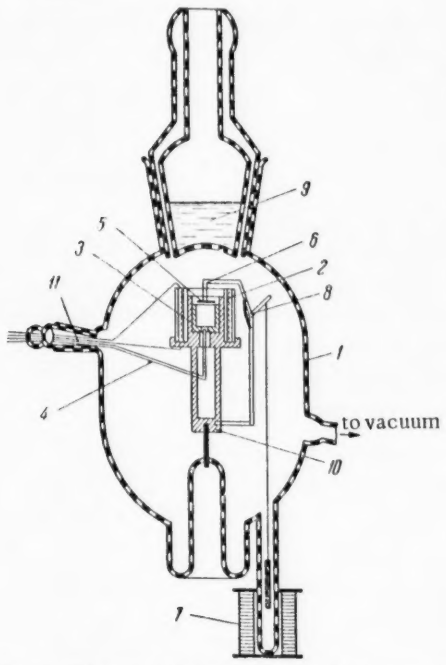

Fig. 1. Diagram of the apparatus for determining the vapor pressure of saturated vapors.

About 0.1 g of the investigated substance was placed in the crucible, after which it was sealed on top with a platinum foil, in the center of which was located a round opening with a diameter of 0.359 mm. The shape and size of the opening was checked using an IZA-2 type of comparator. The crucible was made of graphite. The inside surface of the crucible was polished. A hole was bored in the bottom of the crucible for insertion of thermocouple 4, bored in such manner that the distance between the end of the thermocouple and the investigated substance was at a minimum. For rapid saturation of the vapor the internal dimensions of the crucible were taken h = 5 mm and d = 5 mm.

To avoid evaporation of the substance during heating and cooling the opening of the effusion chamber was covered with lid 5, which was actuated by lever 6 using electromagnet 7. For complete closure with the lid the lever was fitted with spring 8. A condensation dome 9, filled with liquid air, was located over the effusion chamber for collecting the volatilized substance. All of the parts were fastened to a stainless steel base 10.

Sleeve 11 served to lead the thermocouple ends out of the furnace. In order to eliminate the possible influence of crystallization during vaporization on the

experiment results, the radioactive selenium isotope with $T_{1/2}$ = 127 days, prior to experiment, was subjected to crystallization at 135° for an hour, and then at 205-210° for 15 hours (the crystallization was run in a vacuum of the order of 10^{-3} mm Hg). The selenium crystallized completely in this time.

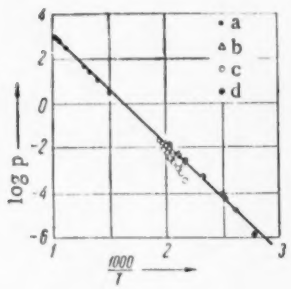

Fig. 2. Relation between log p and the reciprocal of the temperature: a) from [3], b) from [4], c) from [5], d) our data.

The crystallized selenium was crushed to a fine powder and placed in the effusion chamber. The purity of the radioactive selenium was verified by the half-time period, which showed good agreement with the literature data [2]. Then a vacuum of the order of $10^{-5} - 10^{-6}$ mm Hg was created in the apparatus.

When the desired vacuum had been reached the furnace, fed with constant current, was turned on and the crucible heated to the necessary temperature. To completely saturate the vapor before removing the lid the crucible was held at this temperature for an hour.

The temperature was measured with a chromel-alumel thermocouple using a potentiometer. The airtightness of the lid was also checked. For this the crucible was heated to 150°, and then, not removing the lid, after cooling, the activity of the condensation dome was checked. Here the activity did not exceed that of the natural ground.

During the time of making measurements the lid of the crucible was removed for a certain length of time and the selenium vapors, escaping through the effusion orifice, condensed on the dome. After cooling the furnace to room temperature, air was admitted into the furnace, the dome was removed, and the condensed selenium was rinsed off with a carrier which was a solution of inactive selenium in sodium sulfide.

The activity of the rinse solution was read using a B apparatus, and from a comparison with the earlier prepared standard, the amount of selenium was determined.

Knowing the amount g of selenium that vaporized in a certain exposure time t (sec), we calculated the vapor pressure of saturated selenium vapor using the following equation [1]:

$$p = 17{,}14 \frac{g}{kAt} \sqrt{\frac{T}{M}},$$

where A is the area of the orifice in sq cm, k is the Clausing coefficient, T is the absolute temperature, and M is the molecular weight of the vaporized substance in the vapor state.

Following [1], in calculating the vapor pressure of saturated selenium vapor we took the molecular weight of selenium to be six times the atomic weight. The results of our experiments are plotted in Fig. 2, as are also the data of other authors, who studied the vapor pressure of saturated selenium vapors in different temperature ranges [3-5].

It should be mentioned that the linear character of the function log p vs 1/T is proof that the selenium vapors in equilibrium with the solid phase in the temperature range (86-200°) consist of molecules with 6 atoms.

Based on the obtained experimental results the relation between the vapor pressure of selenium vapors and the temperature is expressed by the following equation:

$$\lg p\,(\text{мм}) = 8{,}479 - \frac{5061}{T}.$$

The results of studies [3, 4] and our own data all fall well on a single straight line, which points to the reliability of the indicated data. The data given in [5] are definitely low.

In conclusion the authors wish to thank G. B. Abdullaev, Corresponding Member of the Academy of Sciences of the Azerbaidzhan SSR, for suggesting the problem and for his guidance.

LITERATURE CITED

[1] S. Deshman, Principles of Vacuum Technique (Moscow, 1950).

[2] A. N. Nesmeianov and coworkers, Preparation of Radioactive Isotopes (1954).

[3] G. Preuner and I. Brockmöller, Zs. Phys. Chem. 81, 1 (1912).

[4] J. Jannek, A New Determination of the Atomic Weight of Selenium (Breslau, 1913).

[5] K. Neumann and E. Völker, Zs. Phys. Chem. A, 16 (1932).

Institute of Physics and Mathematics
Academy of Sciences of the Azerbaidzhan SSR

Received February 28, 1958

A CONTRIBUTION TO THE THEORY OF THERMAL CHAIN FLAME PROPAGATION

L. A. Lovachev

(Presented by Academician V. N. Kondrat'ev, March 6, 1958)

A hot flame will be considered to be propagated by a thermal chain if the flame reaction develops according to a chain mechanism in which there is a continuous release of heat and the active centers come from high temperature regions in which their concentration is high. The following simplified scheme represents the chain mechanism for a decomposition reaction involving two active centers of a single type which successively react with the parent substance and regenerate one another [1]:

$$A \longrightarrow 2P \text{ (generation)},$$
$$P + A \longrightarrow 2C + P \text{ (chain)},$$
$$P + P + M \longrightarrow 2C + M \text{ (chain rupture)},$$

Here, A is the parent substance, C is the final product and P is the active center. Writing the product at the density ρ and the coefficient of diffusion of P as $\rho D_p = D$, and supposing the heat capacity, $\underline{c}$, and the thermal conductivity, $\lambda = c\rho D_A$ (D_A being the diffusion coefficient of A) to be independent of the temperature, $T = T' - T'_0$, we obtain for the stationary laminar flame:

$$\lambda pp' - Bcp + Qn = 0, \tag{1}$$
$$Dp^2 n'' - pn'(B - Dp') + R = 0 \tag{2}$$

with the boundary conditions:

$$T = 0, \quad n = n_0, \quad p = 0, \quad pn' = 0; \tag{3}$$
$$T = T_b, \quad n = n_b, \quad p = 0, \quad pn' = 0; \tag{4}$$

$\underline{x}$ being a coordinate; $\underline{u}$, the flow rate; $\underline{n}$ the dimensionless concentration of P; n_A the dimensionless concentration A; $\underline{h}$, the heat of reaction; $K_A(T)$, the rate constant for the reaction; $R(T)$, the rate of generation of P; T'_0, the initial temperature; T'_b, the combustion temperature as determined from the heating value, $h(n_{A_0} - n_{A_b}) = cT_b$; $B = u\rho$; $Q = Q(T) = hK_A(T)n_A(T)$; $Q(0) = Q(T_b) = R(0) = R(T_b) = 0$; $p = \frac{dT}{dx}$ and $p' = \frac{dp}{dT}$ and $n' = \frac{dn}{dT}$.

Dividing the region for the integration of (1) and (2) into a finite number of intervals $\Delta T_i = T_{i+1} - T_i$, and supposing that $n' = \text{const}$ and $n'' = \text{const}$ over each of these, the solution of (2) can be represented in the form:

$$n = n_0 + bT + eT^2, \tag{5}$$

where $\underline{b}$ and $\underline{e}$ are so defined that $n_b = n_0 + bT_b + eT_b^2$, $n' = b + 2eT$ and $n'' = 2e$. Taking this into account, we obtain from (2) and (5):

$$n = n_0 + (l + zT_b)T + zT^2, \tag{6}$$

where

$$l = \frac{n_b - n_0}{T_b} \text{ and } z = \frac{R - lp(B - Dp')}{p(B - Dp')(2T - T_b) - 2Dp^2}. \quad (7)$$

Setting (6) into (1), we obtain for numerical integration:

$$\lambda pp' - Bcp + \Phi_{ch} = 0, \quad (8)$$

where

$$\Phi_{ch} = \Phi_{ch}(T, p, p'; D_P) = Q[(n_0 + lT) - z(T_b - T)T].$$

The relations which are needed for an evaluation of the flame velocity can be obtained from a study of the dependence of B on the maximum value of the temperature gradient, p_m. Taking into account the fact that $p'(T_m) = 0$ and $p(T_m) = p_m$ when $T = T_m$, and setting $(n_0 + lT_m) = t$, $(2T_m - T_b) = s$, $T_m(T_b - T_m) = r$, we have from (8):

$$-Bcp_m + Q_m(l - z_m r) = 0. \quad (9)$$

If it is assumed that $\underline{b}$ and $\underline{e}$ in (5) are fixed for the entire region if integration by their values at $T = T_m$, the approximation relation

$$n = n_0 + (l - z_m T_b)T + z_m T^2. \quad (10)$$

will then be obtained in place of (6). Solving (9) and omitting the root which goes to infinity when $\epsilon = 0$, we find

$$B = \frac{\Phi_{ch}}{cp_m} = \frac{(\alpha p_m^2 + \beta) - \sqrt{(\alpha p_m^2 + \beta)^2 - 4\varepsilon(\gamma p_m^2 + \delta)}}{2\varepsilon p_m}, \quad (11)$$

where

$$\varepsilon = \frac{c}{Q_m} s; \quad \alpha = 2D_m \frac{c}{Q_m}; \quad \beta = st + lr; \quad \gamma = 2D_m t; \quad \delta = R_m r.$$

Differentiating B, (11), with repsect to p_m and equating the numerator of the result to zero, we have the equation

$$a_1 y^3 + a_2 y^2 + a_3 y + a_4 = 0, \quad (12)$$

in which

$$y = p_m^2; \quad a_1 = \alpha^2\gamma; \quad a_2 = -\alpha(2\beta\gamma - 3\alpha\delta);$$
$$a_3 = \beta(\beta\gamma - 2\alpha\delta); \quad a_4 = -\delta(\beta^2 - 4\varepsilon\delta).$$

According to (11), the function B has the form shown in Fig. 1 when the discriminate of Equation (12) is negative. That portion of the function for which differential curves issuing from the point $p = 0$, $T = T_b$ do not satisfy the condition (3), is shown in dotted form. If the diffusion of active centers were not taken into account in the flame propagation, the chain reaction would develop at these temperature only because of generation, just as in the case of spontaneous ignition. In this case, the relation between the concentration of P and the temperature $n_c = n_c(T)$ can be found by simultaneously solving the system of kinetic equations and the equation for heat balance; on setting the result into (1), a single equation is obtained in which the rate of evolution of heat appears as a function of the temperature alone: $\Phi_c = Q(T)n_c(T) = \Phi_c(T)$. Thus, when there is no diffusion of P, B and p_m are related by:

$$B' = \frac{\Phi_{cm}}{cp_m}. \quad (13)$$

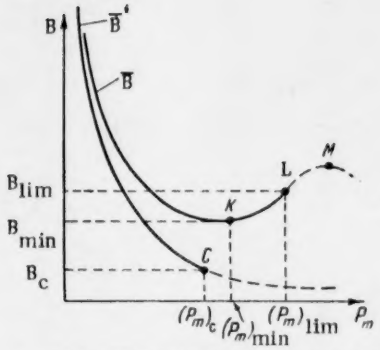

Fig. 1. The relation between the mass velocity, B, and the maximum temperature gradient, $p_m \cdot \bar{B}$) with thermal chain propagation, $\bar{B}'$) neglecting diffusion of the active centers.

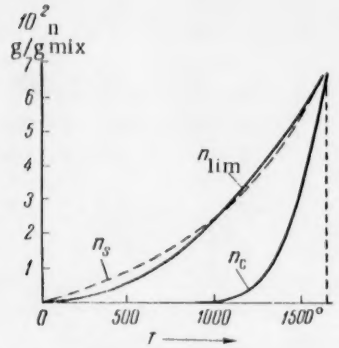

Fig. 2. The relation between the concentration of the active centers P, and the temperature, for the decomposition of hydrazine: n_s in the flame, [1]; n_{lim} in the flame, according to (10); n_c for spontaneous ignition, or in the flame, diffusion of the active centers being neglected [1].

Equation (13) is of the form shown in Fig. 1. For the decomposition of hydrazine, the functions $n_c(T)$ and $\Phi_c(T)$ have been determined in [1] (Figs. 2 and 3). Since there is no basis for selecting a single flame velocity out of the spectrum of values $B' \geq B_c$, the ignition temperature, $T_B > T_0 = 0$, below which no chemical reaction occurs, will be introduced into the theory. In this way there is obtained a certain unique numerical value, B_B, which differs only slightly from B_c when $T_B > 0$ is close to $T_0 = 0$. According to (11), the function B has a fundamentally different form, the function Φ_{ch} depending on the temperature gradient and increasing with an increase in p_m, i.e., with a constriction in the reaction zone, so that there is an increased diffusional flow of P in the region of low and medium temperatures. The limiting value of p_m, $(P_m)_{lim}$, is the maximum permissible p_m under which integral curves will satisfy (4) and still reach the point $p = 0$, $T = 0$. To this value there correspond the maximum possible rate of evolution of heat, $(\Phi_{ch})_{lim} = Q\, n_s \cong Q n_{lim}$, and the limitng parameter value, $B = B_{lim}$. The function n_s and $(\Phi_{ch})_{lim}$ for the hydrazine decomposition flame were determined in [1] by numerical integration of (1) and (2) and are shown in Fig. 2 and 3. In distinction to (13), (11) gives a limiting B_{lim} which corresponds to the state at point , this conditions being stable at stationary propagation if the flame is characterized by a tendency to pass over to states of higher velocity. On the other hand, if the flame has the tendency to propagate with the lowest possible velocity, it will be the state K which will be stable according to (11), and the state C, according to (13). For thermal chain propagation, the B, p_m relation of (11) assures a stable state for every possible tendency. From (11) it follows that the presence of a minimum would indicate, physically, that to each flame velocity between B_{min} and B_{lim} there would correspond two markedly different states. Since spontaneous (natural) processes proceed with maximum increase in the entropy, the part of the curve to the left of K will not be physically realizable from B_{min} to B_{lim} in distinction to the portion to the right of K which corresponds to the maximum departure from the equilibrium process. The principle of determining the flame velocity from the state L, permits an understanding of the limits for the propagation (existence) of the flame, since as the combustion temperature is lowered, the point L moves toward the left, approaches the point K, and finally takes up a position to the left of K.

The exact determination of the limiting values and relations for L calls for the numerical integration of (1) and (2). Relations (11) and (10) prove, however, to give results which are so close to being exact that it is not necessary to have recourse to numerical integration. From the roots of (12), we find the approximate value of the gradient in the point L as the mean:

$$p_L^2 \cong y_{av} = \frac{y_2 + y_3}{2} \cong \frac{\beta}{\alpha}. \qquad (14)$$

By expanding the radical of (11) in a series, and taking (14) into account, we find for the linear flame velocity:

$$u_0 = \frac{1}{\rho_0}\sqrt{\frac{n_b Q_m \rho_m D_{\rho_m}}{2cT_b}}. \qquad (15)$$

In evaluating the quantities which enter into (15), the approximation can be made that $T_m = 0.5\,T_b$ (see Table 1). Using for the spectral limit the approximation relation $B_* = \eta p_*$, where $\eta = \frac{4\lambda_0}{cT_m}$, we find from (9) that:

$$p_*^4(\alpha - \varepsilon\eta)\eta - p_*^2(\gamma - \beta\eta) - \delta = 0. \qquad (16)$$

$T = T_m$ is determined by equating p_* from (16) and p_{lim} from (14).

For testing the resulting approximation relations, numerical calculations were carried out for the hydrazine decomposition flame, all of the necessary values and relations having been obtained in [1] by numerical integration. For an initial mixture at $T_0' = 300°K$, and $T_b' = 1950°K$, all of the starting data could be taken out of [1]. The discriminant of (12) was evaluated and it was established that the relation (11) has in this case the form which is shown in Fig. 1. Calculation gave $T_m = 875°$ and $(p_m)_{lim} = 1.72 \cdot 10^5$ deg/cm. According to [1], the experimentally measured flame velocity for this mixture is $u_0 = 185$ cm/sec.

TABLE 1

Calculated Values of the Flame Velocity, u_0 (cm/sec)

Numerical integration, according to [1]	According to Equa. (11) $T_m = 875°$	According to Equa. (15) $T_m = 875°$	According to Equa. (15) $T_m = \frac{1}{2}T_b = 825°$
160	155	148	147

For the limiting state (point L in Fig. 1), the $\underline{n}$, T relation was established through Equation (10). This function is shown in Fig. 2, where for comparison there has also been plotted this same relation as obtained through numerical integration [1]. It is to be seen that there is a completely satisfactory agreement in all of the results.

By the numerical integration of [1], a flame velocity of $u_0 = 11$ cm/sec was determined for an initial mixture with $T_0' = 300°K$ and $T_b' = 1280°K$. The measured flame velocity was $u_0 = 10$ cm/sec. For this same initial data, calculations according to Equation (15) give $u_0 = 8.6$ cm/sec.

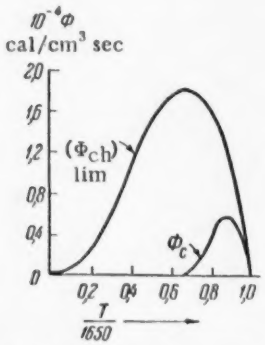

Fig. 3. The relation between the rate of evolution of heat and the temperature, for the decomposition of hydrazine [1]: Φ_c with spontaneous ignition; $(\Phi_{ch})_{lim}$ with the highest possible rate of thermal chain propagation.

It follows from Equation (15) that the flame velocity is inversely proportional to the fourth root of the pressure. If n_b is expressed through an equilibrium constant into which there enters the heat of reaction for the formation of P, Equation (15) then permits the determination of the true energy of activation of the second reaction from the experimentally established relation between the square of the flame velocity and the reciprocal temperature. For thermal chain propagation, the slope of the experimentally determined function depends on both the energy of activation and the heat of reaction.

Chain rupture has been neglected in the present calculations and in [1]. If the rate of rupture were to be taken into account, the n_{lim} curve of Fig. 2 would lie lower. If branching is supposed to occur in the second reaction ($P + A \rightarrow 2C + (i+1)P$) it is then possible, knowing n_{lim}, to find an $\underline{i}$ which would so compensate the chain rupture due to branching that all of the earlier calculated values and relations would remain valid. It has been found that this value is $i = 0.008$. At the same time, this calculation justifies the neglect of chain rupture in solving the initial system of equations.

LITERATURE CITED

[1] D. B. Spalding, Phil. Trans. Roy. Soc. London, 249, 1-25 (1956).

The Institute of Chemical Physics of the
Academy of Sciences of the USSR

Received February 24, 1958

A STUDY OF THE DISSOCIATION OF OXYGEN BEHIND A POWERFUL SHOCK WAVE

S. A. Losev

(Presented by Academician V. N. Kondrat'ev, March 7, 1958)

In the present work an experimental study was made of the rate of thermal dissociation behind a powerful shock wave in oxygen. The source of the shock waves was a shock wave tube whose operational principles have been described in detail in the literature [1, 2]. The state of the gas behind the shock wave was studied by examining the ultraviolet light absorption of the oxygen, heated to a temperature of several thousand degrees by the passage of the shock wave. The light source used was a krypton lamp GSVD-120; the light passed through the gas under study in a given section of the shock wave tube and through a quartz monochromator with two exit slits selecting spectral regions of width $\Delta\lambda = 10$A close to $\lambda_1 = 2272$ A and $\lambda_2 = 2510$ A. The light was subsequently allowed to fall on a FEU-18 photoamplifier. The signals obtained when the shock wave was passed were recorded on the screen of an oscillograph OK-17M (Fig. 1).

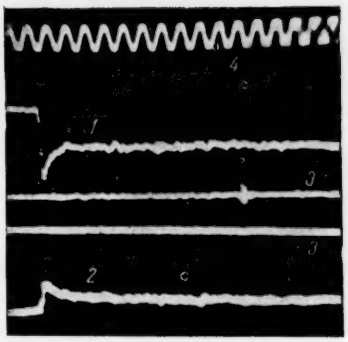

Fig. 1. Oscillogram of the ultraviolet light absorption during the passage of a shock wave through oxygen with a velocity of 3 km/second. 1) In the region $\lambda_1 = 2272$ A; 2) in the region $\lambda_2 = 2510$ A (impulse inverted); 3) corresponding zero lines; 4) calibration sine curve with frequency 500 kilocycles/second.

In order to determine the rate of dissociation, use was made of the ability of molecular oxygen at high temperatures to absorb light in the region 2200-2600 A as a result of movement from the excited vibrational levels of the fundamental electronic state $X^3\Sigma_g^-$ to the state $B^3\Sigma_u^-$ (Schumann–Runge system) [3, 4]. Analysis showed that the oxygen band spectrum is accompanied by a continuous background as a result of broadening of the Schumann–Runge continuum and movements from the $^3\Sigma_g^-$ state to the $^3\Pi_u$ [5]; the lines entering the bands are extensively reabsorbed.

Measurements made (by N. N. Sobolev and coworkers, and also by ourselves) on the temperature of the gas at a given distance from the leading front of the shock wave, from the emission and absorption features of the D-lines from the sodium present as an impurity in the gas, have shown that the temperature of the gas at these points in the stream approximates (at $T < 4000°$ K) to the calculated value obtained from Glugonio's adiabatic curve, assuming equilibrium dissociation and the absence of losses from heat exchange and friction. This has enabled us to establish the relationship between the magnitude of the light absorption in the oxygen and the temperature and concentration of the molecules (for the selected spectral regions).

It was found that under the conditions of our experiments the absorption was dependent to a relatively small extent on the concentration but was dependent to a greater extent on the temperature. It was thus possible to find the temperature distribution immediately behind the shock wave front from the light absorption.

Measurement of the temperature by the method described showed that for a shock wave with velocity 2.7-3 km/second and a pressure before the shock wave of P_0 = 7.6 mm mercury, the temperature of the gas immediately behind the shock wave front has a maximum value and then falls, approaching the value calculated from Giugonio's adiabatic curve assuming equilibrium dissociation (Fig. 2). The extent of this zone decreases as the velocity of the shock wave and the pressure are increased. At high pressures, when there is no detectable dissociation, the temperature maximum behind the wave front is not observed.

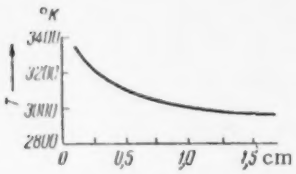

Fig. 2. Temperature distribution behind the front of a shock wave traveling through oxygen with a velocity of 2.8 km/second.

The dimensions of the dissociation zone behind a shock wave in oxygen obtained in a recently published work [6] by measurement of the density gradient using a Tepler apparatus were analogous to our results within the limits of experimental error.

If it is assumed that the zone described, in the conditions given, corresponds to a process which is not in chemical equilibrium, and if it is considered that the thermal dissociation of the oxygen proceeds according to the scheme

$$O_2 + M \rightleftharpoons O + O + M, \qquad (I)$$
$$O_2 + O_2 \rightleftharpoons O_3 + O, \qquad (II)$$
$$O_3 + M \rightleftharpoons O_2 + O + M, \qquad (III)$$

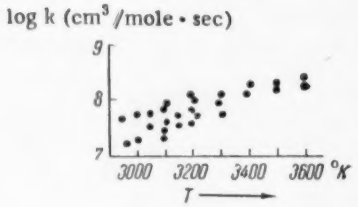

Fig. 3

then it is possible to use the values obtained for the dimensions of the nonequilibrium zone to calculate the value of the reaction rate constant for the oxygen dissociation, since a decrease in the temperature characterizes an increase in the concentration of atomic oxygen, while the concentration change characterizes the rate of the dissociation reaction. It is possible to obtain a quantitative relationship between the temperature gradient behind the shock wave and the rate of dissociation, by making use of the law of conservation of energy for the established one-dimensional current.

At a temperature T = 3000-4000°K, the decomposition of ozone (reaction III) takes place so rapidly that reactions (II) and (III) may be rewritten in the form

$$O_2 + O_2 \rightarrow O + (O + O_2). \qquad (II')$$

The rate constant obtained experimentally for the dissociation of oxygen behind the shock wave (Fig. 3) is a combination of the constant for the direct decomposition of O_2 [reaction (1)] and the rate constant for the breakdown of O_2 with the intermediate formation of ozone [reaction (II)].

The activation energy for reaction (II) is equal to 99.2 kcal/mole [7, 8], which is somewhat lower than the energy of the direct dissociation of oxygen (118 kcal/mole). It would therefore be natural to assume that the oxygen dissociation proceeds according to reaction (II'). If however we use the value for the rate constant of reaction (II) obtained in [8] for the temperature T = 330-385°K, $k_{II} = 6.7 \cdot 10^{12} \exp(-99200/RT)$ cm³/mole · second and assume that it is applicable at high temperatures, then it follows from our experimental results that the dissociation proceeds for the most part by the direct decomposition of O_2. The magnitude of the preexponential factor P in the rate constant for reaction (I), written in the form of the Arrhenius equation $k_1(T) = PZ \exp(-D/RT)$ (where Z – number of molecular collisions per second, D – dissociation energy = 118 kcal/mole), in this case is very much greater than unity and is equal (mean values) to P = 500 at T = 3000° and P = 150 at T = 3600°K. In [7] the value given for the rate constant for reaction (II) is $k_{II} = 3 \cdot 10^{12} \sqrt{T} \exp(-99210/RT)$ cm³/mole · second.

If this value is taken for the evaluation of the rate of reaction (II), the value obtained for the factor P is decreased, but not by more than 10%.

Similar values for P, exceeding unity by several orders of magnitude, have been obtained in the case of the dissociation of certain other diatomic molecules, including bromine [9].

If the rate constant for the reaction $O_2 + O_2 \rightarrow O_3 + O$ at T = 3000-4000°K is in fact greater than the value for k_{II} given above, then it may turn out that this reaction plays an important part in the process of oxygen dissociation. Further experiments are required to clarify this question.

LITERATURE CITED

[1] E. Resler, Sh-C. Lin and A. Kantrowitz, J. Appl. Phys. 23, No. 12, 1390 (1952).

[2] I. I. Glass and G. N. Patterson, J. Aeronaut. Sci. 22, No. 2, 73 (1955).

[3] W. R. Garton and M. W. Feast, Nautre 165, No. 4190, 281 (1950).

[4] A. Hercog and K. Wieland, Helv. Phys. Acta 23, No. 4, 432 (1950).

[5] P. G. Wilkinson and R. S. Mulliken, Astrophys. J. 125, No. 2, 594 (1957).

[6] H. S. Glick and W. H. Wurster, J. Chem. Phys. 27, No. 5, 1224 (1957).

[7] J. O. Hirschfelder, C. F. Curtiss and E. S. Campbell, J. Phys. Chem. 57, No. 4, 403 (1953).

[8] S. W. Benson and A. E. Axworthy, Jr., J. Chem. Phys. 26, No. 6, 1718 (1957).

[9] H. B. Palmer and D. F. Hornig, J. Chem. Phys. 26, No. 1, 98 (1957).

M. V. Lomonosov State University, Moscow

Received March 5, 1958

IRREVERSIBLE CATALYTIC HYDROGEN WAVES IN POLAROGRAPHY

S. G. Mairanovskii

(Presented by Academician A. N. Frumkin, February 27, 1958)

It has been shown earlier [1, 9] that the catalytic liberation of hydrogen at a mercury cathode is not associated with a reduction in the activation energy of hydrogen ion discharge and that it is determined only by the chemical and electrochemical properties of the catalyst material. It has also been shown that the electrochemical stage of the catalytic process in a number of cases may be reversible, and equations have been given for the reversible catalytic hydrogen waves in buffered and nonbuffered solutions. The present work is devoted to a study of irreversible catalytic hydrogen waves.

The catalytic waves chosen for study were those produced by quinine, which has a number of advantages over other catalysts. Quinine has two active groups, differing in their catalytic properties, and therefore gives two catalytic waves which are observed at different potentials: the first wave is shown in acid medium, the second in neutral and weakly alkaline solutions. Both quinine waves, unlike the waves produced by many other catalysts, may be obtained, under appropriate conditions, long before discharge of the support, which facilitates considerably the study of their shape. At the same time, the influence of the concentrations of proton donor and catalyst on the height of the catalytic wave has been studied in considerable detail for the case of quinine [2].

The work was carried out using a visual polarograph at $25 \pm 1^{\circ}$. The dropping electrode with blade for the necessary removal of the drops [3] had the following characteristics: m = 3.82 mg/second, t = 0.26 second. The method of working was the same as that described in previous studies [1, 9].

Analysis of the shape of the waves observed in buffered solutions showed that their lower region, like the ordinary irreversible polarographic waves in the region where concentration polarization is still absent, is described by the equation

$$E = \text{const} - \frac{RT}{\alpha n F} \ln i \qquad (1)$$

(see Curves 2-5 in Fig. 1), where E – potential, i – current strength, n – number of electrons taking part in the electrochemical stage (for catalytic hydrogen currents n = 1), α – transfer coefficient, found equal to 0.6 for both quinine waves, irrespective of the pH of the medium.

The upper part of the waves, however, does not have the limiting current plateau, in place of which the polarograms show a characteristic rounded maximum which is a feature of the irreversible catalytic hydrogen waves. It may be suggested that as the cathode potential is increased, a change takes place in the mechanism of the electrode process, leading to a reduction in the current [4] and distortion of the upper part of the wave. On this assumption, the methods already described [8] were used to find the values for the limiting currents (i_{lim}) of the catalytic waves which would have been observed had there been no reduction in the current. The values of i_{lim} found in this way proved to be proportional to the quinine concentration (when this concentration is not too high). The values of i_{lim} were used to construct the graphs of $E(\lg i/(i_{lim} - i))$ which showed that the irreversible catalytic hydrogen waves, up to potentials corresponding to the start of the reduction in the current, are described by the equation

$$E = E_{\frac{1}{2}} - \frac{RT}{\alpha F} \ln \frac{i}{i_{\text{lim}} - i}. \quad (2)$$

Experiment shows that all the logarithmic graphs obtained with this catalyst at a definite pH lie on the same straight line (see Fig. 1), i.e., for a given wave at the same pH value of the solution, the value of $E_{1/2}$ is independent of catalyst concentration, within the limits of experimental error (2-3 mv).

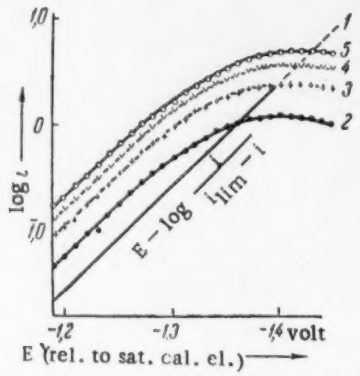

Fig. 1. First catalytic wave for quinine in buffered solution at pH 3.0 ; 2-5) log i (E) curves for quinine concentrations 2.8, 5.5, 7.8, and $10 \cdot 10^{-6}$ respectively; 1) the relationship $\log \frac{i}{i_{\text{lim}} - i}$ (E) for the same solutions.

In order to determine the shape of the curve describing the reduction in current which causes the distortion of the upper part of the irreversible catalytic waves, the observed currents i_{obs} were compared with the values of i_{theor}, which would have been obtained had no reduction in current taken place, i.e., with the values found according to (2). It was found that the curves expressing the magnitudes of the reduction in current Δi (see Fig. 2) are independent of catalyst concentration and may be described by the empirical equation

$$\gamma \lg \Delta i = \gamma \lg (i_{\text{theor}} - i_{\text{obs}}) = E'_0 - E, \quad (3)$$

where E'_0 – a constant, characteristic for a given pH and equal to the potential at which Δi reaches unity; γ – proportionality factor. Figure 2 shows the log Δi(E) curves: 1) for the first wave for 4 quinine concentrations (the same as those for the curves in Fig. 1) in a citrate–phosphate buffer at pH 3.0, and 2) for the second catalytic wave in lithium borate buffer at pH 8.3 for two quinine concentrations. The values of E'_0 for these curves are approximately −1.42 and −2.00 volts respectively, while the value of γ in both cases lies within the limits 60-80 mv. It must be noted that at the potentials where significant decomposition of the support begins, the reduction in current decreases and is no longer described by equation (3). This explains the deviation from the straight line in the curves in Fig. 2.

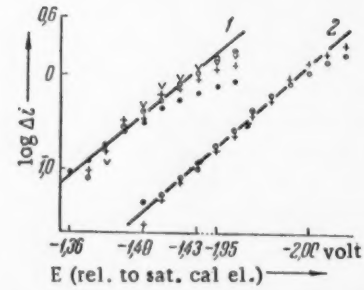

Fig. 2. The relationship between the logarithm of the reduction in current and the potential. 1) For the first catalytic wave at pH 3.0 (for four quinine concentrations); 2) for the second wave at pH 8.3 (for two quinine concentrations).

Figure 3 gives the curves for the catalytic wave observed in a lithium borate buffer at two quinine concentrations (Curves 1 and 2). The upper part of these curves, shown by the dot-and-dash line, was constructed using equation (3). Curve 3 in the upper part of the Figure represents the reduction in current Δi (E); Curve 4 represents the discharge of the support, taking into account the reduction in the charging current caused by adsorption of quinine (linear extrapolation from less negative potentials). The current values in Fig. 3 have been corrected for residual current. A comparison of Curves 1, 2 and 3 shows that the shape of the irreversible catalytic wave (up to potential values preceding noticeable support discharge currents) results from the fact that two processes, represented by Equations (2) and (3), are taking place. The nature of the phenomena leading to the reduction in current is not yet clear; it is being further studied.

The catalytic waves produced by quinine exceed by several orders of magnitude the reversible catalytic waves observed in the presence of pyridine under identical conditions. Since the surface activity of quinine at the mercury–solution boundary is considerably greater than that of pyridine, this phenomenom may explain the greater increase (compared with pyridine) in the concentration of quinine in the layer next to the electrode, relative to its value in the bulk of the solution. In fact, when tetraethylammonium benzenesulfonate (TEABS), which has an extremely high surface activity, is introduced into the solution, the irreversible catalytic waves are considerably reduced. Thus when the solution is made up to 0.1 M in TEABS, the second catalytic quinine wave in lithium borate buffer (pH 8.5) is reduced by a factor of over 30, while the reversible wave produced by pyridine is reduced under such conditions by only 20% [9].

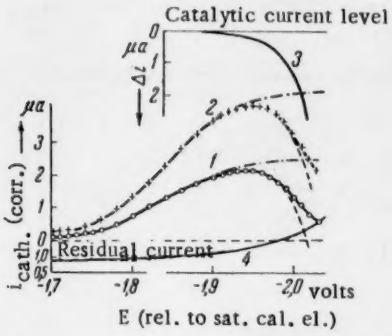

Fig. 3. Catalytic hydrogen waves (1 and 2) at pH 8.3 and quinine concentrations 4.7 and 8.6 · $\cdot 10^{-7}$ M; 3) curve showing fall in current; 4) residual current curve.

Even more important is the fact that the addition of TEABS, in the case of the second quinine wave, shifts the wave toward positive potentials, increases its slope, and eliminates the reduction in current in the upper part of the wave. The graph of $E(\log i/(i_{lim}-i))$ for the catalytic wave in a buffered solution containing 0.1 M TEABS is a straight line with an inverse slope amounting to approximately 60 mv (Fig. 4), i.e., it is very similar to the curve for the reversible pyridine wave observed in the same solution.

It should be noted that at low quinine concentrations in TEABS solution (Fig. 4, 2) the lower part of the waves, as in the case of the waves produced by pyridine, are described by an equation which takes into account the influence of dimerization [1, 9].

$$E = \varepsilon_0 - \frac{RT}{F} \ln \frac{i^{2/3}}{i_{lim} - i} \cdot \qquad (4)$$

These facts show that the addition of TEABS to the solution gives reversible character to the second catalytic quinine wave. Attempts to obtain the first quinine wave in the presence of TEABS were unsuccessful: the catalytic wave is masked by the support current.

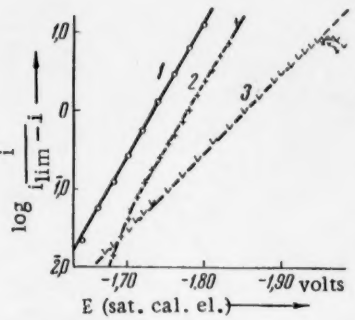

Fig. 4. The graph $\log \frac{i}{i_{lim}-i}$ (E) for the catalytic hydrogen waves in a solution of pH 8.5. 1,2) In the presence of TEABS (0.1 M); 3) without TEABS. Quinine concentrations: 1) 5.6; 2) $1.35 \cdot 10^{-5}$ M; 3) ~4 and ~$8 \cdot 10^{-7}$ M.

The irreversible nature of the catalytic hydrogen wave, at any rate in the case of the wave produced by quinine, is evidently related to adsorption of the oxidized form of the catalyst BH^+ on the electrode surface, leading to retardation of the direct electrode process. R. Brdicka [5] believes that the more extensive adsorption of the oxidized form of the reversibly reducible substance leads to the appearance of a small adsorption step immediately behind the ordinary reversible reduction wave. At a very low concentration of the substance, when the electrode surface is not yet covered with the adsorbed depolarizer, only one ("following") adsorption wave is observed. As the depolarizer concentration is increased, the adsorption wave reaches a limit, corresponding to saturation of the electrode surface by the adsorbed substance, and there appears, before the adsorption wave, the ordinary reversible reduction wave corresponding to the reversible reduction of the nonadsorbed depolarizer [5].

The irreversible catalytic hydrogen wave may be regarded as Brdicka's "following" adsorption wave, the height of which is greatly increased by the catalytic effect. Since the catalyst concentration is usually very

much lower than that required to cover the electrode surface, only one irreversible "adsorption" catalytic wave is observed, corresponding to the catalytic action of the adsorbed quinine (or, more accurately, of its reduction product, since the wave for the reduction of the quinoline nucleus in the quinine precedes the catalytic waves [6]). When TEABS is added to the solution, the catalyst is displaced from the electrode surface, and the desorbed BH^+ particles give a reversible catalytic wave similar to the wave produced by pyridine. Figure 4 gives for comparison the curves for the reversible catalytic waves – in the presence of TEABS (1 and 2) – and the irreversible catalytic waves (3) produced by quinine.

The half-wave potential for the reversible quinine wave in a buffered solution containing TEABS is shifted to quite a considerable extent toward positive values as the quinine concentration increases. This is partly explained by an increase in the rate of dimerization of the reduced form [7].

The author wishes to take this opportunity of expressing his gratitude to Academician A. N. Frumkin for his valuable comments during frequent discussions on this question.

LITERATURE CITED

[1] S. G. Mairanovskii, Proc. Acad. Sci. USSR 114, 1272 (1957).*/**

[2] S. G. Mairanovskii, Bull. Acad. Sci. USSR, Div. Chem. Sci. 805 (1953).**

[3] E. M. Skobets, N. S. Kavetskii, Zavodskaia Lab. 15, 1299 (1949).

[4] S. G. Mairanovskii, Bull. Acad. Sci. USSR, Div. Chem. Sci. 622 (1953).**

[5] R. Brdicka, Coll. trav. chim. Tchecosl. 12, 522 (1947).

[6] I. Bartek, M. Cernoch and F. Santavy, Coll. trav. chim Tchecosl. 19, 605 (1954).

[7] S. G. Mairanovskii, Proc. Acad. Sci. USSR 110, 593 (1956).**

[8] S. G. Mairanovskii, J. Phys. Chem. 32, No. 8 (1958).**

[9] S. G. Mairanovskii, J. Phys. Chem. 32, Nos. 11-12 (1958).**

N. D. Zelinskii Institute of
Organic Chemistry,
USSR Academy of Sciences

Received February 27, 1958

*The following corrections should be made in my paper "Catalytic Hydrogen Currents in Polarography," published in Proc. Acad. Sci. 114, No. 6, 1957:

On page 1272, a minus sign should be placed before i on the left-hand side of equation (2):

$$-i = \varkappa([B]_0 - [B]_s) - sF\mu_1(k_1[DH^+]_s[B]_s - k_2[BH^+]_s[D]_s). \qquad (2)$$

On page 1273, 15 lines from the foot of the page, the phase "..... becomes more negative by 19 mv...." should read "..... becomes more positive by 19 mv....."

**Original Russian pagination. See C. B. Translation.

THE ELECTRICAL CONDUCTIVITY OF n-SEMICONDUCTORS WITH CHEMISORBED ATOMS AND RADICALS

I. A. Miasnikov

(Presented by Academician V. A. Kargin, February 22, 1958)

The chemisorption of atoms and radicals, as our work has shown, brings about a much greater change in conductivity than the chemisorption of molecules. The change in conductivity when molecules are chemisorbed is evidently determined in many cases by the degree of dissociation of the chemisorbed molecules into atoms or radicals [1].

In the present work a study has been made of the influence of the chemisorption of atoms and radicals on the electrical conductivity of electronic semiconductors of the ZnO, TiO_2 type, so that, by avoiding the stage involving the dissociation of chemisorbed molecules according to the scheme:

$$M_2 \rightleftarrows (M_2)_s \rightleftarrows 2(M)_s \rightleftarrows 2(M)'_s + 2n_0, \qquad (1)$$

where M_2 and M are the molecules and atoms, the index s indicates the chemisorbed condition, (M)' indicates ions and n_0 represents the free current carriers, we might make an attempt to examine the behavior of the atoms and radicals on the surface of the adsorbent from the change in its electrical conductivity, assuming that the change in conductivity in this case is determined only by the chemisorption of the atoms and radicals themselves and by transfer of current carriers between the adsorbent and the chemisorbed particles.

The experiments were carried out with atomic hydrogen and nitrogen, and with methyl radicals. The atomic hydrogen and nitrogen were prepared in a stream of molecular hydrogen and nitrogen (pressure 0.7 mm mercury) by means of a silent discharge in a low-power discharge tube (length 40 cm, diameter 2 cm) and also under static conditions by exposing nitrogen and hydrogen to a powerful cobalt γ-source* at a gas pressure of 1 atmosphere.

The methyl radicals were generated in a quartz cell by photolysis of acetone vapor. The specimens of ZnO and TiO_2 semiconducting adsorbents were prepared in the form of fine (3-5μ) films by deposition (spraying) of aqueous suspensions of the appropriate oxides on quartz lining tubes (length 20-25 mm, diameter 5 mm).

The adsorption cells with the films inside were placed in a thermostat. The temperature was checked using thermocouples with their junctions placed on the films. The electrical conductivity of the films was fixed at constant current using a compensation bridge and loop oscillograph.

In the treatment of the experimental data, the change in electrical conductivity caused by chemisorption of the atoms or radicals was related to the change in the surface conductivity of the films, which had a mosaic structure. A basis for this was provided by specially designed experiments on the conductivity of ZnO using alternating current of varying frequency in the presence of oxygen [2].

Before the experiments using atomic hydrogen and nitrogen the film specimens were heated and kept for some time under the experimental conditions (temperature and pressure).

*A. Kh. Breger, V. A. Belynskii, V. L. Karpov, S. D. Prokudin – unpublished.

In the presence of hydrogen or nitrogen, the act of switching on the discharge or the introduction of the γ -source into the chamber led to an increase in the conductivity • (Fig. 1A). In preliminary experiments with the films using γ -radiation in vacuum, no significant change in the conductivity was detected. When the discharge was switched off or the source removed at room temperature or below, the conductivity in the gases remained unchanged, and returned to its previous value only when the film had been heated and subsequently cooled to room temperature. At temperatures above 200°, after removal of the atom sources, the conductivity decreased at an appreciable rate to its previous value without preliminary heating. The higher the temperature, the more rapid the return to the previous state.

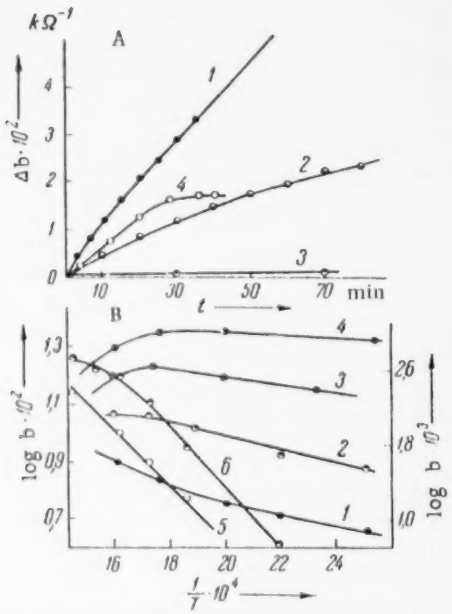

Fig. 1. The change in conductivity of ZnO in H_2 and N_2 under γ -radiation and under a discharge. γ -radiation (A). For H_2: 1) 17°, 2) 200°; 3) 350°; for N_2: 4) 17°. Under discharge (B). For H_2: 1) without discharge, 2) discharge intensity I = 1; 3) I = 2; 4) I = 3 (in arbitrary units); for N_2: 5) without discharge, 6) discharge I = 1.

The kinetics of the increase in conductivity (at some distance from equilibrium) with chemisorption of the atoms and of its reduction in the absence of atoms in the bulk are given accurately by equations of the form:

$$= k_1 [H]_s t, \qquad \frac{1}{\Delta\sigma} = k_2 t + \text{const}, \tag{2}$$

where $\Delta\sigma = \sigma - \sigma_0$, σ_0 – conductivity in the molecular gas, k_1 and k_2 – kinetic constants, $[H]_s$ – stationary concentration of chemisorbed atoms.

These equations are related to reactions involving ionization of the chemisorbed atoms – a first order process – and reactions involving recombination. The activation energies of the conductivity increase with chemisorption of H atoms and of its decrease in the absence of H atoms in the bulk amount of 2 and 36 kcal. respectively. Figure 1B shows the relationship between the change in condutivity produced by the chemisorption of atoms and the temperature at various discharge intensities in the tube.

The intensity of the discharge was checked from the saturation current using two sonde-plates placed inside the discharge tube at right angles to the direction of the field producing the discharge. The decrease in the slope of the straight portions of the curves as the stationary concentration of H atoms is increased is evidently related to the well-known relationship [3] giving the decrease in activation energy of conductivity in semiconductors with increase in the concentration of impurities. In this case however, the effect in question is related to surface impurities – the chemisorbed atoms [4] – and to surface conductivity.

At temperatures over 300°, the increase in conductivity for the same value of the stationary concentration of H atoms in the bulk becomes less. This relationship between the change in conductivity and the temperature is in all probability related to the following competing reactions in the bulk and on the surface:

$$\begin{aligned}
&\text{(a)}\quad M_2 \rightsquigarrow 2M;\\
&\text{(b)}\quad M + M \xrightarrow{\text{a third body}} M_2;\\
&\text{(c)}\quad M \rightarrow (M)_s;\\
&\text{(d)}\quad M + (M)_s \rightarrow M_2;\\
&\text{(e)}\quad (M)_s + (M)_s \rightarrow (M_2)_s \rightarrow M_2;\\
&\text{(f)}\quad (M)_s \rightleftarrows (M)'_s + e;
\end{aligned} \tag{3}$$

• No noticeable change in film temperature due to recombination of the atoms on its surface or absorption of γ -rays took place.

As the temperature is increased, the concentration of H atoms in the bulk remains practically unchanged (the activation energies of reactions (a) and (b) are close to zero), whereas the stationary concentration of the chemisorbed atoms $(M)_s$ is considerably decreased, since reactions (e) and (d) have appreciable activation energies, resulting from migration of the atoms and rupture of the bonds with the surface. At the same time increase in the temperature shifts the equilibrium (f) to give an increase in the concentration of electrons in the conductivity zone. In addition to the experiments described, considerable interest was attached to a study of the change in conductivity of sorbents under the influence of H atoms formed on the surface as the result of heterogeneous chemical reactions, for example, the dehydrogenation of alcohol. For this purpose isopropyl alcohol vapor was passed into a small volume containing a ZnO film (pressure within the volume $5 \cdot 10^{-2}$ mm mercury). The change in conductivity was recorded using a loop oscillograph (see Fig. 2). It was first of all verified that the products of decomposition of the alcohol (acetone and hydrogen), in the concentrations reached after complete decomposition of the alcohol, produced an extremely small change in the conductivity (compared with H atoms) (in the case of H_2 – see Fig. 2). When the pressure of the alcohol is increased by a factor of 5-10, the "conductivity splash" effect decreases, and this is evidently related to an increase in the rate of recombination of the chemisorbed H atoms (increase proportional to the suqare of the concentration) and chemisorption of alcohol vapor (which lowers the conductivity). The activation energy of the increase in conductivity amounts to 46 kcal. (a value very close to the activation energy of the dehydrogenation of isopropyl alcohol on ZnO [6])* while the activation energy of the decrease in conductivity is 37 kcal. (a value close to the value obtained for the activation energy of the decrease in conductivity in the experiments with the discharge).

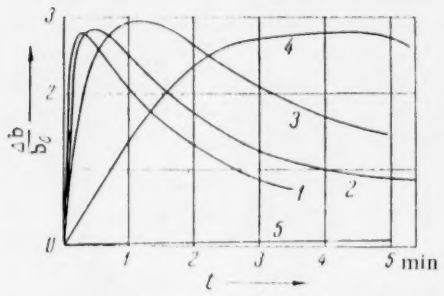

Fig. 2. The change in conductivity of ZnO with passage of alcohol vapor into the reaction vessel. 1) 390°; 2) 370°; 3) 350°; 4) 320°; 5) passage of hydrogen at 390°.

Figure 3 gives the results of experiments on the chemisorption of methyl radicals. The chemisorption of methyl radicals reduces the conductivity. This result is obtained both in the case of acetone photolysis and in the case of dimethyl ether cracking. At room temperature the act of switching off the light does not lead to a reversal of the conductivity change (the film has to be heated). The decrease and increase in the conductivity of n-semiconductors with time are satisfactorily expressed by equations of the form:

$$\lg \sigma = -k_1'[CH_3]_s t + \text{const}, \qquad (4)$$
$$\frac{1}{\Delta\sigma} = k_2 t + \text{const},$$

where k_1' and k_2 – kinetic constants dependent on the temperature; $[CH_3]_s$ – stationary concentration of chemisorbed radicals; $\Delta\sigma = \sigma_0 - \sigma$; σ_0 – conductivity of film with no radicals present; the index s indicates the chemisorbed condition.

These equations may be related to the reactions $(CH_3)_s + e \longrightarrow (CH_3)_s^-$ and $2\,(CH_3)_s^- \longrightarrow C_2H_6 + 2e$, if we consider that in the region of conductivity by impurities, $(CH_3)_s^- = [e]_0 - [e] = \Delta\sigma$.

As the temperature is increased, the values of $k_1 = k_1' \cdot [CH_3]_s$ at first increase (Fig. 3A, part 1a of curve), and afterwards decrease (part 1b), while the values of the stationary conductivity increase with temperature at first slowly and afterwards rapidly (Fig. 3B). These changes in the values of k_1 and the stationary conductivity with change in temperature are related, as in the case of the chemisorption of H radicals (see scheme (3), to the fact that, in the bulk and on the surface, several competing reactions are taking place, with different activation energies, resulting in a reduction in the stationary concentration of chemisorbed radicals $(CH_3)_s$ with increase in temperature, and consequently leading to a reduction in the values of k_1 and an increase in the

*As would be expected, since the activation energy of the reaction $H \longrightarrow (H)_s^+ e$ is small (~ 2 kcal), so that the limiting step of the increase in the conductivity of the ZnO in this process is the decomposition of the alcohol molecule.

stationary conductivity (see Fig. 3B, Curve 2) resulting from a shift in the equilibrium $(CH_3)_s + e \rightleftharpoons (CH_3)_s^-$ to give an increase in the concentration of electrons in the conductivity zone.

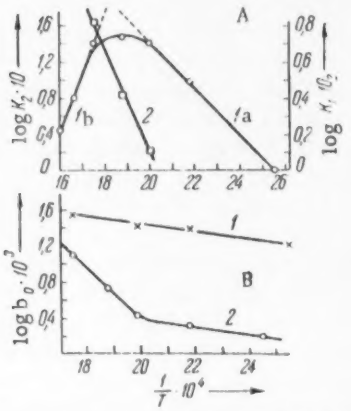

Fig. 3. The change in conductivity of ZnO with chemisorption of methyl radicals. A) The variation of k_1 (1a, b) and k_2 (2) with 1/T; B) the relationship between the stationary conductivity of ZnO and temperature: 1) in acetone vapor; 2) in acetone vapor in the presence of CH_3 radicals.

The activation energies for the elementary surface reactions (I) $CH_3 \rightarrow (CH_3)_s \xrightarrow{+e} (CH_3)_s^-$; (II) $2(CH_3)_s^- \rightarrow (C_2H_6)_s + 2e$ calculated from the results of the conductivity measurements, have the following values: 5 kcal., 27 kcal.

The data obtained in the present work lead to the following conclusions:

1) The processes involved in the chemisorption of atoms and radicals and their subsequent ionization (the formation of $(H)_s^+$, $(N)_s^+$, $(CH_3)_s^+$ for example) take place with activation energies which are considerably lower (from 2 to 5 kcal.) than those of the corresponding processes for molecules (for H_2 30 kcal. [1], in the case of the chemisorption of C_2H_6 the change in conductivity is small, the case of N_2 there is practically no change).

2) The control and measurement of the conductivity of semiconductors during chemical reactions which take place by a mechanism involving radicals may serve as convenient methods for the detection of atoms and radicals, for measuring their concentration, and for studying the elementary stages of surface processes in chemisorption and catalysis.

LITERATURE CITED

[1] I. A. Miasnikov, J. Phys. Chem. 32, No. 4, 841 (1958).•

[2] I. A. Miasnikov, J. Phys. Chem. 31, 172 (1958).•

[3] W. Meyer and H. Neldel, Phys. Zs. 38, 1014 (1937).

[4] V. L. Bonch-Bruevich and F. F. Vol'kenshtein, Coll. Electronic Phenomena in Catalysis,•• (Izd. Acad. Sci. USSR, 1955) p. 218.

[5] I. A. Miasnikov and S. Ia. Pshezhetskii, Prod. Acad. Sci. 99, No. 2, 277 (1954).

L. Ia. Karpov Physicochemical Institute

Received February 5, 1958

•Original Russian pagination. See C. B. Translation.

••In Russian.

APPLICATION OF THE IRREVERSIBILITY OF ADSORPTION OF OPTICAL SENSITIZERS

Z. L. Petrushkina

(Presented by Academician A. N. Terenin, March 3, 1958)

The irreversibility of adsorption of optical sensitizers on silver bromide has been observed on a number of occasions [1, 2]. A more detailed study of the desorption has also been made in [3]. Renwick [4] and Potter [5] have independently patented methods for preparing photographic materials with varying degrees of contrast. The patented layers consist of a mixture of sensitized and unsensitized emulsions. The contrast of the image produced on a photographic layer of this type will vary depending on whether all the grains of the emulsion take part in image formation (exposure with white light) or only part of them (exposure with light corresponding to the sensitization region of one of the emulsions present in the mixture).

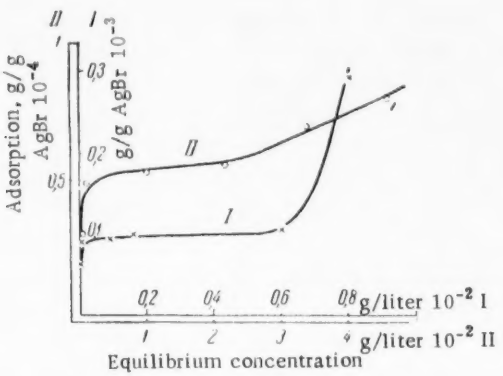

Fig. 1. Adsorption isotherms for the dyes: I) 3,3'-diethyl-4',5'-diphenyl-4-keto-5(3"-ethyl-6",7"-tetramethylenebenzthiazolinylidene-2"-α-phenylethylidene)-thiazolinothiazolocyanine iodide; II) 3,3'-dimethyl-9-ethyloxacarbocyanine iodide.

On the basis of the work described in [3], we have made an attempt to prepare an emulsion layer with two independent sensitization regions. Independent sensitization to different spectral regions reveals the possibility of preparing new photographic layers, color monolayers for example.

The method of study was as follows. Two emulsions were mixed, one sensitized to red and the other to green light, and the mixture was then poured on to a plate to form a single layer.

If the dye is irreversibly adsorbed on the emulsion grains and is not redistributed between them, then it would be expected that when a photographic layer of this type is exposed using light whose wavelength corresponds to the sensitization region of one of the emulsions, it would be possible to obtain an image from the grains of that emulsion only, while the second emulsion in the mixture would remain unexposed. This hypothesis was checked using a spectral sensitometric method.

The experiments were carried out using an ordinary factory production silver iodide–bromide positive emulsion of the "Unibrom" type. One part of the emulsion was sensitized to the red region of the spectrum using the dye 3,3'-diethyl-4',5'-diphenyl-4-keto-5(3"-ethyl-6",7"-tetramethylenebenzthiazolinylidene-2"-α-phenylethylidene)-thiazolinothiazolocyanine iodide. Two parts were sensitized using the orthochromatic dye 3,3'-dimethyl-9-ethyloxacarbocyanine iodide.

A preliminary study was made of the adsorption of the dyes used, on pure silver bromide [3].

Figure 1 shows the adsorption isotherms for the dyes studied. Both dyes are irreversibly adsorbed in

definite amounts on silver bromide, so that the isotherms do not pass through the origin. The emulsion sensitization conditions should be such that only the irreversibly adsorbed quantity of dye remains on the AgBr grains.

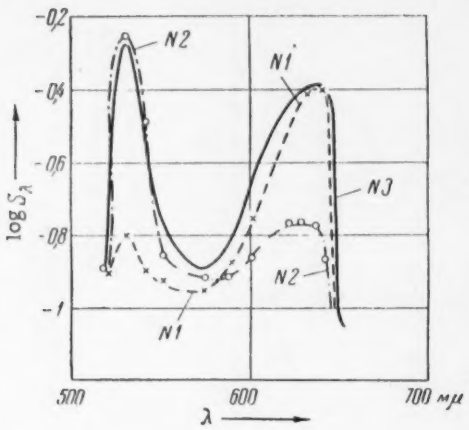

Fig. 2. Spectral light sensitivity curves.

Alcoholic solutions of the dyes, with concentration $1 \cdot 10^{-4}$ molar, were used. 0.05 ml of 3,3'-dimethyl-9-ethyloxacarbocyanine iodide and 0.03 ml of 3,3'-diethyl-4',5'-diphenyl-4-keto-5(3"-ethyl-6",7"-tetramethylenebenzthiazolinylidene-2"-α-phenylethylidene)-thiazolinothiazolocyanine iodide were added to 10 ml of prepared emulsion.

Both sensitized emulsions were coagulated with alcohol in order to remove excess dye from the gelatin and from the grains.

Plate No. 1 was illuminated uniformly with green light. Plate No. 2 was illuminated uniformly with red light. Both plates were developed for 5 minutes in a metol-hydroquinone developer. Thus the grains developed on the first plate were those of the emulsion sensitized to the green region of the spectrum while the grains developed on the second plate were those of the emulsion sensitized to the red region of the spectrum.

The metallic silver was removed from both plates. A panchromatic emulsion should thus have remained on plate No. 1 and an orthochromatic emulsion on plate No. 2.

Both plates, together with a third control plate, were exposed through a yellow light filter to produce spectral sensitivity diagrams which were then given the normal treatment used in sensitometric testing. The spectral sensitivity diagrams were then used to determine the spectral light sensitivity (see Fig. 2).

The control plate was senitive to both red and green light (the $\log S_\lambda = f(\lambda)$ curve has two maxima: $\lambda = 530$ mμ and $\lambda = 640$ mμ). Plate No. 1 retained its sensitivity to red light while its sensitivity to green light was very much reduced, so that evidently only the panchromatic emulsion remained on it before the exposure to produce the spectral sensitivity diagrams. On plate No. 2 the sensitivity to green light remained unchanged, while the sensitivity to red light was reduced.

The results obtained show that it is possible to produce a layer of silver bromide emulsion containing two types of grain: one sensitized to red light and the other sensitized to green light. A photographic layer of this type may be used to obtain images from either type of sensitized grain, depending on the wavelength of the light used. At the same time the results obtained provide proof that irreversible adsorption of sensitizer takes place on silver bromide.

LITERATURE CITED

[1] H. O. Dickinson, Phot. J. 88, B, 97 (1948).

[2] T. H. James and W. Vanseow, J. Am. Chem. Soc. 73, 5617 (1951).

[3] Z. L. Petrushkina, J. Sci. and Appl. Photography and Cinematography 1, 413 (1957).

[4] F. F. Renwick and C. S. Waller, Brit. Pat. 547,883.

[5] R. S. Potter, Brit. Pat. 547,060.

Aeromethods Laboratory,
USSR Academy of Sciences

Received February 7, 1958

THE "DEVIATIONS" FROM RAOULT'S LAW CAUSED BY CHEMICAL INTERACTION BETWEEN THE COMPONENTS

M. Usanovich

(Presented by Academician V. A. Kargin, March 4, 1958)

The customary explanation of deviation from Raoult's law is that the forces of mutual interaction between molecules of different components differ from the mean arithmetic value of the forces of molecular interaction in each of the components separately. From this point of view the sign of the deviation is determined by the direction in which the forces of mutual interaction differ from the mean value; if they exceed it, we have negative deviation, and vice versa.

For all its apparent plausibility, this explanation is not only insufficient, but also unsatisfactory. It excludes, in particular, the deviations of alternating sign which are observed in practice. In addition, from this point of view, chemical interaction between the components of a solution should always lead to negative deviations from Raoult's law, which again does not correspond to reality.

In the first place, the product of chemical interaction, may be, although it rarely is, a more volatile substance than the components. In this case, in spite of the chemical interaction, a positive deviation from Raoult's law may be observed and a positive azeotrope may even appear.

Secondly, chemical interaction may also lead to positive deviations (in partial vapor pressures) from Raoult's law in those cases where a nonvolatile product is formed.

If we have a system of two nonassociated components in which the reaction

$$mA + nB \rightleftarrows A_mB_n, \tag{1}$$

is taking place, and where A_mB_n is a nonvolatile substance, then there will be no positive deviation from Raoult's law only when m = n = 1. Even if only one of the stoichiometric coefficients differs from unity, then a positive deviation should be observed in the partial vapor pressures (albeit in only one of them).

This follows from the following considerations. As a result of reaction (1), the mole fraction of component A becomes equal to $\frac{x-my}{1-(m+n-1)\,y}$, where x – mole fraction of component A in the original mixture and y – mole fraction of compound A_mB_n in the equilibrium mixture. According to Raoult's law the partial vapor pressure of component A is given by

$$p_A = P_A \frac{x - my}{1-(m+n-1)\,y}, \tag{2}$$

and the deviation from Raoult's law is

$$\Delta p_A = P_A \frac{y}{1-(m+n-1)\,y}[(m+n-1)\,x - m]. \tag{3}$$

It follows from (3) that Δp_A changes sign when

$$x = \frac{m}{m+n-1}. \qquad (4)$$

For component B the change in sign of the deviation from Raoult's law takes place similarly when

$$1 - x = \frac{n}{m+n-1}. \qquad (4a)$$

It is apparent that a positive deviation of the vapor pressure in this case is caused by the chemical interaction and by no other process.

An extremely important feature here is that the change in sign of the deviation of the partial vapor pressure from the additive value is determined purely by the stoichiometric coefficients of the equation for reaction (1) and is independent of the equilibrium constant, i.e., of the extent to which the chemical interaction proceeds.

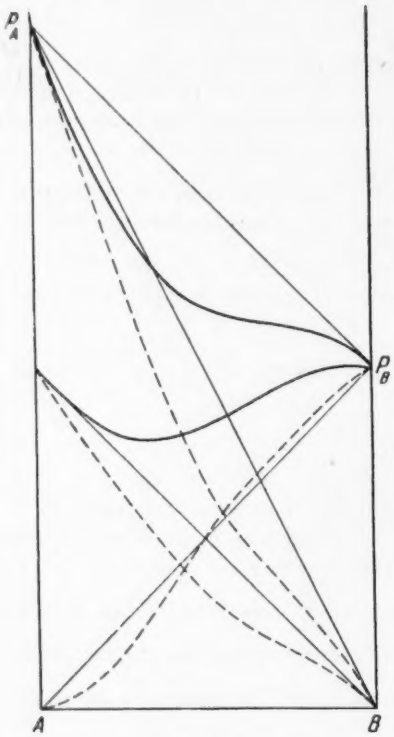

Fig. 1

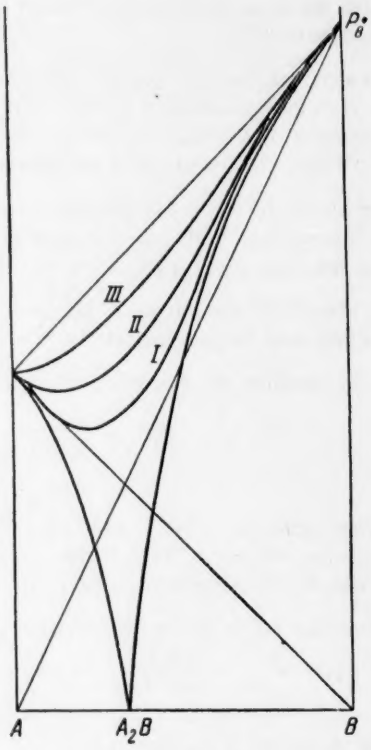

Fig. 2

If the compound A_mB_n is formed (i.e., n = 1), then a positive deviation from Raoult's law is observed only for component B from x = 0 to x = (m − 1)/m. The vapor pressure of component A in this case is lower than the additive pressure at all concentrations.

Figure 1 represents a schematic diagram of the vapor pressure for a binary system A−B in which the compound A_2B is formed. The partial vapor pressure of component B exceeds the additive value when $0 \leq x \leq 0.5$. The straight line AP_B is not a tangent to the partial vapor pressure curve for B at x = 1. Two

versions for the partial vapor pressure of component A are shown (with the same value of K, the constant for the thermal dissociation of the compound formed): one where $P_A = P_B$ and the other where $P_A = 2P_B$. The total vapor pressure curves are shown for both these versions. As the Figure shows, the straight line $P_A P_B$ touches the total vapor pressure curve only at the point P_B, and not at the point P_A. When $P_A = P_B$ the system is necessarily azeotropic; when $P_A \neq P_B$ the appearance of an azeotrope depends on the relationship between P_A, P_B and K.

The influence of K is shown in Fig. 2, which gives, in addition to the limiting case involving information of the undissociated compound A_2B, the total vapor pressure isotherms corresponding to three successively increasing values for the dissociation constant. Curve II is calculated for the same value of K as the vapor pressure curves in Fig. 1.

Our calculations were based on the law of mass action with the assumption that the pseudo-ternary system formed by A, B and A_mB_n obeys Raoult's law, which may be written in the general form

$$P = \sum p_i = \sum P_i x_i, \qquad (5)$$

where P – total vapor pressure of the system and x_i – equilibrium mole fraction of each component. Thus the schematic diagrams shown in Figs. 1 and 2 give the vapor pressure of systems in which chemical reaction is taking place, but which, when full account is taken of this interaction, obey Raoult's law.

It is necessary to apply the law of mass action to the treatment of the chemical interaction. The former has no other adequate expression since the stoichiometric coefficients of the equation for the reaction, which have, as we have shown, a decisive influence on the shape of the vapor pressure curves, figure only in the law of mass action.

It goes without saying that all our discussion relates only to chemical interactions between the components of a solution and cannot be extended to other processes giving deviations from Raoult's law.

S. M. Kirov State Univeristy, Kazakh
Kaz. SSR Academy of Sciences

Received February 3, 1958

ERRATA

Doklady Phys. Chem., Volume 114, Numbers 1-6, 1957

Page	Line	Reads	Should read
331	1 of text	(trans and bent forms)	(trans and skew forms)
382	2 under Fig. 1	3) rarefraction;	3) rarefaction;
	4 under Fig. 1	3) rarefraction;	3) rarefaction;
393	3 under Fig. 1	Rose Begal	Rose Bengal
440	[1] of Lit. Cited	Ya. Seirovsky	J. Heyrovsky